ACTUAL PROBLEMS OF PARTICLE PHYSICS

Proceedings of International School-Seminar

Vol. II

PROCEEDINGS of
INTERNATIONAL SCHOOL-SEMINAR
"ACTUAL PROBLEMS OF PARTICLE PHYSICS"

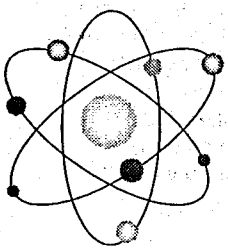

Joint Institute for Nuclear Research (Dubna, Russia),
National Center of Particle and High Energy Physics (Minsk, Belarus),
Institute of Physics (Minsk, Belarus) & Institute of Metal Polymer Systems (Gomel, Belarus) of National Academy of Sciences of Belarus,
Gomel State University,
Gomel Polytechnic Institute

July 30 – August 8, 1999, Gomel, Belarus

Accelerator Physics, LHC Program, Physics "in" and "out" of Framework of Standard Model, Soft and Hard QCD Processes, Quantum Field Theory, Relativistic Nuclear Physics

Edited by the Editorial Board

Vol. II

Dubna, 2000

INTERNATIONAL ADVISORY COMMITTEE:

V.Kadyshevsky JINR (Chairman), N.Amaglobeli IHEP, A.Baldin JINR, M.Danilov ITEP, M.Della Negra CERN, S.Dubnicka IP, V.Dzhelepov JINR, M.Finger Charl. Univ., V.Gaisyonok SCST, P.Jenni CERN, G.Kozlov Min. of Sc., A.Kozulin BSU, A.Logunov IHEP, V.Matveev INR, I.Meshkov JINR, V.Rubakov INR, V.Savrin NPI MSU, D.Shirkov JINR, A.Skrinsky Ac. of Sc. & BINP, R.Sosnovsky INP, P.Spillantini INFN, V.Strazhnev Min. of Ed., N.Tyurin IHEP, H.Vartapetyan ErPI, A.Voytovich Nat. Ac. of Sc., A.Wagner DESY, I.Zalyubovsky KhSU

ORGANIZING COMMITTEE from JINR:

A.Sissakian (Chairman), N.Skatchkov (Vice-Chairman, Rector), S.Shulga (Scientific Secretary), E.Russakovich (School Secretary), P.Bogolyubov, J.Budagov, A.Filippov, I.Golutvin, I.Ivanov, S.Ivanova, V.Kekelidze, A.Kurilin, A.Malakhov, M.Nazarenko, N.Russakovich

ORGANIZING COMMITTEE from BELARUS:

V.Gaisyonok SCST (Chairman), N.Shumeiko NC PHEP (Vice-Chairman), Y.Pleskachevsky IMMPS (Vice-Chairman), N.Maksimenko GSU (Pro-rector), V.Andreev GSU (Scientific Secretary), A.Tolkachev NC PHEP (Scientific Secretary), V.Baryshevsky RINP, A.Bogush SIP, S.Chigrinov "Sosny", V.Davydovych Gomel Executive Committee, N.Kazak SIP, A.Kukharev Council of Ministers, V.Kuvshinov SIP, A.Pankov GSTU, S.Rakhmanov BSU, V.Rumyantsev NC PHEP, S.Scherbakov GUT, A.Shaginyan GSTU, L.Shemetkov GSU, I.Solovtsov GSTU, S.Timoshin GSTU, L.Tomilchik SIP

EDITORIAL BOARD:

A.Bogush, V.Gaisyonok, M.Maksimenko, A.Pankov, S.Shulga, N.Shumeiko, A.Sissakian, N.Skatchkov, P.Starovoitov, A.Tolkachev

ISBN 5-85165-580-1

CONTENTS

Quantum Field Theory

ON THE COMPOSITION LAW OF GROUP VECTOR PARAMETERS: CONSEQUENCES AND APPLICATIONS

A.A.Bogush
B.I.Stepanov Institute of Physics.
National Academy of Sciences of Belarus, Minsk

The efficiency of the Fedorov's three-dimensional vector parametrization (1958-1962) is demonstrated by listing of several applications of the simple composition law for the group parameters in the theory of the Lorentz group as well as in relativistic kinematics, in gauge and other nonlinear field theories. It is also shown that the introduction of the four-dimensional quantum vector parameters reveals new possibilities to use the composition law and related linearity relations by solving specific problems in theory of the simplest quantum group $GL_q(2.C)$, including a realization of the q-deformation procedure in itself.

Introduction.

The crucial constructive role and greatest meaning of the symmetry ideas and invariance (covariance) conditions in the foundation and successive development of the modern theory of elementary particles and their interactions are now very well known and generally accepted. In beginning, to solve the physical problems the simplest infinitely small continuous symmetry transformations were, as a rule, used. In the Lie group theory namely the infinitesimal approach has been worked out very well. The possibility and efficiency of the finite transformation use, in contrast to infinitesimal ones, depend essentially on the convenient choice of the group parameters and on the simplicity of the composition rules connecting these parameters. These aspects of the Lie group theory did not find, in fact, an adequate presentation in the existing scientific literature addressed to physicists during a long time. In order to avoid such difficulties and to fill the related gaps in the group theory, F.I.Fedorov (1911-1994) 40 years ago has developed systematically the vector parametrization (VP) of the rotation group $SO(3.R)$ [1] and firstly worked out (1957-1959) the VP of the Lorentz group $SO(3.1)$ (see [2,3]).

In this review report the main attention will be given to the results which were obtained by developing and applying of the VP during last two decades and not included in the fundamental monograph (1979) of F.I.Fedorov "Lorentz Group" [4].

In the Preface to the monograph [4] it was written: "In this book the complex vector parametrization proposed 20 years ago by the author is

firstly used as the basis of the Lorentz group theory. In the framework of such parametrization all the six parameters of an arbitrary Lorentz transformation are joined into one three-dimensional complex vector obeying the simplest composition law... . The complex vector parameters in conjunction with the composition formula being the group multiplication operation, form a group which is isomorphic to the Lorentz group. Therefore most properties of the Lorentz transformations may by obtained without handling the matrices of these transformations, directly on the level of the related vector parameters themselves... . Thus, the composition law of the parameters plays the most fundamental role in the presented investigations ..."

In the following, some problems connected namely with the composition law and its consequences as well as with several their applications will be mainly considered.

1. Composition law and basic properties of the vector parametrization.

In the framework of the VP **the finite Lorentz transformation matrix** $\mathcal{L} \in SO(3.1)$ of general type is presented as a product of two commuting 4×4-matrices $\alpha_{(+)}$ and $\alpha_{(-)}$ [2,3]:

$$\mathcal{L} = \mathcal{L}(\boldsymbol{q}, \boldsymbol{q}^*) = \alpha_{(+)}(\boldsymbol{q})\alpha_{(-)}(\boldsymbol{q}^*) \in SO(3.1), \tag{1.1}$$

$$\alpha_{(\pm)}(\boldsymbol{q}) = \begin{pmatrix} 1+\boldsymbol{q}^{\times} & \pm\boldsymbol{q} \\ \mp\boldsymbol{q} & 1 \end{pmatrix} (1+\boldsymbol{q}^2)^{-1/2}, \ (\boldsymbol{q}^{\times})_{ac} = \varepsilon_{abc}q_b, \ (a,b,c = 1,2,3);$$

defined correspondingly by the three-dimensional complex vector parameter $\boldsymbol{q} = \boldsymbol{a} + i\boldsymbol{b}$ and its complex conjugated vector parameter $\boldsymbol{q}^* = \boldsymbol{a} - i\boldsymbol{b}$.

As a consequence, the vector parameters $\boldsymbol{q}$ and $\boldsymbol{q}^*$ of the Lorentz transformation matrices $\mathcal{L} = \mathcal{L}(\boldsymbol{q}, \boldsymbol{q}^*)$ (1.1) are composed independently [2,3]:

$$\mathcal{L}\mathcal{L}' = \mathcal{L}'' \rightarrow \begin{cases} <\boldsymbol{q}, \boldsymbol{q}'> = \boldsymbol{q}'', \\ <\boldsymbol{q}^*, \boldsymbol{q}^{*\prime}> = \boldsymbol{q}^{*\prime\prime}; \end{cases} \tag{1.2}$$

$$\mathcal{L}, \mathcal{L}', \mathcal{L}'' \in SO(3.1); \quad \boldsymbol{q}, \boldsymbol{q}', \boldsymbol{q}'' \in Q;$$

with help of **the simplest composition law** [2,3]

$$<\boldsymbol{q}, \boldsymbol{q}'> = (\boldsymbol{q} + \boldsymbol{q}' + [\boldsymbol{q}, \boldsymbol{q}'])(1 - \boldsymbol{q}\boldsymbol{q}')^{-1}, \tag{1.3}$$

which has the same form as in the case of the three-dimensional real vector parameters $\boldsymbol{n}$ of the rotation group $SO(3.R)$ [1].

This main property of Lorentz group VP made it possible to construct all the possible finite dimensional **representation operators** of the $SO(3.1)$ group by making direct use of the results obtained previously in the framework of the $SO(3.R)$ VP [5].

The **geometrical (physical) meaning** of the introduced Lorentz group vector parameters is also investigated with help of composition law (1.3). The complex vector parameter $\boldsymbol{q}$ $(\boldsymbol{q}^*) \in Q$ of the Lorentz group is considered here as a composition of the real vector parameter of the space rotation $\boldsymbol{n}$ and of the imaginary vector parameter of the relative motion $i\boldsymbol{u}$ [2,3]:

$$\boldsymbol{q} = \boldsymbol{a} + i\boldsymbol{b} = <\boldsymbol{n}, i\boldsymbol{u}>, \ \boldsymbol{q}^* = \boldsymbol{a} - i\boldsymbol{b} = <\boldsymbol{n}, -i\boldsymbol{u}>. \tag{1.4}$$

F.I.Fedorov has firstly unveiled the aim, meaning and concrete contents of the procedure called "group parametrization": it is necessary to establish and to formulate explicitly the one-to-one correspondence between a Lie group and its parameters. As a result, it was proved that the multitude Q of vector parameters $\boldsymbol{q}$ of the group $SO(3.1)$ forms a **noncommutative group** Q, for which the nonlinear composition law (1.2), (1.3) plays the role of the group operation [4]. So, with help of this composition law the basic correspondence relations for **the group axioms** are formulated [2,3]. As a consequence, particularly, the following **naturalness conditions** are introduced [2-4]:

$$\mathcal{L} \leftrightarrow (\boldsymbol{q}, \boldsymbol{q}^*), \quad \mathcal{L}^{-1} \leftrightarrow (-\boldsymbol{q}, -\boldsymbol{q}^*), \quad \mathcal{L}_0 = I_4 \leftrightarrow (\boldsymbol{q}_0, \boldsymbol{q}_0^*) = (0,0). \tag{1.5}$$

The composition law (1.2), (1.3) has allowed to treat the VP not only as natural one, but also as a **linear parametrization** [4]. The nonlinear similarity transformation realized, for example, for the 2×2 matrix $L^{(0)} = L(\boldsymbol{q}^{(0)}) \in SL(2.C)$, by means of matrices $L = L(\boldsymbol{q})$ and $L^{-1} = L(-\boldsymbol{q})$ leads to the linear transformation of the vector parameter $\boldsymbol{q}^{(0)}$ with help of the matrix $O(\boldsymbol{q}) \in SO(3.C)$ [2,3]:

$$LL^{(0)}L^{-1} = L(\boldsymbol{q})L(\boldsymbol{q}^{(0)})L(-\boldsymbol{q}) = L(\boldsymbol{q}'^{(0)}) = L'^0 \leftrightarrow$$

$$\leftrightarrow <\boldsymbol{q}, \boldsymbol{q}^{(0)}, -\boldsymbol{q}> = O(\boldsymbol{q})\boldsymbol{q}^{(0)} = \boldsymbol{q}'^{(0)}, \tag{1.6}$$

$$L = L(\boldsymbol{q}) = (1+\boldsymbol{q}^2)^{-1/2}(1 - i\boldsymbol{q}\boldsymbol{\sigma}), \tag{1.7}$$

$$O = O(\boldsymbol{q}) = (1+\boldsymbol{q}^2)^{-1}[1 - \boldsymbol{q}^2 + 2(\boldsymbol{q}\cdot\boldsymbol{q} + \boldsymbol{q}^{\times})], O^{-1} = \tilde{O} = O(-\boldsymbol{q}). \tag{1.8}$$

From the linearity relations (1.6), when considering the similarity transformations as acting on the group generators, but not on the vector parameters, there follow the $SL(2.C)$- **invariance conditions** (similar to ones established in the framework of $SU(2)$ VP in [6]):

$$L(\boldsymbol{q})t^a L(-\boldsymbol{q}) = O_{ba}(\boldsymbol{q})t^b = O(-\boldsymbol{q})_{ab}t^b = t'^a, \qquad (1.9)$$

which define simultaneously the transformation properties of the generators $t^a = \sigma^a/2$ of the group $SL(2.C)$ expressed here in terms of the Pauli matrices $\boldsymbol{\sigma} = (\sigma_a)$. It is easy to see that the linearity relations (1.6) (see [4]) as well as the invariance conditions (1.9) remain to be valid also for arbitrary finite-dimensional representation operators for the group under consideration.

The finite Lorentz transformation matrices and corresponding group representation operators as well as the related vector parameters may be expressed **in terms of physical quantities** used for description of the elementary particle free states, i.e., in terms of energy momentum and spin vectors [7]. In order to realize such possibility the vector parameters which define in most general case the Lorentz transformation matrices $\mathcal{L} = \mathcal{L}(\boldsymbol{q}, \boldsymbol{q}^*)$ connecting two arbitrary fixed four-vectors $p = (\boldsymbol{p}, ip_0)$ and $p' = (\boldsymbol{p}', ip_0')$ $(p^2 = p'^2 = -m^2)$ are found by making direct use of the composition rules (1.4) [7]. On this basis the Lorentz group representation operators $T = T(\boldsymbol{q}, \boldsymbol{q}^*)$ are constructed which realize a transition [7] (see also [4] and [8])

$$T(\boldsymbol{q}, \boldsymbol{q}^*)\psi_1 = \psi_2 \qquad (1.10)$$

where $\psi_1 = \psi^{s_1}(p_1)$ and $\psi_2 = \psi^{s_2}(p_2)$ are the free elementary particle state functions.

The change from the vector parameters $\boldsymbol{q}$ and $\boldsymbol{q}^*$ of the $SO(3.1)$ to the two independent three-dimensional complex vector parameters $\boldsymbol{q} = \boldsymbol{a} + i\boldsymbol{b}$ and $\boldsymbol{g} = \boldsymbol{c} + i\boldsymbol{d}$ leads to the VP of the **complex Lorentz group** $SO(4.C)$. Naturally, these vector parameters obey the same composition law (1.2),(1.3) [9].

The simple operations with vector parameters allow one to separate, classify and describe all the **possible subgroups** of the groups $SO(4.C)$, $SO(3.1)$ and $SO(3.C)$ by making direct use of the composition law (see [4])

The VP allows, as it has been done for the case of the $SO(4.C)$ group, the adequate **quaternionic formulation** [10]. On this basis the consistent **algebraic theory of the vectors in the Lobachevski space**

[11] has been developed by using the composition law (1.3) as summation operation for the introduced vectors (biquaternions). Later, by considering the biquaternions defined over the **complex** as well as the so called **double** and **dual** numbers, in addition to the usual complex Lorentz group $SO(4.C)$, **the two new space-time symmetry groups**, $SO(4.W)$ and $SO(4.V)$, were introduced and studied. These three groups reflect the specific geometrical properties of the Minkowski, Euclidean and Galilei-Newton spaces correspondingly [12,13]. The related vector parameters (biquaternions) obey, naturally, one and the same composition law (1.3).

2. Finite transformations in relativistic kinematics, in gauge and other nonlinear field theories.

a. The finite Lorentz transformations and their representations written in the vector parametrical form have found, first of all, wide applications by solving many problems in relativistic kinematics of the elementary particle interactions.

For example, the covariant approach (1961-1962) to **direct calculation of interaction matrix elements (scattering amplitudes)** for polarized elementary particles was proposed and worked out [7]. It is based on the usage of the constructed in the framework of the VP transition operators (1.10) from one given free particle state to arbitrary other, when using for describing these states the projective dyadic matrices, the general theory of which was worked out by F.I.Fedorov too [14].

The first applications of such covariant calculation technique have shown its efficiency and have originated the wide successful researches in this area which are being continued up to now (see, for example, [4,8]).

The recent extended review paper [8] (1998) sums up the latest developments and wide applications of the covariant approach to the calculation of the scattering amplitudes based on introduction of the so called "diagonal spin basis". In the Summary we read: "The review of recently developed new techniques for covariant calculation of matrix elements in QED, the so-called "formalism of Diagonal Spin Basis" (DSB), is presented. It is applied to calculating of differential cross sections of processes when polarization of particles is to be taken into account... . In contrast to methods of CALCUL-group, etc., the developed approach is valid both for massive fermions and for massless ones... We apply this formalism to the following processes: 1) Möller's and Bhabha's bremsstrahlung ($e^{\pm}e^- \to e^{\pm}e^-\gamma$) ...; 2) Compton back-scattering ... ($e + n\gamma_0 \to e + \gamma$); 3) e^+e^--pair production ... ($\gamma + n\gamma_o \to e^+ + e^-$); 4) Bethe-Heitler process in the case of a

linearly polarized photon emission by an electron with account for proton recoil and formfactors; 5) the reaction $ep \to ep\gamma$ with proton polarizability being taken into account ...; 6) orthopositronium 3-photon annihilation ($e^+e^- \to 3\gamma$). The results obtained with the help of the developed DSB-formalism certify its efficiency for calculating of multiparticle processes when polarization is to be taken into account".

A new efficient and general approach to solve basic problems in relativistic kinematics was also developed [15] (see also monograph [16]) in the framework of the quaternionic formulation of the Lorentz group VP [10] and algebraic theory of the vectors in Lobachevski space [11].

b. In the frames of the VP of $SU(2)$ the transition from the global transformations $U = U(\boldsymbol{n}) \in SU(2)$, to the local (gauge) finite transformations $U(x)$ reduces only to the simple redefinition of the vector parameter: $\boldsymbol{n} \to \boldsymbol{n}(x)$ [6]. All the relations of the VP, including the simple composition law, remain to be valid for the local vector parameters too.

That allowed one to derive firstly the basic relations which define explicitly the transformation properties of the Yang-Mills gauge field vector potentials $\boldsymbol{b}_\mu(x) = (b^a_\mu(x))$ under the **finite** (instead of the infinite small ones, as it has been done previously) gauge (local) transformations $O(x) = O(\boldsymbol{n}(x))$ [6]. As a consequence, some important problems in the gauge field theory were considered on this basis. Particularly, the nonlinear equation and related Lagrangian [17] have been introduced for the principal chiral fields of the $SO(3.R)$ group in the vector parametrical form. This equation becomes solvable in the two-dimensional space-time and allows the existence of soliton-like solutions [18]. **The differential Cartan form** $dU(x)U^{-1}(x)$ has been also expressed in terms of local vector parameters $\boldsymbol{n}(x)$ of the gauge group $SU(2)$ [19] with help of the composition law (see (1.3)), without making direct use of the explicit expressions for the local transformation matrices. The most of these results were later extended to the wide set of gauge (supergauge) groups and effectively used in study of actual nonlinear field models. So, for example, in the Summary of the recent (1994) review paper [20] it was written: "The review is devoted to the development of the method of vector parametrization and its applications to the gauge and chiral field theories. The direct connection between the Cartan forms and the law of composition of parameters is established, not resolving Cartan-Maurer's differential equations. The explicit form of finite gauge transformations for the groups of local unitary, space-time symmetries and supersymmetry, and of the nonlinear realizations of gra-

vity and supergravity are obtained. The Cartan forms, the Lagrangians of the principal chiral and Goldstone fields for unitary groups $U(2)$, $SU(2)$, $U(3)$, $SU(3)$ are found which have the new types of nonlinearity. ... the vector parameters of $SO(3)$ are used as collective coordinates of skyrmions. ..."

3. Composition law for 4-dimensional quantum vector parameters and linearity relations.

a. Recently it was shown that VP may be also extended to the simplest **quantum (q-deformed) groups** (see [21]). Below, as an example, some new possibilities to make direct use of the composition rules for the introduced four-dimensional quantum vector parameters in the theory of the quantum group $GL_q(2.C)$ will be demonstrated.

It is known that the q-deformed group $GL_q(2.C)$ may be defined as a set of the 2×2-matrices

$$M_q^{(0)} = \begin{pmatrix} \hat{a} & \hat{b} \\ \hat{c} & \hat{d} \end{pmatrix} \in GL_q(2.C), \tag{3.1}$$

the elements $\hat{a}$, $\hat{b}$, $\hat{c}$, $\hat{d}$ of which are treated as some operators satisfying the following commutation relations:

$$\hat{a}\hat{b} = q\hat{b}\hat{a}, \hat{b}\hat{d} = q\hat{d}\hat{b}, \hat{b}\hat{c} = \hat{c}\hat{b}, \hat{a}\hat{c} = q\hat{c}\hat{a}, \hat{c}\hat{d} = q\hat{d}\hat{c}, \hat{a}\hat{d} - \hat{d}\hat{a} = (q - q^{-1})\hat{b}\hat{c}; \tag{3.2}$$

whereas the quantum determinant $D_q^{(0)}$ of the matrix $M_q^{(0)}$ (3.1) takes the form:

$$D_q^{(0)} = \det{}_q M_q^{(0} = \hat{a}\hat{d} - q\hat{b}\hat{c} = \hat{d}\hat{a} - q^{-1}\hat{b}\hat{c}. \tag{3.3}$$

(Complex number q is the quantum deformation parameter.)

The basic quantum relations (3.2) and (3.3) may be introduced in various ways. One of them is based on the usage of quantum analogues of the simplectic conditions and (see, for example, [22]) allows one to obtain the explicit quantum expression for the inverse matrix:

$$M_q^{(0)-1} = D_q^{(0)-1} \begin{pmatrix} \hat{d} & -q^{-1}\hat{b} \\ -q\hat{c} & \hat{a} \end{pmatrix}. \tag{3.4}$$

The crucial role in the framework of a such q-deformation procedure based on the independent introduction of the inverse quantum matrix belongs to the evident conditions

$$M_q M_q{}^{-1} = M_q{}^{-1} M_q = I_2, \tag{3.5}$$

as defining ones. The direct substitution of the quantum matrices $M_q^{(0)}$ (3.1) and $M_q^{(0)-1}$ (3.4) into formulas (3.5) leads immediately to the basic quantum relations (3.2) and (3.3).

b. Let us to consider a natural modification of the above q-deformation procedure in itself.

In order to realize such possibility, we define the relations (see (3.1))

$$M = \begin{pmatrix} a & b \\ c & d \end{pmatrix} \to M_q^{(0)} = \begin{pmatrix} \hat{a} & \hat{b} \\ \hat{c} & \hat{d} \end{pmatrix} \to \eta_q M_q^{(0)} \eta_q{}^{-1} = M_q, \tag{3.6}$$

where $M \in GL(2.C)$, $M_q^{(0)}, M_q \in GL_q(2.C)$ and the special transformation 2×2-matrices are introduced

$$\eta_q = \eta(q) = \begin{pmatrix} q^{1/4} & 0 \\ 0 & q^{-1/4} \end{pmatrix}, \eta_q^{-1} = \eta(q^{-1}) = \begin{pmatrix} q^{-1/4} & 0 \\ 0 & q^{1/4} \end{pmatrix}. \tag{3.7}$$

As a result, the new expression for the quantum 2×2-matrix M_q is obtained:

$$M_q = \begin{pmatrix} \hat{a} & q^{1/2}\hat{b} \\ q^{-1/2}\hat{c} & \hat{d} \end{pmatrix}. \tag{3.8}$$

The new inverse quantum matrix

$$M_q{}^{-1} = D_q{}^{-1} \begin{pmatrix} \hat{d} & -q^{-1/2}\hat{b} \\ -q^{1/2}\hat{c} & \hat{a} \end{pmatrix} \tag{3.9}$$

may be also found by introducing, by analogy with formulas (3.6), the following relations:

$$\begin{aligned} DM^{-1} = \begin{pmatrix} d & -b \\ -c & a \end{pmatrix} \to D_q^{(0)} M'^{(0)-1}_q = \begin{pmatrix} \hat{d} & \hat{b} \\ -\hat{c} & \hat{a} \end{pmatrix} \to \\ \to D_q^{(0)} \eta_q^{-1} M'^{(0)-1}_q \eta_q = D_q M_q. \end{aligned} \tag{3.10}$$

The substitution of the new quantum matrices M_q (3.8) and $M_q{}^{-1}$ (3.9) depending now explicitly from two different deformation parameters $q^{1/2}$ and $q^{-1/2}$ into defining conditions (3.5) leads to the same as above basic quantum relations (3.2) and (3.3). In such a way the proposed approach is verified.

c. We will show below that one can reformulate the operations (3.6) and (3.10) in a simple vector parametrical form directly.

First of all, let us remind that the quantum 2×2-matrix $M_q^{(0)}$ (3.1), written in terms of the ordinary Pauli matrices

$$\sigma = (i\sigma_0 = iI_2, \boldsymbol{\sigma}), \quad \boldsymbol{\sigma} = (\sigma_a) \quad \sigma_a\sigma_b = \delta_{ab} + i\varepsilon_{abc}\sigma_c \tag{3.11}$$

takes the following compact form:

$$M_q^{(0)} = -i\hat{m}\sigma = \hat{m}_0 - i\hat{\boldsymbol{m}}\boldsymbol{\sigma} = M_q^{(0)}(\hat{m}) \in GL_q(2.C), \tag{3.12}$$

where namely the set of four quantities

$$(\hat{m}_0, \hat{m}_1, \hat{m}_2, \hat{m}_3) = (\hat{m}_0, \hat{\boldsymbol{m}}) = \hat{m} \tag{3.13}$$

defines the four-dimensional quantum vector parameter of the q-deformed group $GL_q(2.C)$. The auxiliary "inverse" quantum matrix $M'^{(0)-1}_q$ (see (3.4)) entering in the formulas (3.10) may be also written in the vector parametrical form:

$$M_q^{(0)-1} = -iD_q^{-1}\hat{m}'\sigma, \quad \hat{m}' = (\hat{m}_0, -\hat{\boldsymbol{m}}). \tag{3.14}$$

It is easy to establish, by using the properties (3.11) of the Pauli matrices, that for the introduced quantum vector parameters $\hat{m}$ (3.13) of the quantum group $GL_q(2.C)$ the following composition rules (compare with (1.2),(1.3)) are valid [21]:

$$M_q^{(1)} M_q^{(2)} = M_q^{(3)} \to \ll \hat{m}^{(1)}, \hat{m}^{(2)} \gg = \hat{m}^{(3)} = (\hat{m}_0^{(3)}, \boldsymbol{m}^{(3)}):$$

$$\begin{aligned} \hat{m}_0^{(3)} &= \hat{m}_0^{(1)}\hat{m}_0^{(2)} - \hat{\boldsymbol{m}}^{(1)}\hat{\boldsymbol{m}}^{(2)}, \\ \hat{\boldsymbol{m}}^{(3)} &= \hat{m}_0^{(1)}\hat{\boldsymbol{m}}^{(2)} + \hat{\boldsymbol{m}}^{(1)}\hat{m}_0^{(2)} + [\hat{\boldsymbol{m}}^{(1)}\hat{\boldsymbol{m}}^{(2)}]; \\ M_q^{(1)} &= M_q(\hat{m}^{(1)}), M_q^{(2)} = M_q(\hat{m}^{(2)}), M_q^{(3)} = M_q(\hat{m}^{(3)}). \end{aligned} \tag{3.15}$$

Naturally, these composition rules conserve their form for the classical four-dimensional vector parameters of the group $GL(2.C)$ too.

Then, by taking into account the relations (3.6) and (3.10), in which the matrices η_q (3.7) may be treated as classical transformation matrices, we will consider the general case of similarity transformation for the quantum matrix $M_q^{(0)} = M_q(\hat{m}^{(0)}) = M_q(\hat{m}_0^{(0)}, \hat{\boldsymbol{m}}^{(0)})$ (3.12) realized with help of classical 2×2-matrices $M = M(m) = M(m_0, \boldsymbol{m})$ and $M^{-1}(m) = D^{-1}M(m') = D^{-1}M(m_0, -\boldsymbol{m})$:

$$MM_q^{(0)}M^{-1} = M_q \rightarrow$$

$$\rightarrow D^{-1} \ll (m_0, \boldsymbol{m}), (\hat{m}_0^{(0)}, \hat{\boldsymbol{m}}^{(0)}), (m_0, -\boldsymbol{m}) \gg = (\hat{m}'^{(0)}_0, \hat{\boldsymbol{m}}'^{(0)}) : \tag{3.16}$$

$$\hat{m}'^{(0)}_0 = D^{-1}(m_0^2 + \boldsymbol{m}^2)\hat{m}_0^{(0)} = \hat{m}_0^{(0)},$$

$$\hat{\boldsymbol{m}}'^{(0)} = D^{-1}[m_0^2 - \boldsymbol{m}^2 + 2(m_0\boldsymbol{m}^{\times} + \boldsymbol{m}\cdot\boldsymbol{m})]\hat{\boldsymbol{m}}^{(0)};$$

$$\ll (m_0, \boldsymbol{m}), (\hat{m}_0^{(0)}, \hat{\boldsymbol{m}}^{(0)}), (m_0, -\boldsymbol{m}) \gg = \tag{3.17}$$

$$= L(m_0, \boldsymbol{m})(\hat{m}_0^{(0)}, \hat{\boldsymbol{m}}^{(0)}) = (\hat{m}'^{(0)}_0, \hat{\boldsymbol{m}}'^{(0)}) = \hat{m}'^{(0)},$$

$$L = L(m) = L(m_0, \boldsymbol{m}) = \begin{pmatrix} 1 & 0 \\ 0 & O(m) \end{pmatrix},$$

$$O(m) = [m_0^2 - \boldsymbol{m}^2 + 2(m_0\boldsymbol{m}^{\times} + \boldsymbol{m}\cdot\boldsymbol{m})](m_0^2 + \boldsymbol{m}^2)^{-1} \in SO(3.C), \tag{3.18}$$

$$\boldsymbol{m}_a^{\times} = \varepsilon_{abc}m_b, \quad (\boldsymbol{m}\cdot\boldsymbol{m})_{ab} = m_a m_b.$$

d. Now, we can consider the above transformations (3.6) and (3.10) by making direct use of the obtained generalized linearity relations (3.16) -(3.18).

In beginning, let us rewrite in the explicit vector-parametrical form the transformation matrices η_q and η_q^{-1} (3.7):

$$\eta_q = a_0 - ia_3\sigma_3 = M(a), \quad a = (a_0, 0, 0, a_3);$$

$$\eta_q^{-1} = a_0 + ia_3\sigma_3 = M(a'), \quad a' = (a - 0, 0, 0, -a_3); \tag{3.19}$$

$$a_0 = (1/2)(q^{1/4} + q^{-1/4}), \quad a_3 = (i/2)(q^{1/4} - q^{-1/4}).$$

Then, by using the linearity relations (3.16), we can present the transformation (3.6) for the quantum matrix $M_q^{(0)}$ (3.12), in the following form:

$$M(a)M_q^{(0)}(\hat{m})M(a') = M_q(\ll a, \hat{m}, a' \gg) = M_q(m(q^{1/2})). \tag{3.20}$$

where (see (3.17)-(3.19))

$$\ll a, \hat{m}, a' \gg = L(a)\hat{m} = m(q^{1/2}) = [m_0, \boldsymbol{m}(q^{1/2})], \tag{3.21}$$

$$L(a) = \begin{pmatrix} 1 & 0 & 0 & 0 \\ 0 & \omega_{(+)} & i\omega_{(-)} & 0 \\ 0 & -i\omega_{(-)} & \omega_{(+)} & 0 \\ 0 & 0 & 0 & 1 \end{pmatrix}, \quad \omega_{(\pm)} = (1/2)(q^{1/2} \pm q^{-1/2}),$$

$$L^{-1}(a) = \tilde{L}(a) = L(a') = L(a_0, 0, 0, -a_3). \tag{3.22}$$

As a result, we find the four-dimensional quantum vector parameter

$$m(q^{1/2}) = [m_0(q^{1/2}), \boldsymbol{m}(q^{1/2})], \quad m_0(q^{1/2}) = \hat{m}_0,$$

$$\boldsymbol{m}(q^{1/2}) = [m_1(q^{1/2}), m_2(q^{1/2}), m_3(q^{1/2})] =$$

$$= [\omega_{(+)}(\hat{m}_1 + i\alpha\hat{m}_2), \omega_{(+)}(\hat{m}_2 - i\alpha\hat{m}_1), \hat{m}_3]; \tag{3.23}$$

$$-\omega_{(-)}/\omega_{(+)} = (1 - q)/(1 + q) = \alpha(q) = \alpha = -\alpha(q^{-1})$$

which defines the transformed quantum matrix $M_q \in GL_q(2.C)$ (3.8)

$$M_q = M_q[m(q^{1/2})] = M_q[m_0, \boldsymbol{m}(q^{1/2})] = \hat{m}_0 - i\boldsymbol{m}(q^{1/2})\boldsymbol{\sigma}. \tag{3.24}$$

In a similar way, after rewriting the relations (3.10) in the vector parametrical form (see (3.14)) we will have

$$DM^{-1} = D^{-1}M(m_0, -\boldsymbol{m}) = m_0 + i\boldsymbol{m}\boldsymbol{\sigma} \rightarrow$$

$$\rightarrow D_q^{(0)}M_q'^{(0)-1} = \hat{m}_0 + i\hat{\boldsymbol{m}}\boldsymbol{\sigma} \rightarrow D_q{}^{-1}M(a')M_q'^{(0)-1}M(a), \tag{3.25}$$

$$M(a')M_q'^{(0)-1}M(a) = M_q(\ll a', \hat{m}', a \gg) = D_qM_q^{-1},$$

$$\ll a', \hat{m}', a \gg = L^{-1}(a)\hat{m}' = m(q^{-1/2}). \tag{3.26}$$

Hence the explicit expression for the quantum vector parameter $m'(q^{-1/2})$ follows (see (3.19)):

$$m'(q^{-1/2}) = D_q^{-1}m(q^{-1/2}) = D_q^{-1}[m_0(q^{-1/2}), -\boldsymbol{m}(q^{-1/2})],$$

$$m_0(q^{-1/2}) = \hat{m}_0, \quad \boldsymbol{m}(q^{-1/2}) = (m_1(q^{-1/2}), m_2(q^{-1/2}), m_3(q^{-1/2})) = \tag{3.27}$$

$$= \{w_{(+)}(\hat{m}_1 - i\alpha\hat{m}_2), w_{(+)}(\hat{m}_2 + i\alpha\hat{m}_1), \hat{m}_3\},$$

whereas the related inverse quantum matrix $M_q{}^{-1}$ (3.9) takes the following vector-parametrical form:

$$M_q{}^{-1} = M_q[m'(q^{-1/2})] = M_q[D_q^{-1}m(q^{-1/2})] = D_q^{-1}[\hat{m}_0 + i\boldsymbol{m}(q^{-1/2})\boldsymbol{\sigma}]. \tag{3.28}$$

It is clear that for the obtained quantum matrices $M_q[m(q^{1/2})]$ (3.24) the composition law (3.15) remains to be valid, provided the evident change of the quantum vector parameters is taken into account (see (3.13) and (3.23))

$$\hat{m} = (\hat{m}_0, \hat{\boldsymbol{m}}) \to m(q^{1/2}) = (\hat{m}_0, \boldsymbol{m}(q^{1/2})).$$

Now, by substituting the quantum matrices M_q (3.24) and M_q^{-1} (3.28) into basic conditions (3.5) and applying the composition law (3.15) only ($I_2 = M_q(1,0)$):

$$M_q M_q^{-1} = I_2 \to D_q{}^{-1} \ll m(q^{1/2}), m(q^{-1/2}) \gg = (1,0),$$

$$M_q{}^{-1} M_q = I_2 \to D_q{}^{-1} \ll m(q^{-1/2}), m(q^{1/2}) \gg = (1,0)$$

we get the basic quantum relations (3.2) and (3.3) written in the following compact vector parametrical form (see [21]):

$$\begin{aligned} [\boldsymbol{m}(q^{1/2})\boldsymbol{m}(q^{-1/2})] &= -\hat{m}_0 \boldsymbol{m}(q^{-1/2}) + \boldsymbol{m}(q^{1/2})\hat{m}_0, \\ [\boldsymbol{m}(q^{-1/2})\boldsymbol{m}(q^{1/2})] &= \hat{m}_0 \boldsymbol{m}(q^{1/2}) - \boldsymbol{m}(q^{-1/2})\hat{m}_0; \end{aligned} \tag{3.29}$$

$$D_q = \det{}_q M_q = \hat{m}_0 \hat{m}_0 + \boldsymbol{m}(q^{1/2})\boldsymbol{m}(q^{-1/2}). \tag{3.30}$$

e. All the above investigations may be also extended on the cases when the q-deformed Lie algebra of the quantum group is introduced and used. In order to realize such a possibility let us return to the formula (1.9) which follows directly from the linearity relations (1.6) and defines the transformation properties of the Pauli matrices. In fact, starting from the similarity transformations (3.6) and (3.10) taken in the four-dimensional vector parametrical forms (3.20)-(3.22) and (3.25), (3.26), in accordance with the generalized relations (3.15)-(3.19), we can write

$$\eta_q M_q^{(0)} \eta_q^{-1} = -iM(a)\hat{m}\sigma M(a') = -i(L(a)\hat{m})\sigma = -i\hat{m}L^{-1}(a)\sigma = M_q, \tag{3.31}$$

$$M_q = -i\hat{m}\sigma_q = \hat{m}_0 - i\hat{\boldsymbol{m}}\boldsymbol{\sigma}_q, \quad \sigma_q = L^{-1}(a)\sigma \tag{3.32}$$

and correspondingly:

$$\begin{aligned} D_q^0 \eta_q^{-1} M_q^{(0)-1} \eta_q &= -iM(a')\hat{m}'\sigma M(a) = \\ &= -i(L^{-1}(a)\hat{m}')\sigma = -i\hat{m}'L(a)\boldsymbol{\sigma} = -i\hat{m}'\bar{\sigma}_q = D_q M_q^{-1}, \end{aligned} \tag{3.33}$$

$$M_q^{-1} = D_q^{-1} M_q(\hat{m}') = -iD_q^{-1}\hat{m}'\bar{\sigma}_q = D_q^{-1}(\hat{m}_0 + i\hat{\boldsymbol{m}}\bar{\boldsymbol{\sigma}}_q), \quad \bar{\sigma}_q = L(a)\sigma. \tag{3.34}$$

As a result, we obtain two sets of the q-deformed Pauli matrices:

$$\begin{aligned} &\sigma_{0q} = \sigma_0 = \begin{pmatrix} 1 & 0 \\ 0 & 1 \end{pmatrix}, \ \sigma_{1q} = \omega_{(+)}\sigma_1 - i\omega_{(-)}\sigma_2 = \begin{pmatrix} 0 & q^{-1/2} \\ q^{1/2} & 0 \end{pmatrix}, \\ &\sigma_{2q} = \omega_{(+)}\sigma_2 + i\omega_{(-)}\sigma_1 = \begin{pmatrix} 0 & -iq^{-1/2} \\ iq^{1/2} & 0 \end{pmatrix}, \ \sigma_{3q} = \sigma_3 = \begin{pmatrix} 1 & 0 \\ 0 & -1 \end{pmatrix}; \end{aligned} \tag{3.35}$$

$$\begin{aligned} &\bar{\sigma}_{0q} = \sigma_0 = \begin{pmatrix} 1 & 0 \\ 0 & 1 \end{pmatrix}, \ \bar{\sigma}_{1q} = \omega_{(+)}\sigma_1 + i\omega_{(-)}\sigma_2 = \begin{pmatrix} 0 & q^{1/2} \\ q^{-1/2} & 0 \end{pmatrix}, \\ &\bar{\sigma}_{2q} = \omega_{(+)}\sigma_2 - i\omega_{(-)}\sigma_1 = \begin{pmatrix} 0 & -iq^{1/2} \\ iq^{-1/2} & 0 \end{pmatrix}, \quad \sigma_{3q} = \sigma_3. \end{aligned} \tag{3.36}$$

The both sets of matrices σ_q (3.35) and $\bar{\sigma}_q$ (3.36) satisfy the same as in classical case relations (3.11): $\sigma_{aq}\sigma_{bq} = \delta_{ab} + i\varepsilon_{abc}\sigma_{cq}$ and $\bar{\sigma}_{aq}\bar{\sigma}_{bq} = \delta_{ab} + i\varepsilon_{abc}\bar{\sigma}_{cq}$. In order to reflect the specific quantum properties of the q-deformed group $GL_q(2.C)$ we introduce the evident relations connecting among themselves the above two sets (see (3.32), (3.34)):

$$\begin{aligned} \sigma_{cq}\bar{\sigma}_{dq} &= (L^{-1}(a))_{ca}(L(a))_{db}(\delta_{ab} + i\varepsilon_{abf}\sigma_f), \\ \bar{\sigma}_{cq}\sigma_{dq} &= (L(a))_{ca}(L^{-1}(a))_{db}(\delta_{ab} + i\varepsilon_{abf}\sigma_f). \end{aligned} \tag{3.37}$$

Actually, by substituting, as above, the quantum matrices $M_q = -i\hat{m}\sigma_q$ (3.32) and $M_q^{-1} = -iD_q^{-1}\hat{m}'\bar{\sigma}_q$ (3.34) into defining conditions (3.5) and by using namely the relations (3.37) we get to the basic commutation relations (see (3.2)) [21]:

$$[\hat{m}_1, \hat{m}_2]_- = 0, \quad 2[\hat{m}_3, \hat{m}_0]_- = -i(q - q^{-1})(\hat{m}_1^2 + \hat{m}_2^2),$$

$$[\hat{m}_1, \hat{m}_3]_\pm = i\alpha(\pm q)[\hat{m}_1, \hat{m}_0]_\mp, \quad [\hat{m}_2, \hat{m}_3]_\pm = i\alpha(\pm q)[\hat{m}_2, \hat{m}_0]_\mp,$$

which coincide, naturally, with the general relations (3.29) (see explicit expressions for $m(q^{1/2})$ (3.23) and $m(q^{-1/2})$ (3.27)).

At last, the following schema for transition $GL(2.C) \to GL_q(2.C)$ in the framework of the VP may be given:

$$M \to M_q^{(0)} \to M_q = \eta_q M_q^{(0)} \eta_q^{-1}:$$

$$m, \ \sigma; \to \hat{m}, \ \sigma; \to \begin{cases} m(q^{1/2}) = L(a)\hat{m}, & \sigma; \\ \hat{m}, & \sigma_q = L^{-1}(a)\sigma; \end{cases}$$

$$M^{-1} \to M_q'^{(0)-1} \to M_q^{-1} = \eta_q^{-1} M_q'^{(0)-1} \eta_q :$$

$$m, \ \sigma; \to \hat{m}', \ \sigma; \to \begin{cases} m(q^{-1/2}) = L^{-1}(a)\hat{m}', \ \sigma; \\ \hat{m}', \ \bar{\sigma}_q = L(a)\sigma. \end{cases}$$

Thus, we have demonstrated that in the framework of the four-dimensional VP the basic problems of the q-deformed group $GL_q(2.C)$, including the q-deformation procedure in itself, may be solved in simple and natural way by making use of composition law and linearity relations, i.e., by operating only with the quantum vector parameters, without making direct use of the explicit expressions for the finite quantum transformation matrices.

Conclusion.

Finally, we can conclude that the vector parametrization worked out by F.I.Fedorov 40 years ago turned out to be very general and fruitful method in the Lie group theory and in its physical applications. This approach may be indeed considered as forming a foundation for elaboration of the general finite symmetry (geometrical, dynamical and quantum) transformation technique for using in the theory of elementary particles and their interactions.

The work is supported by Belarussian Republican Foundation for Advanced Studies.

References

[1] Fedorov F.I. *Doklady Akademii Navuk BSSR.* V.2. 1958. P.408.

[2] Fedorov F.I. *Doklady Akademii Nauk BSSR.* V.5. 1961. Pp.101, 194.

[3] Fedorov F.I. *Doklady Akademii Nauk SSSR.* V.143. 1962. P.56.

[4] Fedorov F.I. *Lorentz Group.* M. 1979.

[5] Tkharev E.E., Fedorov F.I. *Yadernaya Fizika.* V.5. 1967. P.1112; *Vesti Akad. Nav. BSSR. Ser.fiz.-matem.nav.* N 1. 1967. P.101.

[6] Bogush A.A. *Introduction to the Field Theory of Elementary Particles.* Nauka i tekhnika. Minsk. 1981.

[7] Bogush A.A., Fedorov F.I. *Vesti Akad.Nav. BSSR. Ser. fiz.-tekhn. nav.* N 2. 1962. P.26.

[8] Galynskij M.V., Sikach S.M. *Elementary Particles and Atomic Nuclei.* Dubna. V.29. 1998. P.1133.

[9] Bogush A.A., Fedorov F.I. *Teoret. i matem. fizika.* V.13. 1972. P.67.

[10] Bogush A.A., Kurochkin Yu.A., Lapkovski A.K., Fedorov F.I. *Vesti AN BSSR. S. f.-m.n.* N1. 1976. P.69.

[11] Kurochkin Yu. A. *Quaternions and its applications in physics.* Preprint N 109. Institute of Physics AN BSSR, Minsk 1976.

[12] Kurochkin Yu. A., Tolkachev E.A. *Dokl. Ak. Nav. BSSR.* V.34. 1990. P.695.

[13] Bogush A.A., Kurochkin Yu.A. *Dokl. Akad. Nauk Belarusi.* V.39. 1995. P.39.

[14] Fedorov F.I. *Zhurn. experim. i teoret. fiziki.* V.35. 1958. P.483.

[15] Bogush A.A., Kurochkin Yu.A., Fedorov F.I. *Dokl. AN SSSR.* V.231. 1976. P.312.

[16] Berezin A.V., Kurochkin Yu.A., Tolkachev E.A. *Quaternions in Relativistic Physics.*, Nauka i tekhnika, Minsk. 1989.

[17] Bogush A.A., Zhirkov L.F. In: *Covariant Methods in Theoretical Physics. Physics of Elementary Particles and Relativity Theory.* IP AN BSSR, Minsk. 1981. P.5.

[18] Doktorov E.V. Ibid. 1991. P.64.

[19] Berezin A.V, Kuvshinov V.I., Tho N.V. Ibid. 1991. P.21.

[20] Kuvshinov V.I., Tho N.V. *Physics of Elementary Particles and Atomic Nuclei.* Dubna. V.25. 1994. P.603

[21] Bogush A.A. *Dokl. Akad. Nauk Belarusi.* V.36. 1992. P.407; V.40. 1996. P.50; *Vesti. Nat. Akad. Nauk Belarusi. Ser.fiz.-matem. navuk.* N 4. 1997. P.57.

[22] Vokos S.P., Zumino B. and Wess J. *Z.Phys.C.* V.48. 1990. P.65.

TWO-GAUGE VERTEX FUNCTION IN METHOD OF FUNCTIONAL INTEGRATION

A. Fursin
GSTU, Belarus

Abstract

Gauge invariation exactly dictates a kind of interaction between fundamental fields. Special attention must be attached to the development of methods of the gauge field theory. In the article presented, with the help of mathematical apparatus of functional integration, the gauge equation for Lagrangians has been obtained which are invariant towards local transformation of groups U(1), SU(2), SU(3). With the help of generating functionals, calculated in the raw according to perturbation theory, these equations are checked in bottom orders.

Pointing independence of Lagrangian L towards gauge transformations, generating functional will be infinite. To obtain the final value, it is necessary to fix qauge quotient. As the result, functional integral will not be taken according to fields, connected with each other by gauge transformations. Strict mathematical description of this evidence, quotes in case of non-abelian fields to coming out of non-physical fields of Faddeev-Popov. The above mentioned words can be considered as, at some extend, mathematical trick, and by choosing of specific gauge calibration their contribution can be eliminated . Such gauges exist, for example, axial, determined by relation

$$t^\mu A^a_\mu = 3D0, \quad t^\mu t_\mu = 3D - 1. \tag{1}$$

1. U(1)-symmetry. Quantum Electrodynamics.

The gauge equation for 1-photon vertex function was considered in [1-2]. For the case of non-abelian group, this consideration was generalized in [3-4]. The equation for 2-photon function follows from the gauge invariation of quantum electrodynamics (QED). This principle results in equation [5]:

$$\partial^\mu \frac{\delta\tilde{\Gamma}}{\delta A_\mu(x)} + ie\frac{\delta\tilde{\Gamma}}{\delta\psi(x)}\psi(x) + ie\overline{\psi}(x)\frac{\delta\tilde{\Gamma}}{\delta\overline{\psi}(x)} == 3D0. \tag{2}$$

Executing the third functional derivative of the equation (2) according to fields $A_\mu, \overline{c}, c$ and make an equal to $\overline{c} = 3Dc = 3DA_\mu = 3D0$, we obtain in th= e momentum representation

$$\tilde{Q}^{\mu\nu}(p,0,0;p) = 3D\frac{\partial^2\tilde{S}^{-1}(p)}{\partial p_\mu \partial p_\nu}. \tag{3}$$

This equation is determined for 2-photon vertex function. Decomposing generating functional in the raw, we have to check this formula in the two bottom orders. We have

$$Q^{\mu\nu}(p,0,0,p) = 3D0. \tag{4}$$

As the opposite electron propagator $S^{-1}(p) = 3D\gamma_\mu p^\mu - m =$ in bottom order

$$\frac{\partial^2 S^{-1}(p)}{\partial p_\mu \partial p_\nu} = 3D0. \tag{5}$$

In the next order the investment in $\tilde{Q}^{\mu\nu}(p,0,0,p)$ and after all transformations gives only one diagram of generating functional

$$\begin{aligned} &Q^{(2)\mu\nu}(p,0,0,p) = \\ &= 3Die^2\int \gamma^\lambda S(p-k)\gamma^\mu S(p-k)\gamma^\nu S(p-k)\gamma^\omega S(p-k)D_{\lambda\omega}(k)dk \\ &+ie^2\int \gamma^\lambda S(p-k)\gamma^\nu S(p-k)\gamma^\mu S(p-k)\gamma^\omega S(p-k)D_{\lambda\omega}(k)dk. \end{aligned} \tag{6}$$

As the opposite electron propagator in the second order of momentum representation has the form

$$S^{(2)-1}(p) = 3Die^2\int \gamma^\lambda S(p-k)\gamma^\omega D_{\lambda\omega}(k)dk. \tag{7}$$

we obtain the coincidence in the formula of right-hand and left-hand sides in the second order.

2. Non-abelian gauge fields. SU(2)-symmetry. Spinor case.

Let spinor ψ is the dublet of group SU(2), then the law of its transformation

$$\psi \longrightarrow \psi' = 3Dexp(i\frac{1}{2}\vec{\tau}\vec{\Lambda})\psi, \tag{8}$$

where $\vec{\tau}$– Pauli-matrix, $\vec{\Lambda}$– arbitrary real functions.

Let's impose the consideration of gauge independence upon the generating functional

$$\delta\tilde{Z} = 3D0. \tag{9}$$

The unknown before equation has the form

$$\frac{\delta\tilde{\Gamma}}{\delta\vec{A}_\mu(x)} \times \vec{A}_\mu(x) + \frac{1}{g}\partial^\mu \frac{\delta\tilde{\Gamma}}{\delta\vec{A}^\mu(x)} - \\ -\frac{1}{2}i(\frac{\delta\tilde{\Gamma}}{\delta\psi(x)}\vec{\tau}\psi(x) + \overline{\psi}(x)\vec{\tau}\frac{\delta\tilde{\Gamma}}{\delta\overline{\psi}(x)}) = 3D0. \tag{10}$$

Executing the second functional derivative of the last equation according to fields $\overline{\psi}(x_1)$, $\psi(y_1)$ putting down $\overline{\psi} = 3D\psi = 3D\vec{A}_\mu = 3D0$. As the result we will have in the momentum representation

$$\tilde{\vec{\Gamma}}_\mu(p,0,p) = 3D - \frac{\vec{\tau}}{2}\frac{\partial\tilde{S}^{-1}(p)}{\partial p^\mu}. \tag{11}$$

We will obtain gauge equation for double-fermions vertex function. Executing functional derivative (10) according to fields $\overline{\psi}$, ψ, A_μ and consider them equal to zero. We have

$$\tilde{Q}^{ab}_{\mu\nu}(p,0,0;p) = 3D\frac{1}{4}\delta^{ab}\frac{\partial l^2\tilde{S}^{-1}(p)}{\partial p^\mu \partial p^\nu}. \tag{12}$$

As the bottom order the quantity $\tilde{Q}^{ab}_{\mu\nu}(p,0,0;p)$ is zero. We have also zero value in the right part (12), because $S^{-1} = 3D\gamma^\mu p_\mu - m$.

3. Non-abelian gauge case. SU(2) - symmetry. Vector case.

Let field $\overline{\phi}$ has three components $\vec{\phi} = 3D(\phi_1, \phi_2, \phi_3)$ and has the following law of transportation

$$\vec{\phi} \longrightarrow \vec{\phi}' = 3De^{(i\vec{I}\vec{\Lambda})}\vec{\phi}, \tag{13}$$

where I - matrix generators $(I_i)_{mn} = 3D - i\epsilon_{imn}$. Imposing condition of gauge independence (9) upon the generating functional we will have the following equation

$$\frac{\delta\tilde{\Gamma}}{\delta\vec{A}_\mu(x)} \times \vec{A}_\mu(x) + \frac{1}{g}\partial_\mu\frac{\delta\tilde{\Gamma}}{\delta A_\mu(x)} + \frac{\delta\tilde{\Gamma}}{\delta\vec{\phi}(x)} \times \vec{\phi}(x) = 3D0. \tag{14}$$

Executing the second functional derivative of the last equality in the momentum representation we will have

$$\tilde{\Gamma}^{\epsilon d,a}_\mu(p,0,p) = 3Di\epsilon^{\epsilon da}\frac{\partial\tilde{S}^{-1}(p)}{\partial p^\mu}. \tag{15}$$

We will obtain gauge equation for two-bozone vertex function. As the result we have

$$q^\mu l^\nu \tilde{Q}^{\epsilon d,af}_{\mu\nu}(p,0,0;p) = 3D\frac{1}{2}(\epsilon^{bea}\epsilon^{bdf} + \epsilon^{bef}\epsilon^{bda})\frac{\partial\tilde{S}^{-1}(p)}{\partial p^\mu \partial p^\nu}. \tag{16}$$

For proving of this equation let's make calculation of quantity $\tilde{Q}^{\epsilon d,af}_{\mu\nu}(p,0,0;p)$ in the bottom order:

$$Q^{\epsilon d,af}_{\mu\nu}(p,0,0;p) = 3D\delta_{\mu\nu}(\epsilon^{bea}\epsilon^{bdf} + \epsilon^{bef}\epsilon^{bda}). \tag{17}$$

The second derivative $S^{-1} = 3Dp^2 - m^2$ has the value $2\delta_{\mu\nu}$, what proves the gauge equation in the bottom order.

4. Non-abelian case. SU(3)-symmetry. Gauge equation for two-gluon function.

Let field $q^i(x)$ has the following law of transformation

$$q\beta q' = 3De^{(-igt^a\Lambda_a)}q, \tag{18}$$

where t^a– Gel-Mann matrix , Λ_a– arbitrary real functions. Let's impose the consideration of gauge independence upon the generating functional. Futher transformations bring into the following equation

$$r^\mu\tilde{\Gamma}^a_\mu(p,r;p+r) = 3Dt^a(\tilde{G}^{-1}(p+r) - \tilde{G}^{-1}(p)). \tag{19}$$

Let r to the zero we obtain

$$\tilde{\Gamma}^a_\mu(p,0,p) = 3Dt^a\frac{\partial\tilde{G}^{-1}(p)}{\partial p^\mu}. \tag{20}$$

We will obtain the gauge equation for two-gluon function, executing functional derivative and consider them equal to zero. We have in the momentum representation

$$\tilde{Q}^{ad}_{\mu\nu}(p,0,0;p) = 3D\frac{1}{2}\frac{\partial\tilde{G}^{-1}(p)}{\partial p^\mu \partial p^\nu}[t^a, t^d]_+. \tag{21}$$

5.Conclusion

Let generators M^a determine some representation of group U(1), SU(2) and SU(3). Then, the above obtained gauge equations can be generalized:

$$\tilde{\Gamma}^a_\mu(p,0,p) = 3D - M^a \frac{\partial \tilde{S}^{-1}(p)}{\partial p^\mu}, \tag{22}$$

$$\tilde{Q}^{ab}_{\mu\nu}(p,0,0;p) = 3D\frac{1}{2}\frac{\partial^2 \tilde{S}^{-1}(p)}{\partial p^\mu \partial p^\nu}[M^a M^b]_+. \tag{23}$$

The gauge equation obtained in the presented article, can be used in the overnormalized theory. The method described in this article presents interest in finding gauge equations for connected states, because only in connected states, the gauge equation theories run into-essential difficulties.

Bibliography

1. Ward J.C., Phys. Review, 1950. - 82. - p. 182
2. Takahashi Y., Nuovo Cim., 1957. - p. 371
3. Taylor J.C., Nucl. Phys., 1971. - p. 436
4. Slavnov A., Sov. Journ. Part. and Nucl., 1974 - 5.2. - p. 755
5. Ramond P., Field Theory, The Benjamin/Cummings Publishig Company, Inc., 1981
6. Yang L.N., Mills R.L., Phys. Rev., 1954. - 96, - p. 191
7. Slavnov A., Faddeev L., Introduction to quantum theory of gauge fields. - M.: Nauka, 1988

Realistic Quantum Field Theories with Non-Compact Group Symmetry.

A.E. Margolin & V. I. Strazhev
National Centre of the High Energy and Particle Physics,
Bogdanovich str.153, Minsk 220040, Belarus,
e-mail: alexm@hep.by

July 10, 2000

Abstract

We investigate two wide classes quantum field models with non-compact group symmetry: Yang-Mills theories with non-compact semi-simple groups symmetries and non-compact sigma model. We show that quantization of this models are self-consistent and describe by unitary physical S-matrix. The conditions of absence of chiral anomalies in both types of models are considered. General principles of correct quantization realistic quantum field theries with indefinite metrics are stated.

1 Introduction

Recently the non-compact groups of the internal symmetry very often appear in different models of quantum field theory.We enumerate papers on nonlinear non-compact sigma models [1], gauge theorics including gravitation[2],Grand Unification Theory [3], superstrings [4]and others.However, the use of the non-compact groups in particle physics generates some difficulties. In particular if the unitary representation of such groups which are infinite dimentional are used, a general principle of separation from such representations the finite dimentional subspaces with physical content is necessary.If the finite-dimensional (non-unitary) representations are used, an indefinite metric appears in the quantum state space of the corresponding theory, providing a positive hamiltonian definiteness and as a consequence there is a possibility of the appearance of the negative probabilities and S-matrix nonunitary. There are two methods of the obtaining the self-consistentnt quantum theories in the spaces with the indefinite metrics.The first one is to eliminate this metrics in the physical space states the appropriate condition on the state vectors. Such a method is good enough for a relativistic invariant formulation of the non-abelian Yang-Mills field with compact group in the procedure of the BRST-quantization[5] , the theory of the bosonic strings and superstrings[6], other quantum field theories . However, it

seems that this method isn't suitable for many theories with non-compact group of the symmetries. In particular it is impossible to formulate a self-consistent Yang-Mills quantum theory with non-compact group without the negative norm and it was already shown for the "minimum" non-abelian non-compact group SL (2,C) in Ref.7. The same is in the non-compact sigma models: the quantization in the space with definite norm is incorrect[8]. In the present report, we show that two wide classes of the quantum theories with non-compact groups of the internal symmetry: Yang-Mills field with non-compact semi-simple group and non-compact sigma model are correct quantized with using space with indefinite metric.We give sufficient condition to garantee that the quantum field model with indefinite metric had correct quantization.

2 Spaces of states with indefinite metric.

2.1 Operationals decompositions in the space with indefinite metric.

Let us consider space with non-degenerated indefinite metric $\langle , \rangle$ and fixed decomposition

$$H = H^+ \oplus H^- \tag{2.1}$$

We exclude degenerated states $| v\rangle$ with property $\langle H \mid v\rangle = 0$.We shall term such spaces in the further as the Krein spaces according to used terminology[9]. Then following propositions about H take place[10,11]

Proposition1. Let $A[H]$ is an algebra of operators on the H. Then there is unique decomposition for any operator $\varkappa \in A[H] : \varkappa = \varsigma + \upsilon$ where operator ς preserves Hilbert sectors H^+, H^- i.e. $\varkappa : H^+ \longrightarrow H^+ , H^- \longrightarrow H^-$ and υ mixes theirs $\upsilon : H^+ \longrightarrow H^-, H^- \longrightarrow H^+$.So we have decomposition $A[H]$ in the direct sum

$$A[H] = A_0[H] \oplus A_1[H] \tag{2.2},$$

where $A_0[H]$ is an operator algebra , presrerving H^+, H^- and $A_1[H]$ is the subspace mixing theirs.

Let ς and υ be a diagonal and cross-diagonal part of the operator $\varkappa$ respectively.

Evidently that ς can be considered as an operator in Hilbert spaces H^+, H^- but only with different sign of metrics. In order there not be any confusion, we shall use notations of the hermitian conjugation and hermiticity of the operator , which are similarly used in the sign-defined metrics. It is stated in Ref4 the correspondence of such a terminology with case of the mathematical Krein spaces.

Proposition 2. Let (2.2) be a canonical development of the operator $\varkappa$ in the Krein space H with the indefinite metrics. Then if $\varkappa$ is hermitian (cross-hermitian) then the operators ς and υ are the same.

2.2 Observables in the space of states with indefinite metric.

However not all operators in the space with indefinite metrics may be considered as observables. In particular for the operators of the type $A_1[H]$, i.e. the operators which coincide with their cross-diagonal part, it is true the following.

Proposition 3. Average value of the any $\upsilon \in A_1[H]$ hermitian (cross-hermitian) operator for any eigen state is zero.

If we suppose a existence of the full system of mutally orthogonal eigen states for any physical interesting operator from $A[H]$, then one can obtain immediately

Proposition 3*. Average value of the any $\upsilon \in A_1[H]$ hermitian (cross-hermitian) operator for any state $\Theta \in H$ is zero, i.e.$\langle \Theta \mid \upsilon \mid \Theta \rangle$.

Such operators $\varkappa \in A[H]$ with non-zero υ can not be observables. That is why it is important to consider only operators of the diagonal type as observables. Each operator of such a type is reduced to two operators on the Hilbert spaces wich sign-defined norm respectively. The operator of a such type obviously has a spectrum which is a unification of its spectra on H^+, H^-, and obviously it is the same system of eigen states. It is necessary to note that canonical Krein symmetry J on H has the following properties: $J_{H^+} = 1$, $J_{H^-} = -1$ [Ref.9], commutates with algebra $A_0[H]$ and anticommutates with space $A_1[H]$. Consequently, if H is the quantum state space of some physical system then canonical Krein symmetry J commutates with arbitrary observable and vice versa : the observable in H is described by the operators , which commutes with the canonical Krein symmetry J . Therefore, we have the following

Statement : let we have physical system with Lagrangian L generating space of states with indefinite metric $H = H^+ \oplus H^-$ in the secondary-quantized theory. And theory has a discrete symmetry D which induced canonical Krein operator J on H.

Then D is defined the superselection rule for the given theory.

2.3 Cluster property.

Let us consider the problem on cluster property in the considered theory. The property of cluster decomposition may be formulated, for example, in the following way:

$$\langle vac \mid C(x)B(y) \mid vac\rangle \underset{x-y\longrightarrow\infty}{\longrightarrow} \langle vac \mid C(x) \mid vac\rangle\langle vac \mid B(y) \mid vac\rangle \tag{2.3}$$

where $C(x)$, $B(y)$ are two local operators. Equation (2.3) is valid for the operators $A_0[H]$, at least, for the H^+ sector. In particular it is true when $(C(x)$, $B(y)) \in A_0[H^+]$ is the cluster property, it is equal to vacuum unique existence

according to proposition 7.1 of Ref.12. Taking into account the above mentioned it is evident that if the $C(x), B(y)$ arethe operators belong to $A(H)$, then (2.3) will not be fulfilled as it is generally impossible "to divide"the $A(x)B(y)$ product into two operators. If they belong to $A_1(H)$ (e.g.), then the left part of (2.3) can and can not be equal to zero, at the same time the right part, in this case,is always equal to zero. It means in the discussed theory that it is impossible to select a partical state with the opposite (here negative) sign of the norm from the multipartical state. Actually it can be treated in this theory as the presence of the property of confinement. Note also that while considering the cluster property we imply imlicitly or explicitly that the state space is Hilbert space with a sign-defined metric but it is not pseudo-Hilbert space as otherwise a zero norm may appear in the intermediate states . But of course, it is realised, if in the space with indefinite metric the cluster property may be implied in the projection on the superselected sectors.Naturally the above mentioned is not final conclusion and a further analysis is neccessary as the given problem appears in any theory of supergravitation in which a scalar sector is described as a non-compact sigma model.

3 Yang-Mills quantum fields with non-compact semi-simple group.

3.1 D-symmetry of the Quantum Lagrangian

The effective quantum Lagrangian of the Yang-Mills field with non-compact semi-simple group $\hat{G}$ has the form

$$L^{\hat{G}}_{Q} = \eta_{AB}\,(\tfrac{1}{4}F^{A}_{\mu\nu}F^{\mu\nu,B} + i\partial^{\mu}c^{A}(D_{\mu}\bar{c})^{B} + \partial_{\mu}B^{A}A^{B}_{\mu} - \tfrac{\alpha_0}{2}B^{A}B^{B}) \qquad (3.1)$$

where $c^A, \bar{c}^B$ are ghost (antighost) fields respectively, the multiplet of Nakanishi-Lautrup fields B^A appears as in Ref.13 and two last terms in (3.1) fix gauge; the Killing metric η_{AB} of the group $\hat{G}$ is negative on some maximal compact subalgebra $g \subset \hat{g}$ and positively defined on the orthogonal complement $\hat{g}^{\perp}$ to g : $\hat{g} = g + g^{\perp}$,where $\hat{g}$ is algebra Lie of $\hat{G}$ and g is on some maximal compact subgroup $G \subset \hat{G}$.

The Cartan involution D on $\hat{g}$,retaining g and being a reflection on $g^{\perp}$ may be extended to the fields $c^A, \bar{c}^B, B^M, A^N_{\mu}$

$$D(\tau^A) = -\eta_{AB}\tau^B \qquad (3.2)$$

where τ is any of the above mentioned fields.

Taking into account the commutatition relations on $\hat{g}$

$$[g,g] \subseteq g,\ [g,g^{\perp}] \subseteq g^{\perp},\ [g^{\perp},g^{\perp}] \subseteq g \qquad (3.3)$$

one can see that D acts self-consistenly on $F_{\mu\nu}$

$$D(F^A_{\mu\nu}) = -\eta_{AD}F^B_{\mu\nu} \qquad (3.4)$$

and hence retains $L^{\hat{G}}_{Q}$. Thus, D is the discrete symmetry of Lagrangian [11,14]. As is known such Lagrangian has BRST symmetry[5], its transformations have the form

$$\delta A^A_{\mu}(x) = \lambda(D_{\mu}c(x))^A \qquad (3.5A)$$

$$\delta c^A(x) = -\tfrac{\lambda}{2}f^A_{\overline{B}\overline{C}}c^{\overline{B}}(x)c^{\overline{C}}(x) \qquad (3.5B)$$

$$\delta\bar{c}^A(x) = i\lambda B^A(x) \qquad (3.5C)$$

$$\delta B^A(x) = 0 \qquad (3.5D)$$

here $f^A_{\overline{B}\overline{C}}$ are structural constant $\hat{g}$, λ is the Grassmanian parameter.Obviously the operator D commutes with BRST charge Q_B :

$$[D, Q_B] = 0 \qquad (3.6)$$

Actually the formula (3.6) is a direct consequence of (3.5).

3.2 Quantization. Superselection rule.

The realization of the quantization procedure on the basis (3.1) differs from the compact case only by the use of the additional sign-indefinite multiplier η_{AB} .In particular,the total space of the asymptotic states V has the additional indefiniteness which is connected to η_{AB}. If $H \subset V$ is a subspace, generated by the transverse modes of the gauge fields, then H has nondegenerated indefinite metric and H is a direct sum of H^+ and H^-

$$H = H^+ \oplus H^- \qquad (3.7)$$

where $H^+$is generated by the arbitrary number of operators of the asymptotic fields $a_{\lambda}(k)(a_{\lambda'}(k'))$ with $\eta_{BB} = -1$ and their even numbers with $\eta_{BB} = 1$; the definition of H^- is characterized by the same assumption but one can consider also the odd numbers of operators with $\eta_{BB} = 1$. Here $\lambda', \lambda = 1, 2$ characterizes the polarization value and operator commutators have the form

$$[a^B_{\lambda}(k), a^{B'+}_{\lambda'}(k')] = -\eta^{BB'}\delta_{\lambda\lambda'}\,\delta_{kk'} \qquad (3.8)$$

Defining V_{phys} by the standard way:

$V_{phys} = \{|\, v >\in V : Q_B \,|\, v >= 0 \ \ or \ \ KerQ\ \}$ (3.9)

we obtain that D retains V_{phys},according to (3.6), it also retains H by the definition of D and $H \subset V_{phys}$ so that Q_B has the form

$$Q_B = i\eta_{AB}\int d^3k(b^{A+}(k)c^B(k) - c^{A+}(k)b^B(k)) \qquad (3.10)$$

In (3.10) $b^{A+}(k)(b^B(k))$ and $c^{A+}(k)(c^B(k))$ are operators of the creation and annihilation fields B,c respectively. One can state that $V_{phys} = H \oplus V^0$, where V^0 is the degenerated state subspace V_{phys}. It is clear that V^0 retains D and cannot be mixed with states H, lying on the zero cone $\Lambda^0 = \{|\, w\rangle \in H : \langle w \mid w\rangle = 0\}$ by virtue of nondegeneration of the latter. That is why S-matrix

following from (3.1) retains V^0 , commutates with D and therefore we can define S_{phys} as

$$S_{phys} = P^+SP \qquad (3.11)$$

where $P = P_H$ is a projector. As $D_{H^+} = 1$, $D_{H^-} = -1$, $[D, S_{phys}] = 0$

Immediately we obtain that

$$S_{phys}(H^+) = H^+, \quad S_{phys}(H^-) = H^- \qquad (3.12A)$$

$$S_{phys}S^+_{phys} = S^+_{phys}S_{phys} = (1_{H^+}, 1_{H^-}) \qquad (3.12B)$$

(3.12B) follows from (3.12A) and (pseudo)unitarity S on V, V_{phys}.

Thus the quantum gauge theory,which is based on (3.1), is physically acceptable and D is an operator defining the superselection rule in this theory, according to last statement of the section 2. All S-matrix elements and their corresponding amplitudes of the transition probability don't depend on the selection of the decomposition of $\hat{g}$into g and $g^\perp$,as η_{AB} is $\hat{G}$-invariant:

$$P_{\varsigma f,\varsigma\tau} = \frac{|<\varsigma f|s|\varsigma\tau>|^2}{||\varsigma f||||\varsigma\tau||} = \frac{|<f|s|\tau>|^2}{||f||||\tau||} = P_{f,\tau}, \text{ for } \quad \forall\varsigma \in \hat{G} \qquad (3.13)$$

It follows from (3.13) that in the theory there is no negative probability: $P_{f,\tau} = 0$, if $| f >\in H^+$,$| \tau >\in H^-$. Note that unlike Refs.13,15 H is not the space with positively defined norm. In particular in Ref. 15, only such field components of A_μ are considered to be physical (condition 6) which commutate with Q_B and have a positive norm. However,in the present case the fulfilment of the last statement of this condition is not required,as in the theory there is the superselection rule,defined by the operator of the discrete symmetry.

All considerations,mentioned above,are true if V_{phys} is"narrowed" by the additional condition $Q_c \mid v >= 0$,where Q_c is a charge of the ghost transformations[13].

Actually as $[D, Q_c] = 0$ the whole quantization sheme does not change except only the "decrease" V_0 at the expense of the superselection by the zero quantum number of the ghosts. As BRST-transformations are multiplicatively renormalized , $[D, Q^{ren}_B] = 0$,where $Q^{ren}_B = (\widetilde{Z}_3/Z_B)^{1/2}Q_B$ is a renormalized BRST- charge, $\widetilde{Z}_3$ and Z_B are constants of the field renormalization c and B respectively[14].That's why the described scheme of the quantization is invariant to the renormalization procedure.The constructed S-matrix is gauge-invariant i.e. it doesn't depend on the selection of gauge: in (1) we used

D -invariant gauge explicitely. But if the theory is constructed with the fixed gauge term, which isn't retained by D,then using the results[16] we come to the same S_{Pphys} . The corresponding quantization scheme is readily extended to the Lagrangian describing interactions of the gauge fields with matters fields of the spinor or scalar type.We note only that correspondent representation ρ of the group $\hat{G}$ under contraction on the maximal compact subgroup necessarily must be reducible

$$\rho_G = \rho_1 \oplus \rho_2$$

3.3 Involution and Z_2 -graduation.

Let us note that the theory with the non-compact gauge group generates Z_2-graduation. Actually in $\hat{g}$ it is fixed by the selection $g = g_0$, $g^\perp = g_1$ and commutative relations (3.3). In H we have $H^+ = H_0$, $H^- = H_1$ and a product, being a tensor product of the different states. In operator algebra $A(H)$, $A_0(H) = \{\alpha \mid \alpha(H^\pm) \subseteq H^\pm\}$, $A_1(H) = \{\beta \mid \beta(H^\pm) \subseteq H^\mp\}$ and product is the Lie bracket (section 2). D is the involution in each of these spaces. D is transformed as $D \longmapsto D^\gamma$ under the action of the group $\hat{G}$,as $g \longmapsto g^\gamma$, $g^\perp \longmapsto g^{\perp\gamma}$, $H \longmapsto H^\gamma$, $A(H) \longmapsto A(H)^\gamma$ for any element $\gamma \in \hat{G}$ so all physical expressions remain invariant, in particular (3.3).

Note that in the discussed case the cohomologies $H(Q_B) = KerQ_B/ImQ_B$ are different from the compact Yang-Mills case[13] and the relativistic string[6], furthemore some are free of states with the negative norm,generated by the Lorentz metric $g_{\mu\nu}$. Actually as in our case $Q^2_B = 0$, $Q^+_B = Q_B$, that $ImQ = V^0$, $H(Q_B) = H$ -is the space with nondegenerated indefinite metric,generated only by η_{AB}.

3.4 Chiral anomalies

L.AIvares-Gaume and E.Witten showed [17]that non-abelian gauge theories can give chiral anomalies only in the complex representations, therefore if $\hat{G}$ is non-compact then in accordance with the statement proved above all D-symmetric representations automatically haven't anomalies or $\hat{G}$-invarianting and D-symmetric Lagrangian haven't chiral anomalies. Thus the condition of the existence of D-symmetry for the non-compact theories is a sufficient condition for anomalies absence. However, this condition is not necessary for anomalies absence. In general we recall that condition of the anomalies absence is:

$$\sum_{T_L} STr(T^{a_1}_L ... T^{a_{n+1}}_L) - \sum_{T_R} STr(T^{a_1}_R ... T^{a_{n+1}}_R) = 0,$$

where T_L, T_R stands for the representations of $\hat{G}$ left (right-) handed fermions and STr means the symmetrized trace over group generators involved, 2n is the dimension of the space-time [18]. It is known that the whole thing comes down to computation of $tr_{(r)}F^{\tilde{n}}$ for the arbitrary generator F of Lie algebra $\hat{G}$ in the representation r : if $tr_{(r)}F^{\tilde{n}} = 0$ then representation r is free-anomalies.

For the odd $\tilde{n}$ there is a correct analysis, which comes to this situation to the compactification of $\hat{G}$. Namely let $\widetilde{G}$ be the "compactification" of $\hat{G}$ in the representation r i.e. generators of $\hat{G}$ are divided into two parts $\{K, S\}$, where K are Hermitian (compact) and S are skew-Hermitian. Then the map $\{K, S\} \longrightarrow \{K, iS\}$ is a compactification of $\hat{G}$, because it reflects non-compact Lie algebra $\hat{g}$ of $\hat{G}$ into compact Lie algebra $\tilde{g}$ of the compact group $\widetilde{G}$. Let $\tilde{r}$ be the corresponding r of representation of $\tilde{g}$. Then if $\tilde{r}$ is real or pseudoreal and $dim\tilde{r} = 2k+1$, then $\tilde{r}$ is anomaly-free, because $tr_{(\tilde{r})}\widetilde{F}^{2k+1} = 0$ for any generator $\widetilde{F}$ of $\tilde{g}$, but then, $tr_{(r)}F^{2k+1} = 0$ for any $F \in \hat{g}$ and r is anomaly-free too. In particular, for non-compact simple groups we can easily identify which groups and which representations are automatically safe in $4k$ dimensions, reducing

this question to a compact case. We have the following safe groups:

1) $SO(p,q)(p+q=2k+1)$

2) $SO(p,q)(p+q=4k)$

3) $Sp(p,q)(for\ all\ p,q)$

4) non-compact forms of exeptional groups G_2, F_4, E_7, E_8.

For the groups of $SU(p,q)$ types additional computations are necessary.

4 Quantum non-compact sigma models.

4.1 Introduction

The non-compact σ models, investigated by many authors [1,19], describe a scalar sector of supergravitation [20], and in particularly $N = 8$ supergravitation, a candidate for the unification of all interactions [21]. Besides within the scope of the σ model (compact or not), the dynamic creation of the composite gauge boson [22], appearing during the procedure of compactification in the theory of superstrings[4,6], is described.

At the same time the quantum description of the non-compact σ models contain such problems as the construction of the unitary S-matrix, the treatment of the spontaneous symmetry breakdown, etc. In ref.8 it was shown that the non-compact σ model can be correctly quantized only in the case of a state space with indefinite metric. The quantization in the sign-defined Fock space[23] leads to contributions breaking the unitarity of the multiloop amplitudes. In ref.24 the non-compact two-dimensional σ model was quantized in the positively defined state space, containing an even number of states with negative norm. However, one has also analogous problems in this case.

In the present section we will show that a superselection rule is present in the non-compact σ model . It has an algebraic origin and it is generated by the Cartan involution of a Lee algebra $\hat{g}$ of the non-compact group $\hat{G}$. We consider also the spontaneous breakdown of a non-compact symmetry[11,25].

4.2 Superselection rule.

Let us consider the case $\hat{G} = O(N,1)$ without loss of generality. The general case and in particular $\hat{G} = SU(N,I)$ (CP^{N+1}model) does not differ substantially from it. It is known that hamiltonian of the non-compact $O(N,1)$ σ model has the form

$$h = \tfrac{1}{2}[(\partial_o \Pi)^2 + (\partial_i \Pi)^2 - (\partial_o \sigma)^2 - (\partial_i \sigma)^2 + \lambda(\Pi^2 - \sigma^2 + \tfrac{1}{2} f_0] \qquad (4.1)$$

where $\Pi = (\Pi_1, ..., \Pi_N)$ is a field multiplet. (Π, σ) is transformed by the fundamental representation of the group $O(N,1)$,

$$(\partial_o \Pi)^2 = \sum_{n=1}^{N} (\partial_0 \Pi_n)^2, \quad \Pi^2 = \sum_{n=1}^{N} \Pi_n^2$$

f_0 is the coupling constant of the model, λ is the lagrangian multiplier. The presence of the negative square of the field σ in (4.1) leads to the state space with indefinite metric

$$H = H^+ \oplus H^- \qquad (4.2)$$

where H^+, H^- are Hilbert subspaces, containing an even and an odd number of the creation operators of the field σ, respectively, and an arbitrary number of all other fields. The states are generated by the positively defined vacuum $|\,0)$. The representation

(Π, σ) is decomposed on the restriction $\hat{G}$ to the maximal compact subgroup $G = O(N)$ into the sum of two irreducible representations $\{\Pi\}$ and $\{\sigma\}$. Let us consider the Cartan involution of the Lee algebra $\hat{g} = O(N,1)$. In the matrix form this involution is defined by the matrix

$$D = \begin{pmatrix} 1_N & 0 \\ 0 & -1 \end{pmatrix} \qquad (4.3)$$

The generators Q^A of the Lee algebra $\hat{g}$ obey the following transformation law:

$$D(Q^A) = -\eta_{AB} Q^B \qquad (4.4)$$

where η_{AB} is the Killing (sign-variable) metric. The η_{AB} is negative on the maximal compact subalgebra $g \subset \hat{g}$ and positively defined on the orthogonal complement $g^{\perp}$to $g : \hat{g} = g \oplus g^{\perp}$. The Cartan involution D on $\hat{g}$ may be extended to the fields (Π, σ). In the representations (Π, σ) we have

$$D : \begin{pmatrix} \Pi \\ \sigma \end{pmatrix} \longmapsto \begin{pmatrix} \Pi \\ -\sigma \end{pmatrix} \qquad (4.5)$$

The considerations are the following. In the quantum field theory the generators of the discussed non-compact group are constructed from (Π, σ) fields. This conclusion is a direct consequence of the Noether theorem. The transformation laws (4.4), (4.5) are in accordance with this construction. Let us note that it is possible, or course, to postulate

(4.5) and then to connect it with the Cartan involution of the generators. Note that the analogous D-action is induced in the Z_2-graduation operator algebra $A(H) = A_0(H) \oplus A_1(H)$, how in the Yang-Mills non-compact case (subsection 3.3)

$$D(v) = (-1)^i v_i, \qquad (4.6)$$

where $v \in A(H)$, and v_i are graduated components of the v. The unique choice of transformation law (4.5) can be guaranteed by the above mentioned algebraic considerations [eq. (4.6)]. The hamiltonian h and the S-matrix are invariant under the action of D. Obviously, D generates the canonical Krein operator J in H and therefore it is superselection rule in the theory according of the results of the section 2. Such one can choose observables only from $A_0(H)$, which is also D-invariant. The calculations performed in Refs. 22,24 give us the independent proof of this statement. In Ref.24, the S-matrix unitarity in H^+ was proved in the two-dimensional case within the scope of the $1/N$ decomposition. It is similarly proved also for H^-. Let us note that it is not necessary to project H onto the positive norm (physical) subsector H^+.

The full Krein space $H = H^+ \oplus H^-$ one can consider as a physical space. This conclusion is based on the fact that the transitions between subsectors

H^+ and $H^-$are forbidden by the above stated superselection rule. That is why negative probabilities are absent in the theory. The presence in the theory of the two sectors H^+, H^- can be interpreted as the existence of states in the theory with multiplicative quantum number with values $\pm$ 1.

4.3 Spontaneous non-compact symmetry breakdown

The mechanism of spontaneous symmetry break-down has some peculiar features in the theory under discussion. They are the following:

(I) The state space is the space H with indefinite metric. The vacuum state $\mid 0 >$ in the subsector H^+.

(2) The generators of the compact part $Q^A \in O(N)$ do not mix the sectors H^+ and H^- i.e. belong to $A_0(H)$, and the generators of the non-compact part $Q^B \in g^\perp$ mix $H^+$and H^-, i.e. belong to $A_1(H)$.

The Goldstone theorem has therefore the following form:

(a) If the non-compact symmetry is spontaneously broken only by the generators of the compact part $[Q^A \mid 0 > \neq 0, Q^A \in O(N)\ ]$, the Goldstone particles appear only in H^+.

(b) If the non-compact symmetry is spontaneously broken only by the generators of the non-compact part $[Q^B \mid 0 > \neq 0, Q^B \in g^\perp]$ the Goldstone particles appear only in H^-.

(c) In the case of non-compact symmetry breakdown by g and $g^\perp$ simultaneously, the Goldstone particles appear with both norm signs.

It is necessary to note that case (a) actually is not realized, as its realization contradicts the commutative relations in the Lee algebra $\hat{g} : [g^\perp, g^\perp] \subset g$.

Two stationary pointswere obtained in Ref.8 within the scope of the I/N decomposition for (4.I),

$$\frac{\sigma^2}{N+1} = \mu^{d-2}\left(\frac{1}{2f} - \frac{1}{2f_c}\right), \quad \Pi = \lambda = 0 \tag{4.7A}$$

$$\sigma = \Pi = 0, \ \frac{\lambda}{\mu^2} = \left(1 - \frac{f_c}{f}\right)^{2/d} \tag{4.7B}$$

at $I/f > I/f_c$, and one stationary point,

$$\frac{\Pi^2}{N+1} = -\mu^{d-2}\left(\frac{1}{2f} - \frac{1}{2f_c}\right) \tag{4.7C}$$

Here μ is the renormalization point, f is the renormalized coupling constant, f_c is the critical coupling constant, d is the space-time dimension. It is supposed that the symmetry breakdown occurs in such a way that $< 0 \mid \sigma^2 \mid 0 > > 0$. But the hermitian operator $\sigma \in A_1(H)$ has a spectrum in $iR \cup \{0\}$. That is why it is reasonable to consider the case $< 0 \mid \sigma^2 \mid 0 > < 0$. But if, in the case of symmetry breakdown, the averages of the operators remain the continuous functions in the topology of the "initial" space H, then $< 0 \mid \sigma^2 \mid 0 >$ cannot be more than 0. Then the points (4.7A), (4.7C) correspond to the case $1/f < l/f_c$ i.e., spontaneous symmetry breakdown, and in the case (4.7A) the symmetry is broken up to the maximal compact subgroup $0(N)$ [case (b) of the Goldstone theorem], but up to the non-compact group $O(N-1,1)$ in the case (4.7C)[8]. It

is necessary to note that then in the case (4.7A) the Green function will not have the tachyonic poles in the euclidean momentum,

$$\det G^{-1} = \frac{N+1}{8} p^2 \int \frac{d^d}{(2\pi)^d} \frac{1}{k^2(k-p)^2} - \frac{1}{4}\sigma_0^2 \tag{4.8}$$

because $\sigma_0^2 < 0$ [σ_0 is the non-zero vacuum expectation σ].

4.4 Chiral anomalies in non-compact sigma models.

One of the most important problems in quantum exposition of sigmas - models is also examination of anomalies and, in particular, chiral of anomalies. In a compact case this problem is well enough investigated [10,11]. In the present operation the necessary requirements of absent anomalies in noncompact sigmas - models are obtained which in a series of cases are sufficient and, essentially, are based on the fact presence of superselection rule.

In G/H-sigma-model. the is supposed, that H and G - Lie group, H is subgroup$G$. In a reference case it is meant[12], that both they semi-simple and are compact. In our

case the first requirement (semisimplicity) is maintained, to the second requirement (compactness) will be already to satisfy only group H, the group G is supposed semisimple and noncompact. Moreover, we shall suppose, that $H \subset G$ is maximum compact subgroup G, as all examples[5-7], originating in a high-energy physics, are reduced to this case.

Then, as is known[11,12], G/H - symmetrical space, i.e. $T = (H, X)$ - the set of generators G is divided into a skew-Hermitian part $\{H_i\}$ laying in H, and Hermite,$\{X_a\}$ belonging to some noncompact addition, concerning the metric of the Killing : $[H_i, H_j] = f_{ij}^k\ H_k$, $[H_i, X_a] = f_{ia}^b\ X_b$, $[X_a, X_b] = f_{ab}^i\ H_i$

The systematic application such G/H of spaces (with compact G) to low-energetical physics and algebra of currents was advanced in papers of Callan,Coulmen, Wess and Zumino[13]. Let's mark also, that it is models with the spontaneously broken symmetry, where H is subgroup, which preserves ground state, i.e.goldstouns correspond to generators $\{X_a\}$. The anomalies in sigmas - models occur at exposition of interaction of gauge fields with chiral fermions. The fermion fields of matter are transormated on some representation ρ of group H, which, generally speaking, can be both nonreducible, and reduced. The relevant Lagrangian L_m looks like:

$$L_m = \bar{\psi} i\gamma_\mu(\partial_\mu + \omega_\mu)\, p_+\, \psi \tag{1},$$

where $\partial_\mu = \frac{\partial}{\partial x_\mu}$, γ_μ are matrixes of the Dirac, $p_+ = \frac{(1+\gamma_5)}{2}$

ψ is correspondent fermion multiplet, ω_μ is the canonical connectedness correspondent H.

Thus, as a gauge field the H-canonical connectedness appears in case of sigma - model. Therefore examination of anomalies in this case in many respects identically to study of a similar problem in the gauge theories. In particular, all is reduced to an evaluation of a functional integral

$$e^{-\Gamma_{eff}[\omega]} = \int\limits_{\psi,\bar{\psi}} e^{-\int d^{2n}x L_m} d\psi d\bar{\psi}$$

at transformation of a fermion effective action $\Gamma_{eff}[\omega]$ concerning global G-isometries:

$$l(\varphi) \longrightarrow g\, l(\varphi)\, h^{-1}(\varphi, g),\ \omega \longrightarrow h(\omega + d)\, h^{-1},\ f \longrightarrow hf \qquad (2)$$

where $l(\varphi)$ is the local section of a principal H - bundle, $g \in G$, $h^{-1}(\varphi, g)$ is compensating H-transformation. As the canonical connectedness ω_μ is transformated as a H-gauge field relativity an action of G, the modification of an effective operation concerning infinitesimal G-transformations is given by the known formula for gauge anomalies .

The build-up of a correct quantum theory for nonlinear sigma - model, which at a Lagrangian has terms of interaction with chiral fermions is reduced, essentially to a solution of two basic problems:

1) What groups H do not give anomalies?

2) If the anomalies are present, in what cases are possible contrterms, cutting them?

As in a case, considered in section, the group H - compact, then the answer to a problem 1) does not depend on a type of model (it is compact whether or not), i.e. list of anomalous - safe groups H for these two types same. In particular, on a role H the groups suit: $SO(N), N \neq 6; SU(2); Sp(2N), N \neq 3$ etc., the situation is completely identical with a usual compact case. But for a problem 2) there are distinctions. It is known , that the anomalies, if they are available, are possible to reduce by adding contrterm, depending from coordinates on G/H, and for this purpose such is necessary to have representation $\hat{\rho}$ groups G, that $\hat{\rho}/H = \rho$. This representation $\hat{\rho}$ in a noncompact case impose on ρ essential restriction: the representation ρ of group H should be reduced.

Really, as $\hat{\rho}$ is finite-dimensional and, therefore is nonunitary representation of noncompact group G, correspondent contrterm generates in quantum description the indefinite metric. And that the unitarity of the theory was not broken, the restriction $\hat{\rho}/H = \rho$ should consist at least of two representations generating states both with positive, and with negative signs of norms, which the superselection operator D, entered in[8,9], separates from each other.

Besides the performance ρ of group H should not be complex[11] (and it already for all types of models), for in this case it fails to regularizate the correspondent functional integral.

In outcome we come to the following deduction:

That noncompact G/H - the sigma - model, where H - the maximum compact subgroup of group G, had no of chiral anomalies, is necessary, that the relevant representation of a group H in space of fermions was reducible, real and rising up to group G, or the group H was from the very beginning ... . Thus, basic difference from a general case is reducibility of correspondent chiral represantation.

From here also follows, that the fundamental representations of complex semisimple groups are unsuitable, as remain nonreducible at restriction on the material shape (therefore, on a maximum compact subgroup). And on the contrary, well known examples non-anomalies of noncompact sigmas - models $SO(p,q)/SO(p) \times SO(q)$,

$SU(p,q)/SU(p) \times SU(q) \times U(1)$ are confirmation of outcome of operation, as the performances of maximum compact subgroups $SO(p) \times SO(q)$ and $SU(p) \times SU(q) \times U(1)$ accordingly completely satisfy to all enumerated requirements. Thus, in case of noncompact G/H-sigma-model of pseudoorthogonal and pseudounitary types the obtained criterion of absent chiral anomalies is sufficient.

REFERENCES.

1. Y.Cohen and E.Rabinovici, Phys.Lett. B124 (1983) 371; A.C.Davis, A.J.Mactorlane and J.W.van Holten, ibid B125 (1983) 151.
2. L.Smolin, Phys.Rev. D30 (1984) 2159.
3. J.Dell, J.L.deLyra and L.Smolin, Phys.Rev. D34 (1986) 3012.
4. M.B.Green and J.H.Schwarz, Phys.Rep. 89 (1982) 224.
5. C. Becchi, A. Rouet and R.Stora, Ann. Phys. 98(1976) 273; I.V.Tyutin, FIAN preprint N.39 (1975).
6. M.B.Green, J.H.Schwarz and E.Witten, Superstring theory
7. M.D.Xsu and G.P.Xin, Phys.Rev. D24 (1981) 471.
8. O. Morozumi and S. Nojiri, Prog. Theor. Phys. 75 (1986) 677.
9. T.Ya.Azizov and I.S.Iohvidov, Foundation of the linear operator theory in the space with indefinite metric (Moscow,Nauka,1986), p.352.
10. A.E. Margolin and V.I.Strazhev, Izv. AN BSSR 3 (1989) 79 (in Russian).
11. A.E.Margolin, Ph. D. Thesis, Minsk 1989 (in Russian).
12. N.N.Bogoliubov et al General principles of the quantum field theory (Moscow "Nauka" 1987).
13. T.Kugo and I. Ojima, Suppl. Prog. Theor. Phys. 66, (1979) 1.
14. A.E.Margolin and V.I.Strazhev, Mod.Phys.Lett. A7 (1992) 2747.
15. A.A.Slavnov, Phys.Lett. 217B (1989) 91.
16. L.Baulieu, Phys.Rep. 129 (1985) 1;J.C.Collins Renormalization. An introduction to renormalization, the renormalization group,and the operator-product expansion (Cambridge University Press, 1984).
17. L.AIvarez-Gaume and E.Witten, Nucl.Phys. B234 (1984) 269.
18. L.AIvarez-Gaume, in Fundamental problems gauge fields theory, Roc.6 course int. sch. erice, Jule 1-14,1985 (N.Y.,London 1986).
19. D.J. Amit and A.C. Davis, Nucl. Phys. B225 (1983) 221.
20. E.Cremer and B.Julia, Nucl.Phys. B159 (1979) 141.
21. E.Cremer and B.Julia, ibid B229 [FS9](1983) 221.
22. M. Gomes and Y.K. Ha, Phys. Rev. Lett. 58 (1987) 2390.
23. G.W. van Holten, J. Math. Phys. 28 (1987) 1420.
24. S.A.Brunini, M.Gomes and A.J.de Silva, Phys.Rev. D38 (1988) 706.
25. A.E. Margolin and V.I.Strazhev, Phys. Lett. 249B (1990) 438.

NEW CRITERION OF THE INSTANTONS IDENTIFICATION IN DEEP INELASTIC SCATTERING

V.Kuvshinov[1] and R.Shulyakovsky[2]
Institute of Physics
National Academy of Sciences of Belarus
Scarina av.,68, Minsk 220072
BELARUS

Factorial, cumulant and H_q-moments in dependence on their rank q for the *instanton-induced* deep inelastic scattering (DIS) in the frameworks of QCD are calculated and analysed. The obtained correlation moments behaviour has specific form, which can be considered as a new criterion of the QCD-instantons identification on experiment at HERA.

1 Introduction

As it is known, such gauge theories as SM of electroweak interactions and QCD have degenerated vacuum structure on the *classical* level [1]: potential energy is periodic with respect to the Chern-Simons number

$$N_{cs} = \frac{g^2}{16\pi^2}\int d^3x\varepsilon_{ijk}\Big(A_i^a\partial_j A_k^a + \frac{g}{3}\varepsilon^{abc}A_i^aA_j^bA_k^c\Big). \qquad (1)$$

Minimal energy (classical vacua) corresponds to integer N_{cs}. Neighbouring vacua are separated by a potential barrier of height E_{sp} (Fig.1).

[1]kuvshino@dragon.bas-net.by
[2]shul@dragon.bas-net.by

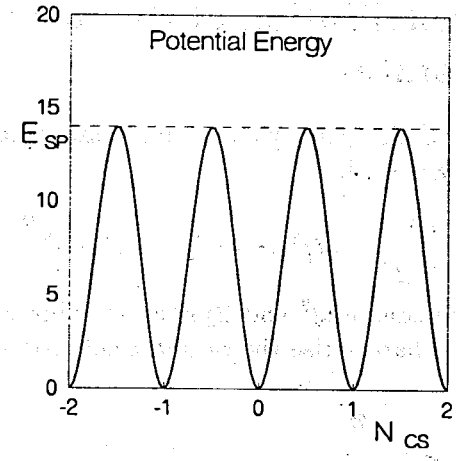

Fig.1. Schematic dependence of potential energy of gauge fields on Chern-Simons number N_{cs}. Gauge condition $A_0 = 0$ is used. E_{sp} is so-called sphaleron mass.

Usual perturbative theory (Feynman rules) describes phenomena with $N_{cs} = 0$ only. *Quantum* tunnelling transitions between neighbouring vacua can be described by means of *instantons*, which are classical solutions of the Euclidean field equations with finite action [2]. Taking into account such tunnelling transitions leads to the baryon number violation in SM [3], which is connected with the problem of matter and antimatter asymmetry in the Universe [4]. In QCD instantons lead to the chirality violation, allow to solve U(1)-problem [3], give contribution to the confinement [5]. Therefore, the experimental discovery of instantons would be of fundamental significance for particle physics.

It was suggested probability of the instanton transitions can increase in high energy collisions [6]. There is a possibility of the instanton-induced events identification in the electron-proton DIS at HERA (DESY) [7]. Instanton induced DIS final states can be distinguished from ordinary (perturbative) ones through some features:
- *high multiplicity* (the average number of partons ~ 10 [7]);
- *isotropic* distribution of partons in the instanton rest system and presence, practically, of *all* light quarks (u, d, s) in each events [3];
- specific behaviour of gluon structure functions [8] and gluon correlation characteristics [9].

In our report additional "footprints" of QCD-instantons (factorial, cumulant and H_q-moments) are studied.

2 Multiplicity distribution of the instanton-induced final states

In DIS instantons can appear in the quark-gluon subprocesses (Fig.2). The following usual designations are used:

$$Q^2 = -q^2, \qquad x = \frac{Q^2}{2Pq}, \qquad Q'^2 = -q'^2, \qquad x' = \frac{Q'^2}{2pq'}, \tag{2}$$

where transferred momentum square Q^2 and Bjorken variable x describe total DIS process; Q'^2 and x' characterise the *insanton* subprocess.

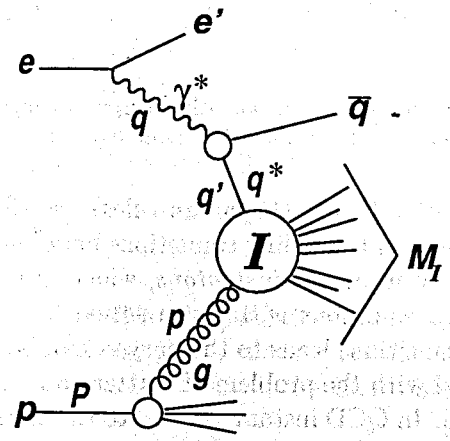

Fig.2. Instanton induced DIS (figure was taken from [10]).

As it was mentioned above high parton multiplicity is one of the main characteristics of the instanton-induced events. The distribution on numbers of gluons in the instanton-induced events is given by the expression:

$$P_n^{(g)} = \frac{1}{\sigma_{tot}} \frac{1}{n!} \int d^4k_1 ... d^4k_n \left| T(k_1, ..., k_n) \right|^2, \tag{3}$$

where σ_{tot} – total cross-section, $T(k_1, ..., k_n)$ is the amplitude of the production of gluons with the energy-momentum 4-vectors $k_1, ..., k_n$. It is calculated by means of LSZ-technique applying to the Euclidean n-points Green function, which is given by the following Feynman path integral (in the quasiclassical approximation):

$$\int DA e^{-S^e[A]} A^{I\ a_1}_{\mu_1}(x_1) ... A^{I\ a_n}_{\mu_n}(x_n). \tag{4}$$

where $S^e[A]$ is QCD Euclidean action, $A^{I\ a}_{\mu}(x)$ – instanton configuration [2]. In quasiclassical approximation Gauss integral (4) is known calculable expression. The integration is carried out on the gluon fields, which connect neighbour classical vacua. Factorisation in (4) leads to the Poisson distribution on the final gluon number [8, 9]:

$$P_n^{(g)} = e^{-<n_g>} \frac{< n_g >^n}{n!}, \quad < n_g >= \frac{16\pi^2}{g^2} \left(\frac{1 - x'}{x'} \right)^2, \quad 0.5 < x' < 1. \tag{5}$$

The quarks production in the instanton processes is described by the well-known fixed multiplicity distribution (if we take into account zero modes only [3]):

$$P_n^{(q)} = \delta_{2n_f, n}, \tag{6}$$

where n_f is a number of massless quark flavours. We suggest that masses of u, d, s are equal to zero.

Thus, if we take into account both gluons and quarks, then the following distribution is obtained:

$$P_n = e^{-<n_g>} \frac{< n_g >^{n-2n_f}}{(n - 2n_f)!} \Theta(n - 2n_f). \tag{7}$$

3 Calculation of the correlation moments for the instanton DIS processes

Study of the correlation moments is more useful sometimes than study of the multiplicity distribution [11]. Let us remind the well-known definition of the normalised factorial moments:

$$F_q = \frac{1}{< n >^q} \left. \frac{d^q Q(z)}{dz^q} \right|_{z=1}, \qquad Q(z) = \sum_{n=1}^{\infty} P_n z^n, \qquad 0 \le z \le 1. \tag{8}$$

where $< n >$ is the average multiplicity, $Q(z)$ – generating function.

In the case of the instanton-induced multiparticle production processes $Q(z)$ and $< n >$ have the following forms:

$$Q(z) = \sum_{n=2n_f}^{\infty} e^{-<n_g>} \frac{< n_g >^{n-2n_f} z^n}{(n-2n_f)!} = z^{2n_f} e^{<n_g>[z-1]}, \quad < n >=< n_g > +2n_f. \tag{9}$$

The corresponding normalised factorial moments dependence on q is shown on the Fig.3. It is well-known, that normalised factorial moments for ordinary perturbative processes of the particle production increase with increasing q. Therefore the behaviour of the moments for the instanton-induced processes can be used as a new instanton identification criterion.

Also we can consider the normalised cumulant moments:

$$K_q = \frac{1}{< n >^q} \frac{d^q ln Q(z)}{dz^q}\bigg|_{z=1}. \tag{10}$$

It is not difficult to calculate K_q for the instanton distribution (10):

$$K_q = \frac{2n_f(-1)^{q-1}q! + < n_g > \delta_{q1}}{(< n_g > +2n_f)^q}. \tag{11}$$

It is more interesting to consider the instanton contribution to the ratio of the cumulant and factorial moments:

$$H_q = \frac{K_q}{F_q}. \tag{12}$$

These moments have the following properties for the perturbative QCD: decreasing oscillations, presence of the negative correlations, there is the first minimum at $q = 5$ [11].

Unlike this, for the instanton distribution (7) H_q-moments have the first minimum at $q = 2$ (Fig.4), oscillations, which magnitude increases at large q numbers (Fig.5).

4 Conclusion

The obtained dependences of the factorial, cumulant and H_q-moments on their rank have specific forms. Therefore, the behaviour of the correlation moments can be used as a new signal of the QCD nonperturbative vacuum

phenomenon in addition to the well-known "footprints". Of course, we need to take into account hadronization stage. Local parton-hadron duality [12] allows to apply the obtained results for the experimental QCD-instantons search.

We propose the following procedure for the experimental QCD instantons search at HERA:
1) selection of the events with high multiplicity. For our approximations $n_{hadrons} \geq 12$ (local parton-hadron duality gives number of the final hadrons $n_{hadrons} = 2n_{partons} \geq 2n_{quarks} = 4n_f = 12$);
2) analysis of the correlation moments for the *selected* events and comparison with theoretical predictions.

References

[1] R.Jackiw and C.Rebbi, *Phys.Rev.Lett.* **37** (1976) 172.

[2] A.Belavin, A.Polyakov, A.Schwarz and Yu.Tyupkin, *Phys.Lett.* **B59** (1975) 85.

[3] G.'t Hooft, *Phys.Rev.Lett.* **37** (1976) 8,
G.'t Hooft, *Phys.Rev.* **D14** (1976) 3432.

[4] A.Sakharov, *JETP Lett.* **5** (1967) 1.

[5] A.Polyakov, *Phys.Lett.* **B59** (1975) 82.

[6] A.Ringwald, *Nucl.Phys.* **B330** (1990) 1.

[7] I.Balitsky and V.Braun, *Phys.Lett.* **B314** (1993) 237.

[8] S.Moch, A.Ringwald, F.Schrempp, *Nucl.Phys.* **B507** (1997) 134.

[9] V.Kuvshinov and R.Shulyakovsky, *Acta Phys.Pol* **B28** (1997) 1629, hep-ph/9902403;
V.Kuvshinov and R.Shulyakovsky, *Acta Phys.Pol* **B30** (1999) 69, hep-ph/9902379.

[10] T.Carli, M.Kuhlen, *DESY preprint* **97-151** (August,1997), hep-exp/9708008.

[11] I.Dremin, *Phys. Rev. Lett.* **313** (1993) 209;
I.Dremin, *Proceed. of the 7th Workshop on Multiparticle Production "Correlations and Fluctuations" (June 30 - July 6, 1996, Nijmegen, The Netherlands)*, (1997) 313.

[12] Ya.Azimov, Yu.Dokshitzer, V.Khoze, S.Troyan, *Z.Phys.* **C27** (1985) 65.

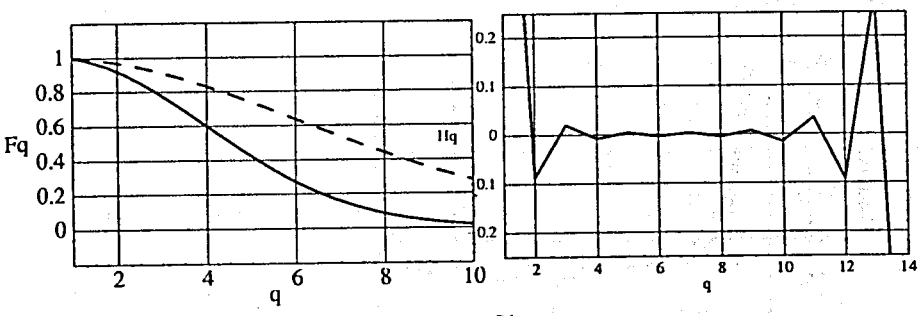

Fig.3. The dependence of the normalised factorial moments on their rank q for the different average gluon numbers: $< n_g >= 2$ (solid line), $< n_g >= 8$ (dash line); $n_f = 3$.

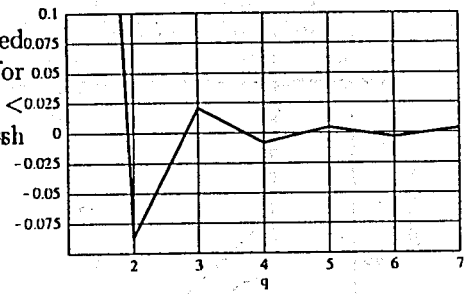

Fig.4. H_q as the function of q, $< n_g >= 2$, $n_f = 3$: upper curve – full plot, lower – first part of the plot.

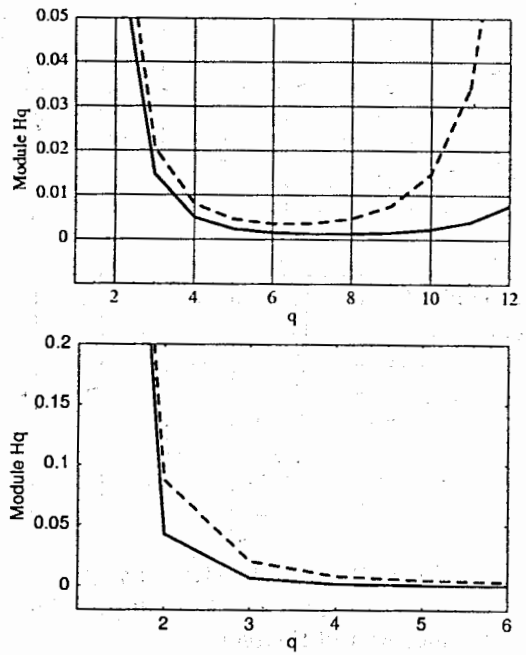

Fig.5. Absolute values of H_q as the function of q. Upper curve corresponds to the full plot ($< n_g >$=3 for solid line, $< n_g >$= 2 for dash line), lower - first part of the plot ($< n_g >$=6 for solid line, $< n_g >$= 2 for dash line).

Coherent atomic beam generator and its potential applications

A. V. Soroko*

National Centre of Particle and High Energy Physics, Belarusian State University, Bogdanovich Street 153, Minsk 220040, Belarus

The concept and properties of a coherent atomic beam generator are discussed. The techniques which are necessary to demonstrate the atom laser based on the Raman cooling below the gravitational limit are presented. Potential applications of the atom laser in the field of atom optics are also discussed. In particular, it is shown that at certain physical conditions the diffraction of an coherent atomic beam by the inhomogeneous laser field can be interpreted as if the beam passes through a three-dimensional hologram. On this basis a new method for reconstruction of the object image with matter waves is offered. The latter may have useful practical applications ranging from atom lithography to the manufacturing of microstructures, or quantum microfabrication.

03.75.Be, 42.50.Vk, 42.50.Ct, 03.75.Fi

I. INTRODUCTION

A coherent atomic beam generator (CAB) or atom laser is analogous to an optical laser, but it emits matter waves instead of electromagnetic waves. Its output is a coherent matter wave, which means, for instance, that atom laser beams can interfere with each other. Compared to an ordinary beam of atoms, the beam of an atom laser is also extremely bright. Thus, the brightness and coherence are the essential features, which pick out coherent atomic beam generators among other atomic sources.

A number of theoretical atom laser schemes have already been proposed [1–6], and only one of them [1] is realized experimentally in MIT up to now. These schemes have involved some method of cooling atoms in an atomic cavity, and a coupling the atoms to the external atomic modes. So, the main parts of an atom laser include a cavity (resonator), an active medium, and an output coupler. For example, in the MIT atom laser, the resonator is a magnetic trap in which the atoms are confined by magnetic mirrors. The active medium is a thermal cloud of ultracold atoms, and the output coupler is an rf pulse which controls the reflectivity of the magnetic mirrors.

In the reported models of CAB the ground state of an atomic trap or cavity (the lasing mode) is filled with a large number of atoms by using the higher energy modes of the trap as a continuously pumped atomic source. The coupling between higher energy modes and the laser mode is achieved through cooling. Different cooling mechanisms sufficiently discriminate proposed schemes of the atom lasers. So, in the experiment [1], the coupling is done by evaporative cooling, where the evaporation process creates a cloud which is not in thermal equilibrium and relaxes towards colder temperatures. This results in growth of the condensate, i.e., the lasing mode population. Conversely, in reference [2] the mechanism is dark state laser cooling, and atoms are transferred from the source to the lasing mode irreversibly due to spontaneous emission. In the scheme proposed by Spreeuw *et al.* [3] the cold atoms will be dropped from the trap

onto a so-called atomic trampoline, consisting of a repulsive evanescent wave at a glass-vacuum interface. In the turning point the atoms will be optically pumped into the other hyperfine ground state. The atoms accumulate in an optical cavity for matter waves, enhancing the transition probability for additional atoms by Bose statistics. Holland *et al.* [4] and Guzman *et al.* [5] use inelastic binary collisions to transfer atoms from the source mode to the lasing mode. In these approaches, two atoms collide to produce one atom in the lasing mode, and another in a higher energy mode. This process is made irreversible by using evaporative cooling to rapidly remove the higher energy atom from the system. Conceptually this methods are similar to that used in [1].

The number of atoms in the lasing mode depends on the pumping and loss rates. Above threshold the number of atoms in the lasing mode saturates. In a conventional laser, stimulated emission of photons causes the radiation field to build up in a single mode. In an atom laser, the presence of N atoms in the lasing mode, causes stimulated transition into that mode, i.e., enhances the probability that an atom will be scattered into the lasing mode by $N + 1$.

This is required to have a reasonably well defined number of atoms in a single cavity mode and hence a state that closely approximates a coherent state. The proposed methods of output coupling to this state have involved either quantum mechanical tunneling [2] or periodically turning off the cavity mirrors [5]. Turning off the cavity mirrors, while effective for output coupling, will not provide a continuous beam. Therefore Moy *et al.* [6] have present an atom laser scheme using two atomic cavities - one for the source atoms and an effectively single mode cavity for the lasing mode. Higher modes of the lasing cavity cannot be reached as their energy is larger than that of the incoming atoms. Raman transitions are used to change the state of the atoms to a non-trapped state, to allow the output coupling of the atoms from the lasing mode.

There are many applications in fundamental research and industry where atomic beams are used, e.g., atomic clocks, atom optics, precision measurements of fundamental constants, tests of fundamental symmetries, atomic beam deposition for chip production (atom lithography), and, more generally, nanotechnology. The CAB may have an impact on all of these applications, if indeed will provide the necessary brightness and coherence. But as a rule, the detrimental influence of the gravity effects is ignored in the schemes mentioned above, whereas only freely traveling matter waves can be sufficiently coherent.

Two ways are envisioned to prepare a stable quantum state of matter in the gravitational field: to bound particles or to suspend them free in an inhomogeneous magnetic field using Stern-Gerlach effect. In the first approach atoms are confined by a conservative trapping potential which can be realized, e.g., in a far-off-resonance or a dipole trap, where an intensity gradient provides a spatially dependent ac Stark shift. In momentum space, up to now only the existence of an approximate dark state (DS), which in turn may be used as a lasing mode, has been demonstrated [7]. This state does not interact with the photons in the process of laser cooling and characterized by a decay rate in a special 1D atomic and laser field configuration much smaller than that of all other states in the trap. The finite lifetime of approximate DS evidently restricts the cooling possibilities in a trap, leaving the question about going below the gravitational limit to be clarified. However, a scheme [8] which is based on the creation of a dark state in position space with the help of an appropriate spatial profile of the cooling laser, e.g., in a doughnut mode, seems to be much more efficient, allowing to cool a significant fraction of atoms to the ground state of the trapping potential.

Another approach may be applied to atoms possessing a magnetic moment. Superimposing a weakly inhomogeneous magnetic field onto the path of pre-polarized particles and appropriately adjusting the field gradient it is possible to compensate for the effects of gravity for a definite internal atomic state. However, the magnetic field induces spatially dependent shifts of the Zeeman levels, which lead to unwanted residual excitation from the DS in the framework of any traditional subrecoil cooling method, such as velocity selective coherent population trapping (VSCPT) [9] and Raman cooling [10]. Moreover, in the case of VSCPT the dark state cannot be an eigenvector of the total Hamiltonian since only one of the internal states forming the superposition which is not coupled to the laser field may escape gravity. Thus, both VSCPT and Raman cooling mechanisms in their standard form are incompatible with the last approach.

To resolve this problem we suggest a modification of Raman cooling method [11], in which the ground-level atoms are made motionally free with the Stern-Gerlach effect and the DS is created and supported in momentum space of these atoms with additional velocity-selective two-photon transitions. The transitions couple external momentum states of the same ground internal level and are organized in such a manner that DS cyclically occupies different thin sets of velocity modes while remaining unreachable for the Raman excitation-repumping pulse sequences at all times.

In a bosonic system, where the losses in DS population can be compensated by the quantum-statistical enhancement of feeding rate, our cooling mechanism may be used as the basis for extensive CAB implementation. An easy tunable wavelength will be one of the advantages of such a device, because as we will see below the momentum of a cooled atom is readily defined by the geometry of laser beams.

In Sec. II we specify the magnetic field to compensate for the gravity effects. In Sec. III a detailed qualitative treatment of the cooling mechanism is given, and numerical simulation in one dimension is presented. An application of the coherent atomic beams to the atom-optics holography [12] is demonstrated in Sec. IV, namely, the inhomogeneous laser radiation is shown to behave like a three-dimensional hologram with respect to the coherent matter wave. Section IV concludes with a summary of the results.

II. COMPENSATION FOR GRAVITY

Consider for definiteness an atom with a $J = \frac{1}{2}$ to $J = \frac{3}{2}$ transition, e.g., sodium or cesium. The magnetic field $\mathbf{B}(\mathbf{r})$ applied to compensate the gravity is supposed to contain a homogeneous component $\mathbf{B}_0$ directed along the gravity acceleration $\mathbf{B}_0 \uparrow\uparrow \mathbf{g}$. The remaining inhomogeneous part of the field $\mathbf{B}_1(\mathbf{r}) = \mathbf{B}(\mathbf{r}) - \mathbf{B}_0$ should be small compared to this component,

$$|\mathbf{B}_1(\mathbf{r})| \ll B_0 = |\mathbf{B}_0|. \tag{2.1}$$

As we will see below, to fulfil this condition it is necessary to take B_0 in the range $10^3 \div 10^4$ G. In practice such a field is strong enough to induce Zeeman shifts which considerably exceed the hyperfine splitting intervals $\sim \hbar\omega_{\mathrm{HFS}}$ (but not the multiplet ones). Therefore an internal atomic eigenstate $|J, I, M_J, m_I\rangle$ may be well described using the set of quantum numbers consisting of the angular momenta of the electronic shell J and the nucleus I, and their local projections M_J, m_I on the direction of the magnetic field.

In the framework of perturbation theory, $|J, I, M_J, m_I\rangle$ represents a combination of eigenstates $|J, I, M_J, m_I\rangle^{(0)}$ related to the atomic Hamiltonian without the hyperfine interaction,

$$|J, I, M_J, m_I\rangle = |J, I, M_J, m_I\rangle^{(0)} + \frac{a}{2\mu_B g_L B_0} \times \Big\{ [(J + M_J)(J - M_J + 1)]^{1/2} [(I + m_I + 1)(I - m_I)]^{1/2} \times |J, I, M_J - 1, m_I + 1\rangle^{(0)} - [(J + M_J + 1)(J - M_J)]^{1/2} [(I + m_I)(I - m_I + 1)]^{1/2} \times |J, I, M_J + 1, m_I - 1\rangle^{(0)} \Big\}, \quad (2.2)$$

where a is the hyperfine coupling constant ($a \propto \hbar\omega_{\rm HFS}$, e.g., for Na $a/\hbar = 885.8$ MHz) and g_L denotes the Lande factor. The corresponding energy eigenvalue is determined not only by the multiplet level E_J but also by the magnetic field $B(\mathbf{r}) = |\mathbf{B}(\mathbf{r})|$ and therefore is spatially dependent

$$E_{|J,I,M_J,m_I\rangle}(\mathbf{r}) = E_J + aM_J m_I + (\mu_B g_L M_J - \mu_{\rm nuc} m_I) B(\mathbf{r}), \quad (2.3)$$

where $\mu_{\rm nuc}$ is the nuclear magnetic moment. Because of the condition (2.1) such a spatial dependence, however, mainly arises from the longitudinal ($B_1^{\parallel}(\mathbf{r}) = \mathbf{B}_0 \cdot \mathbf{B}_1(\mathbf{r})/B_0$), rather than the transverse ($\mathbf{B}_1^{\perp}(\mathbf{r})$) component of the vector $\mathbf{B}_1(\mathbf{r})$, provided that the components are defined relative to $\mathbf{B}_0$. This is evident from the expression

$$B(\mathbf{r}) = \sqrt{\left[B_0 + B_1^{\parallel}(\mathbf{r})\right]^2 + \left[\mathbf{B}_1^{\perp}(\mathbf{r})\right]^2} \simeq B_0 + B_1^{\parallel}(\mathbf{r}) + \left[\mathbf{B}_1^{\perp}(\mathbf{r})\right]^2/(2B_0), \quad (2.4)$$

where the term containing $\mathbf{B}_1^{\perp}(\mathbf{r})$ is small and can be neglected. Consequently, by adjusting the gradient of the field $B_1^{\parallel}(\mathbf{r})$ one can achieve translational invariance of the ground state $|1\rangle = |1/2, I, -1/2, I\rangle$ in three dimensions:

$$E_{|1\rangle}(\mathbf{r}) - M\mathbf{g} \cdot \mathbf{r} = \text{const}. \quad (2.5)$$

For example, to balance the gravitational force in this way for sodium it is necessary to create a gradient $\nabla B_1^{\parallel}(\mathbf{r}) = b_1 \mathbf{g}/|\mathbf{g}|$, where $b_1 = -4.033$ G/cm. This condition does not contradict the Maxwell equation $\nabla \cdot \mathbf{B}_1(\mathbf{r}) = 0$, because variation of $\mathbf{B}_1^{\perp}(\mathbf{r})$ is not restricted. Note also that the choice $B_0 = 10^3 \div 10^4$ G maintains the condition (2.1) very well within a spatial region of the size ~ 10 cm.

All the other levels are affected by the residual external potential. In particular, after a transition from $|1\rangle$ to the neighboring state $|2\rangle = |1/2, I, -1/2, I - 1\rangle$ the atom experiences a force

$$\mathbf{f}_2 = \frac{M\mu_{\rm nuc}\mathbf{g}}{(1/2)\mu_B g_L + \mu_{\rm nuc} I}. \quad (2.6)$$

III. COOLING SCHEME

In our scheme, we use pulses of laser light at frequencies ω_1 and ω_2 which are roughly tuned to the $|1\rangle \to |3\rangle$ and $|2\rangle \to |3\rangle$ transitions, where $|3\rangle = |3/2, I, -3/2, I\rangle$ is an excited state with the lowest energy. The typical size $2L$ of atomic sample is restricted by the condition $L \ll a/(Mg)$, which allows to regard $E_{|3\rangle}(\mathbf{r})$ as the closest to resonance excited level within the whole interaction domain. Indeed, the force $\mathbf{f}_3$ acting on the atoms in the state $|3\rangle$ may be estimated from Eqs. (2.3) and (2.5) as $|\mathbf{f}_3| \sim Mg$. The maximal spatial shift of the level $\sim MgL$ which it induces is much less than the hyperfine splitting intervals ($MgL \ll a \sim \hbar\omega_{\rm HFS}$), and the hierarchy of detunings is retained. Therefore an atom initially in $|1\rangle$ or $|2\rangle$ state behaves as a three-level system with respect to the processes with stimulated emission of photons.

Since the atomic dipole momentum operator $\mathbf{d}$ is diagonal in quantum numbers I and m_I in the basis $|J, I, M_J, m_I\rangle^{(0)}$, the transitions which change m_I, e.g., $|2\rangle \to |3\rangle$, are allowed only due to hyperfine interaction, as is seen from Eq. (2.2). The value of any matrix element like $|\langle 3|\mathbf{d}|2\rangle|$ is approximately $\propto \eta_{\rm HF}|\langle 3|\mathbf{d}|1\rangle|$, where $\eta_{\rm HF} = a/(2\mu_B g_L B_0) \ll 1$. As a consequence, the upper state $|3\rangle$ decays to the lower ones preferentially in the channel $|3\rangle \to |1\rangle$ (with the rate γ). This circumstance makes it possible to deal with an atom as a three-level system even if spontaneous photon emission takes place.

When the atom is irradiated with two laser beams at frequencies ω_1 and ω_2, the two-photon Raman transition from $|1\rangle \to |2\rangle$ has twice the Doppler sensitivity of a single-photon transition provided that $\omega_1 - \omega_2 \sim \omega_{\rm HFS}$ and the beam wave vectors $\mathbf{k}_1$, $\mathbf{k}_2$ are opposite [10]. However, if we take into account the force (2.6), a wide set of atomic momenta $\mathbf{p}$ may satisfy the resonance condition, as follows from the energy conservation:

$$\hbar\Delta_1 - 2\mathbf{p} \cdot \boldsymbol{\Delta}_p/M = \hbar\Delta_2 - \mathbf{f}_2 \cdot \mathbf{r} + 2\Delta_p^2/M. \quad (3.1)$$

Here detunings $\Delta_m \equiv \omega_m + [E_{|m\rangle}(0) - E_{|3\rangle}(0)]/\hbar$, $m = 1, 2$, are defined in the center of atom-laser interaction region ($\mathbf{r} = 0$), $\boldsymbol{\Delta}_p = \hbar(\mathbf{k}_1 - \mathbf{k}_2)/2$, and $\Delta_p = |\boldsymbol{\Delta}_p|$. The dip in the velocity dependence of absorption rate broadens so that the width of the trapping zone [13] becomes

$$\delta v \sim L|\mathbf{f}_2|/(2\Delta_p). \quad (3.2)$$

As a consequence, since the sample of unconfined particles considered in this paper may spread up to $L \sim 1$ cm during the cooling, the effective temperature of atoms left in the state $|1\rangle$, which constitutes $\sim M(\delta v)^2/(2k_B)$, generally lies far above the gravitational limit [14] $k_B T_G = Mg/k$. For example, in the case of sodium, where $\Delta_p/\hbar = 1.07 \times 10^5$ cm^{-1} and $|\mathbf{f}_2|/\hbar = 7.3 \times 10^4$ cm^{-1} s^{-1}, such a temperature may reach $6.4T_G$.

Despite insufficient velocity selectivity of the $|1\rangle \to |2\rangle$ transition, state $|2\rangle$ may be used in Raman excitation cycle. To avoid unwanted radiation impact on the selected group of particles, which are referenced here as the DS atoms, one should move them in momentum space to another place, where the resonance condition (3.1) brakes down. It can be achieved by means of a two-photon $|1\rangle \to |1\rangle$ transition while the atom is irradiated with two noncolinear laser beams at the same frequency ω_1.

If the ground-level initial momentum distribution along the direction of vector $\boldsymbol{\Delta}_p$ were as shown in Fig. 1(a), such a transition would have selectively brought particles

concentrated near the point $-\Delta_p$ (the DS, as we will see below) to the point Δ_p, and vice versa. To prove this imagine an atom with momentum p passing through a superposition of two laser beams. The superposition may be treated as a diffraction grating in the case $\mathbf{k}_1 \uparrow\downarrow \mathbf{k}_2$ (standing wave) [15,16], or as an effective atomic hologram when directions of the wave vectors are arbitrary [12]. At low laser light intensity and large detuning Δ_1 only the first-order Bragg scattering is of importance. In this case, two diffraction modes with indices 0 and 1 resonantly couple with each other. Physically, the first-order Bragg resonance corresponds to an absorption and stimulated photon emission process from one laser beam to another. As a consequence of the atomic kinetic energy conservation one gets the Bragg resonance condition

$$\pm \mathbf{p} \cdot \mathbf{\Delta}_p = \Delta_p^2, \tag{3.3}$$

which is satisfied for any momentum with the component $p = \pm\Delta_p$ along the vector $\mathbf{\Delta}_p$. Figure 1(b) contains the final distribution, the peak around Δ_p being the moved DS. So the *first step* of our scheme consists in the momentum transfer of DS as it is indicated with arrows in Fig. 1(a).

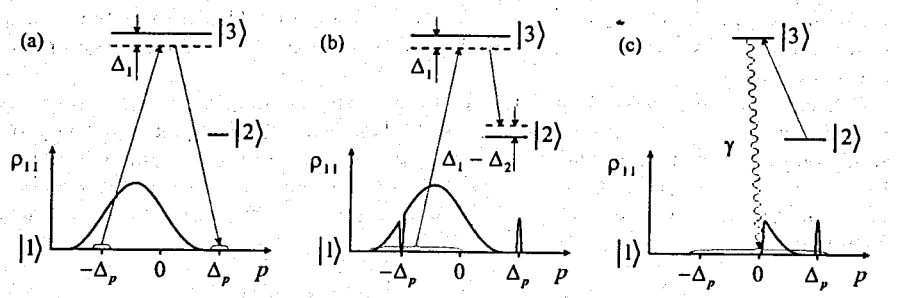

FIG. 1. Energy level diagram and profile of ground state atomic distribution ρ_{11} as a function of p, the momentum component along the direction of vector $\mathbf{\Delta}_p$: (a) before DS transfer with the two-photon $|1\rangle \rightarrow |1\rangle$ transition; (b) before the Raman excitation $|1\rangle \rightarrow |2\rangle$ cycle; and (c) before the optical repumping pulse tuned to the $|2\rangle \rightarrow |3\rangle$ transition. The curly braces denote momentum intervals involved in each of these processes.

In the *second step* of cooling, the Raman excitation cycle [10] takes place. In accordance with Eq. (3.1), atoms with any negative p can be transferred to state $|2\rangle$ by varying the difference of beam frequencies. Due to the finite width of trapping zone atoms with positive $p < M\delta v$ also have a chance to undergo transition. The DS, being hidden near the point $p = \Delta_p > M\delta v$, does not take part in this process, as illustrated in Fig. 1(b).

In the *third step*, an optical pumping pulse at frequency ω_2 is used to return the atoms back to the state $|1\rangle$. It is important that the ground level appears to be far off resonance and laser light does not affect DS directly. The population of DS rises during the spontaneous emission process, which randomizes the atomic momenta [see Fig. 1(c)].

Then the sequence of *steps 1 - 3* is repeated with opposite directions of $\mathbf{k}_1$ and $\mathbf{k}_2$ involving residual positive-momentum atoms of the ground level in DS filling and

finishing a 1D cooling cycle along $\mathbf{\Delta}_p$. After this stage the DS occupies its initial place near the point $-\mathbf{\Delta}_p$.

By choosing linearly independent vectors $\mathbf{\Delta}_p^m$ in a set of two ($m = 1,2$) or three ($m = 1,2,3$) 1D cooling cycles one can proceed with decreasing the temperature in two or three dimensions by repeatedly applying such sets.

To increase the efficiency of DS filling one can admit several Raman and optical pumping pulses, i.e., a number of *steps 2 and 3*, between two consecutive *first steps*. It can be done, for example, as in the classical method [10], where every Raman transition is followed by the optical repumping, or by applying a series of cycles, each including multiple Raman and one optical pumping pulses.

Since the time necessary to collect all the atoms in DS is, generally speaking, infinitely long, it may be useful to separate the DS from background with the final *first-step* transitions (on one for each dimension) so that the DS and background atoms will move in opposite directions and eventually will not spatially overlap. In particular, when vectors $\mathbf{\Delta}_p^m$, $m = 1,2,3$, form an orthogonal basis, our scheme will produce a cooled atomic beam with the average momentum $\mathbf{\Delta}_p^1 + \mathbf{\Delta}_p^2 + \mathbf{\Delta}_p^3$ as follows from Eq. (3.3). The minimum allowed temperature (but not the intensity) of such a beam is obviously determined by the width of velocity selection specific to *first-step* transitions and therefore can be much less than the gravitational limit.

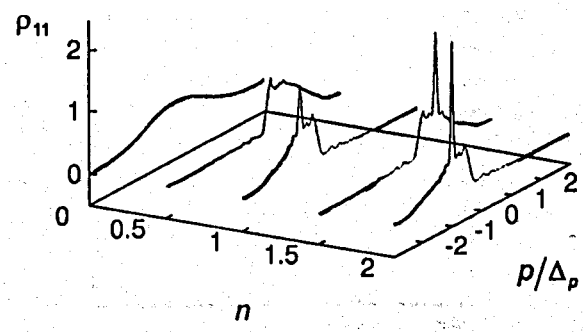

FIG. 2. One-dimensional ground-state distribution ρ_{11} for Na as a function of atomic momentum p and the number n of cooling cycles normalized to 1 on the scale p/Δ_p. Half-integer values of n correspond to the beginning of the second stage of each cooling cycle which starts when laser beams reverse. The curve with $n = 0$ gives the initial distribution. The highest peaks of the function represent the DS.

A. Numerical results

In the following we present one-dimensional results obtained for Na assuming that all vectors have only z-components, i.e., lie on the same axis with the gravitational force, and the laser beams with $\mathbf{k}_1$ and $\mathbf{k}_2$ are counterpropagating. An initial distribution of ground-state atoms is considered to be Gaussian. Since in our scheme we imply

that an atomic sample precooled to the recoil limit is used, it is reasonable to take the wave number of laser light $k = 1.07 \times 10^5$ cm^{-1} as an input for momentum dispersion σ_p. Note that for the considered laser-beams geometry $\Delta_p/\hbar = k$. We also take the parameter $\eta_{HF} = 2.5 \times 10^{-2}$, which corresponds to $B_0 = 10^3$ G.

In the numerical simulation of a cooling cycle each *first-step* pulse was followed by five repetitions of a set involving seven Raman and one optical pumping pulses. Both *first* and *second steps* of cooling continued during π-pulse times. The duration of the optical pumping pulse was taken to provide a complete depopulation of the $|2\rangle$ state. The remaining parameters were chosen as follows. For the *first step*: the Rabi frequencies $\Omega_1 = \Omega_2 = 0.08\gamma$, and the detuning $\Delta_1 = -16\gamma$. For the *second step*: $\Omega_1 = 0.4\gamma$, $\Omega_2 = 0.04\gamma$, and all seven Raman pulses were detuned to the red so that the sum $\Delta_1 + \Delta_2 = -32\gamma$ remained constant while the difference $\Delta_1 - \Delta_2$ was increased by -135, 118, 372, 625, 880, 1135, and 1393 kHz. Such a choice of detunings was tailored both to span the momentum interval $0 \le p \le 3\Delta_p$ and to minimize the losses of DS population due to parasitic excitation by sidelobes in the frequency spectrum of Raman transitions. For the *third step* we put $\Omega_2 = 0.1\gamma$, and $\Delta_2 = 0$. The initial size of atomic sample was taken $L = 1$ cm. However, for the given set of Raman light parameters this, or indeed any smaller, value of L means that the width of velocity selection does not depend on L. Therefore our results remain correct for all $L \le 1$ cm.

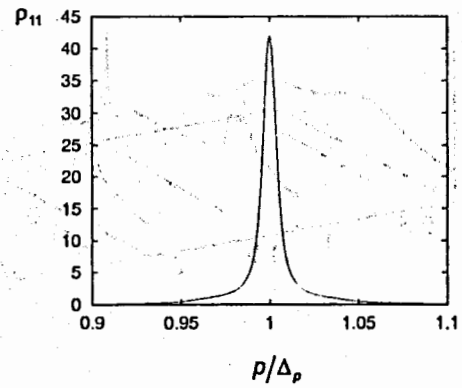

FIG. 3. Final ground-state distribution ρ_{11} of atoms with positive momenta as a function of p. The full-scale distribution is normalized as in the Fig. 2 whereas the plotted part contains $\sim 59\%$ of all particles.

Figure 2 shows the initial momentum distribution $\rho_{11}(p, p, 0)$ and the formation of a DS peak during two first cooling cycles including intermediate stages when the position of this peak is alternated. Although each $|1\rangle \to |1\rangle$ transition captures atoms in a rather wide momentum interval $\sim 2\delta p \approx 0.28\Delta_p$, the width of the DS peak (at half-maximum) decreases rapidly with the number of applied cycles because of a pronounced maximum in the transition rate profile. After 10 cycles the decrease slows down and approaches at $0.005\Delta_p$ by the end of cooling. At the same time, the peak height growth is far

from saturation, and after 100 cooling cycles this value exceeds the initial distribution maximum in more than 98 times.

The fraction of cold atoms in the interval $-\Delta_p - \delta p \le p \le -\Delta_p + \delta p$ depends on the difference between the feeding rate due to optical pumping and losses during DS transfer, and constitutes about 65 % by the end of cooling.

When separated from the background by the final *first-step* transition which transfers the aforementioned interval to positive momentum half-axis, the DS peak acquires a shape represented in the Fig. 3. As a result, the effective temperature calculated as a mean kinetic energy of the atoms distributed within the domain $\Delta_p - \delta p \le p \le \Delta_p + \delta p$ reaches 0.4 nK or $0.015T_G$.

IV. ATOM-OPTICS HOLOGRAPHY

A. Typical layout design

In our scheme the atom moves inside a superposition of the reference and the object beams

$$\mathbf{E}(\mathbf{r}, t) = \mathbf{E}_s(\mathbf{r}, t) + \mathbf{E}_r(\mathbf{r}, t), \tag{4.1}$$

where the laser light has the frequency ω

$$\mathbf{E}_{\{s,r\}}(\mathbf{r}, t) = \mathbf{E}_{\{s,r\}}(\mathbf{r})\epsilon^{-i\omega t} + \text{c.c.} \tag{4.2}$$

Each beam is represented as a discrete sum of plane monochromatic electromagnetic waves. In particular, we use the following decomposition of the electric field in the object beam:

$$\mathbf{E}_s(\mathbf{r}) = \sum_{m \ge 1} \mathbf{E}_m \exp(i\mathbf{k}_m \cdot \mathbf{r}), \tag{4.3}$$

where $\mathbf{E}_m$ and $\mathbf{k}_m$ stand for the complex amplitude of the mode m and its wave vector, respectively. Such an approach does not restrict the generality of our consideration, because the expression (4.3) must well describe the real laser field only in the atom-laser interaction region. Evidently, the latter requirement can always be satisfied by decreasing the minimal angle between the mode wave vectors. In this case we can also regard the reference beam as a single mode (with the index $m = 0$),

$$\mathbf{E}_r(\mathbf{r}) = \mathbf{E}_0 \exp(i\mathbf{k}_0 \cdot \mathbf{r}) \tag{4.4}$$

which just as the condition

$$|\mathbf{E}_0|^2 \gg |\mathbf{E}_m|^2, \quad m \ge 1, \tag{4.5}$$

is a typical arrangement for optical holography. The layout design of laser and atomic beams may be as shown in the Fig. 4.

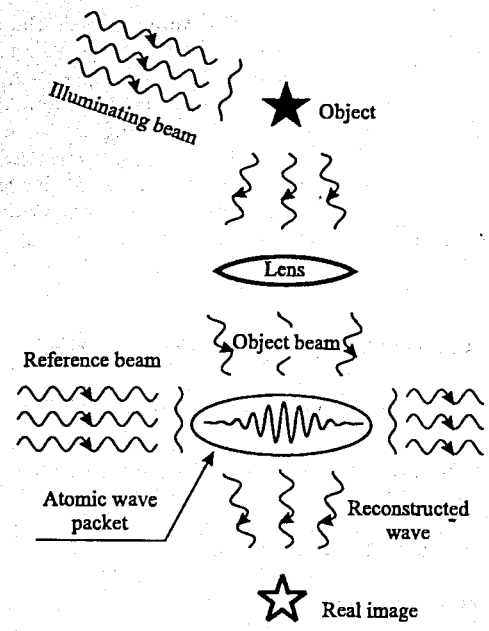

FIG. 4. Typical layout design of laser beams and matter wave packets suitable for atomic holography.

B. Off-resonance solution of the master equation

We are considering the case when laser frequency is far off resonance and ultracold atoms in the beam are supposed to move with momenta close to the photon ones. Then the one-particle atomic density matrix can be represented as the sum

$$\rho_{ab}(\mathbf{r}_1,\mathbf{r}_2,t)=\rho^{\mathrm{E}}_{ab}(\mathbf{r}_1,\mathbf{r}_2,t)+\rho^{\mathrm{R}}_{ab}(\mathbf{r}_1,\mathbf{r}_2,t)+\rho^{\mathrm{W}}_{ab}(\mathbf{r}_1,\mathbf{r}_2,t), \tag{4.6}$$

where the term $\rho^{\mathrm{E}}_{ab}(\mathbf{r}_1,\mathbf{r}_2,t)$ arises due to stimulated scattering of light, the term $\rho^{\mathrm{R}}_{ab}(\mathbf{r}_1,\mathbf{r}_2,t)$ is responsible for the effects of spontaneous emission and the term $\rho^{\mathrm{W}}_{ab}(\mathbf{r}_1,\mathbf{r}_2,t)$ describes dipole-dipole and other atomic interactions. Here indices $a,b\ldots$ span the internal atomic states.

Since the inhomogeneous magnetic field applied to compensate for the gravity creates large enough Zeeman splitting to suppress shifted stimulated photon scattering we get non-vanishing ρ^{E}_{ab} in agreement with the energy-momentum conservation only when we take into account those two-photon processes which leave atoms in the ground state $|g\rangle$. Below we also assume almost critical cross correlation of the laser field, which, for instance, can be achieved when all field modes originate from one initial laser mode. Therefore after stochastic averaging over the laser field fluctuations outside the atomic beam the perturbation theory gives the result

$$\rho^{\mathrm{E}}_{ab}(\mathbf{r}_1,\mathbf{r}_2,t)=\int d\nu d\varepsilon f(\nu,\varepsilon)\times\phi(\mathbf{r}_1,t;\nu,\varepsilon)\,\dot{\phi}\,(\mathbf{r}_2,t;\nu,\varepsilon)\delta_{ag}\delta_{bg}, \tag{4.7}$$

where

$$\phi(\mathbf{r},t;\nu,\varepsilon)=\frac{M}{2\pi\hbar^2}\int d\mathbf{r}' G_g(\mathbf{r}-\mathbf{r}';\varepsilon)\times\alpha_{ln}(\mathbf{r}')\,\dot{E}^{l}\,(\mathbf{r}')E^{n}(\mathbf{r}')\phi_0(\mathbf{r}',t;\nu,\varepsilon), \tag{4.8}$$

and $f(\nu,\varepsilon)$ is atomic beam distribution function on energy ε and quantum numbers ν, which define the wave function $\phi_0(\mathbf{r},t;\nu,\varepsilon)$ of a free particle with the mass M. In the Eq. (4.8) $G_g(\mathbf{r};\varepsilon)$ denotes the Green function of the Helmholtz equation, and $\alpha_{ln}(\mathbf{r})$ stands for the coherent-scattering tensor weakly dependent on $\mathbf{r}$ because of the external magnetic field inhomogeneity. In fact, expressions (4.7),(4.8) describe the scattering of atoms by a lightshift potential in a regime when it can be treated perturbatively and when spontaneous emission and collective effects are negligible.

C. Atom-optics interpretation

To get the atom-optics interpretation of the solution (4.7),(4.8) we will assume the atomic beam aperture to be wide enough in the region of atom-field interaction and will regard $\phi_0(\mathbf{r},t;\nu,\varepsilon)$ as a wave function of a free definite-momentum particle, using the de Broglie wave vector $\mathbf{k}_a$ as an equivalent of quantum numbers $\{\nu,\varepsilon\}$. On analogy with conventional optics, this function can be well approximated by the plane wave having a finite spatial extension along diaphragm forming the beam (see Fig. 5 for details).

It is convenient to put the origin of a reference frame at the center of region where both reference and object wave cross the atomic beam as illustrated in Fig. 5. Near a point of radius-vector $\mathbf{R}$, the integral in Eq. (4.8) can be calculated within the Kirchhoff-Fresnel approximation if typical longitudinal ($2L$) and transversal ($2D$) dimensions of the region with respect to $\mathbf{R}$ satisfy the conditions: $\lambda\ll\{L,D\}\ll R\ll D^2/\lambda$, where λ is the laser wavelength. As a result one gets

$$\langle\rho^{\mathrm{E}}_{gg}(\mathbf{r}_1,\mathbf{r}_2,t)\rangle=g(\mathbf{r}_1-\mathbf{r}_2)\Psi(\mathbf{r}_1)\,\dot{\Psi}\,(\mathbf{r}_2), \tag{4.9}$$

where

$$\Psi(\mathbf{r})=\frac{2ML}{\hbar^2 k_0}\,\dot{E}^{l}_{0}\,\alpha_{lm}(\mathbf{r})E^{m}_{s}(\mathbf{r}), \tag{4.10}$$

$$g(\mathbf{r})=\int d\mathbf{k}_a f(\mathbf{k}_a)J^2[k_0^{-1}(\hat{\mathbf{k}}-\mathbf{k}_0)\cdot(\mathbf{k}_a-\mathbf{k}_0)]\times\exp[i(\mathbf{k}_a-\mathbf{k}_0)\cdot\mathbf{r}], \tag{4.11}$$

and $J(k)=\sin(kL)/(kL)$.

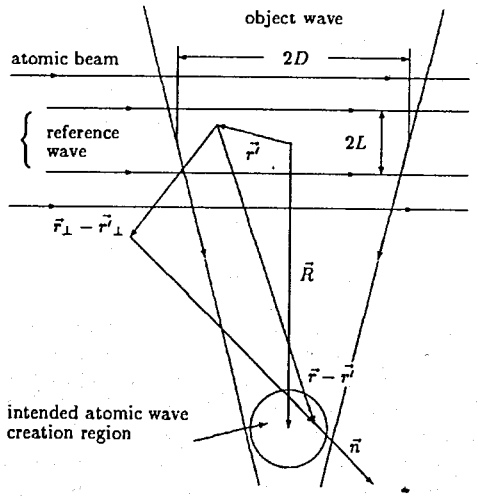

FIG. 5. Typical geometry of laser and atomic beams.

On analyzing the expression (4.11) with respect to the peak shape of the function $J(k)$ one may easily find the density matrix (4.9) to describe the coherent state (4.10) as soon as the atomic distribution is compatible with the condition

$$|(\tilde{\mathbf{k}} - \mathbf{k}_0) \cdot (\mathbf{k}_a - \mathbf{k}_0)| \leq \pi k_0/(2L). \tag{4.12}$$

where $\tilde{\mathbf{k}}$ is some typical wave vector in the object beam.

On the other hand, the spatial concentration of atoms is defined at $\mathbf{r}_1 = \mathbf{r}_2$ and would be received independently from mentioned condition as if all particles had the same wave function $[g(0)]^{1/2}\Psi(\mathbf{r})$. So in both cases because tensor $\alpha_{lm}(\mathbf{r})$ varies slowly in the interaction region, one deals with the atomic wave reproducing the amplitude and phase characteristics of the object wave.

D. Physical conditions

1. Applicability of the perturbation theory

The formula (4.10) remains correct provided that $|\Psi(\mathbf{r})| \ll |\phi_0(\mathbf{r}, t; \mathbf{k}_a)|$, or that the perturbation of the incident atomic beam is weak. This in turn sets an upper limit on the object wave amplitude

$$|E_s^m(\mathbf{r})| \ll \frac{\hbar^2 k_0}{2ML} |E_0^l \alpha_{lm}(\mathbf{r})|^{-1}. \tag{4.13}$$

Note, that correspondingly low values of the object wave intensity result in the linear response of the atomic system to the laser-field inhomogeneity.

2. Compensation for gravity

Another important prerequisite for successful wave front reconstruction with massive particles concerns the need to compensate for the potentially detrimental influence of gravitational effects. This can be done as described in Sec. II

3. Reducing background from the spontaneous emission

First of all we must insure a small background arising from the spontaneous emission of atoms, i.e.,

$$\langle \rho_{ab}^{\mathrm{E}}(\mathbf{r}_1, \mathbf{r}_2, t) \rangle \gg \langle \rho_{ab}^{\mathrm{R}}(\mathbf{r}_1, \mathbf{r}_2, t) \rangle. \tag{4.14}$$

This condition fulfils if the object wave amplitude is large enough

$$|\mathbf{E}_s(\mathbf{r})|^2 \gg 2\hbar^2 k_0^4/(3MLP), \tag{4.15}$$

where $P \equiv g(0)/n_{\mathrm{b}}$ represents the part of particles distributed due to peak shape of function $J(k)$ within the domain (4.12).

4. Reducing effects of the interatomic collisions

Since our model neglects all atomic interactions apart from dipole-dipole interaction (i.e. relevant at short interatomic distances), it can only be used for systems that are not too dense. In particular, the mean field interaction energy per particle [17] must be much less than the typical kinetic energy of an atom, whence

$$n_{\mathrm{b}} \ll \mathbf{k}_a^2/(8\pi a_{\mathrm{sc}}), \tag{4.16}$$

where n_{b} denotes spatial concentration of atoms, and a_{sc} is the scattering length directly related to the low energy S-wave cross section ($\sigma_{\mathrm{S}} = 4\pi a_{\mathrm{sc}}^2$).

5. Elimination of the dipole-dipole interactions

Condition (4.16), however, do not fix completely possible range of n_{b}. To satisfy the inequality

$$\langle \rho_{ab}^{\mathrm{E}}(\mathbf{r}_1, \mathbf{r}_2, t) \rangle \gg \langle \rho_{ab}^{\mathrm{W}}(\mathbf{r}_1, \mathbf{r}_2, t) \rangle, \tag{4.17}$$

we must also provide elimination of the dipole-dipole interactions. In the framework of the mean-field approach one can readily get an additional restriction on the spatial concentration of atoms

$$n_{\mathrm{b}} = \int d\mathbf{k}_a f(\mathbf{k}_a) \ll (8\pi ||\alpha_{lm}(\mathbf{r})||)^{-1}. \tag{4.18}$$

E. Numerical example

The method of atomic wave creation, we have just considered theoretically, proves to be currently available. In particular, it is possible to choose the beam and laser field parameters so that all necessary conditions may be satisfied whereas the amplitude $|[g(0)]^{1/2}\Psi(\vec{r})|$ of desired wave would be sufficient.

For example, let us take the atomic beam with $n_b \sim 10^{10-11}$ cm^{-3} as typical for Raman cooling experiments [10]. Such a concentration is obviously compatible with the conditions (4.16),(4.18) because for most atoms, the scattering length does not exceed $10^2 a_B$, and in nonresonance case the components of tensor $\alpha_{lm}(\mathbf{r})$ are of the order a_B^3, where a_B denotes the Bohr radius.

If the width of atomic beam is imagined to be about 1 cm, and intensity of background wave is $\sim$ 1 W/cm^2, then mean intensity $\sim$ 0.1 W/cm^2 of the object wave will not violate the conditions (4.13),(4.15), where we have substituted $P \simeq 2 \times 10^{-5}$. At such parameters, the atomic wave amplitude will be $|[g(0)]^{1/2}\Psi(\mathbf{r})| \sim 10^{1-2}$ cm$^{-2/3}$ leading to quite observable concentration $n_s \sim 10^{2-4}$ cm^{-3} of atoms in the created wave.

A way to enhance this concentration consists in preparing the atomic beam appropriately. Since only the part P of all atoms undergoes the stimulated photon scattering giving contribution to the wave $[g(0)]^{1/2}\Psi(\mathbf{r})$, we should cool the beam as much as possible. If, for instance, $P \simeq 1$, then we get $n_s \sim 10^{8-9}$ cm^{-3} in the same experimental situation as above. An extraordinary role here may be played by coherent atomic-beam generators [1–6], that are under development now.

V. CONCLUSIONS

In conclusion, creation of an atom laser based on the cooling scheme below the gravitational limit seems to be possible, but more thorough investigations are necessary. A large number of atom optics applications requires such a device, for instance, the atom-optics holography, which will be a powerful tool to manipulate atoms. A way to enhance diffraction efficiency of an atomic hologram consists in using of the coherent atomic beam so that all the particles get the same momentum as the momentum of photons in the reference wave, and a special role here may be played coherent atomic-beam generators, which are under development now.

---

* Electronic address: soroko@hep.by

[1] M.-O. Mewes, M. R. Andrews, D. M. Kurn, D. S. Durfee, C. G. Townsend, and W. Ketterle, Phys. Rev. Lett. **78**, 582 (1997).
[2] H. M. Wiseman and M. J. Collett, Phys. Lett. A bf 202, 246 (1995).
[3] R. J. C. Spreeuw, T. Pfau, U. Janicke, and M. Wilkens, Europhys. Lett. **32**, 469 (1995).
[4] M. Holland, K. Burnett, C. Gardiner, J. I. Cirac, and P. Zoller, Phys. Rev. A **54**, R1757 (1994).
[5] A. M. Guzman, M. Moore, and P. Meystre, Phys. Rev. A **53**, 977 (1996).

[6] G. M. Moy, J. J. Hope, and C. M. Savage, Phys. Rev. A **55**, 3631 (1997).
[7] T. Pellizzari, P. Marte, and P. Zoller, Phys. Rev. A **52**, 4709 (1995).
[8] G. Morigi, J. I. Cirac, K. Ellinger, and P. Zoller, Phys. Rev. A **57**, 2209 (1998).
[9] A. Aspect, E. Arimondo, R. Kaiser, N. Vansteenkiste, and C. Cohen-Tannoudji, Phys. Rev. Lett. **61**, 826 (1988); J. Lawall, S. Kulin, B. Saubamea, N. Bigelow, M. Leduc, and C. Cohen-Tannoudji, *ibid.* **75**, 4194 (1995).
[10] M. Kasevich and S. Chu, Phys. Rev. Lett. **69**, 1741 (1992); N. Davidson, H. J. Lee, M. Kasevich, and S. Chu, *ibid.* **72**, 3158 (1994); H. J. Lee, C. S. Adams, M. Kasevich, and S. Chu, *ibid.* **76**, 2658 (1996).
[11] A. V. Soroko, Phys. Rev. A **58**, 3963 (1998).
[12] A. V. Soroko, J. Phys. B. **30**, 5621 (1997).
[13] J. Reichel, F. Bardou, M. Ben Dahan, E. Peik, S. Rand, C. Salomon, and C. Cohen-Tannoudji, Phys. Rev. Lett. **75**, 4575 (1995).
[14] R. Dum and M. Ol'shanii, Phys. Rev. A **55**, 1217 (1997).
[15] P. E. Moskowitz, P. L. Gould, S. R. Atlas, and D. E. Pritchard, Phys. Rev. Lett. **51**, 370 (1983).
[16] P. J. Martin, B. C. Oldaker, A. N. Miklich, and D. E. Pritchard, Phys. Rev. Lett. **60**, 515 (1988).
[17] M. Lewenstein, L. You, J. Cooper, and K. Burnett, Phys. Rev. A **50**, 2207 (1994).

Confining Properties of a Conformally Flat Effective Metric

L.M.Tomilchik
B.I.Stepanov Institute of Physics
National Academy of Sciences of Belarus
Minsk

Abstract

The confining aspects of the conformally flat metric are discussed. It is shown that the Lorenz-scalar potential and the damping normalizing factor introduced in some nowadays relativistic fenomenological quarkonim models for providing quark confinement arise pure geometrically as a consequence of the existence of the conformally flat static effective metric. The classical (geodesic equations) and quantum (Dirac and Klein-Fock-Gordon equations) cases are considered. The possibility of treating the conformally flat metric appearence as a kinematic effect connected with existence of the maximal acceleration or the maximal rate of energy change is discussed. The expression for the generalized linear element for the particle moving in a given external field is proposed.

Coordinate – dependent mass as a confining condition

It is well known that the standard confining potentials $V(\underline{r})$ being used in phenomenological relativistic quark models based on Dirac equation with the Hamiltonian

$$H = \alpha_\kappa \rho_\kappa + \beta m_o + V(\underline{r}), \qquad (1)$$

don't give necessary asymptotic (at $r \to \infty$) behaviour.

However the problem can be solved via including in (1) some Lorenz-scalar potential what is equivalent to introducing the coordinate – dependent rest mass. Then we have instead of (1) the Hamiltonian

$$H = \alpha_\kappa \rho_\kappa + \beta m_o U(\underline{r}) + V(\underline{r}), \qquad (2)$$

where U(r) is some function of spatial coordinates[1].

The necessary condition of the corresponding analytical behaviour of solutions is the following: the Lorenz scalar potential $(U(r))$ must increase with a distance more fast than the time-like component of the vector one $(V(\underline{r}))$[2]

This circumstance can be easily demonstrated using (1+1) version of Dirac equation, which can be presented in the following form:

$$\left(-i\sigma_2 \frac{d}{dx} + \sigma_3 m\right)\psi = \varepsilon\psi, (\hbar = c = 1); \qquad (3)$$

where $\psi = \begin{pmatrix} \psi_1 \\ \psi_2 \end{pmatrix}$, $\sigma_1 = \begin{pmatrix} 0 & 1 \\ 1 & 0 \end{pmatrix}$, $\sigma_3 = \begin{pmatrix} 1 & 0 \\ 0 & -1 \end{pmatrix}$,

m – rest mass, ε – energy.

Considering m and ε as the coordinate – dependent quantities (i.e. $m = m(x)$, $\varepsilon = \varepsilon(x)$) we obtain the following two equations

$$\begin{cases} -i\dfrac{d\psi_2}{dx} + \phi(x)\psi_1 = 0, \\ -i\dfrac{d\psi_1}{dx} - \eta(x)\psi_2 = 0, \end{cases} \qquad (4)$$

where $\phi(x) = m(x) - \varepsilon(x), \eta(x) = m(x) + \varepsilon(x)$.

The quadrized equation (for ψ_2) is:

$$\frac{d^2\psi_2}{dx^2} + \left(\frac{1d\phi}{\phi dx}\right)\cdot\frac{d\psi_2}{dx} - \eta(x)\phi(x)\psi_2 = 0. \qquad (5)$$

If $m(x)$ und $\varepsilon(x)$ are both increasing functions of x the second term under $x \to \infty$ in (5) can be neglected and asymptotically we have equation (omitting the index "2")

$$\frac{d^2\psi}{dx^2} - \{m^2(x) - \varepsilon^2(x)\}\psi = 0. \qquad (6)$$

We see that the asymptotic behaviour of ψ is unambiguosly determined by the sign of difference $m^2(x) - \varepsilon^2(x)$ in the region under consideration. We have exponentially descreasing solutions if $m^2(x) > \varepsilon^2(x)$ and the oscillating ones in the case $m^2(x) < \varepsilon^2(x)$. Eg. (6) clearly demonstrates the crucial role of the mass coordinate dependence as the neccessary confining condition:

If $m^2(x) = m_0^2$, we obtain equation

$$\frac{d^2\psi}{dx^2}+\varepsilon^2(x)\psi=m_0{}^2\psi$$

admittind asymptotically (at $x\to\infty$) oscillating solutions only.

Let us demonstrate that such a coordinate dependence arises purely geometrically when equations of motion are defined in space possessing conformally flat static metric [3], [4]

1.Classical picture: Geodesic equations in the conformally flat static metric.

Geodesic equation in general case is:

$$\frac{d^2x^\mu}{d\tau^2}+\Gamma^\mu_{\alpha\beta}\frac{dx^\alpha}{d\tau}\frac{dx^\beta}{d\tau}=0 \qquad (7)$$

where $\Gamma^\mu_{\alpha\beta}$ are the standard Christoffel symbols, dτ is the proper time element.

Let us consider the conformally flat metric with

$$g_{\mu\nu}=U^2(x)\eta_{\mu\nu}\,,\quad \eta_{\mu\nu}=diag(1,-1,-1,-1)\,, \qquad (8)$$

where $U(x)$ is some function, which depends on x^μ only.

The connection between the elements of proper time (dτ) and the laboratory one (dt) is:

$$d\tau=dtU(x)\sqrt{1-\frac{v^2}{e^2}} \qquad (9)$$

Geodesic equation (7) in the case of the metric (8) can be written in the following form:

$$\frac{d}{dt}\left(U^2\frac{dx^\mu}{d\tau}\right)-\frac{c^2}{2U^2}\eta^{\mu\nu}\frac{\partial(U^2)}{\partial x^\nu}=0\,, \qquad (10)$$

Being multiplied by the constant m_0 with the dimension of mass Eq. (10) can de written in the following noncovariant form:

$$\frac{d\underline{p}}{dt}+\frac{m_0^2c^2}{2M}grad(U^2)=0\,, \qquad (11a)$$

$$\frac{dE}{dt}-\frac{m_0^2c^2}{M}\frac{\partial(U^2)}{\partial t}=0 \qquad (11b)$$

where $\underline{p}=M\underline{v}$, $E=Mc^2$,

$$M=\frac{m_0U(x)}{\sqrt{1-\frac{v^2}{c^2}}} \qquad (12)$$

If the conformally flat metric is static one, i.e. $U(x)=U(\underline{r}),\frac{\partial(U^2)}{\partial t}=0$, equation (11b) leads to $\frac{dM}{dt}=0$ the "mass" M determined by (12) is conserved quantity (integral of motion) and one obtaines from (11a) the following equation:

$$M\frac{d^2r}{dt^2}+\frac{m_0^2}{M}grad(U^2)=0 \qquad (13)$$

This equation coincides formally with the nonrelativistic equation of motion of a "particle" possessing the "mass" M in a "potential field".

$$\underline{F}=-\frac{m_0c^2}{M}grad(U^2) \qquad (14)$$

The essentially new feature of the solutions of equation (13) is the existence of the peculiar parametric dependence on the initial comditions, because the integrals of motion appear in (13) instead of numerical constants.

We see that momentum $\underline{p}$ and energy E are connected by the standart condition

$$E^2-c^2p^2=m_0^2U^2(\underline{r})\,c^4$$

which showes that the quantity $m_0U(\underline{r})$ plays the role of coordinate-dependent rest mass. The same results can be certainly obtained via standard variational procelure with an action determined by linear element

$$ds=\left(g_{\mu\nu}dx^\mu dx^\nu\right)^{1/2}$$

defined by metric (8).

The corresponding Lagrangian is:

$$L = -m_0 c^2 U(\underline{r})\sqrt{1-\frac{v^2}{c^2}}.$$

2. Dirac eguation

Let us consider Dirac equation in the general covariant form [5]:

$$\gamma^\mu\left\{\partial_\mu\psi+\frac{1}{4}\gamma^\nu\left(\partial_\mu\gamma_\nu-\Gamma^\alpha_{\mu\nu}\gamma_\alpha\right)\psi\right\}+m_0\psi=0. \qquad (15)$$

Here γ^μ are generalized Dirac matrices satisfying the standard condition

$\gamma^\mu\gamma^\nu+\gamma^\nu\gamma^\mu=2g^{\mu\nu}$, $\Gamma^\alpha_{\mu\nu}$ are Christoffel symbols, m_0 is the rest mass.

Bispinor ψ satisfies the condition

$$i\int\bar{\psi}\gamma^\mu\psi df_\mu=1 \qquad (16)$$

$x^o = t = cons\ t$

$\bar{\psi}$ is the Dirac conjugated bispinor, df_μ is hypersurface $x^o = t = cons\ t$ element.

In the case of metric (8) γ matrices can be chosen in the following form:

$$\gamma_\mu = U(\underline{r})\overset{o}{\gamma}_\mu \qquad \left(\gamma^\mu = U^{-1}(\underline{r})\overset{o}{\gamma}^\mu\right), \qquad (17)$$

where $\overset{o}{\gamma}_\mu$ are constant Dirac matrices corresponding to the flat space-time, i.e.

$$\overset{o}{\gamma}^\mu\overset{o}{\gamma}^\nu+\overset{o}{\gamma}^\nu\overset{o}{\gamma}^\mu=2\eta^{\mu\nu}.$$

After substituting (17) in equations (15) and (16) we obtain Dirac equation in the following form:

$$i\frac{\partial\psi}{\partial t}=\left\{\alpha^\kappa\left(P_\kappa-\frac{3i}{2}U^{-1}\partial_\kappa U\right)+\beta m_o U\right\}\Psi, \qquad (18)$$

where $\alpha^\kappa=\overset{o}{\gamma}_o\overset{o}{\gamma}^\kappa, \beta=-i\overset{o}{\gamma}_o, P_\kappa=-i\partial_\kappa, c=\hbar=1$.

The normalizing condition (16) takes the form:

$$\int\psi^+\psi U^3 d^3x=1 \qquad \left(d^3x=dx^1dx^2dx^3\right)$$

$x^o = t = cons\ t$.

After introducing the new wave function

$$\Phi = U^{3/2}\Psi \qquad (19)$$

which satisfies the conventional normalization condition

$$\int\Phi^+\Phi d^3x=1$$

$x^o = t = cons\ t$

we obtain Dirac equation in the form

$$i\frac{\partial\phi}{\partial t}=\left\{\alpha^\kappa P_\kappa+\beta m_o U(\underline{r})\right\}\Phi \qquad (20)$$

We see that Dirac equation for the particle with rest mass m_o in conformally flat static metric $g_{\mu\nu}=U(\underline{r})\eta_{\mu\nu}$ coincides formally with Dirac equation for particle with some coordinate – dependent effective rest mass $m(\underline{r})=m_oU(\underline{r})$ in flat space–time.

The external fields can be included in (20) in a standard way.

3.Klein - Fock - Gordon (KFG) equation

The KFG equation

$$(\Box+\mu_o^2)\varphi=0 \qquad \left(\mu_o\frac{1}{\lambda}=\frac{m_oc}{\hbar}\right),$$

where

$$\Box=\frac{1}{\sqrt{-g}}\partial_\mu\left(\sqrt{-g}\ g^{\mu\nu}\partial_\nu\right)$$

in the case of metric (8) can be written in the following form:

$(\Box+\mu_o^2)\varphi =$

$$=\frac{1}{U^2}\left(\frac{1}{c^2}\frac{\partial^2}{\partial t^2}-\partial_\kappa^2\right)\varphi-\frac{2}{U^3}(\partial_\kappa U)\partial_\kappa\varphi+\mu_o^2\varphi=0 \qquad (21)$$

The term in (21) containing the first derivative $\partial_\kappa\varphi$ is excluded by the substitution:

$$\varphi=U^{-1}\phi.$$

Then (taking into account the condition $\frac{\partial u}{\partial t}=0$) KFG equation for the function ϕ is :

$$\left\{\frac{1}{c^2}\frac{\partial^2}{\partial t^2}-\partial_\kappa^2+U^{-1}\partial_\kappa^2 U+\mu_o^2U^2\right\}\phi=0 \qquad (22)$$

Thus we obtain the equation for the "particle", possessing the effective (coordinate-dependent) mass μ_o - determined by formula

$$M_o^2=\mu_o^2U^2+U^{-1}\partial_\kappa^2U$$

It is interesing to notice that conformally flat metric gives us some peculiar mechanism of "mass gneration': initially massless (m_o = o) particle behaves as the massive one possessing the coordinat-dependent mass

$$M_o=\left(U^{-1}\partial_\kappa^2U\right)^{\frac{1}{2}}$$

As an illustrative example let us consider the function

$$U=1+e^{-\kappa_o r}$$

corresponding to the metric which differs from flat one in the restricted space region $r\le\kappa_o^{-1}$ only and is asymptotically flat.

In this case we have

$$U^{-1}\partial_\kappa^2U=\left(e^{\kappa_o r}+1\right)^{-1}\left(\kappa_o^2-\frac{2\kappa_o}{r}\right).$$

This expression obviously trends to zero at r→∞. However at the small distances one obtaines

$$U^{-1}\partial_\kappa^2U_{at\ \ \kappa_o r\ll 1}\approx\kappa_o^2-\frac{\kappa_o}{r}-\frac{\kappa_o^3}{2}\cdot r$$

The KFG equation (22) for massless particle (m_o = 0) in this case takes the form:

$$\left\{\frac{1}{c^2}\frac{\partial^2}{\partial t^2}-\partial_\kappa^2+\kappa_o^2-\frac{\kappa_o}{r}-\frac{\kappa_o^3}{2}\cdot r\right\}\phi=0,$$

which corresponds the spinless particle possessing **rest mass** κ_o, moving in the static external field which is the sum of the Coloumb attractive and the lineary increasing repulsive potentials.

Phenomenological relativistic quark models and conformally-flat metric

As we have seen, making suitable choice of the conformally flat static metric, one can obtain confining solutions of Dirac equation, which is used in phenomenological relativistic quark models.

For example in the "new hadronization model" proposed in[6],[7] to explain the present data on charmed meson decays the quarks satisfy a generalized Dirac equation with the Hamiltonian

$$H_D=\alpha^\kappa\left(-i\partial_\kappa-ix_\kappa/x_o^2\right)+\beta m. \qquad (23)$$

The quark wave function therefore has the form:

$$\psi(\underline{r},t)=e^{-\frac{r^2}{2x_o^2}}e^{ip_\mu x^\mu} \qquad (24)$$

i.e. $\psi(\underline{r},t)$ is the plane wave damped by a gaussian factor $\left(e^{-\frac{r^2}{2x_o^2}}\right)$, x_o is the effective hadronization radius.

Comparing eq.(23) with Dirac equation (18) in the general case of the conformally flat static metric

$$g_{\mu\nu}=U^2(\underline{r})\eta_{\mu\nu},$$

and taking into account the general formula (19) $\Psi=U^{-3/2}\phi$ in the private case when $\phi=\exp\{ip_\mu x^\mu\}$, we obtain $U^{-3/2}(r)=e^{-\frac{r^2}{2x_o^2}}$, or $U(r)=e^{\frac{r^2}{3x_o^2}}$.

Thus we see that authors [6,7] actually deals with Dirac equation in the case of following conformally flat metric:

$$g_{\mu\nu}=e^{\frac{2r^2}{3x_o^2}}\eta_{\mu\nu} \qquad (25)$$

as it was shown in the paper [4].

In the case of metric (25) we obtain

$$U^{-1}\partial_\kappa^2U=\left(e^{-\frac{r^2}{3x_o^2}}\right)\partial_\kappa^2\left(e^{\frac{r^2}{3x_o^2}}\right)=\frac{2}{x_o^2}+\frac{4}{9}\frac{r^2}{x_o^4}.$$

The corresponding KFG equation (21) takes the form:

$$\left\{\frac{1}{c^2}\frac{\partial^2}{\partial t^2}-\partial_\kappa^2+m_o^2e^{\frac{2r^2}{3x_o^2}}+\frac{2}{x_o^2}+\frac{4}{9}\frac{r^2}{x_o^4}\right\}\phi=0 \qquad (26)$$

what coincides with the result obtained in[8]

To estimate the numerical value of x_o one can consider the small distance approximation (r/x_o « 1) to eg. (26). In this case to first order in

r^2/x_o^2 eq. (26) coincides formally with the energy eigenvalue equation for an isotropic harmonic oscillator.

The allowed values of the square of mass (M^2) in this approximation are given by (see[8]): $M^2 = m_o^2 + \frac{2}{x_o^2} + \frac{2m}{x_o}\cdot\sqrt{\frac{2}{3}}\cdot\left(1+\frac{2}{3m^2x_o^2}\right)^{1/2}\left(2n+\ell+\frac{3}{2}\right)$

(27)

(h = c = 1)

We see that in this picture the slope α' of a Regge trajectory depends on parameters m and x_o. In the case of sufficiently light confined particles ($mx_o \ll 1$) eq. (27) gives $\alpha' \cong \frac{3x_o^2}{4}$, and since $\alpha' \cong 1 Gev^{-2}$ we obtain an estimate of the parameter x_o: $x_o \approx 1{,}2$ Gev^{-1} in good agreement with the experimental value, $x_o \approx 1$ -1,5 Gev^{-1}, obtained from the data on charm decay.

Possible origin of the effective conformally-flat metric

The hypothesis of maximal acceleration was conjectured by Caianiello[9]. Different aspects, formulation and consequences of the possible existence of a limiting value to the proper acceleration of a particle were advanced on classical and quantum grounds by several authors (see, for example [10], [11] and the references there).

In particular the effective conformally flat metric can arise as an straight consequence of the existence of maximal acceleration.

The model proposed by Caianiello and his coworkers to include the effects of a maximal acceleration in a particle dynamics consisted in enlargihg the space – time manifold to an eight-dimensional space – time tangent bundle, where the coordinates are $X^a = \left\{x^\mu; \frac{c}{A}\dot{x}^\mu\right\}$, μ=1, ... 4, $\dot{x}^\mu = \frac{dx^\mu}{d\tau}$, A is the parameter whose dimension is acceleration.

The fundamental infinitesimal interval for a particle is the folloving eight-dimensional line element:

$$dS^2 = dx^\mu dx_\mu + \frac{c^2}{A^2} d\dot{x}^\mu d\dot{x}_\mu \qquad (28)$$

Assuming the background metric as the Minkowski one, i.e. $g_{\mu\nu} = \eta_{\mu\nu}$ = diag (1, -1, -1, -1) and taking into account $d\dot{x}^\mu = \ddot{x}^\mu d\tau$ we obtain from (28)

$$dS^2 = \left(1+\frac{\ddot{x}^\mu \ddot{x}_\mu}{A^2}\right)ds^2 \qquad (29)$$

where $\ddot{x}^\mu = \frac{d^2x^\mu}{d\tau^2}$, $ds^2 = dx^\mu dx_\mu = c^2 d\tau^2$, $\ddot{x}^\mu$ is a space-like vector (i.e. $\ddot{x}^\mu \ddot{x}_\mu < 0$. The explicit form of $\ddot{x}^\mu \ddot{x}_\mu$ in noncovariant notations is:

$$\ddot{x}^\mu \ddot{x}_\mu = -\left(1-\frac{v^2}{c^2}\right)^{-3}\left\{\underline{a}^2 - \frac{1}{c^2}(\underline{a}\times\underline{v})^2\right\} \qquad (30)$$

where $\underline{v} = \frac{d\underline{r}}{dt}$, $\underline{a} = \frac{d^2\underline{r}}{dt^2}$.

In the case $\underline{v} = 0$ (classical returning point) we obtain from (29), (30) the formula

$$dS^2 = c^2 d\tau^2\left(1-\frac{\underline{a}^2}{A^2}\right)$$

which demonstrate the limiting role of A.

The use of line element (29) as a starting point of particle dynamics (both classical and quantum) obviously leads as to the theory with high derivatives.

It is more productive to consider the acceleration field $\ddot{x}^\mu \ddot{x}_\mu$ of the particle as a result of its interaction with an external fields.

If one considers for simplicity the case of non-relativistic electron in an electrostatic external field $\underline{E}(r)$ the term $\ddot{x}^\mu \ddot{x}_\mu$ reduces to

$$|\ddot{\underline{r}}|^2 = \frac{e^2}{m^2}\cdot\underline{E}^2(r),$$

where if neglecting terms of order A^{-4} $\underline{E}(r)$ restricts to central electric field $E(r) = ze^2/r^2$.

Then from (29) we obtain

$$ds^2 = \left(1+\frac{1}{A^2}\ddot{x}^\mu \ddot{x}_\mu\right)ds^2 = \left(1-\left(\frac{r_o}{r}\right)^4\right)ds^2 = U^2 ds^2, \qquad (31)$$

where

$$U(r) = \left\{1-\frac{z^2e^4}{m^2A^2}\cdot\frac{1}{r^4}\right\}^{\frac{1}{2}} \qquad r_o = \left(\frac{Ze^2}{mA}\right)^{\frac{1}{2}} \qquad (32)$$

is the conformal factor.

The maximal acceleration corrections to the Lamb shift of one-electron atoms were calculated in [11] starting from the Dirac equation in conformally flat metric with the conformal factor determined by (32).

An interesting apporoach to explain the connection between maximal acceleration and the effective geometry proposed in[12].

They considered a particle of mass m and charge q moving in background Minkowski metric under the action of an externally applied electromagnetic field. The classical equation of motion is

$$dx^{\mu} = \frac{q}{mc} F^{\mu}_{\nu} dx^{\nu} \qquad (33)$$

This equation can be taken as the first order approximation to the real velocity fields of the particle. If one substitute (33) in (28) one can calculate the correction of order A^{-2} to the classical background metric $\eta_{\mu\nu}$. This procedure can be iterated, by calculating the new velocity field and substituting it again into the metric to obtain the corrections A^{-4} and so on. Because the value of the maximal acceleration is very high we can neglect $0(A^{-4})$ terms.This leads to metric

$$ds^2 = g_{\mu\nu} dx^{\mu} dx^{\nu},$$

where

$$\bar{g}_{\mu\nu} = \eta_{\mu\nu} - \frac{q^2}{A^2 m^2} F_{\mu\nu} F^{\alpha}_{\nu} \qquad (34)$$

The effective geometry is curved by the acceleration due to the interaction of the charges particle with the electromagnetic field and this curvature affects the motion of the particle itself.

The modifield equation of motion of the charged particle may be obtained from the action

$$S = \int \left\{ -mc^2 \left(\bar{g}_{\mu\nu} dx^{\mu} dx^{\nu} \right)^{\frac{1}{2}} + qA_{\mu} x^{\mu} \right\} d\tau .$$

Now we notice that the alternative starting point to introduce the fundamental infinitesimal interval of the type given by (28) is the Born reciprocity principle[13]. The corresponding reciprocity-invariant interval is:

$$dS^2 = ds^2 + \frac{1}{\kappa_0^2} d\rho^{\mu} d\rho_{\mu}, \qquad (35)$$

where ρ^{μ} is a momentum, and κ_0 is a constant, whith dimention momentum/length or energy/time. This constant was introduced by author

in 1974 [14]. $\kappa_0 = \frac{dm_0}{d\tau}$. Inthe limit $\kappa_0 \to \infty \left(\frac{dm}{d\tau} << x_0 \right)$ arises two independent Lorenz-invariant intervals in Minkovski and momentum spaces correspondingly. The connection between κ_0 and the maximal acceleration is : $A = m^{-1} c \kappa_0$

The interval (35) can be written in the following form

$$dS^2 = \left(1 + \frac{1}{\kappa_0^2} \frac{d\rho^{\mu}}{ds} \frac{d\rho_{\mu}}{ds} \right) ds^2 \qquad (36)$$

Using the equation of motion $\frac{d\rho^{\mu}}{ds} = \frac{e}{c^2} F^{\mu}_{\nu} U^{\nu}$ and introducing a new constant $g_0 = \frac{c\kappa_0^2}{\hbar}$ with dimention of energy density (maximal energy density) we obtain

$$dS^2 = \left\{ 1 + \frac{\alpha_0}{\rho_0} F_{\mu}^{\alpha} F_{\nu\alpha} U^{\mu} U^{\nu} \right\} ds^2, \qquad (37)$$

where $\alpha_0 = e^2 / \hbar c$.

Being expressed by the standard electromagnetic energy-momentum tensor $T^{(e\text{-}m)}_{\mu\nu}$ notations formula (37) gives:

$$dS^2 = \left\{ 1 - \frac{4\pi\alpha_0}{\rho_0} \left(c^{-2} T^{(e-m)}_{\mu\nu} U^{\mu} U^{\nu} + L^{(e-m)} \right) \right\}^2 ds^2, \qquad (38)$$

where $L^{(e\text{-}m)}$ is the standard electromagnetic field Lagrandian.
In the comoving reference frame we obtain from (38):

$$dS = \left(1 - \frac{\alpha_0}{\rho_0} \underline{E}^2 \right)^{\frac{1}{2}} ds$$

($\underline{E}$ – is the electric fields vector). This leads exactly to the conformal factor introduced in [11] by calculating maximal acceleration cirrection to the Lamb shift. Itis very tempting to suppose that (38) gives us some universal rule, which is suitable for any particles interacting with corresponding external field via coupling constant α. I.e.

$$dS = \left\{ 1 - \frac{4\pi\alpha}{\rho_0} \left(\frac{1}{c^2} T^{(f)}_{\mu\nu} U^{\mu} U^{\nu} + L^{(f)} \right) \right\}^{\frac{1}{2}} ds$$

where $T_{\mu\nu}^{(f)}$ and $L^{(f)}$ are the external field energy-momentum tensor and Lagrangian correspondingly.

References

[1] Calucci G.Lett.Nuovo Cim.,1979, **26**,449.Ono S.Phys.Rev.,1982, **D26**, 2510. Ravndal P.Phys.Lett., 1982, **113B**, 57.

[2] Bykov A.A., Dremin I.M.., Leonidov A.B.. Pisma JETP, 1983, **193**, 33. Usp.Fiz.Nauk, 1984, **143**,3.

[3] Gorbatsevich A.K., Tomilchik L.M. (1986). Preprint N415 Phys.Inst.Ac.Sci. of Belarus, Minsk: High Energy Physics Problems (Proc. IX Seminar, Protvino, 1987, Moscow, "Science", pp.378-383. (in russian)

[4] Gasperini M., 1987, Phys.Lett. **B195**, 453.

[5] Schmutzer E. Relativistische Physik, 1968, Leipzig.

[6] Basdevant J.L., Bediaga I., Predazzi, (1987), Nuclear Physics **B294**, 1054-1070.

[7] Basdevant J.L., Bediaga I., Predazzi E., Tiomno J. Ibid. 1071-1080.

[8] Caianiello E.R., Gasperini M., Predazzi E., Scarpetta G., 1988, Phys.Lett.**A132**, 82-84.

[9] Caianiello E.R. 1981, Lett.Nuovo Cimento, **32**, 65; Rivisita del Nuovo Cimento, 1992, **15**, p.4.

[10] Papini G., Feoli A., Scarpetta G. 1995, Phys.Lett. **A202**, 50.

[11] Lambiase G., Papini G., Scarpetta G., 1997, hep-th/9702130, 17 Feb.

[12] Feoli A., Lambiase G., Papini G., Scarpetta G. (1997), hep-th/9702131, 17 Feb.

[13] M.Born. Rev.Mod.Phys, 21, 463 (1949).

[14]Tomilchik L.M. Vesti AN BSSR, ser. Fiz.-mat.nauk, N4,1974, p.72. (Proc.Belorussian Ac.Sci. in russian).

Relativistic Physics of hadrons and nuclei

The mesons in relativistic Hamiltonian dynamics

V. V. Andreev [1]
Gomel State University, Physics Department, 246699 Gomel, Belarus

Abstract

We consider a model of meson, based on the Poincare'-covariant quark model with analytical solution of the mass spectrum. We investigate possible limitations of model parameters, implied from the lepton decay constants as well as from the mass spectrum of light mesons.

1 Introduction

The investigation of bound states of particles is one of the effective methods to study the properties and dynamics of the interaction of particles. This method is widely used in various areas of nuclear physics and physics of elementary particles. In studies of properties of quarks, of which the mesons and baryons consist, this method has important value, as the quarks are not observed as free states. Today, the electroweak decays of hadrons enable us to measure the parameters of the Standard Model (SM), and also these decays are the tool of exploration of effects of new physics i.e. physics beyond the SM. In particular, the hadronic decays allow determining the elements of a mass matrix, as well as angles of mixing. The leptonic decays of pseudoscalar mesons in a model with two charged Higgs bosons become sensitive to masses of these bosons [1]. Information about the structure of hadrons are required for these investigations and it is important to have the description of properties of hadrons in the framework the relativistic models of bound states.

Many different descriptions of relativistic bound systems have been developed and even a brief survey of the vast literature on this subject goes far beyond the scope of this paper. In the present work, for the description of bound states, we use a Poincare'-covariant model of hadrons. The basis of this model is a constituent quark model and Relativistic Hamiltonian Dynamics (RHD)[2] .

The aim of this work is to present combined description of lepton decay constants of pseudoscalar meson and Regge trajectories of light meson in the Poincare' covariant quark model, based on the point form of the RHD. We consider a simple model with an analytical solution of the mass spectrum and investigate the possible limitations of model parameters, implied from the lepton decay constants as well as the mass spectrum of light mesons.

2 Bound quark–antiquark of a state in the RHD

In the quark model the mesons represent a system consisting of a quark and an antiquark. In the framework of RHD, the interaction, which is determined by the generators of the Poincare' group $\hat{P}_\mu$ and $\hat{M}^{\mu\nu}$ is introduced as follows. The construction of generators

[1]E-mail: andreev@gsu.unibel.by

for a system of interacting particles starts from the generators of an appropriate system composed out of noninteracting particles (further we shall note such operators without "hat"), and then add interaction so that the obtained generators also satisfy the commutation relations of Poincare' group. Unlike the case of a usual nonrelativistic quantum mechanics, in the relativistic case it is necessary to add interaction $\hat{U}$ in more than one generator to satisfy the algebra of the Poincare' group . Dirac [3] has shown that there is no unambiguous separation of generators into the dynamic set (generators containing the interaction $\hat{U}$) and a kinematic set. There are three versions of separation on dynamic and kinematic sets (so-called RHD forms): the point, instant form and dynamics on light front. In all three forms the interaction contains mass operator $\hat{M}$ i.e. $\hat{M} \equiv M_0 + \hat{U}$, where M_0 is an effective mass of a system of noninteracting particles. In an instant form the interaction enters also in the operator of a boost $\vec{N} = (\widehat{M}^{01}, \widehat{M}^{02}, \widehat{M}^{03})$, which makes wave functions of mesons Lorentz -noninvariant. In the dynamics on light front the interaction is contained with components J_1, J_2 of the operator of an angular momentum $\vec{J} = \vec{J}$ $(\vec{J}=(\widehat{M}^{23}, \widehat{M}^{31}, \widehat{M}^{12}))$, that results in violation of a rotational covariance. In a point form RHD 4-velocities of bound and noninteracting systems are equal, i.e.

$$\hat{V} = \hat{V}_{12}, V = P/M, \quad V_{12} = P_{12}/M_0, \tag{1}$$

where P and P_{12} are the 4-momenta of the bound and free from the interactions of particle system. In all forms of the RHD 4-momentum of a bound system P and total momentum of free particles are not equal, i.e. $P \neq P_{12}$.

Let's consider in the context of RHD, a bound state with momentum P, mass M, spin J and it's projection μ consisting of two particles. Let these particles have the following characteristics: momenta p_1 and p_2, masses m_1, m_2, spins s_1 and s_2, projection of spins λ_1 and λ_2. The construction of a bound two-particle state includes the following stage [2]:

1. Definition of the two-particle Hilbert space as the tensor product of the one-particle spaces and of the appropriate basis:

$$|p_1\lambda_1\rangle\,|p_2\lambda_2\rangle \equiv |m_1 s_1; p_1\lambda_1\rangle \otimes |m_2 s_2; p_2\lambda_2\rangle \tag{2}$$

with the normalization

$$\langle p_1'\lambda_1'|\,\langle p_2'\lambda_2'|\,|p_1\lambda_1\rangle\,|p_2\lambda_2\rangle = \delta_{\lambda_1'\lambda_1}\delta_{\lambda_2'\lambda_2}\delta(\vec{p}_1' - \vec{p}_1)\delta(\vec{p}_2' - \vec{p}_2).$$

2. The Clebsch-Gordon coefficients of the Poincare' group are constructed and are used to reduce the two-particle representation of a Poincare' group to linear superposition (direct integral) of irreducible representations. As result we obtain the basis:

$$\left|\vec{P}_{12}, \mu, [J, M_0(k)], (ls); [m_1 s_1; m_2 s_2]\right\rangle =$$

$$\sum_{ls}\sum_{\lambda_1\lambda_2}\int d\tilde{\vec{k}}\sqrt{\frac{\omega_{m_1}(\vec{p}_1)\,\omega_{m_2}(\vec{p}_2)\,M_0}{\omega_{m_1}(\vec{k})\omega_{m_2}(\vec{k})\omega_{M_0}(\vec{P}_{12})}}$$

$$\sum_{m\lambda}\sum_{\nu_1\nu_2}\langle s_1\nu_1, s_2\nu_2|\,s\lambda\rangle\,\langle lm, s\lambda|\,J\mu\rangle\,Y_{lm}\left(\tilde{\vec{k}}\right)$$

$$D^{1/2}_{\lambda_1\nu_1}(\vec{n}\,(p_1, P_{12}))\,D^{1/2}_{\lambda_2\nu_2}(\vec{n}\,(p_2, P_{12}))\,|p_1\lambda_1\rangle\,|p_2\lambda_2\rangle\,, \tag{3}$$

We used the following notations:

$$P_{12} = p_1 + p_2$$

is the total momentum of a free system, whereas

$$\vec{k} = \vec{p}_1 + \frac{\vec{P}_{12}}{M_0}\left(\frac{\vec{P}_{12}\cdot\vec{p}_1}{\omega_{M_0}(\vec{P}_{12}) + M_0} + \omega_{m_1}(\vec{p}_1)\right), \widehat{\vec{k}} = \vec{k}/\left|\vec{k}\right|$$

is the relative momentum of two particles, and $\langle s_1\nu_1, s_2\nu_2|\,s\lambda\rangle$, $\langle lm, s\lambda|\,J\mu\rangle$ are Clebsch-Gordon coefficients of SU(2)-group. The function $Y_{lm}(\tilde{\vec{k}})$ is spherical harmonics and $D^{1/2}(\vec{n}) = 1 - i\vec{n}\cdot\vec{\sigma}/\sqrt{1+\vec{n}^2}$ is the D-function of Wigner rotation, which is determined by the vector-parameter $\vec{n}(p_1, p_2) = \vec{u}_1 \times \vec{u}_2/(1 - \vec{u}_1\cdot\vec{u}_2)$ with $\vec{u} = \vec{p}/\,(\omega_m\,(\vec{p}) + m)$. Apart from that, the following reductions are used:

$$\begin{aligned} M_0 &= M_0(k) = \omega_{m_1}(\vec{k}) + \omega_{m_2}(\vec{k}), \\ \omega_m(\vec{k}) &= \sqrt{k^2 + m^2}, k \equiv \left|\vec{k}\right|. \end{aligned} \tag{4}$$

The following step consists of adding the interaction $\hat{U}$ to the mass operator of a noninteracting system:

$$\widehat{M} = M_0 + \hat{U}.$$

If the operator $\hat{U}$ satisfies the conditions:

$$\hat{M} = \hat{M}^\dagger, \quad M > 0,$$

$$[\vec{P}_{12}, \hat{U}]_- = [i\vec{\nabla}_{\vec{p}_{12}}, \hat{U}]_- = [\vec{J}, \hat{U}]_- = 0 \tag{5}$$

then a similar set of interacting particles will satisfy the same commutation relations as the set of non-interacting system.

The problem of eigenvalues of the mass of a bound system can be expressed in three equivalent forms in the Hilbert space[2]:

$$\widehat{M}\mid\Psi> \equiv (M_0 + \hat{U})\mid\Psi> = M\mid\Psi>,$$

$$M_0^2 + \widehat{W}_U\mid\Psi> = M^2\mid\Psi>, \widehat{W}_U = \widehat{M}^2 - M_0^2,$$

$$(k^2 + \hat{W})\mid\Psi> = \eta\mid\Psi>, \widehat{W} = \frac{1}{4}\left[\left(\widehat{M}^2 - M_0^2\right) + \left(m_1^2 - m_2^2\right) * \left(\frac{1}{\widehat{M}^2} - \frac{1}{M_0^2}\right)\right], \tag{6}$$

where M and η are connected:

$$M^2 = 2\eta + m_1^2 + m_2^2 + 2\sqrt{\eta(\eta + m_1^2 + m_2^2) + m_1^2 m_2^2}. \tag{7}$$

The solution of the problem (6) will allow to find wave functions, which determine the vertex of the transition from free from interaction to a bound system of particles. In the point form this wave function is determined as follows:

$$\left\langle \vec{V}_{12}, J, \mu, k, (ls)\left|\vec{V}, J', \mu', M\right.\right\rangle = \delta_{JJ'}\delta_{\mu\mu'}\delta(\vec{V} - \vec{V}_{12})\Psi^{J\mu}(k\,l\,s)\,. \tag{8}$$

Wave function generally satisfies the integro-differential equation, which follows from Egs.(6) and (8):

$$\sum_{l's'}\int_0^\infty < k\,l\,s \parallel \widehat{W}^J \parallel k'\,l'\,s' > \Psi^J(k'\,l'\,s';\,M)k'^2dk' +$$

$$+k^2\Psi^J(k\,l\,s) = \eta\Psi^J(k\,l\,s) \qquad (9)$$

with the reduced matrix element of operator $\widehat{W}$

$$\left\langle \vec{V}_{12}, J, \mu, k, (ls)\right|\widehat{W}\left|\vec{V}'_{12}, J', \mu', k', (l's')\right\rangle =$$

$$\delta_{JJ'}\delta_{\mu\mu'}\delta(\vec{V}_{12}-\vec{V}'_{12})\left\langle k,(ls)\right\|\widehat{W}^J\left\|k',(l's')\right\rangle. \qquad (10)$$

The wave functions are normalized:

$$N_c\sum_{ls}\int_0^\infty dk\,k^2\left|\Psi^J(kls)\right|^2 = 1, \qquad (11)$$

where N_c is the number of quark colors. Thus in the point form the meson state is defined as state of on-shell quark and antiquark with the meson wave function $\Psi^J(kls)$

$$\begin{aligned}\left|\vec{P},J,\mu,M\right\rangle &= \sqrt{\frac{M}{\omega_M\left(\vec{P}\right)}}\sum_{ls}\sum_{\lambda_1\lambda_2}\int d^3k\sqrt{\frac{\omega_{m_1}\left(\vec{p}_1\right)\omega_{m_2}\left(\vec{p}_2\right)}{\omega_{m_1}\left(\vec{k}\right)\omega_{m_2}\left(\vec{k}\right)}}\\ &\Psi^J(kls)\sum_{m\lambda}\sum_{\nu_1\nu_2}\left\langle s_1\nu_1,s_2\nu_2\right|s\lambda\rangle\left\langle lm,s\lambda\right|J\mu\rangle Y_{lm}\left(\vec{\widehat{k}}\right)\\ &D^{1/2}_{\lambda_1\nu_1}\left(\vec{n}\left(p_1,P_{12}\right)\right)D^{1/2}_{\lambda_2\nu_2}\left(\vec{n}\left(p_2,P_{12}\right)\right)\left|p_1\lambda_1\right\rangle\left|p_2\lambda_2\right\rangle. \qquad (12)\end{aligned}$$

Let's mark, equation (9) for a wave function is a similar radial equation in a quantum mechanics (only the impulse representation).

3 Regge trajectories of mesons in Poincare'-covariant quark model

In this section we apply the formalism developed above to calculate the mass spectra of mesons containing u, d and s quarks. To choose the appropriate interquark potential we use the well-known experimental fact that light hadrons populate approximately linear Regge trajectories, i.e. $M^2 \simeq \beta l + const$, with the same slope $\beta \simeq 1.2\ GeV^2$, for all trajectories (see, for example, [4]). We take the effective model potential $\widehat{W}$ in the oscillator form with spin-spin interaction $a_s\left(\vec{\widehat{s}}_1\vec{\widehat{s}}_2\right)$

$$\hat{W}(r) = W_0\,\delta(\vec{r}) + \beta^4_{qQ}\vec{r}^2 + a_s\left(\vec{\widehat{s}}_1\vec{\widehat{s}}_2\right) \qquad (13)$$

where W_0, a_s and β_{qQ} are free parameters.

Using standard relations for the coordinate operator, orbital momentum and spin operators we reduce the integro-differential equation of RHD (9) to the ordinary quantum-mechanical radial equation with the oscillator potential (only impulse representation)

$$\left[\frac{\partial^2}{\partial k^2}+\frac{2}{k}\frac{\partial}{\partial k}-\frac{l(l+1)}{k^2}-\frac{k^2}{\beta^4_{qQ}}\right]\Psi(kls) = \frac{\widetilde{W}_0-\eta}{\beta^4_{qQ}}\Psi(kls),$$

$$\widetilde{W}_0 = W_0 + a_s\left(-\delta_{s0}\frac{3}{4}+\delta_{s1}\frac{1}{4}\right). \qquad (14)$$

The eigenfunctions of Eq. (14) are

$$\Psi(kls) = N_{nl}\exp\left(-\frac{k^2}{2\beta^2_{qQ}}\right)\left(\frac{k}{\beta_{qQ}}\right)^l F\left(-n,l+\frac{3}{2},\frac{k^2}{\beta^2_{qQ}}\right) \qquad (15)$$

with

$$N_{nl} = \frac{\beta_{qQ}^{-l-3/2}}{\Gamma(l+3/2)}\sqrt{\frac{\Gamma(n+l+3/2)}{\Gamma(n+1)}},$$

where $n, l = 0, 1, 2\ldots$, $F(a,b,z)$ is the hypergeometric function, $\Gamma(n)$ is the Gamma function. Note that the wave function of the ground state $(n, l = 0)$ has the oscillator form, which is used in many relativistic models of hadrons:

$$\Psi(kls) \equiv \Psi(k,\beta_{qQ}) = 2/\left(\beta^{3/2}_{qQ}\pi^{1/4}\right)\exp\left(-\frac{k^2}{2\beta^2_{qQ}}\right). \qquad (16)$$

Quantization condition is defined by

$$\eta = W_0 + 2\beta^2_{qQ}\left(2n+l+3/2\right) + a_s\left(-\delta_{s0}\frac{3}{4}+\delta_{s1}\frac{1}{4}\right). \qquad (17)$$

The spectra of mesons, composed of quarks with equal masses ($m_q = m_Q \equiv m$) are given by:

$$M^2_{qQ}(l) = 4\left(m^2 + W_0 + a_s\left(-\delta_{s0}\frac{3}{4}+\delta_{s1}\frac{1}{4}\right)\right) + 8\beta^2_{qQ}\left(2n+l+\frac{3}{2}\right). \qquad (18)$$

Thus we reproduce the linear dependence of $M^2(l)$ in the framework of the two-body relativistic equation (9).

Now we determine possible limitations on parameters of the bound systems with equal quark masses ($u-d$ and $s-\bar{s}$ states), which are implied from meson Regge trajectories.

The parameters $\widetilde{W}_0$ and β_{uu} have been found from fitting the ρ-Regge trajectories (see Fig.1):

$$m_u^2 + W_0 + a_s\frac{1}{4} = -0.28962 \pm 0.0264\,GeV^2, \beta_{uu} = 0.3818 \pm 0.0116\,GeV. \qquad (19)$$

If we assume that $\beta_{uu} = \beta_{ud} = \beta_{dd}$, we obtain that the differences of the squared masses of spin-singlet and spin-triplet for $u-d$ systems are determined by $M^2_{S=1}(l=0) -$

$M^2_{S=0}(l=0) = 4a_s$. Using that $M^2_\rho - M^2_\pi = 0.5711\,GeV^2$ we see that parameter of spin-spin interaction have value:

$$a_s = 0.14275 \pm 0.00025\,GeV^2. \tag{20}$$

Experimentally, the differences of the squared masses of corresponding spin-singlet and spin-triplet quarkonium states, which contain at least one light quark, weakly depend from quark masses. For example

$$M^2_\rho - M^2_\pi = 0.5711\,GeV^2, M^2_{K^*} - M^2_K = 0.55\,GeV^2, M^2_{D^*} - M^2_D = 0.55\,GeV^2.$$

Therefore we suggest that parameter a_s does not depend from masses of quarks. Thus we have that

$$m_u^2 + W_0 = -0.3253 \pm 0.0264\,GeV^2. \tag{21}$$

There are eight meson Regge trajectories populated by $u-d$ bound states (for each isospin I and angular momenta $J = l+1, J = l, J = l-1$ and total spin S of qQ system-$S = 0, 1$). Some of the trajectories are plotted in Fig.2 using parameters (19)-(21). We observe that all experimental data are in good agreement with the spectrum given by Eq.(9) for $S = 1$ (Fig.2a-2b). As in the case of bound states with $S = 0$, the agreement between our theoretical predictions and the existing experimental data is not good (see Fig.2c-2d). Such deviations can be explained by the absence of tensor spin-dependent terms, short-distance term of the potential and octet-singlet mixing for the η-meson trajectory.

If we shall assume "ideal" mixing for ϕ meson i.e. the mesons, which correspond to ϕ-meson Regge trajectory (see Fig.3), consist of only s-quarks, from linear fit (18), we obtain

$$\begin{array}{c} \beta_{ss} = 0.400077 \pm 0.00841\,GeV, \\ m_s^2 + W_0 = -0.26486 \pm 0.02013\,GeV^2. \end{array} \tag{22}$$

We can also find a ratio between masses of quarks. It is easy to verify, that m_s and m_u have the relation

$$m_s^2 - m_u^2 = 0.06044 \pm 0.0332\,GeV^2. \tag{23}$$

Thus, using Regge trajectories of mesons containing quarks with equal masses we have the following limitations of model parameters:

$$\begin{array}{rcl} a_s & = & 0.14275 \pm 0.00025\,GeV^2, \\ \beta_{uu} & = & \beta_{ud} = \beta_{dd} = 0.3818 \pm 0.0115\,GeV, \\ \beta_{ss} & = & 0.400077 \pm 0.00841\,GeV, \\ m_u^2 + W_0 & = & -0.3253 \pm 0.0264\,GeV^2, \\ m_s^2 + W_0 & = & -0.26486 \pm 0.02013\,GeV^2. \end{array} \tag{24}$$

As is easy to see, our method for bound systems with different quark masses does not require a special procedure to solve the main equation of RHD (9), as was pointed out in [4] (introduction of additional parameter). When the masses of the quark and antiquark are different, using Eq.(7) M^2_{qQ} can be written

$$\begin{array}{c} M^2_{qQ}(l) = \\ 2\eta + m_q^2 + m_Q^2 + 2\sqrt{\eta(\eta + m_q^2 + m_Q^2) + m_q^2 m_Q^2} = \\ \left(2\eta + m_q^2 + m_Q^2\right)\sqrt{1 - \left(m_q^2 - m_Q^2\right)^2 / \left(2\eta + m_q^2 + m_Q^2\right)^2}, \end{array} \tag{25}$$

where the quantization condition of the η is defined by Eq.(17). The dependence $M^2_{qQ}(l)$ is also linear if we assume that in Eq.(25)

$$\left(m_q^2 - m_Q^2\right)^2 / \left(2\eta + m_q^2 + m_Q^2\right)^2 \ll 1.$$

However, from the analysis the Regge of trajectories, we cannot fix masses of the quarks. Therefore the additional experimental data are necessary for further analysis. We shall consider the limitations that we can obtain from alternative experimental data. Then we shall again pass to the construction of the Regge trajectories of mesons with strange quark.

Concluding this section, we remark that, the analytical solution of a main equation of the RHD can be used as zero approximation for solving the problem with more realistic potentials.

4 Leptonic decays in a Poincare'-covariant model of mesons

In this section we shall consider possible constraints on the parameters of the model, which can be obtained from leptonic decays of pseudoscalar mesons (pion, kaon). In the SM the width of purely leptonic decays of charged mesons $P^+(Q\bar{q}) \to l^+\nu_l$ has the expression:

$$\Gamma_{SM}\left(P^+ \to l^+\nu_l\right) = \frac{G_F^2}{8\pi}|V_{qQ}|^2 f_P^2 m_l^2 M_P \left(1 - \frac{m_l^2}{M_P^2}\right)^2, \tag{26}$$

where G_F is a Fermi constant and m_l,M_P are the masses of the charged lepton l^+ and of the pseudoscalar meson P, respectively. The leptonic decay constant f_p of a pseudoscalar meson $P(Q\bar{q})$ is defined by the matrix element

$$\left\langle 0\left|\hat{J}^h_\mu(0)\right|\vec{P}, M_P\right\rangle = i\,(1/2\pi)^{3/2}\frac{1}{\sqrt{2\omega_{M_P}\left(\vec{P}\right)}}P_\mu f_P, \tag{27}$$

where $\hat{J}^h_\mu(0)$ is the operator of the meson current.

Using the relativistic impulse approximation and Eqs.(8),(12) we find that in the point form dynamics

$$\begin{array}{c} f_P(m_q, m_Q, \beta_{qQ}) = \\ N_c/\left(\pi\sqrt{2}\right)(m_q + m_Q)\int_0^\infty dk\,k^2\,\Psi(k, \beta_{qQ})\sqrt{\frac{M_0^2 - (m_q - m_Q)^2}{\omega_{m_q}\left(\vec{k}\right)\omega_{m_Q}\left(\vec{k}\right)M_0^3}}, \end{array} \tag{28}$$

where N_c is the number of colors, m_q and m_Q are the masses of the quarks. If $m_q = m_Q$, the leptonic decay constant is defined by

$$f_P(m_Q, \beta_{qQ}) = \frac{N_c m_Q}{\pi}\int_0^\infty \frac{dk\,k^2\Psi(k, \beta_{qQ})}{\omega^{3/2}_{m_Q}\left(\vec{k}\right)}. \tag{29}$$

For further calculations we shall use the wave function of oscillator form (16), which is the solution equation of the relativistic bound states with model potential (13). Using the experimental values of the pion and kaon decay constants and the theoretically calculated formula we shall receive the limitations on parameters of the model. The modern experimental data give the following values of constants of decays of a pion and kaon [5]:

$$f_\pi^{\exp} = 0.130.7 \pm 0.00046 \;\; GeV, \quad f_K^{\exp} = 0.1598 \pm 0.00188 \, GeV.$$

The π-meson decay constant is defined by

$$f_\pi(m_u, \beta_{ud}) = \frac{\sqrt{3} m_u}{\pi^{5/4}\Gamma\left(-\frac{1}{4}\right)} \left[2^{3/4}\Gamma\left(-\frac{1}{4}\right)\Gamma\left(\frac{3}{4}\right) {}_1F_1\left(\frac{3}{4}; \frac{1}{4}; \frac{m_u^2}{2\beta_{ud}^2}\right) - \frac{2 m_u^{3/2}\sqrt{\pi}}{\beta_{ud}^{3/2}}\Gamma\left(-\frac{3}{4}\right) {}_1F_1\left(\frac{3}{2}; \frac{7}{4}; \frac{m_u^2}{2\beta_{ud}^2}\right)\right]. \quad (30)$$

For the decay of the K-meson, which consists of quarks of different mass, the decay constant is set by Eq.(28). To obtain the limitations on the parameters of model, it is necessary to solve the set of equations:

$$f_\pi(m_u, \beta_{ud}) = f_\pi^{exp}, \;\; f_K(m_u, m_s, \beta_{us}) = f_K^{exp}. \quad (31)$$

For the solution of this system of equations we use the following procedure: we get the limitations on m_u, β_{ud}, which follow from the first equation of a system (31). Further let's assume, that

$$m_s = a * m_u, \beta_{us} = V * \beta_{ud}, \quad (32)$$

where a, V are some numbers. The values of a and V are obtained by minimization of deviation

$$|f_K(m_u, \beta_{ud}, a, V) - f_K^{\exp}|.$$

Graphically it means, that the solution points coincide for both experiments on the plane $m_u - \beta_{ud}$. The result of the procedure are displayed in Fig.4. The coincidence curve is achieved at $a = 1.48, V = 1.236$. If we assume that $\beta_{ud} = 0.329 \, GeV$ (see Fig.4), we receive

$$\begin{aligned} cm_u &= 0.250 \, GeV, \;\; m_s = 0.370 \, GeV, \\ \beta_{us} &= 0.407 \, GeV. \end{aligned} \quad (33)$$

This result (33) agrees with the results obtained in the instant form of the RHD for oscillator wave function [6]. In the dynamics of light front for the data of the quark masses and the parameter β of the wave function are approximately equal numerically (33) [7]. Now we shall use the value of the parameters β_{ud}, which we have found from the analysis of the Regge trajectories (see (24))-$\beta_{ud} = 0.3818 \, GeV$. In this case we obtain, that

$$m_u = 0.216 \pm 0.02 \, GeV, \;\; m_s = 0.320 \pm 0.03 \, GeV.$$

We shall return to the analysis of the Regge trajectories. When the masses of quarks are fixed we can calculate the remaining parameters of a model potential. So from a ratio (24) we receive for the parameter W_0 the following value:

$$W_0 = -0.3720 \pm 0.0264 \, GeV^2.$$

Using mass pseudoscalar K-meson $m_K = 0.4937 \, GeV$ and equation (25) we obtain, that parameter of a wave function β_{us} is equal:

$$\beta_{us} = 0.3925 \pm 0.06 \, GeV.$$

Thus for mesons containing u, d and s quark with the interquark potential (13) we have:

$$\begin{aligned} a_s &= 0.14275 \pm 0.00025 \, GeV^2, \\ \beta_{uu} &= \beta_{ud} = \beta_{dd} = 0.3818 \pm 0.0115 \, GeV, \\ \beta_{us} &= 0.3925 \pm 0.06 \, GeV, \\ \beta_{ss} &= 0.400077 \pm 0.00841 \, GeV, \\ W_0 &= -0.3720 \pm 0.0264 \, GeV^2 \\ m_u &= m_d = 0.216 \pm 0.02 \, GeV, \\ m_s &= 0.320 \pm 0.03 \, GeV. \end{aligned} \quad (34)$$

Let's remark, that the squared masses of the u and s-quarks, obtained from the leptonic decay constants, and from the analysis of the ϕ-meson Regge trajectories are approximately agreed (see (23) and (34))

$$\begin{aligned} m_s^2 - m_u^2 &= 0.056 \pm 0.021 \, GeV^2 - leptonic \; decays, \\ m_s^2 - m_u^2 &= 0.06044 \pm 0.0332 \, GeV^2 - Regge \; trajectories. \end{aligned}$$

The evalutations of parameter $V = \beta_{us}/\beta_{ud}$ are agreed little a bit worse

$$\begin{aligned} V &= 1.236 \pm 0.020 - leptonic \; decays, \\ V &= 1.02 \pm 0.30 - Regge \; trajectories. \end{aligned}$$

We compute the strange meson Regge trajectories using Eqs.(25) and (34) (see Fig.5). The model describes two Regge trajectories with $S = 1$ and and one with $S = 0$ in quite a satisfactory way (see Fig.5a, 5b, 5d). But for the K^*-meson trajectory the agreement between the model and the experimental data is not good (see Fig.5c)

Thus, in the framework of the model of the mesons based on a point form of the RHD with seven parameters we have a satisfactory description of decay constants of pseudoscalar mesons and their masses. Also the model potential, which solves the equation of the bound two-particle relativistic system with an adequate accuracy reproduces the Regge trajectories of light mesons. But a realistic potential (one boson exchange + nonperturbative part of potential+$\cdots$) is necessary for a more satisfactory description of the spectrum of masses.

References

[1] W.S.Hou, Phys. Rev.D, **48** (1993), P.2342.

[2] B.D.Keister, W.N.Polyzou, Adv. Nucl. Phys., **20** (1991), P.225.

[3] P.A.M. Dirac, Rev.Mod. Phys., **21** (1949), P.392.

[4] E. Di Salvo, L. Kondratyuk, P. Saracco, Z.Phys., C69 (1995), P.149.

[5] Review of Particle Properties, Phys. Rev.D, 54 (1996), P.1.

[6] A.F.Krutov,Sov J. Nucl. Phys., 60 (1997), P.1442.

[7] W.Jaus, Phys. Rev.D, 44 (1991), P.2851.

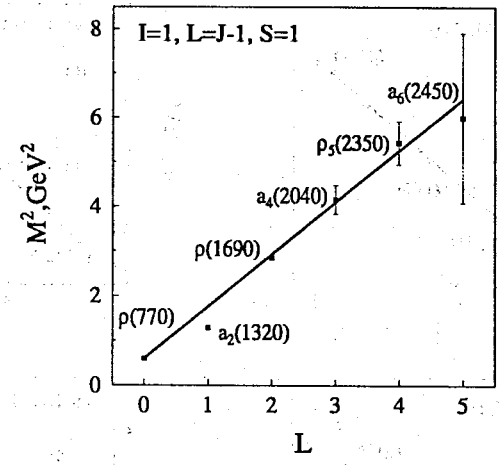

Figure 1: ρ-meson trajectory

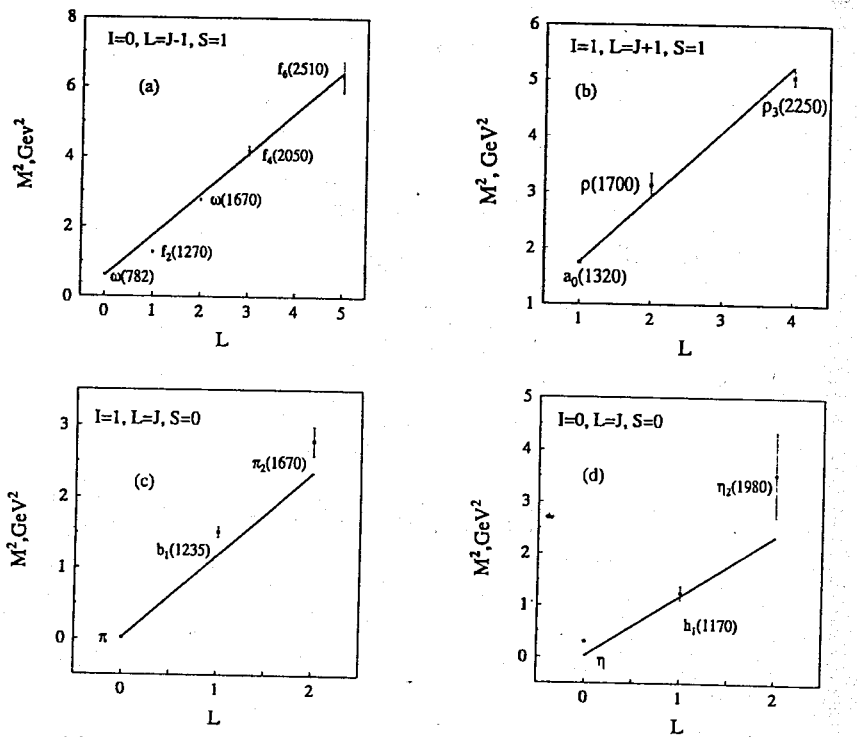

Figure 2: (a)- ω-meson Regge trajectory, (b)- a_0-meson Regge trajectory, (c)- π-meson Regge trajectory, (d)- η-meson Regge trajectory

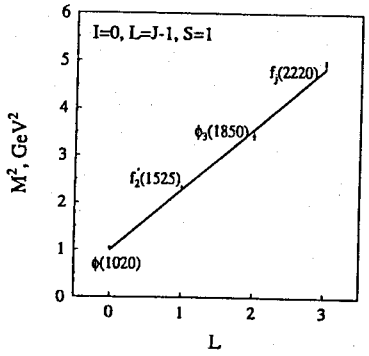

Figure 3: ϕ-meson trajectory

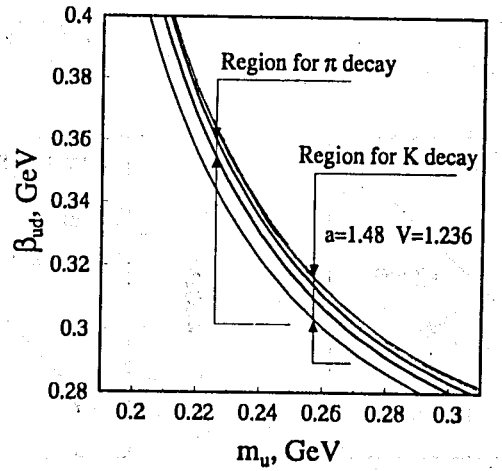

Figure 4: Allowed regions for leptonic decays

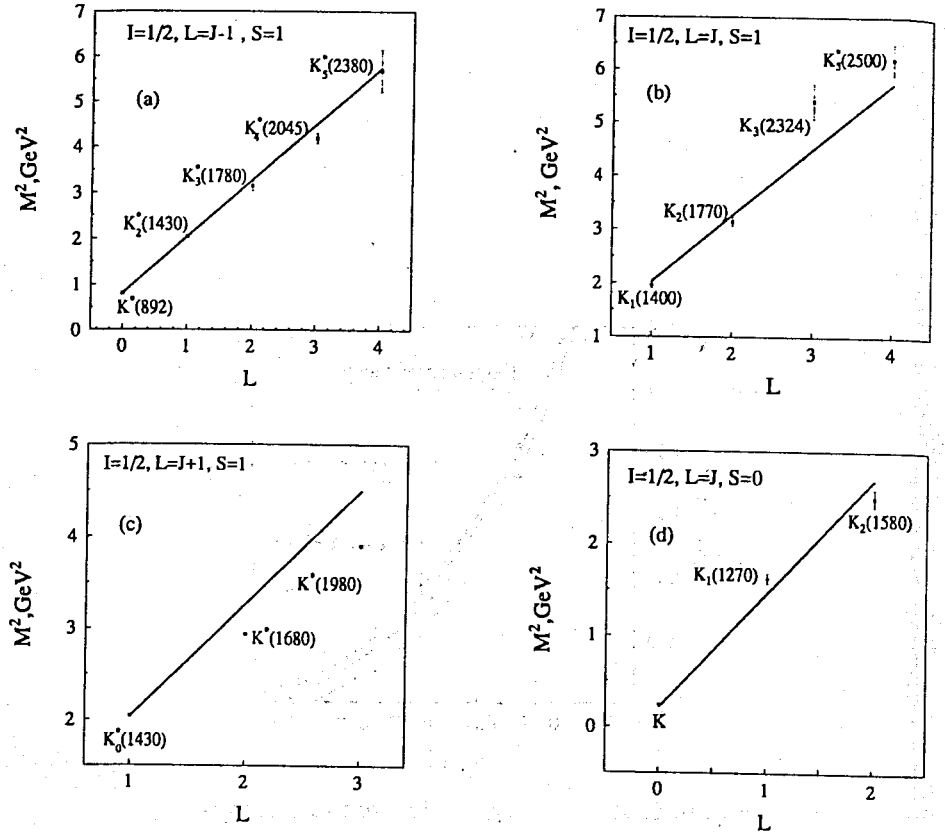

Figure 5: K-meson trajectories

TIME-REVERSAL-VIOLATING OPTICAL GYROTROPY

Vladimir G.Baryshevsky
Nuclear Problem Research Institute,
Bobruiskaya Str.11, Minsk 220080 Belarus.
Electronic address: bar@inp.minsk.by
Tel: 00375-172-208481, Fax: 00375-172-265124

Time-reversal-violating interactions of the electrons and nucleus cause the appearance of new optical phenomena. These phenomena are not only very interesting from fundamental point of view, but give us a new key for studying the time-reversal-violating interactions of the elementary particles.

Violation of time reversal symmetry has been observed only in K_0-decay many years ago [1], and remains one of the great unsolved problems in elementary particle physics. Since the discovery of the CP-violation in decay of K_0-mesons, a few attempts have been undertaken to observe this phenomenon experimentally in different processes. However, those experiments have not been successful. At the present time novel more precise experimental schemes are actively discussed: observation of the atom [2] and neutron [3] electric dipole moment, T-violating (time reversal) atom (molecule) spin rotation in a laser wave and T-violating optical activity of an atomic or molecular gas [4, 5].

According to [6] a new optical phenomenon appears due to violation of the time reversal symmetry: the photon polarization plane rotation and circular dichroism in an optically homogeneous isotropic medium exposed to an electric field. This T-odd phenomenon is a kinematic analog of the famous T-even phenomenon of the photon polarization plane rotation in the medium exposed to a magnetic field (Faraday phenomenon) (see figure.1). One more T-odd phenomenon of photon polarization plane rotation and circular dichroism appears at photon passing through non-center-symmetrical diffraction grating [6].

In the present paper the T-odd phenomena of photon polarization plane rotation by an electric field and by a diffraction grating are considered. The magnitude of effects are estimated and the possibilities of experimental observation are discussed.

1. Phenomenon of the time-reversal-violating photon polarization plane rotation by an electric field.

where f_s is the P-,T- invariant scalar amplitude, f_s^P is the P-violating scalar amplitude, and f_s^T is the P-,T- violating scalar amplitude.

It can easily be found from (7,8) that the term proportional to $\beta_s^T\left(f_s^T\right)$ vanishes in the case of forward scattering $\left(\vec{n}' \to \vec{n}\right)$. Vice versa, in the case of back scattering $\left(\vec{n}' \to -\vec{n}\right)$ the term proportional to $\beta_s^P\left(f_s^P\right)$ gets equal to zero.

Thus, one can conclude that the T-violating interactions manifest themselves in the processes of scattering by atoms (molecules). However, the scattering processes are usually incoherent and their cross sections are too small to hope for observation of the T-violating effect. Another situation takes place for diffraction gratings in the vicinity of the Bragg resonance where the scattering process is coherent. As a result, the intensities of scattered waves strongly increase: for instance, in the Bragg (reflection) diffraction geometry the amplitude of the diffracted-reflected wave may reach the unity. It gives us an opportunity to study the T-violating scattering processes [5].

To include the P, T violating processes into the diffraction theory, let us consider the microscopic Maxwell equations:

$$\begin{aligned} curl\vec{E} &= -\frac{1}{c}\frac{\partial \vec{B}}{\partial t} \quad , \quad curl\vec{B} = \frac{1}{c}\frac{\partial \vec{E}}{\partial t} + \frac{4\pi}{c}\vec{j} \quad , \\ div\vec{E} &= 4\pi\rho \quad , \quad div\vec{B} = 0 \quad , \quad \frac{\partial \rho}{\partial t} + div\vec{j} = 0 \quad . \end{aligned} \tag{9}$$

where $\vec{E}$ is the electric field strength and $\vec{B}$ is the magnetic field induction, ρ and $\vec{j}$ are the microscopic densities of the electrical charge and the current induced by an electromagnetic wave, c is the speed of light. The Fourier transformation of these equations (i.e. $\vec{E}(\vec{r},t) = \frac{1}{2\pi^4}\int \vec{E}\left(\vec{k},\omega\right) e^{i\vec{k}\vec{r}} e^{-i\omega t} d^3k d\omega$ and so on) yields to equation for $\vec{E}\left(\vec{k},\omega\right)$:

$$\left(-k^2 + \frac{\omega^2}{c^2}\right)\vec{E}\left(\vec{k},\omega\right) = -\frac{4\pi i\omega}{c^2}\left[\vec{j}\left(\vec{k},\omega\right) - \frac{c^2k^2}{\omega^2}\vec{n}\left(\vec{n}\vec{j}\left(\vec{k},\omega\right)\right)\right], \tag{10}$$

where $\vec{n} = \frac{\vec{k}}{k}$.

In linear approximation, the current $\vec{j}(\vec{r},\omega)$ is coupled with $\vec{E}(\vec{r},\omega)$ by the well-known dependence: $j_i(\vec{r},\omega) = \int d^3r' \sigma_{ij}\left(\vec{r},\vec{r}',\omega\right) E_j\left(\vec{r}',\omega\right)$ with

$\sigma_{ij}\left(\vec{r},\vec{r}',\omega\right)$ as the microscopic conductivity tensor being a sum of the conductivity tensors of the atoms (molecules) constituting the diffraction grating: $\sigma_{ij}\left(\vec{r},\vec{r}',\omega\right) = \sum_{A=1}^{N}\sigma_{ij}^A\left(\vec{r},\vec{r}',\omega\right)$, here σ_{ij}^A is the conductivity tensor of the A-type scatterers. The summation is done over all atoms (molecules) of the grating. In a diffraction grating, the tensor $\sigma_{ij}\left(\vec{r},\vec{r}',\omega\right)$ is a spatially periodic function. Therefore, $j_i\left(\vec{k},\omega\right)$ can be written as follows:

$$j_i\left(\vec{k},\omega\right) = \frac{1}{V_0}\sum_{\vec{\tau}}\sigma_{ij}^c\left(\vec{k},\vec{k}-\vec{\tau},\omega\right)E_j\left(\vec{k}-\vec{\tau},\omega\right) \tag{11}$$

where σ_{ij}^c is the Fourier transform of the conductivity tensor of a grating's elementary cell, $\vec{\tau}$ is the reciprocal lattice vector of the diffraction grating.

Using current representation (11), one can obtain from (10):

$$\left(-k^2 + k_0^2\right)E_i\left(\vec{k},\omega\right) = -\frac{\omega^2}{c^2}\sum_{\vec{\tau}}\hat{\chi}_{ij}\left(\vec{k},\vec{k}-\vec{\tau}\right)E_j\left(\vec{k}-\vec{\tau}\right) \tag{12}$$

Tensor of the diffraction grating susceptibility is given by

$$\hat{\chi}_{ij}\left(\vec{k},\vec{k}-\vec{\tau}\right) = \left(\delta_{il} - n_in_l\right)\chi_{lj}\left(\vec{k},\vec{k}-\vec{\tau}\right) \tag{13}$$

with

$$\chi_{lj}\left(\vec{k},\vec{k}-\vec{\tau}\right) = \frac{4\pi i}{V_0\omega}\sigma_{lj}\left(\vec{k},\vec{k}-\vec{\tau}\right) = \frac{4\pi c^2}{V_0\omega^2}F_{lj}\left(\vec{k},\vec{k}-\vec{\tau}\right).$$

Here $F_{lj}\left(\vec{k},\vec{k}-\vec{\tau}\right) = \frac{i\omega}{c^2}\sigma_{lj}\left(\vec{k},\vec{k}-\vec{\tau}\right)$ is the amplitude of coherent elastic scattering of an electromagnetic wave by a grating elementary cell from a state with the wave vector $(\vec{k}-\vec{\tau})$ to a state with the wave vector $\vec{k}$.

The amplitude F_{lj} is obtained by summation of atomic (molecular) coherent elastic scattering amplitudes over a grating's elementary cell:

$$F_{lj}\left(\vec{k}' = \vec{k}+\vec{\tau},\vec{k}\right) = \left\langle \sum_{A=1}^{N_c} f_{lj}^A\left(\vec{k}' = \vec{k}+\vec{\tau},\vec{k}\right)e^{-i\vec{\tau}\vec{R}_A}\right\rangle, \tag{14}$$

where f_{lj}^A is the coherent elastic scattering amplitude by an A-type atom (molecule), $\vec{R}_A$ is the gravity center coordinate of the A-type atom (molecule), N_c is the number of the atoms (molecules) in an elementary cell, angular brackets denote averaging over the coordinate distribution of scatterers in a grating's elementary cell.

The amplitude f_{ij} has been given by equation (7,8).

From (13), (14) and (8) one can obtain an expression for the susceptibility χ_{ij} of the elementary cell of an optically isotropic material:

$$\chi_{ij}\left(\vec{k},\vec{k}-\vec{\tau}\right)=\chi_{s\vec{\tau}}\delta_{ij}+i\chi^{P}_{s\vec{\tau}}\varepsilon_{ijf}\nu^{\vec{\tau}}_{1f}+\chi^{T}_{s\vec{\tau}}\varepsilon_{ijf}\nu^{\vec{\tau}}_{2f} \qquad (15)$$

where

$$\chi^{(P,T)}_{s\vec{\tau}}=\frac{4\pi e^2}{V_0\omega^2}\left\langle\sum_{A=1}^{N_c}f^{A(P,T)}_{s}\left(\vec{k},\vec{k}-\vec{\tau}\right)e^{-i\vec{\tau}\vec{R}_A}\right\rangle,$$

$\chi_{s\vec{\tau}}$ is the scalar P-, T- invariant susceptibility of an elementary cell, $\chi^{P}_{s\vec{\tau}}$ is the P-violating, T- invariant susceptibility of the elementary cell, and $\chi^{T}_{s\vec{\tau}}$ is the P- and T- violating susceptibility of the elementary cell,

$$\vec{\nu}^{\vec{\tau}}_{1}=\frac{2\vec{k}-\vec{\tau}}{\left|2\vec{k}-\vec{\tau}\right|}\quad,\quad\vec{\nu}^{\vec{\tau}}_{2}=\frac{\vec{\tau}}{\tau}.$$

Then, using (12,13,15) one can derive a set of equations describing the P and T violating interaction of an electromagnetic wave with a diffraction grating

$$\begin{aligned}\left(-\frac{k^2}{k_0^2}+1\right)E_i\left(\vec{k}\right) &= -\left(\delta_{ij}-n_in_j\right)\chi_{s0}E_j\left(\vec{k}\right)-\\ &-i\chi^{P}_{s0}\left(\delta_{il}-n_in_l\right)\varepsilon_{ljf}n_fE_j\left(\vec{k}\right)-\\ &-\sum_{\vec{\tau}\neq0}\{\left(\delta_{ij}-n_in_j\right)\chi_{s\vec{\tau}}E_j\left(\vec{k}-\vec{\tau}\right)+\\ &+i\chi^{P}_{s\vec{\tau}}\left(\delta_{il}-n_in_l\right)\varepsilon_{ljf}\nu^{\vec{\tau}}_{1f}E_j\left(\vec{k}-\vec{\tau}\right)+\\ &+\chi^{T}_{s\vec{\tau}}\left(\delta_{il}-n_in_l\right)\varepsilon_{ljf}\nu^{\vec{\tau}}_{2f}E_j\left(\vec{k}-\vec{\tau}\right)\},\end{aligned} \qquad (16)$$

where $k_0=\frac{\omega}{c}$

Assuming the interaction to be P, T invariant $\left(\chi^{P}_{s}=\chi^{T}_{s}=0\right)$, eqs. (16) are reduced to the conventional set of equations of dynamic diffraction theory [9]. The detailed analysis of these equations was done in [6].

According to [6] the angle of the photon polarization plane rotation out of Bragg conditions is defined by

$$\vartheta=-k_0Re\chi^{P}_{s}(0)\,L+2k_0\alpha_\tau^{-1}Re\left[\chi_{1s}(\vec{\tau})\,\chi^{T}_{2s}(\vec{\tau})-\chi_{2s}(\vec{\tau})\,\chi^{T}_{1s}(\vec{\tau})\right]L \qquad (17)$$

So, the T-violating rotation arises in the case of nonzero odd part of the susceptibility: $\chi_2(\vec{\tau})\neq0$. Such a situation is possible if an elementary cell of the diffraction grating does not posses the center of symmetry.

In accordance with (17), the angle of the T-violating rotation grows at $\alpha_\tau\to0$. However, the condition $\alpha_\tau\left|\chi_s(\vec{\tau})\right|\ll1$ is violated at $\alpha_\tau^{-1}\to0$, when the amplitude of diffracted and transmitted waves are comparable: $E\left(\vec{k}-\vec{\tau}\right)\simeq E\left(\vec{k}\right)$ and, consequently, the perturbation theory gets unapplicable. A rigorous dynamical diffraction theory must be applied in this case.

Let the Bragg condition is fulfilled only for the diffracted wave. It allows us to use the two-wave approximation of the dynamical diffraction theory [9]. Then, the set of equations (10) is reduced to two coupled equations, which for the back-scattering diffraction scheme $\left(\vec{k}_0\parallel\vec{\tau}\right)$ take the form [6]

$$\begin{aligned}\left(\frac{k^2}{k_0^2}-1\right)E_j\left(\vec{k}\right)&=\chi_s(0)\,E_j\left(\vec{k}\right)+i\chi^{P}_{s}(0)\,\varepsilon_{jmf}E_m\left(\vec{k}\right)n_f+\\ &+\chi_s(\vec{\tau})\,E_j\left(\vec{k}-\vec{\tau}\right)+\chi^{T}_{s}(\vec{\tau})\,\varepsilon_{jmf}E_m\left(\vec{k}-\vec{\tau}\right)\nu^{\vec{\tau}}_{2f},\\ \left(\frac{\left(\vec{k}-\vec{\tau}\right)^2}{k_0^2}-1\right)E_j\left(\vec{k}-\vec{\tau}\right)&=\chi_s(0)\,E_j\left(\vec{k}-\vec{\tau}\right)+\\ &+i\chi^{P}_{s}(0)\,\varepsilon_{jmf}n_f\left(\vec{k}-\vec{\tau}\right)E_m\left(\vec{k}-\vec{\tau}\right)+\\ &+\chi_s(-\vec{\tau})\,E_j\left(\vec{k}\right)+\chi^{T}_{s}(-\vec{\tau})\,\varepsilon_{jmf}\nu^{\vec{\tau}}_{2f}E_m\left(\vec{k}\right),\end{aligned} \qquad (18)$$

$\vec{n}\left(\vec{k}-\vec{\tau}\right)=\frac{\vec{k}-\vec{\tau}}{\left|\vec{k}-\vec{\tau}\right|}$. These set of equations can be diagonalized for the photon with a certain circular polarization. Let the right-circularly polarized photon $(\vec{e}_+)$ be incident on the diffraction grating. Then, the diffraction process yields to the appearance of a back-scattered photon with the left circular polarization $\left(\vec{e}^{\vec{\tau}}_{-}\right)$ (this is because the momentum of the back-scattered photon $\vec{k}'=\vec{k}-\vec{\tau}$ is antiparallel to the momentum $\vec{k}$ of the incident one). And visa versa obviously the left-circularly polarized photon will produce a right-circularly polarized back-scattered one.

Thus, for circularly polarized photons the set of vector equations (18) can be split into two independent sets of scalar equations [6]. The explicit solution of these equations yield to the following expression for the transmitted wave amplitude [6] (all the symbols are defined in [6]):

$$\vec{E}_{\pm}=\vec{e}_{\pm}(-1)^b\,e^{i\varphi_{\pm}},$$

where

$$\varphi_{\pm} = k_0 \left[\frac{1}{2} \varepsilon^{\pm} (\alpha_{1,2}) - \frac{k_0 (\alpha_{1,2} - 2\chi_s(0)) L}{8\pi b} \Delta^{\pm} \right] L$$

Using this equation one can find the angle of the polarization plane rotation

$$\vartheta = Re(\varphi_+ - \varphi_-) = \vartheta^P + \vartheta^T_{1,2},$$

where $\vartheta^P = -k_0 Re \chi^P_s(0) L$ - defines the P-violating T-invariant rotation angle and $\vartheta^T_{1,2}$ corresponds to the T-violating rotation:

$$\vartheta^T_{1,2}(\alpha_{1,2}) = \mp \frac{k_0^3 L^3}{8\pi^2 b^2} \sqrt{4(\chi^2_{1s} + \chi^2_{2s}) + \left(\frac{4\pi b}{k_0 L}\right)^2} \times \left[\chi_{1s}(\vec{\tau}) Re\chi^T_{2s}(\vec{\tau}) - \chi_{2s}(\vec{\tau}) Re\chi^T_{1s}(\vec{\tau}) \right], \quad (19)$$

the sign $(-)$ corresponds to α_1 , the sign $(+)$ corresponds to α_2.

The imaginary part of the T-violating polarizability $Im\chi^T_{s1,2}$ is responsible for the T-violating circular dichroism. Due to that process, a linearly polarized photon gets a circular polarization at the diffraction grating's output. The degree of the circular polarization of the photon is determined from the relation:

$$\delta_{1,2} = \frac{\left|\vec{E}_+\right|^2 - \left|\vec{E}_-\right|^2}{\left|\vec{E}_+\right|^2 + \left|\vec{E}_-\right|^2} \simeq Im\varphi_- - Im\varphi_+ = k_0 Im\chi^P_s(0) L \pm \quad (20)$$

$$\pm \frac{k_0^3 L^3}{8\pi^2 b^2} \sqrt{4(\chi^2_{1s} + \chi^2_{2s}) + \left(\frac{4\pi b}{k_0 L}\right)^2} \left[\chi_{1s}(\vec{\tau}) Im\chi^T_{2s}(\vec{\tau}) - \chi_{2s}(\vec{\tau}) Im\chi^T_{1s}(\vec{\tau}) \right]$$

It should be pointed out that the resonance transmission condition is satisfied at a given b for two different values of α. This is because there is a possibility to approach to the Brilluan (the total Bragg reflection) bandgap both from high and low frequencies. The T-violating parts of the rotation angle are opposite in sign for α_1 and for α_2. It gives the addition opportunity to distinguish the T-violating rotation from the P-violating T-invariant rotation. Indeed, the P-violating rotation does not depend on the

back Bragg diffraction in the general case because the P-violating scattering amplitude equals zero for back scattering (see [6]). In accordance with (19,20) the T-violating rotation and dichroism grow sharply in the vicinity of the resonance Bragg transmission. At the first glance, one could expect for ϑ^T the dependence $\vartheta^T \sim k_0 Re\chi^T_{s1,2}(\vec{\tau}) L$ (see (17)). However, in the vicinity of resonance, the rotation angle ϑ^T turns out to be multiplied by the factor $B = (8\pi^2 b^2)^{-1} k_0 \sqrt{4\left(\chi^2_{1s} + \chi^2_{2s}\right) + \left(\frac{4\pi b}{k_0 L}\right)^2} L k_0 \chi_{s1,2} L$ which provides the above mentioned growth (for example, $B \sim 10^5$ at $\chi_s \simeq 10^{-1}$, $k_0 \simeq 10^4 \div 10^5 cm^{-1}$, $L = 1cm$, $b = 1$).

Now, let us estimate the effect magnitude. To do that we must determine, in accordance with formula (19) for ϑ^T, the T-violating susceptibility $\chi^T_{s1,2}$, which is proportional to the T-violating atomic polarizability β^T_s. The estimate carried out by [4, 5, 7] gives $\beta^T_s \sim 10^{-3} \div 10^{-4} \beta^P_s$, where β^P_s is the P-violating T-invariant scalar polarizability. The polarizability β^P_s was studied both theoretically and experimentally [7]. Particularly, the theory gives $\beta^P_s \cong 10^{-30} cm^3$ for atoms analogous to Bi, Tl, Pb. It yields the estimate $\cong 10^{-33} \div 10^{-34} cm^3$ for the T-violating atomic polarizability. The polarizability β^P_s causes the P-violating rotation of the polarization plane by the angle $\vartheta^P = kRe\chi^P_s(0) L \cong 10^{-7}$ rad/cm×L for the gas density $\rho = 10^{16} \div 10^{17} cm^{-3}$. As a result, in our case the parameter $\varphi = k\chi^T_s(\tau) L$ turns out to be $\varphi \cong 10^{-10} \div 10^{-11}$ rad/cm×L and can be even less by the factor h/d, where h is the corrugation amplitude of the diffraction grating while d is the distance between waveguide's mirrors. Assuming this factor to be $\sim 10^{-1}$, we shall find $\varphi \cong 10^{-11} \div 10^{-12}$ rad/cm×L. Thus, the final estimate of the T-violating rotation angle ϑ^T is

$$\vartheta^T \cong 10^{-11} \div 10^{-12} \frac{rad}{cm} k_0^2 \chi^2_s(\tau) L^3 \quad (21)$$

In real situation the susceptibility of a grating $\chi_s(\tau)$ may exceed the unity. However, our analysis has been performed under the assumption $\chi_s \ll 1$. If, for example, we take $\chi_s = 10^{-1}$, $k_0 = 10^4$ then $\vartheta^T \simeq 10^{-6} \div 10^{-7} L^3$ and, consequently, for L= 1 cm we will have the rotation angle $\vartheta^T \simeq 10^{-6} \div 10^{-7} rad$.

As it is seen, we have obtained the T-violating rotation angle ϑ^T of the same order of ϑ^P. It makes possible experimental observation of the phenomenon of the T-violating polarization plane rotation.

It should be noted that the manufacturing of diffraction gratings for the range being more longwave than the visible light one may be sim-

pler. That is why we would like to attract attention to the possibility of studying of the T-violating polarization plane rotation in the vicinity of frequencies of atomic (molecular) hyperfine transitions; for example, for Ce (the transition wavelength is $\lambda = 3.26$ cm) and Tl ($\lambda = 1.42$ cm).

Thus, we have shown that the phenomenon of the T-violating polarization plane rotation appears while the photon is scattered by a volume diffraction grating. The phenomenon grows sharply in the vicinity of the resonance transmission condition. An experimental scheme based on a waveguide, containing a diffraction grating and gas, has been proposed that enables real experiments on observation of the T-violating polarization plane rotation to be performed. The rotation angle has been shown to be $\vartheta^T = 10^{-6} \div 10^{-7} L^3$, where L is the waveguide length (thickness of the equivalent volume diffracting grating).

The possibility to observe the phenomena experimentally can be discussed now. In accordance with (6) the angle of the T-odd rotation in electric field can be evaluated as follows:

$$\vartheta^T \sim \frac{2\pi\rho\omega}{c}\beta_E^T L \sim \frac{\beta_E^T}{\beta_S^P}\vartheta^P \sim \alpha^{-1}\frac{\langle dE\rangle}{\Delta}\frac{\langle V_w^T\rangle}{\langle V_w^P\rangle}\vartheta^P. \qquad (22)$$

According to the experimental data [12, 13] being well consistent with calculations [7] the typical value of ϑ^P is $\vartheta^P \sim 10^{-6} rad$ (for the length L being equal to the several absorption lengths of the light propagating through a gas L_a).

For the electric field $E \sim 10^4 V \cdot cm^{-1}$ the parameter $\frac{\langle dE\rangle}{\Delta}$ can be estimated as $\frac{\langle dE\rangle}{\Delta} \sim 10^{-5}$ for Cs, Tl and $\frac{\langle dE\rangle}{\Delta} \sim 10^{-4}$ for Yb and lead. Therefore, one can obtain $\vartheta^T \sim 10^{-13} rad$ for Cs, Tl and $\vartheta^T \sim 10^{-12} rad$ for Yb and lead. For the two-atom molecules (TlF, BiS, HgF) the angle ϑ^T can be larger, because they have a pair of degenerate opposite parity states.

The final estimate for the T-noninvariant effect in a diffraction grating gives for the T-violating rotation angle ϑ^T

$$\vartheta^T \cong 10^{-11} \div 10^{-12}\frac{rad}{cm} k_0^2 \chi_s^2(\tau)\, L^3 \qquad (23)$$

In real situation the susceptibility of a grating $\chi_s(\tau)$ may exceed the unity. However, our analysis has been performed under the assumption

$\chi_s \ll 1$. If, for example, we take $\chi_s = 10^{-1}$, $k_0 = 10^4$ then $\vartheta^T \simeq 10^{-6} \div 10^{-7} L^3$ and, consequently, for L= 1 cm we will have the rotation angle $\vartheta^T \simeq 10^{-6} \div 10^{-7} rad$.

As it is seen, we have obtained the T-violating rotation angle ϑ^T of the same order of ϑ^P. It makes possible experimental observation of the phenomenon of the T-violating polarization plane rotation.

It should be noted that the classical up-to-date experimental techniques allow to measure angles of light polarization plane rotation up to $4,3 \cdot 10^{-11} rad$ [14].

A way to increase the rotation angle ϑ^T is to increase the length L of the path of a photon inside a medium (see (6)). It can be done, for example, by placing a medium (gas in an electric field or non-center-symmetrical diffraction grating) in a resonator or inside a laser gyroscope. This becomes possible due to the fact that in contrast with the phenomenon of P-odd rotation of the polarization plane of photon the T-odd rotation in an electric field (as well as in a diffraction grating) is accumulated while photon is moving both in the forward and backward directions.

For the first view the re-reflection of the wave in resonator (or light multiple passing over circle resonator of a laser gyroscope) can not provide the significant increase of the photon path length L in comparison with the absorption length L_a because of the absorption of photons in a medium. Nevertheless this difficulty can be overcome when the part of resonator is filled by the amplifying medium (for example, inverse medium). As a result, the electromagnetic wave being absorbed by the investigated gas is coherently amplified in the amplifier and then is refracted to the gas again. Consequently, under the ideal conditions the light pulse can exist in such resonator-amplifier for arbitrarily long time and, for example, the polarization plane of the wave rotates around the $\vec{E}$ direction i.e. the peculiar "photon trap" appears (phase difference of waves with right and left circular polarizations moving in the opposite directions in a laser gyroscope increases in time). The angle of rotation $\vartheta^T = \Omega^T \cdot t$, where Ω^T is the frequency of the photon polarization plane rotation around the $\vec{E}$ direction, t is the time of electromagnetic wave being in a "trap". It is easy to find the frequency Ω^T from (6): $\Omega^T = \frac{\vartheta^T}{L} c = 2\pi\rho\omega\beta_E^T$. From the estimates of ϑ^T it is evident that for $\vartheta^T \sim 10^{-12} rad$ (Lead, Yb) the frequency Ω^T appears to be $\Omega^T = \frac{\vartheta^T}{L_a} c \sim 10^{-4}\,\mathrm{sec}^{-1}$. Therefore $\vartheta^T \sim 10^{-4} t$

and for the time t of about 3 hours the angle ϑ^T becomes ~ 1 *rad*. The similar estimates for the atoms Cs, Tl ($\vartheta^T \sim 10^{-13}$ *rad*) give that for the same time the angle $\vartheta^T \sim 10^{-1}$ *rad*.

The time t is limited, in particular, by spontaneous radiation of photons in an amplifier that gradually leads to the depolarization of photon gas in resonator. Surely, it is the ideal picture, but here is the way to further increase of the experiment sensitivity.

All the said can be applied not only for the optical range but for the radio frequency range as well where the observation of the mentioned phenomenon is also possible by the use of the same atoms and molecules [6].

Thus, we have shown that the T-odd and P-odd phenomena of photon polarization plane rotation and circular dichroism in an electric field are expected to be observable experimentally.

It should be noted, that the new T-odd and P-odd phenomenon of photon polarization plane rotation (circular dichroism) in an electric field has general meaning. Due to quantum electrodynamic effects of electron-positron pair creation in strong electric, magnetic or gravitational fields, the vacuum is described by the dielectric permittivity tensor ε_{ik} depending on these fields[11, 15]. The theory of ε_{ik} [11, 15] does not take into account the weak interaction of electron and positron with each other. Considering the weak interaction between electron and positron in the process of pair creation in an electric (gravitational) field one can obtain that the permittivity tensor of vacuum in strong electric (gravitational) field contains the term $\varepsilon_{ik}^{vac} \sim i\beta^T_{vac} \overrightarrow{E} \varepsilon_{ikl} n_{lE}$ ($\varepsilon_{ik}^{vac} \sim i\beta^T_{vac} \overrightarrow{g} \varepsilon_{ikl} n_{lg}, \overrightarrow{n_g} = \dfrac{\overrightarrow{g}}{g}, \overrightarrow{g}$ is the free fall acceleration), and as a result, the polarization plane rotation (circular dichroism) phenomena exist for photons moving in an electric (gravitational) field in vacuum. And visa versa γ-quanta appeared under single-photon electron-positron annihilation in an electric (gravitational) field will have the admixture of circular polarization, caused by T-odd P-odd weak interactions.

References

[1] Christenson J.H., Cronin J.W., Fitch V.L. and Turlay R. Phys. Rev. Lett. 3 (1964) 1138.

[2] Lamoreaux S.K. Nucl. Instrum. Methods. A284 (1989) 43.

[3] Forte M.J. Journ. Of Phys. G.: Nucl. Part. Phys. G9 (1983) 745.

[4] Baryshevsky V.G. Phys. Lett A177 (1993) 38.

[5] Baryshevsky V.G., Baryshevsky D.V. Journ. Of Phys. B: At. Mol. Opt. Phys. 27 (1994) 4421.

[6] Baryshevsky V.G. J.High Energy Phys. 04 (1998) 018.

[7] Khriplovich I.B. Parity Nonconservation in Atomic Phenomena. 1991 (London: Gordon and Breach).

[8] Baryshevsky V.G. Phys. Lett A260 (1999) 24.

[9] Shi-Lin Chang. Multiple Diffraction of X-rays in Crystals. 1984 (Springer-Verlag Berlin Heidelberg New-York Tokyo)

[10] Landau L., Lifshitz E. Quantum mechanics, 1989, Moscow Science.

[11] Berestetskii V., Lifshitz E., Pitaevskii L. Quantum electrodynamics, 1989, Moscow Science.

[12] Meekhof D.H., Vetter P.A., Majumber P.K., Lamoreaux S.K. and Fortson E.N. Phys. Rev. A52 (1995) 1895

[13] Edwards N.H., Phipp S.J., Baird G. and Nakayama S. Phys. Rev. Lett 74 (1995) 2654

[14] Cameron R., Cantatore G., Melissinos A.C. et. al. Phys. Rev. D 47 (1993) 3707

[15] Bunch T.S., Davies P.C.W. Proc.Roy.Soc. Lond. A356(1977) 569.

COVARIANT DEFINITION OF TENSORS OF HADRON POLARIZABILITIES BASED ON THE SYMMETRY PROPERTIES OF TWO-PHOTONS PROCESSES

O.M.Deryuzhkova, E.N.Kalantai, N.V.Maksimenko

Skaryna University, Sovietskaya Str., 104, 246699, Gomel, Belarus

It is known that hadrons are structural particles. For that reason we can define their properties by their electromagnetic characteristics, such as $\langle r^2 \rangle$, polarizabilities and gyrations or, as the latter is presently known, spin polarizabilities [1-4, 5].

The introduction of hadron electromagnetic characteristics in the effective Lagrangians is unambiguous in the non-relativistic physics. However, while moving to the relativistic theoretical-field description of the hadron polarizabilities, their ambiguous definition appears in the amplitudes of two-photon processes [3].

Therefore, to construct the effective relativistic Lagrangians of the interaction between the electromagnetic field and hadrons, we can use the principle of correspondence of the classical electrodynamics of moving mediums, the relativistic quantum field theory [6], and the Poinare group algebra of the operators and matrices, contained in the hadron motion equations.

The classical non-relativistic part of Hamiltonian of the interaction of the electromagnetic field with neutral isotropic medium is [7,8]

$$H_I = -2\pi \left(\vec{P}\vec{E} + \vec{M}\vec{H} \right). \tag{1}$$

If we take only the medium polarizability into consideration then

$$\vec{P} = \hat{\alpha}\vec{E}, \quad \vec{M} = \hat{\beta}\vec{H}. \tag{2}$$

The polarizability tensors $\hat{\alpha}$ and $\hat{\beta}$ for spinless particles are

$$\alpha_{ij} = \alpha_0 \delta_{ij}, \ \beta_{ij} = \beta_0 \delta_{ij}. \tag{3}$$

Let us consider the low-energy Compton scattering for structural particles with 0, 1/2 and 1 spin. We will assume that the tensors $\hat{\alpha}$ and $\hat{\beta}$ depend on spin operators which satisfy some commutative relations. This

statement is in full agreement with the fact that the polarizabilities tensors can be expressed with the amplitude of Compton scattering. This amplitude is based on the invariance relative to P- and T- transformation and rotation group [9]. Under such approach there is no a physical interpretation of scalar functions.

The amplitude of scattering of low-energy photons is defined by the expression

$$F = \omega^2 \{ \vec{e}\,' \hat{\alpha} \vec{e} + (\vec{n}'\vec{e})(\vec{n}\hat{\beta}\vec{e}\,') + (\vec{n}\vec{e}\,')(\vec{e}\hat{\beta}\vec{n}') +$$

$$+ (\vec{e}\,'\vec{e})(\vec{n}\hat{\beta}\vec{n}') - (\vec{n}'\vec{n})(\vec{e}\hat{\beta}\vec{e}\,') + (\vec{n}\vec{n}' \cdot \vec{e}\,'\vec{e} - \vec{n}'\vec{e} \cdot \vec{n}\vec{e}\,') Sp(\hat{\beta}) \}, \tag{4}$$

where ω is a frequency of incoming wave, $\vec{n}$ and $\vec{n}'$ are unit vectors of incoming and scattered waves, $\vec{e}$ and $\vec{e}\,'$ are unit polarization vectors of incoming and scattered waves respectively.

To determine the tensors α_{ij} and β_{ij} in terms of spin operators $\hat{\vec{S}}$ for structural particles of spin 1/2 and 1, we use the commutative relations of the spin operators components.

In both cases the expression

$$\left[\hat{S}_i, \hat{S}_j \right] = i\varepsilon_{ijk} \hat{S}_k \tag{5}$$

is true. In this expression ε_{ijk} is a completely anti symmetrical unit tensor.

For particles of spin 1/2 operators $\hat{S}_i$ can be also defined by the expression

$$\hat{S}_i \hat{S}_j = \frac{1}{4}\delta_{ij} + \frac{i}{2}\varepsilon_{ijk}\hat{S}_k. \tag{6}$$

According to this statement tensors are expressed as

$$T_{ij}(\hat{\vec{S}}) = T_0 \delta_{ij} + iT_1 \varepsilon_{ijk} \hat{S}_k. \tag{7}$$

(We imply that T_{ij} are tensors α_{ij} and β_{ij})

On the other hand, structural particles of spin 1 are defined by:

$$\hat{S}_i \hat{S}_j \hat{S}_k = i\varepsilon_{ijk} + \frac{1}{2}(\hat{S}_i \delta_{jk} + \hat{S}_k \delta_{ij}) + \frac{i}{2}\varepsilon_{lik}(\hat{S}_j \hat{S}_l + \hat{S}_l \hat{S}_j). \tag{8}$$

That's why tensors α_{ij} and β_{ij} can be represented by the expansion by the following independent combinations

$$T_{ij}(\hat{\vec{S}}) = T_0 \delta_{ij} + iT_1 \varepsilon_{ijk} \hat{S}_k + T_2(\hat{S}_i \hat{S}_j + \hat{S}_j \hat{S}_i). \tag{9}$$

Based on (4), (7) and (9) the scattering amplitude can be represented by

$$F = \omega^2 \chi^+ \{\alpha_0(\vec{e}\,'\vec{e}) + i\alpha_1(\hat{\vec{S}}[\vec{e}\vec{e}\,']) + \alpha_2\{\hat{\vec{S}}\vec{e}\,', \hat{\vec{S}}\vec{e}\} + \\ + \beta_0([\vec{e}\vec{n}][\vec{e}\,'\vec{n}']) + i\beta_1(\hat{\vec{S}}[[\vec{e}\,'\vec{n}'][\vec{e}\vec{n}]]) + \\ + \beta_2\{\hat{\vec{S}}[\vec{e}\vec{n}], \hat{\vec{S}}[\vec{e}\,'\vec{n}']\}\}\chi, \qquad (10)$$

where χ and χ^+ are the spin functions of the particles, the square brackets represent a vector multiplication, the braces represent a commutator. ¿From the equation (10) one can be see that

1) the scattering amplitude of a scalar particle is defined by α_0 and β_0;
2) the scattering amplitude of a spinor particle is defined by the polarizabilities $\alpha_0, \beta_0, \alpha_1$ and β_1;
3) the scattering amplitude of a vector particle contains α_0, β_0 and the spinor polarizabilities $\alpha_1, \alpha_2, \beta_1$ and β_2.

For the amplitude (10) of the second order in terms of the frequency to satisfy the condition of cross-symmetry, it is needed to set the spin polarizabilities α_1 and β_1 to zero.

Using the low-energy expansion of Born's part of the scattering amplitude and the expression (4), one can obtain that the averaged Compton scattering amplitude for particles with spin 1 is

$$\Phi(\omega) = -\frac{\alpha}{M} + \frac{\alpha\omega^2}{3M^3}\left(2\mu^2 - 4\mu + 2Q\right) + \\ + \frac{\omega^2}{3}(3\alpha_0 + 3\beta_0 + 4\alpha_2 + 4\beta_2), \qquad (11)$$

where $\alpha = e^2/4\pi$ is the fine structure constant. Let us assume that the amplitude Φ satisfies the dispersional relations with one subtraction

$$\Phi(\omega) = \Phi(\omega = 0) + \frac{\omega^2}{2\pi}\int \frac{Im\Phi(\omega')d\omega'}{\omega'(\omega'^2 - \omega^2)}. \qquad (12)$$

Based on the optical theorem, the expression (12) can be written as

$$\Phi(\omega) = \Phi(\omega = 0) + \frac{2\omega^2}{\pi}\int \frac{\sigma_{tot}d\omega'}{\omega'^2 - \omega^2}. \qquad (13)$$

By comparing (11) and (13), the following rules of sums can be obtained:

$$\frac{1}{2\pi^2}\int \frac{\sigma_{tot}d\omega'}{\omega'^2} = (\alpha_0 + \beta_0) + \frac{4}{3}(\alpha_2 + \beta_2) + \frac{2e^2}{3M^3}(Q + \mu^2 - 2\mu). \qquad (14)$$

Similar rules of sums were obtained in [10]. However, in this work the authors introduced four constants C_1, C_2, C_3 and C_4, that do not have a physical interpretation. ¿From the expression (14), one can see that these constants are nothing but polarizabilities α_0 and β_0, and spin (tensor) polarizabilities α_2 and β_2.

According to the relativistic electrodynamics of the moving mediums the effective Lagrange function is [7]:

$$L_{eff}^{pol} = 2\pi\{e^\mu\alpha_{\mu\nu}e^\nu + h^\mu\beta_{\mu\nu}h^\nu\}. \qquad (15)$$

In this expression $e_\mu = F_{\mu\nu}U^\nu$, $h_\mu = \tilde{F}_{\mu\nu}U^\nu$, $\tilde{F}_{\mu\nu} = \frac{i}{2}\varepsilon_{\mu\nu\rho\sigma}F^{\rho\sigma}$, where $F_{\mu\nu}$ and $\tilde{F}_{\mu\nu}$ are the tensors of the electromagnetic field, $\alpha_{\mu\nu}$ and $\beta_{\mu\nu}$ are tensors that are expressed by the polarizabilities in a medium at rest. U_μ is the 4-dimensional velocity of the medium.

By analogy with the non-relativistic quantum theory let us consider that tensors $\alpha_{\mu\nu}$ and $\beta_{\mu\nu}$ depend on the momentum operator and the Pauli-Lubanski vector-operator

$$\alpha_{\mu\nu} = \alpha_{\mu\nu}(\hat{W}_\mu, \hat{p}_\mu).$$

The operators $\hat{W}_\mu$ and $\hat{p}_\mu$ are subordinated to commutative correlations in the limits of quantum-mechanical Poincare group [11]. If these commutative expressions are used, then we obtain the following expansions:

1) for particles with spin 1/2

$$\alpha_{\mu\nu} = \alpha_0\delta_{\mu\nu} + \alpha_1\varepsilon_{\mu\nu\rho\sigma}\hat{W}^\rho\hat{p}^\sigma, \qquad (16)$$

$$\beta_{\mu\nu} = \beta_0\delta_{\mu\nu} + \beta_1\varepsilon_{\mu\nu\rho\sigma}\hat{W}^\rho\hat{p}^\sigma; \qquad (17)$$

2) for particles with spin 1

$$\alpha_{\mu\nu} = \alpha_0\delta_{\mu\nu} + \alpha_2(\hat{W}_\mu\hat{W}_\nu + \hat{W}_\nu\hat{W}_\mu), \qquad (18)$$

$$\beta_{\mu\nu} = \beta_0\delta_{\mu\nu} + \beta_2(\hat{W}_\mu\hat{W}_\nu + \hat{W}_\nu\hat{W}_\mu). \qquad (19)$$

According to the cross-symmetry laws, α_1 and β_1 in (16) and (17) are equal to zero. However, in (18) and (19) α_2 and β_2 differ from zero. Consequently, as one can be see from (15), in the second order of the photon frequency, the effective Lagrangians of hadrons with spin 0 and 1/2 are defined only by α_0 and β_0.

The effective Lagrangians of the interaction of the electromagnetic field and hadrons with spin 1 in the same approximation, depend on the operators $\hat{W}_\mu$ (relativistic generalization of spin) and are defined by the coefficients α_2 β_2, which, according to (18), (19), can be called spin (tensor) polarizability.

If we move from the Lagrangian (15) to the theoretical-field Lagrangian on the basis of the correspondence principle, then we obtain [4]:
1) for particles with spin 0

$$L_{eff}^{pol} = \frac{\pi}{4M^2}\left[(\partial_\mu\varphi^+)(\partial_\nu\varphi) + (\partial_\mu\varphi)(\partial_\nu\varphi^+) - (\varphi^+\partial_\mu\partial_\nu\varphi + \varphi\partial_\mu\partial_\nu\varphi^+)\right] K^{\mu\nu}. \tag{20}$$

2) for particles with spin 1/2

$$L_{eff}^{pol} = \frac{\pi}{m}\left(\bar{\psi}\gamma_\mu(\partial_\nu\psi) - (\partial_\nu\bar{\psi})\gamma_\mu\psi\right) K^{\mu\nu}, \tag{21}$$

where $K_{\mu\nu} = \alpha_0 F_{\mu\rho}F^\rho_\nu + \beta_0 \tilde{F}_{\mu\rho}\tilde{F}^\rho_\nu$. φ and ψ are the wave functions of particles with spin 0 and 1/2.

If the medium is isotropic-gyratropycal [8]

$$\vec{P} = \hat{\alpha}\vec{E} + \hat{\eta}\left[\vec{\nabla}\vec{E}\right], \tag{22}$$

$$\vec{M} = \hat{\beta}\vec{H} + \hat{\kappa}\left[\vec{\nabla}\vec{H}\right]. \tag{23}$$

where $\hat{\eta}$ and $\hat{\kappa}$ are the gyration tensors.

For relativistic moving mediums L_{eff} is [7]:

$$L_{eff} = 2\pi\left\{\epsilon^\mu\alpha_{\mu\nu}\epsilon^\nu + h^\mu\beta_{\mu\nu}h^\nu + \eta^{\mu\nu\rho}F_{\mu\sigma}\partial_\nu F^\sigma_\rho + \kappa^{\mu\nu\rho}\tilde{F}_{\mu\sigma}\partial_\nu\tilde{F}^\sigma_\rho\right\}. \tag{24}$$

As it follows from the correspondence principle and expression (24), the theoretical-field effective Lagrangian of the interaction between the electromagnetic field and spinless hadrons will not satisfy the law of parity preservation, if the components $\eta_{\mu\nu\rho}$ $\kappa_{\mu\nu\rho}$ differ from zero. However, if we proceed to the definition of Lagrangians of the interaction between the electromagnetic field and hadrons with spin that is different from zero, then, using a vector - operator $\hat{W}_\mu$, it is possible to construct the structures of Lagrangian that satisfies the law of parity preservation.

On the basis of commutative relations between $\hat{W}_\mu$ and $\hat{p}_\mu$ it is possible to show, that

$$\eta_{\mu\nu\rho} = \eta_0\varepsilon^\sigma_{\mu\nu\rho}\hat{W}_\sigma. \tag{25}$$

The similar expression is also fair for $\kappa_{\mu\nu\rho}$. In expression (25) η_0 and κ_0 are the gyrational scalar factors or, as we call them now, spin polarizabilities.

The theoretical-field effective Lagrangian of the interaction between the electromagnetic field and hadrons with spin 1/2, in this case is

$$L_{eff} = L_{eff}^{pol} + L_{eff}^{Sp}. \tag{26}$$

In (26) L_{eff}^{pol} is defined by ratio (21), and

$$L_{eff}^{Sp} = \eta_0\left\{\bar{\psi}\overleftrightarrow{\partial}_\nu\hat{\sigma}_{\mu\rho}\psi F^{\nu\mu}\overleftarrow{\partial}_\sigma F^{\rho\sigma} - \bar{\psi}\overleftrightarrow{\partial}_\sigma\hat{\sigma}_{\mu\rho}\psi F^{\nu\mu}\vec{\partial}_\nu F^{\rho\sigma}\right\} +$$

$$+k_0\left\{\bar{\psi}\overleftrightarrow{\partial}_\nu\hat{\sigma}_{\mu\rho}\psi\,\tilde{F}^{\nu\mu}\overleftarrow{\partial}_\sigma\tilde{F}^{\rho\sigma} - \bar{\psi}\overleftrightarrow{\partial}_\sigma\hat{\sigma}_{\mu\rho}\psi\,\tilde{F}^{\nu\mu}\vec{\partial}_\nu\tilde{F}^{\rho\sigma}\right\}, \tag{27}$$

where $\hat{\sigma}_{\mu\rho} = \frac{i}{2}(\gamma_\mu\gamma_\rho - \gamma_\rho\gamma_\mu)$, $\overleftrightarrow{\partial}_\mu = \overleftarrow{\partial}_\mu - \vec{\partial}_\mu$.

The effective Lagrangian satisfies the cross-symmetry and also satisfies all requirements of relativistic quantum field theory. Besides, as follows from expression (27), spin polarizability for hadrons with spin 1/2 gives the contribution to the effective Lagrangian. Structures of this Lagrangian are proportional to the third order of the radiation frequency. In low-energy approximation in the terms of order $O(\omega^3)$ an amplitude (27) has a form:

$$L_{eff}^{Sp} = i\omega^3\chi^+\{\eta_0'\{2(\vec{\sigma}[\vec{e}\,'\vec{e}]) - 2(\vec{n}\vec{n}')(\vec{\sigma}[\vec{e}\,'\vec{e}]) +$$

$$+(\vec{n}\vec{e}\,')(\vec{\sigma}[\vec{n}'\vec{e}]) - (\vec{n}'\vec{e})(\vec{\sigma}[\vec{n}\vec{e}\,'])\} +$$

$$+k_0'\{-2(\vec{\sigma}[[\vec{n}'\vec{e}\,'][\vec{n}\vec{e}]]) + (\vec{\sigma}[[\vec{n}'\vec{e}\,'][\vec{n}'\vec{e}]]) - (\vec{\sigma}[[\vec{n}\vec{e}][\vec{n}\vec{e}\,']])\}\}\chi. \tag{28}$$

If take into account the invariant spin structure or Lagrangian [4], it is not difficult to confirm that the amplitudes for Compton scattering coincide with such as one in works [1,4,5].

This work was supported by grant No. F98-105 (01.03.99) from the Foundation for Fundamental Research of the Republic of Belarus.

[1] D.Babusci,J.Jiordano, A.J.L'vov, J.Matone, A.M.Nathan. Low-Energy Compton Scattering of Polarized Photons on Polarized Nucleons. Hep-ph/980334/.

[2] V.A. Petrun'kin. Physics of Elementary Particles and Atomic Nuclei 12. 1981. P.692.

[3] A.J.L'vov. Preprint FIAN. N344. 1987.

[4] N.V.Maksimenko, L.G.Moroz. In Proc. 11 Intern. Scool on High Energy Physics and Relativistic Nucl. Phys. Dubna JINR. D2-11707. 1979. P.533-543.

[5] M.I.Levchuk. L.G.Moroz. Vesci AN BSSR. Ser.: fiz.-mat. nauk 1. 1985. P.49.

[6] ..Bogush, L.G.rz. Introduction in clasic fields theory. Nauka i tehnika. Minsk. 1968.

[7] B.V.Bokut', A.N.Serdyukov. Jornal of Applied Spectroscopy 11. 1969. P.704.

[8] B.V.Bokut', A.N.Serdyukov, F.I.Fedorov. Jornal of Applied Spectroscopy 19. 1973. P.377.

[9] V.G.Barishevski. Nuclear optics of polarized media. . Energoizdat. 1995.

[10] K.Y.Lin, I.C.Chen. Phys.J: Nucl.Phys. 1975. Vol.1. N4. P.394-399.

[11] Yu.V.Novojilov. Introduction in theory of elementary particles. Nauka. . 1972.

Production of the cumulative particles in the FRITIOF model

A.S. Galoyan, V.V. Uzhinskii
Joint Institute for Nuclear Research
Laboratory of High Energies
Dubna, Russia

June 6, 2000

In the framework of the modified FRITIOF model, the inclusive spectra of the cumulative π^0-mesons produced in the forward direction in the nucleus-nucleus interactions at 4.5 GeV/c/nucleon are calculated. It is shown that the model reproduces qualitatively, and i= n some cases quantitatively the main experimental regularities. Accordi= ng to the model, the production of the cumulative particles is connected with the mechanism of the "soft" nucleon-nucleon interaction, and with the character of the QCD string fragmentation. Fermi motion does not play an essential role. Possibilities of the model in an application to the cumulative particle production processes are discussed.

According to the generally accepted view point, the cumulative particle production is caused by the existence in the nuclei heavy compact objects called "fluctons". An alternative possibility of the cumulative particle creation as a result of the so-called "hot" process does not consider now. However, the "hot" models ideas have found an extraordinary application in high energy physics in some modified forms. They are used in the well-known models of multi-particle production as FRITIOF [3], RQMD [4], and HIJING [5]. The common assumption of the models is that the soft inelastic hadron-hadron collisions have a binary character $a + b \to a' + b'$, where a'- and b'- are excited hadrons. The excited hadrons with masses $m_{a'}, m_{b'} > m_a, m_b$ are considered as QCD-strings, and LUND-model [7] is used to describe their decays.

In the case of hadron-nucleus interactions, the models assume that an excited hadron a' can collide with other nuclear nucleons and increase its mass. The same can take place in nucleus-nucleus interactions.

As one can easily mark, the general representation of the hadron-nucleus interactions assumed by the models is almost similar to that considered in Ref. [1]. The authors of Ref. [1] supposed, heave hadron system (a fireball) which does not include a leading particle, is created in the first collision of projectile hadron with a nuclear nucleon. The fireball moving in the nucleus collides with other nucleons, slows down and increases its mass. As a results, a production of particles in the regions kinematically forbidden in free hadron-nucleon collisions becomes possible. Thus, one can expect that the cumulative particles have to appear in the models, in particular, in the FRITIOF model.

Figs. 1, 2 show the experimental data [8] on fast π^0- mesons production in nucleus-nucleus interactions at $P = 3D$ 4.5 A GeV/c with FRITIOF model calculations taking into account the last corrections [9]. As seen, the FRITIOF model predicts the cumulative particle production.

π^0- mesons production in the pC-, pCu-, αC-, αCu-, CC- and CGu-interactions at momentum 4.5 A_p GeV/c have been studied experimentally in Refs. [8]. γ- quanta were registered at the experiments by 90-channel Cherenkov γ-spectrometer of LHE FOTON setup. π^0- mesons with the angles in laboratory system (in the rest frame of target) $\theta_\pi \leq 16^0$ and energies $E_\pi \geq 2$ GeV were considered after estimation background conditions and π^0 identification.

In Fig.1, the experimentally measured invariant cross-sections of π^0-mesons production per mass number of projectiles (A_p) as a function of cumulative number X are presented by circles. The variable X was determined as

$$X = 3D\frac{m_N E_{\pi^0} - m^2_{\pi^0}/2}{E_N m_N - E_N E_{\pi^0} - m^2_N + P_N P_{\pi^0} cos\theta_{\pi^0}},$$

where m_N and m_{π^0} are nucleon and meson masses, respectively, P_N is the momentum of projectile per nucleon ($P_N = 3D4.5$ GeV/=E1) P_{π^0} is π^0 momentum, $E_N = 3D\sqrt{M^2_N + P^2_N}$, $E_{\pi^0} = 3D\sqrt{m^2_{\pi^0} + P^2_{\pi^0}}$. The systematic errors of the cross-section is about ~ 20 %. The statistical errors are in the circle limits.

In fig1, histograms demonstrate calculations of the cross-sections of π^0- mesons production at $E_{\pi^0} \geq 2$ GeV and $\theta_{\pi^0} \leq 16^0$ performed within

the framework of FRITIOF model. The calculation results are normalized on the nucleus-nucleus interactions cross sections obtained in Glauber approach [10]. As seen, the slopes of experimental and the calculated curves are close, but the calculated cross-sections overestimate the experimental values 2-3 times.

Fig. 2 illustrates a better agreement between calculations and experimental data. Fig. 2 gives the invariant cross-sections of π^0-mesons production with respect to the π^0 -meson transverse momentum. The model reproduces both spectrum forms and the absolute values of the cross-sections. The reason of such different descriptions of experimental data of fig. 1 and fig. 2 is not clear for us.

The model FRITIOF allows one to decipher the cumulative particle production mechanism in detail. The different characteristics of CC-interaction events accompanied by the fast π^0 -meson production are presented in fig. 3. Fig. 3a shows the yields into the invariant inclusive cross-section of projectile and target nucleons (dashed and dotted curves, respectively). The relative yields are given in fig. 3c. As seen, the contribution of the target nucleons is about ~ 25 %.

Fig. 3d shows the average lougitudinal momenta of projectile and target nucleons before and after the interaction (solid and dashed curves, respectively). According to the figure, more and more energetic projectile nucleons are selected with increase the cumulative number. Accounting the Fermi-motion is not critical for the description of the inclusive cross-sections because without the Fermi-motion the cross-section in the region of $X \sim 0.9 - 1.3$ does not decrease in needed quantity, the slope of the cross-section is only changed (see fig. 4). It is natural that the longitudinal momenta of projectile nucleons decrease some during the interaction, but this takes place below $X \sim 1.5$. The nucleons acquired the momenta larger than momenta of incident nucleons, give the contribution in the region of large X.. It is clearly seen in the calculations performed without taking the Fermi-motion into account (see insert in fig. 4). The considered effect of the nucleon acceleration is a specific feature of the assumed nucleus-nucleus interaction mechanism.

Fig. 3e gives the analogous characteristics of the target nucleons. The longitudinal momenta of target nucleons are small before the interaction (see dashed curve). In the course of the interaction, the nucleons have to acquire significant longitudinal momenta for the cumulative particle production in the forward direction (see solid curve).

Fig. 3f shows the masses of the projectile and target nucleons which give the cumulative meson, after the interaction (see solid and dashed curves). As seen, the projectile nucleons acquire larger excitations then the target nucleons. These coincide with the main imaginations of the "hot" models with the exception of the possibility of the nucleon acceleration.

The presented results allow one to expect a description of spectra of cumulative π- and K- mesons. Most probably, a problem of a cumulative proton production will take place. The matter is Glauber approach used in the FRITIOF model underestimates multiplicity of ejected nucleons. So, taking into account additional destruction of nuclei is needed what can be done, for example, within the framework of approach of Ref. [11]. In this case, the Fermi-motion manifests itself stronger. Probably, a relativistic quantum molecular dynamics (RQMD) model [4] application allows one to avoid the problem, because the model describes the proton production taking into account the secondary interactions in nuclear residuals. However, the models can not predict the yields of deuterium, tritium and helium nuclei. Perhaps, one should take into account the multi-quark states in the nuclei and their fragmentation.

The first task is to calculate the absolute values of the inclusive cross-sections. The questions about fluctons in nuclei will be arisen if the calculated values are less than the experimental ones. In order to solve the problem we are going to turn to the hadron-nucleus interaction data.

The authors express their sincere gratitude to Kh.U. Abraamyan, G.L. Melkumov and A.G. Litvinenko for their fruitful discussions and valuable remarks.

References

[1] Gorenstain M.I., Zinovjev G.M., Shelest V.P.// Phys. Lett. B, 1977, V. **67**, P. 100; Yad. Fiz., 1977, V. 26, P. 788.

[2] Kalinkin B.N., Shmonin V.L.// Phys. Scripta, 1990, V. **42**, P. 393;

[3] Andersson B. et al.// Nucl. Phys. B, 1987, V. **281**, P. 289;

Nilsson-Almquist B., Stenlund E.// Comp. Phys. Comm., 1987, V. **43**, p. 387.

[4] Sorge H., Stöker H., Greiner W.// Ann. of Phys. (N.Y.), 1989, V. **192**, P. 260; Sorge H., Winckelmann L.A., Stöker H., Greiner W.//Zeit. Phys. C, 1993, V. **59**, P. 85.

[5] Gyulassy M., Plumer M.// Phys. Lett. B, 1990, V. **243**, p. 432; Wang X.-N., Gyulassy M.// Phys. Rev. C, 1991, V. **44**, P. 3501.

[6] Adamovich M.I. et al. (EMU-01 Collaboration)// Zeit. für Phys. A, 1997, V. **358**, P. 337.

[7] Sjöstrand T.// Comp. Phys. Commun., 1986, V. **39**, P. 347;

Sjöstrand T., Bengtsson M.// Comp. Phys. Commun., 1987, V. **43**, P.367.

[8] Abraamyan Kh.U. et al.// JINR preprint, 1992, E1-92-307, Dubna; Phys. Lett. B, 1994, V. 323, p. 1; Kh.U. Abraamyan et al.// Yad. Fiz, 1996, V. 59, P. 271; Kh.U. Abraamyan et al.// Yad. Fiz., 1997, V. 60, P. 2014.

[9] G. Ganhuyag, V.V. Uzhinskii// JINR Commun., 1997, **=901-97-315**, Dubna; JINR Commun., 1997, **=902-97-397**, Dubna.

[10] Shmakov S.Yu. Uzhinski V.V., Zadorojny A.M.// Comp. Phys. Commun., 1989, V. **54**, P. 125.

[11] El-Waged Kh., Uzhinskii V.V.// =9F=94, 1997, =92. **60**, =91. 925.

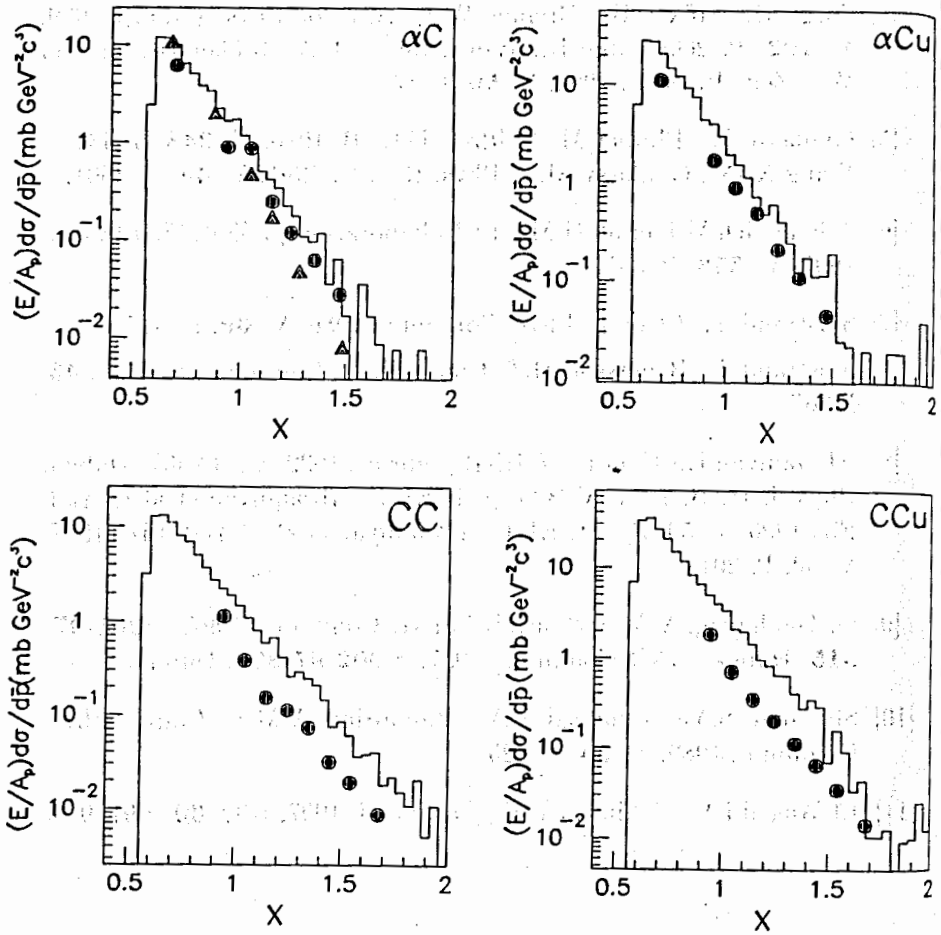

Figure 1: Invariant inclusive cross-sections of π^0-mesons production in nucleus-nucleus interactions at 4.5 GeV/c/nucleon. The points are experimantal data [8], histograms are the FRITIOF model calculations.

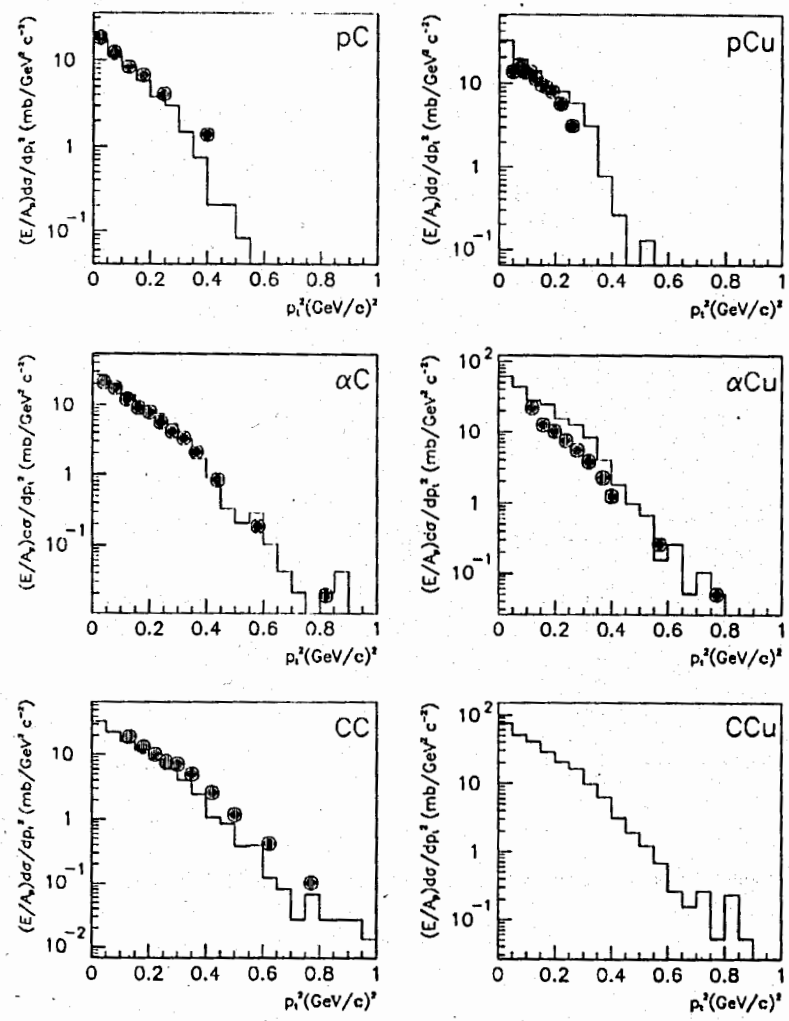

Figure 2: Invariant inclusive cross-sections of π^0-mesons production in nucleus-nucleus interactions at 4.5 GeV/c/nucleon. The notation is identical to that in fig. 1.

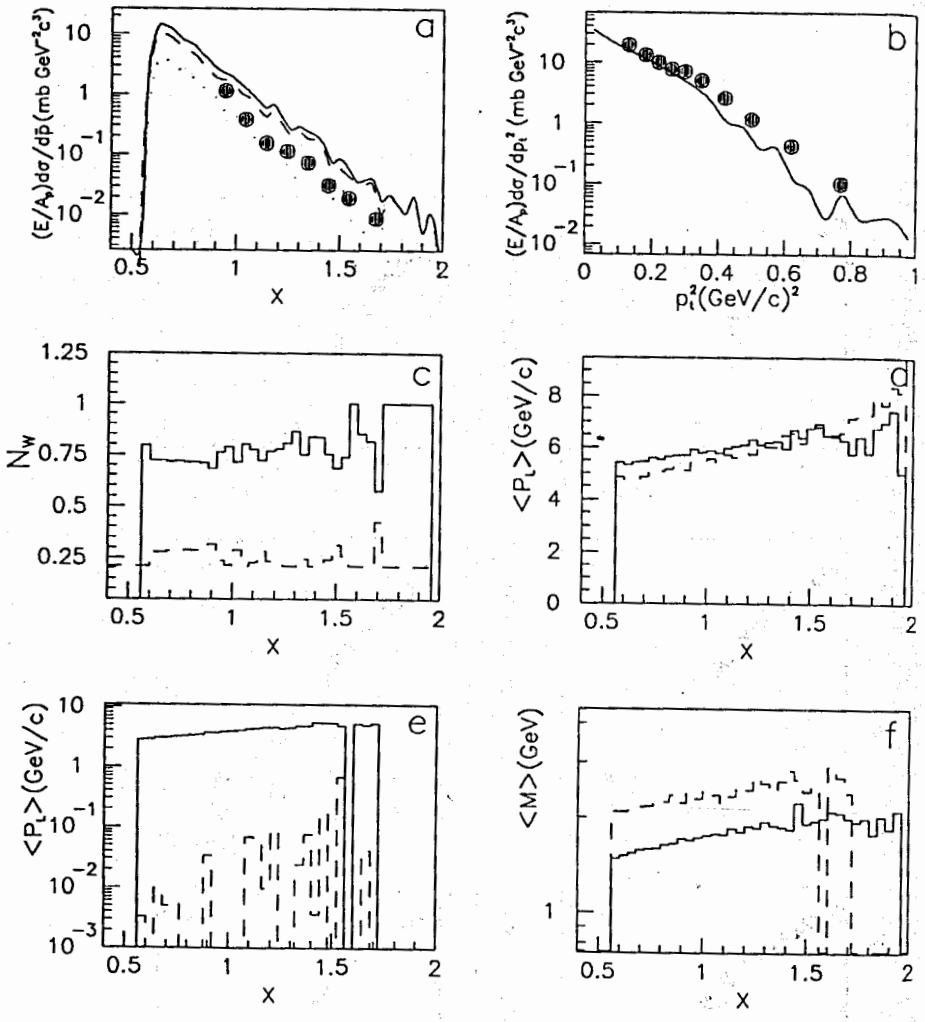

Figure 3: Various characteristics of CC-interactions with fast π^0-mesons production.

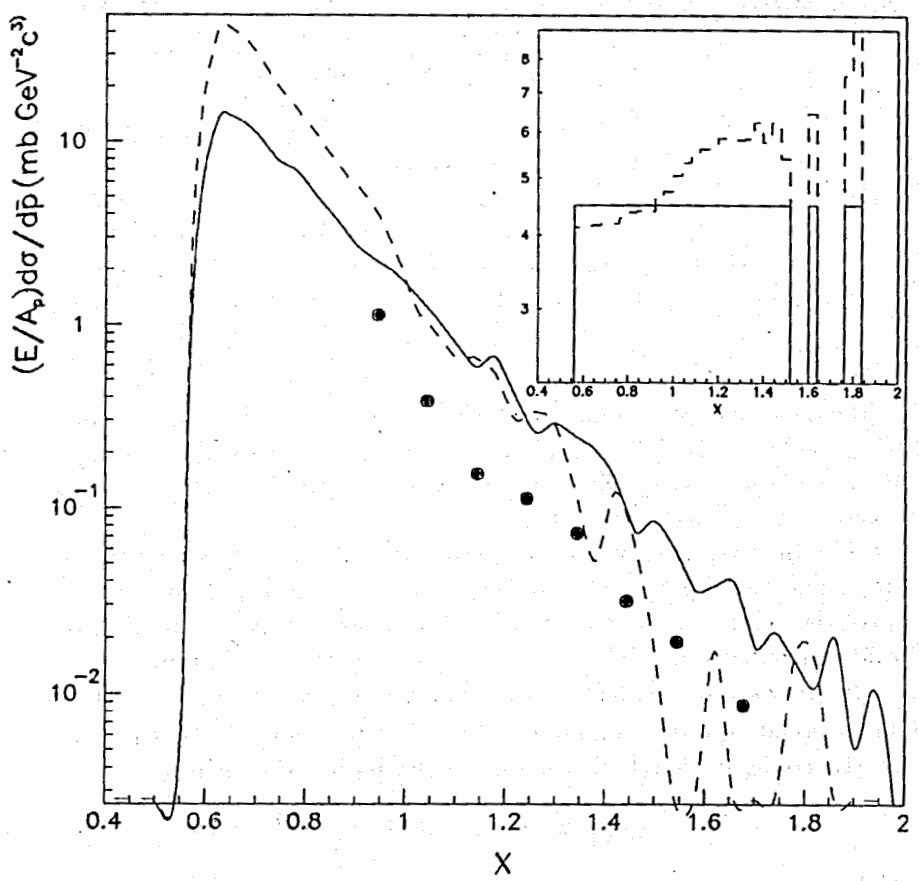

Figure 4: Invariant inclusive cross-sections of π^0-mesons production in CC - interactions at 4.5 GeV/c/nucleon. The points are experimantal data [8], the curves are the FRITIOF model calculations.

One-dimensional relativistic bound state problem for superposition of N δ-potentials

V.N.Kapshai, T.A.Alferova

Gomel State University, Sovetskaia str., 102, Gomel, 246699, Belarus

Abstract

The one-dimensional relativistic bound state wavefunctions for four kinds of quasipotential equations for superposition of N δ-potentials are obtained. The quantization condition for such kind of potentials is studied in details.

In the past models of point interaction have been much developed in quantum mechanics [1]-[3]. At this time the one-dimensional Shrödinger and Dirac equations with point interactions and their generalizations have attracted a lot of attention [4]-[7].

The investigation of the relativistic two-particle equations [8, 9] with single and two δ-potentials has been started in [10, 11]. Now our aim is to solve the relativistic quasipotential equations with N δ-potentials and to study the effects, available for such potentials for bound states.

In the case of particles with equal masses ($m_1 = m_2 = m$) the one-dimensional equation for bound state wavefunctions $\Psi^{(j)}_{iw}(\rho)$ in the relativistic configurational representation (RCR) has the form

$$\Psi^{(j)}_{iw}(\rho) = \int g^{(j)}_m(E_{iw};\rho,\rho')\,V(\rho')\,\Psi^{(j)}_{iw}(\rho')\,d\rho', \tag{1}$$

where

$$E_{iw} = \sqrt{m^2 + (iw)^2} = m\cos\xi, \tag{2}$$

and $g^{(j)}_m(E_{iw};\rho,\rho')$ are relativistic Green functions in the RCR. In this paper we consider four kinds of quasipotential equations. The Logunov-Tavkhelidze equation for two scalar particles ($j = 1$) and Kadyshevsky equation for two spinor particles ($j = 2$) contain the following Green functions [12]:

$$g^{(1)}_m(E_{iw};\rho,\rho') = \frac{-1}{m\sin 2\xi}\frac{\sinh\left[\left(\frac{\pi}{2}-\xi\right)m(\rho-\rho')\right]}{\sinh\left[\frac{\pi}{2}m(\rho-\rho')\right]}, \tag{3}$$

$$g^{(2)}_m(E_{iw};\rho,\rho') = \frac{-1}{m\sin 2\xi}\frac{\sinh\left[(\pi-\xi)m(\rho-\rho')\right]}{\sinh\left[\pi m(\rho-\rho')\right]} + \frac{(4m\cos\xi)^{-1}}{\cosh\left[\frac{\pi}{2}m(\rho-\rho')\right]} \tag{4}$$

For the modified Logunov-Tavkhelidze ($j = 3$) and modified Kadyshevsky ($j = 4$) equations the Green functions are

$$g^{(3)}_m(E_{iw};\rho,\rho') = \frac{-1}{2m\sin\xi}\frac{\cosh\left[\left(\frac{\pi}{2}-\xi\right)m(\rho-\rho')\right]}{\cosh\left[\frac{\pi}{2}m(\rho-\rho')\right]}, \tag{5}$$

$$g^{(4)}_m(E_{iw};\rho,\rho') = \frac{-1}{2m\sin\xi}\frac{\sinh\left[(\pi-\xi)m(\rho-\rho')\right]}{\sinh\left[\pi m(\rho-\rho')\right]}. \tag{6}$$

Our purpose is to investigate relativistic two-particle equations (1)-(6) with some superposition of N δ-potentials (V_s are real)

$$V(\rho) = \sum_{s=1}^{N} V_s\delta(\rho-a_s); \quad a_s = 2a(s-1). \tag{7}$$

The wavefunctions of equation (1) with potential (7) can be obtained easily:

$$\Psi^{(j)}_{iw}(\rho) = \sum_{s=1}^{N} g^{(j)}_m(E_{iw};\rho,a_s)\,V_s\Psi^{(j)}_{iw}(a_s), \tag{8}$$

where constants $\Psi^{(j)}_{iw}(a_s)$ ($s = 1 \div N$) should be solutions of the following algebraic system

$$M^{(j)}_{ks}(E_{iw})\Psi^{(j)}_{iw}(a_s) = 0; \quad M^{(j)}_{ks}(E_{iw}) = \delta_{ks} - g^{(j)}(E_{iw},m;a_k,a_s). \tag{9}$$

The quantization condition can be determined as follows

$$\det M^j(E_{iw}) = 0. \tag{10}$$

Let us consider the potential as a superposition of N δ-"holes"($V_s = -V < 0$). The curves for the energy levels E as functions of the "hole depth" V for the superposition of 3 δ-"holes" with the same value of parameter a are given in figure 1. Number of energy levels is equal to the number of δ-"holes" (see figure 2(a)).

In order to compare the relativistic and non-relativistic results let us consider the parameters V and E in the range of value corresponding to the non-relativistic case: $V \le m$, E is close to m. To emphasize the descriptive behaviour of the curves let us choose the parameter a as large as there is only the first energy level. The behaviour of the first level for all four relativistic equations and Shrödinger equation as a function of

parameter V is given in figure 2(b). In the region of small values of V the relativistic results coincide well with the non-relativistic one.

The behaviour of energy levels of the Logunov-Tavkhelidze equation as a function of V and a function of a are given in figure 3. The wavefunctions of all the considered relativistic quasipotential equations are presented in figure 4.

References

[1] A.I.Baz, Y.B.Zeldovich, A.M.Perelomov. Scattering, Reactions and Decay in Nonrelativistic Quantum Mechanic. Moscow: Nauka. 1971.

[2] Y.N.Demkov, V.N.Ostrovsky. Zero-range Potentials and their Applications in Atomic Physics. New York-London: Plenum Press Translation of the Russian edition:Leningrad Univ.Press Leningrad.1988.

[3] S.Albeverio et al . Solvable Models in Quantum Mechanics. New-York: Springer-Verlag. 1988.

[4] S. Albeverio, L.Dabrowski, P.Kurasov // Lett. Math. Phys. 1998. V.45 P.33

[5] P.Kurasov// J. Math. Anal. Appl. 1996. V.201. P.297.

[6] J.Dittrich, P.Exner, P.Seba// J. Math. Phys. 1989. V.30. P.2875.

[7] M.G.Calkin, D.Kiang, Y.Nogami// Phys. Rew. C. 1988. V.38. P.1076.

[8] A.A. Logunov, A.N. Tavkhelidze// Nuovo Chimento, 1963 V.29. P.380.

[9] V.G.Kadyshevsky // Nucl. Phys. B, 1968 V.6. P. 125.

[10] V.N.Kapshai, T.A.Alferova//Proceed. of Intern. School-Seminar "Actual Problems of Particle Physics", Dubna 1998. V.1. P.294.

[11] V.N.Kapshai, T.A.Alferova// J.Phys.A: Math.Gen. 1999 V.32. P.5329.

[12] V.N.Kapshai, T.A.Alferova// In summaries "Kovariantnye metody v teor.fizike", 1997. V.4. P.88.

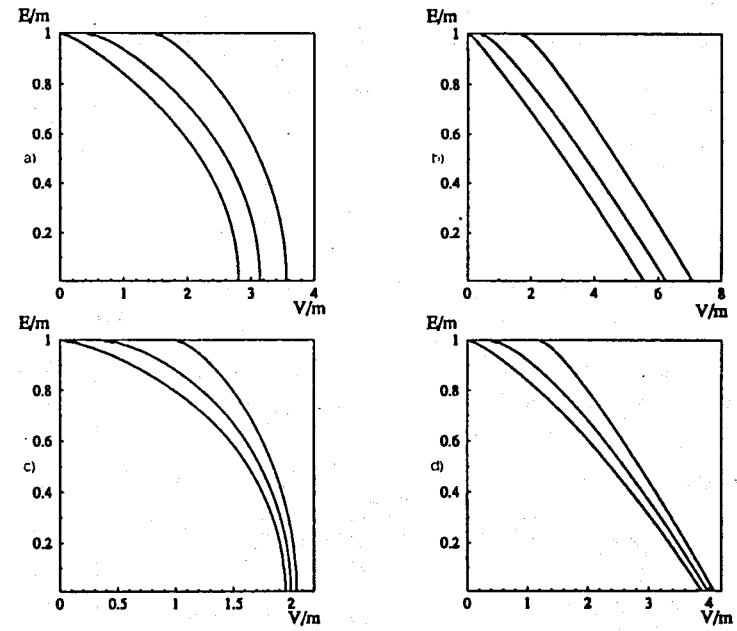

Figure 1: Energy levels as a function of V for $ma = 1.5$, $N = 3$ a) the Logunov-Tavkhelidze equation; b) the Kadyshevsky equation; c) the modified Logunov-Tavkhelidze equation; d) the modified Kadyshevsky equation.

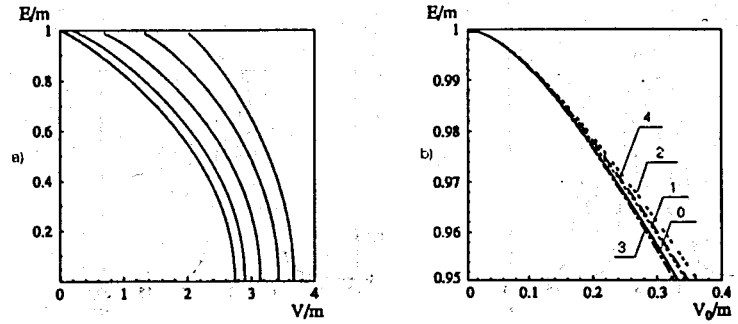

Figure 2: $N = 5$: a) energy levels as a function of V for $ma = 1.5$ for the Logunov-Tavkhelidze equation; b) the first energy level as a function of V for $ma = 1$: 0- for the Shrödinger equation; 1- for the Logunov-Tavkhelidze equation: 2- for the Kadyshevsky equation; 3- for the modified Logunov-Tavkhelidze equation: 4- for the modified Kadyshevsky equation.

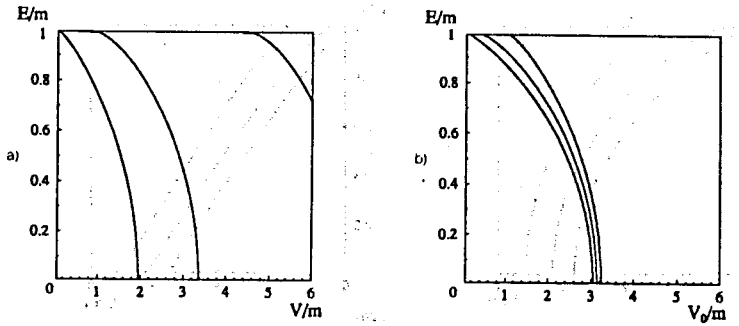

Figure 3: Energy levels as a function of V for the Logunov-Tavkhelidze equation $N = 3$: a) $a = 0.8$; b) $a = 2$.

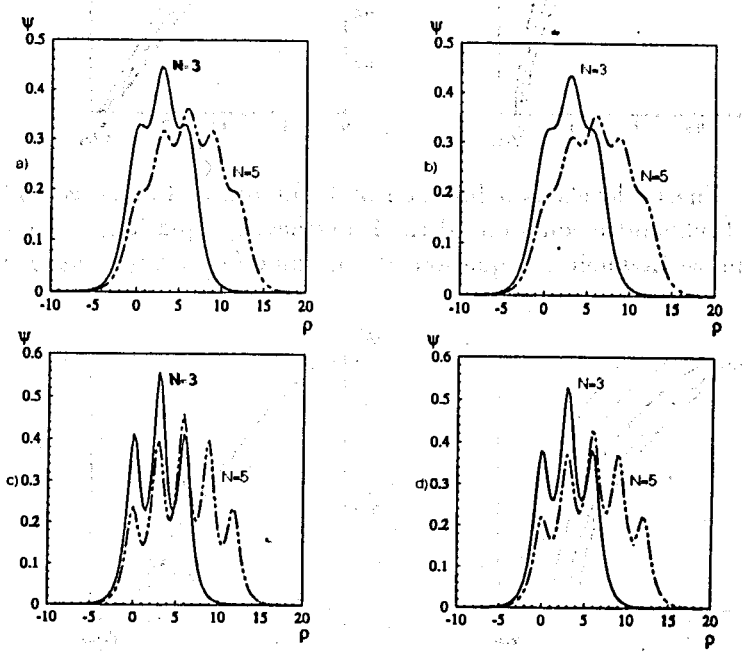

Figure 4: Wavefunctions of the ground state at $ma = 1.5$, $E_{iw} = 0.5m$: a) the Logunov-Tavkhelidze equation: b) the Kadyshevsky equation; c) the modified Logunov-Tavkhelidze equation: d) the modified Kadyshevsky equation.

Physics in and beyond the framework of Standart Model

Effects of fermion and boson mixing at e^+e^- linear collider

A. A. Babich

Gomel State Technical University named by Pavel Sukhoy, Gomel, 246746 Belarus

Abstract

This lecture contains a brief introduction to the formalism of fermion and gauge boson mixing. Separately considered the mixing in charge and neutral fermion sectors. The effects of simultaneous fermion and gauge boson mixing are discussed too. The modern experimental constrains on the some common mixing parameters are represented.

1 Introduction.

Grand unified theories (GUT's) are an attractive extension of the standard model (SM), allowing us to understand the relative values of the gauge couplings, the quantization of the electric charge, as well as successfully predicting some fermion mass ratios. Furthermore, GUT's are a natural outcome of more fundamental theories such as superstrings. As soon as one considers unification groups beyond the simplest $SU(5)$, two general consequent result: (i) the low–energy gauge group often contains extra $U(1)$ factors; (ii) the fermionic sector is enlarged, since the matter multiplets are in larger representations [**16** for $SO(10)$, **27** for E_6, etc.]. Moreover, since with the fermion content of the SM no new anomaly–free currents are possible beyond those of $SU(5)$, the presence of new fermions in any extended unified gauge model is a necessary condition to ensure anomaly cancellation.

In many models the masses of the new fermions arise from the same vacuum expectation values (VEV's) that give mass to the extra gauge bosons, and hence are expected to be not much larger than $M_{Z'}$ itself. If new fermions are present, there are good reasons to believe that they will mix with the known states: for the neutral fermions the mixing naturally arise in seesaw models, which provide a nice explanation for the lightness of the known neutrinos. For the charged fermions, a mixing would provide a natural channel for the decay of heavy ones, avoiding cosmological consequences that would be problematic if the heavy fermions were stable [1], [2]. Hence, in the presence of a light ($100\ GeV$ - $1\ TeV$) Z' boson, one also expects some light ($\lesssim 1\ TeV$) fermions mixing with the known ones, and the modifications on the electroweak observables induced by the presence of both these kinds of new states may well complete, so that it is important to consider all effects simultaneously.

¿From the phenomenological point of view much effort has been devoted to constrain a Z' boson associated with an extra $U(1)$ surviving below the TeV scale via its indirect effects [3] - [6]. In addition to the direct searches for new particles, strong bounds have been also set on the mixing between the known fermions and heavy new ones, which would affect the couplings of the light states to the standard gauge bosons [7]-[9]. While rather exhaustive analysis exist where either only the modification due to an extra neutral boson, or only the mixing effects induced by the new fermions, are considered, at present only a few steps have been done in trying to take into account these two effects simultaneously [10]-[12]. The aim of the present report is to study in detail the interrelation between the two possible sources of deviations from the SM predictions.

2 Exotic fermions.

In the SM, all left-handed (L) fermions transform as doublets under weak $SU(2)_W$, while all right-handed (R) fermions are singlets:

$$\begin{pmatrix} \nu_e \\ e^- \end{pmatrix}_L \begin{pmatrix} \nu_\mu \\ \mu^- \end{pmatrix}_L \begin{pmatrix} \nu_\tau \\ \tau^- \end{pmatrix}_L \begin{pmatrix} u \\ d \end{pmatrix}_L \begin{pmatrix} c \\ s \end{pmatrix}_L \begin{pmatrix} t \\ b \end{pmatrix}_L , \qquad (1)$$

$$e_R^- \quad \mu_R^- \quad \tau_R^- \quad u_R \quad c_R \quad t_R \qquad (2)$$
$$d_R \quad s_R \quad b_R$$

Many models which go beyond the SM predict the existence of new

fermions which transform in a non-standard way under $SU(2)_W$. in E_6 models, for example, in the 27-plet one finds, in addition to the ordinary particles, vector singlet quarks and vector doublet leptons. Vector singlet (doublet) fermions refer to particles whose L and R components both transform as singlets (doublets) under $SU(2)_W$. One also finds new $SU(2)_W$ - singlet Weyl neutrinos in the 27-plet. Mirror fermions are another type of exotic fermion, whose transformation properties under $SU(2)_W$ are opposite those of ordinary fermions, i.e. left-handed singlets and right-handed doublets. These appear, for instance, in grand unified theories which include family unification.

The possibilities for new fermions are listed below:

- Canonical $SU(2)_W \times U(1)$ assignments

  a) sequential fermions

$$\begin{pmatrix} N \\ E^- \end{pmatrix}_L \quad E_R, \quad \begin{pmatrix} U \\ D \end{pmatrix}_L \quad \begin{matrix} U_R \\ D_R \end{matrix} \qquad (3)$$

- Non-canonical $SU(2)_W \times U(1)$ assignments

  a) vector doublets

$$\begin{pmatrix} N \\ E^- \end{pmatrix}_L \quad \begin{pmatrix} N \\ E^- \end{pmatrix}_R , \quad \begin{pmatrix} U \\ D \end{pmatrix}_L \quad \begin{pmatrix} U \\ D \end{pmatrix}_R \qquad (4)$$

  b) mirror fermions

$$E_L^- \quad \begin{pmatrix} N \\ E^- \end{pmatrix}_R , \quad \begin{matrix} U_L \\ D_L \end{matrix} \quad \begin{pmatrix} U \\ D \end{pmatrix}_R \qquad (5)$$

  c) vector singlets

$$E_L^- \quad E_R^- , \quad \begin{matrix} U_L & U_R \\ D_L & D_R \end{matrix} \qquad (6)$$

  d) Weyl neutrinos

$$N_L \quad N_R \qquad (7)$$

Here pairs of particles enclosed in parenthesis indicate $SU(2)_W$ doublets and otherwise they are $SU(2)_W$ singlets; N - neutral lepton, E - charge lepton, U - up-quark ($+\frac{2}{3}$) and D - down-quark ($-\frac{1}{3}$). In following all particles with unconventional isospin assignments (left-handed singlets or

right–handed doublets) will be denoted as *exotic* fermions, and all remaining new fermions as well as all the standard ones, which have conventional assignments, are referred to as *ordinary*. Since no new fermions have been directly observed yet, if new states exist they should be rather heavy ($m_{new} \geq E_{beam}/2$, where E_{beam} – beam energy modern electron–positron colliders (LEP2, SLC)), with possible exception of the singlet neutrinos. However, since the light mass eigenstates will in general correspond to superpositions of the known and new states, the new fermions could manifest themselves indirectly through a mixing with the known ones.

3 Fermion mixing formalism.

Now we discuss the fermion mixing formalism between the known and new states in general context. Since $SU(1)_{em}$ and $SU(3)_c$ are unbroken, different gauge eigenstates can mix only when they have the same electric and color charges, and hence the electromagnetic and color currents of the mass eigenstates are not modified by the fermion mixing. So fermions can be divided into four categories, a namely, u – type with $Q_{em} = 2/3$, d – type with $Q_{em} = -1/3$, e – type with $Q_{em} = -1$ and n – type with $Q_{em} = 0$. The case of mixing in neutrino sector is more complicated and we consider the charged fermion mixing and the neutral fermion mixing separately.

3.1 Charged fermion mixing

As known in the gauge currents chirality is conserved, and it is convenient to group the fermions with the same electric charge and chirality $\alpha = L, R$ in column vector of the known and new gauge eigenstates $\Psi^0_\alpha = (\Psi^0_\mathcal{K}, \Psi^0_\mathcal{N})^T_\alpha$. The eigenstates in Ψ^0_α can be mixed via the mass matrix, and their relation with the corresponding light and heavy mass eigenstates $\Psi_\alpha = (\Psi_l, \Psi_h)^T_\alpha$ is given by a unitary transformation

$$\begin{pmatrix} \Psi^0_\mathcal{K} \\ \Psi^0_\mathcal{N} \end{pmatrix}_\alpha = U_\alpha \begin{pmatrix} \Psi_l \\ \Psi_h \end{pmatrix}_\alpha, \text{ where } U_\alpha = \begin{pmatrix} A & G \\ F & H \end{pmatrix}_\alpha, \ \alpha = L, R \qquad (8)$$

The submatrices A and F describe the overlap of the light eigenstates with the known and the new states, respectively. The unitarity of U_α requires

$$A^\dagger A + F^\dagger F = A A^\dagger + G G^\dagger = I, \qquad (9)$$

and so the matrix A deviates from unitary one by small light–heavy mixing effects contained in F.

In terms of the fermion mass eigenstates the neutral current corresponding to a generator $\mathcal{Q}$ is

$$J^\mu_\mathcal{Q} = \sum_{\alpha=L,R} \bar{\Psi}_\alpha \gamma^\mu U^\dagger_\alpha \mathcal{Q}_\alpha U_\alpha \Psi_\alpha. \qquad (10)$$

Here $\mathcal{Q}$ represents a generic diagonal matrix of the charges for the chiral fermions. From (10) one readly notes that if in one subspace of states with equal electric charge and chirality the matrix $\mathcal{Q}_\alpha$ is proportional to the identity, the current for these fermions is not modified in going to the base of the mass eigenstates, and the corresponding gauge couplings are not affected. This happens for example in the SM, where for a given electric charges and chirality the eigenvalues of T_3 are indeed the same, implying in particular the absence (at the tree level) of flavor–changing neutral current (GIM mechanism).

In model with new fermions, the matrices $\mathcal{Q}_\alpha$ have the general form $\mathcal{Q}_\alpha = \text{diag}(\mathcal{Q}^\mathcal{K}_\alpha, \mathcal{Q}^\mathcal{N}_\alpha)$. Also, if the gauge group is generation independent all the known states appearing in one vector Ψ^0_α have the same eigenvalues with respect to the generators of the gauge symmetry, and hence $\mathcal{Q}^\mathcal{K}_\alpha = q^\mathcal{K}_\alpha I$ with $q^\mathcal{K}_\alpha = t_3(f^\mathcal{K}_\alpha), q_1(f^\mathcal{K}_\alpha)$. This also happens for the new charged states in E_6, i.e., $\mathcal{Q}^\mathcal{N}_\alpha = q^\mathcal{N}_\alpha I$. In contrast, since more different types of neutrino are present in E_6, for the neutral states appearing in $\Psi^0_\mathcal{N}$, $\mathcal{Q}^\mathcal{N}_\alpha$ is not proportional to the identity.

Keeping only those terms which involve just light states the weak neutral current can now be expressed as

$$J^\mu_{l\mathcal{Q}} = \sum_{\alpha=L,R} \Psi_{l\alpha} \gamma^\mu \left[q^\mathcal{K}_\alpha A^\dagger_\alpha A_\alpha + F^\dagger_\alpha \mathcal{Q}^\mathcal{N}_\alpha F_\alpha \right] \Psi_{l\alpha} \qquad (11)$$

$$= \sum_{\alpha=L,R} \Psi_{l\alpha} \gamma^\mu \left[q^\mathcal{K}_\alpha + (q^\mathcal{N}_\alpha - q^\mathcal{K}_\alpha) F^\dagger_\alpha \mathcal{Q}^\mathcal{N}_\alpha F_\alpha \right] \Psi_{l\alpha}. \qquad (12)$$

The first form (11) is general, and describes the effects of fermion mixing in the neutral current of light states for a wide class of model, while the second form (12), obtained via the unitarity relation (9), holds when the mixing is with only one type of new states that have the same $q^\mathcal{N}_\alpha$ charges, as is the case for the charged fermions of E_6 and the neutrinos in $SO(10)$.

The important point to recognize here is that, since neither A_α nor F_α is unitary, $A^\dagger_\alpha A_\alpha$ and $F^\dagger_\alpha F_\alpha$ are not necessary diagonal. In other words, FCNC

will in general be induced among the light particle. However, extremely stringent constraint exist on μe, sd and bd transitions, and imply that the corresponding terms are at most $\sim 10^{-4}$ [13]. Tight bounds $\sim 10^{-2}$ exist for bs, τe and $\tau\mu$ flavor changing parameters as well [13]. Hence, if flavor changing vertices exist in Z_0 interactions, most of them must be negligible, and it is then reasonable to concentrate in constraining possible deviations in flavor diagonal couplings. Assuming the absence of FCNC is equivalent to assume that different light mass eigenstates are not mixed with the same exotic partner, in which case the $F^\dagger F$ terms corresponding to ordinary - exotic mixing are diagonal. With this assumption, we can define the mixing angles $\theta^f_{L,R}$ that describe the mixing between L or R ordinary and exotic partners through

$$(F^\dagger_\alpha F_\alpha)_{ff'} = (s^f_\alpha)^2\delta_{ff'}, \quad f_\alpha, f'_\alpha = e_R, \mu_R, \tau_R, d_L, s_L, b_L, \tag{13}$$

where $(s^f_{L,R})^2 \equiv 1-(c^f_{L,R})^2 \equiv \sin^2\theta^f_{L,R}$. The flavor diagonal chiral coupling to the Z_0 of the corresponding light mass eigenstates then read as

$$\begin{aligned} \varepsilon_{0R}(f) &= -\frac{1}{2}(s^f_R)^2 + s^2_W, \quad f = e, \mu, \tau \\ \varepsilon_{0L}(f) &= -\frac{1}{2}(c^f_L)^2 + \frac{1}{3}s^2_W, \quad f = d, s, b. \end{aligned} \tag{14}$$

Similarly, the chiral couplings in the J^μ_1 current are also flavor diagonal, and we find

$$\varepsilon_{1R}(f) = q_1(f_\alpha) + (s^f_\alpha)^2[q_1(f^{\mathcal{N}}_\alpha) - q_1(f_\alpha)], \; f = e_R, \mu_R, \tau_R, d_L, s_L, b_L. \tag{15}$$

If $t_3(f^{\mathcal{N}}) = t_3(f^{\mathcal{K}})$, as in case the left-handed charged leptons and right-handed $q_{em} = -\frac{1}{3}$ quarks in E_6, then, since the coefficient of the $F^\dagger F$ term in (12) vanishes identically, the J^μ_0 current is not modified in going to the mass eigenstate basis, and the chiral couplings of the corresponding fermions conserve the standard form

$$\varepsilon_{0L}(e) = -\frac{1}{2} + s^2_W, \quad \varepsilon_{0R}(d) = \frac{1}{3}s^2_W. \tag{16}$$

In contrast, in general $q_1(f^{\mathcal{N}}) \neq q_1(f^{\mathcal{K}})$, and the mixing between the ordinary known and new fermions will indeed affect the ε_1 couplings. Unfortunately, since Z_0 interactions cannot provide information on the $F^\dagger F$ parameters, there is not possibility to derive constraints on ordinary–ordinary mixings.

Fermion mixing affect the charged current sector as well. For the hadrons, since the only exotic quarks present in E_6 are d_L type, the general formalism acquires a much simpler form. In the standard base, where the gauge and mass eigenstate up quarks coincide, the charged current between light mass eigenstate quarks is

$$\frac{1}{2}J^\mu_W = \bar{\Psi}^u_{lL}\gamma^\mu A^d_L \Psi^d_{lL}, \tag{17}$$

where $\Psi^u_{lL} = (u, c, t)^T_L$ and $\Psi^d_{lL} = (d, s, b)^T_L$. A^d_L here plays the role of an apparent CKM mixing matrix, but clearly it is not unitary due to the mixing with the exotic quarks.

3.2 Neutral fermion mixing

For the neutral fermions situation is more complicated and a few specific assumptions have to be formulated as well. At first, neutral fields with three different weak –isospin assignments can mix simultaneously in the presence of Majorana mass term. In fact, in addition to the known neutrinos in SM there are new *ordinary* neutrinos in the L doublets $(N\ E^-)^T$. The *exotic* neutral states with $t_3 = -\frac{1}{2}$ appearing in $(E^+\ N^c)^T_L$ can also mix with the known neutrinos through lepton–number violating $\Delta L = \pm 2$ Majorana mass terms, and finally, for each fermion family. In E_6 two $SU(2)$ exotic singlets ν^c_L and S_L are also present.

At second, there is the lack of experimental constraints on neutrino FCNC's so that, as for the ordinary–ordinary mixing, again we cannot make any assumption on the form of the $F^\dagger F$ term in (11). However, in all the measurements the final–states neutrinos are not detected, so that a sum over the flavor of the final mass eigenstates has to be taken. Under this condition, we can again account for the mixing effects in the neutral sector without introducing explicit FCNC parameters. A further assumption has to be made regarding the number of light neutrinos. For simplicity we assume that only the three known neutrinos, which are mainly ordinary states, are light.

In analogy with the charged fermions, it is convenient to introduce a vector $n^0_L = (\nu^0_{\mathcal{K}}, \nu^0_{\mathcal{N}})^T_L$ for the known and new neutral gauge eigenstates and a vector $n_L = (n_l, n_h)^T_L$ for the light– and heavy–mass eigenstates, to label the elements of the basis with indices $a, b...$ and $i, j...$, respectively, and to drop the index $\mathcal{K}$ when no confusion can arise. We will also not distinguish

between left-handed neutrinos and antineutrinos. They are all described by field n_L. The right-handed fields will be denoted as $n_R^c = C\bar{n}_L^T$, and clearly $n_R^{0c} = U_R n_R^c$ with $U_R = U_L^*$. Hence it is understood that (11) has to be restricted only to L-chirality states in this case.

It is useful to decompose the vector of newstates and the matrix F_L, relating the new state with the light ones, as

$$\nu_{NL}^0 = (N, N^c, S)_L^T, \quad F_L = (O, E, S)_L^T, \tag{18}$$

where each submatrix describes the overlap of the light states with the new ordinary, exotic doublet, and exotic singlet neutrinos, respectively. Three light neutrino states are the standard ν_K^0 neutrinos, and the matrix A_L, describing the overlap of the light neutrinos with the ordinary known ones, is 3×3 and deviates from a unitary one only by small mixing effects in F_L.

In the flavor basis such that the charged lepton flavor eigenstates coincide with the charged mass eigenstates up to light-heavy mixing effects, the charged current between light states is

$$\frac{1}{2} J_W^\mu = \bar{n}_L \gamma^\mu A_L^\dagger e_L + \bar{n}_R^c \gamma^\mu E_R^\dagger s_R^e e_R. \tag{19}$$

In the first term in this equation the overall strength of the left-handed is reduced by the effect of light-heavy mixing appearing in the $A_L^\dagger$ neutrino projector, while the second term corresponds to an induced right-handed current that will produce neutrinos of the nonconventional helicity in weak decays. It is convenient to introduce the leptonic analog of the CKM matrix, K_l, by writing $A^\dagger = K_l \mathcal{A}^{\nu\dagger}$. The matrix K_l is unitary and is nontrivial if nondegenerate masses and mixing are present for the light neutrinos. The exotic mixing appear only in $\mathcal{A}^\nu$, which can be chosen to be Hermitian, and deviates from the identity by terms of $\mathcal{O}(s^2)$. For instance, in a weak decay involving the $e_a \to n_i$ transition, the change with respect to the SM decay rate Γ_0 induced by the corresponding mixing is

$$\frac{1}{\Gamma_0} \sum_i \Gamma(e_a \to n_i) = (A_L A_L^\dagger)_{aa} + (s_R^{e_a})^2 (E_R E_R^\dagger)_{aa}. \tag{20}$$

The first term $(A_L A_L^\dagger)_{aa} = (\mathcal{A}^\nu)_a^2 \equiv (c_L^{\nu_a})^2 = 1 - (s_L^{\nu_a})^2$ accounts for the reduction in the light neutrinos coupling strength, and we see that the information in K_l is lost when the sum over the unobserved final neutrino

eigenstates. The second term, in which $(E_R E_R^\dagger)_{aa} \equiv (s_R^{\nu_a})^2$, appears only both the light neutrino and the R charged lepton mix with components of an exotic doublet (as is required by helicity conservation in the W interaction), and is $\mathcal{O}(s^4)$ in the light-heavy mixing. Each $(s_R^{\nu_a})^2$ represents an additional mixing parameter that ia in principle unrelated to the corresponding $(s_L^{\nu_a})^2$. For $\nu_a = \nu_e, \nu_\mu$, the existing direct constraints on the right-handed currents (RHC's) [13] ensure that it is safe to neglect the $\mathcal{O}(s^4)$ terms. However for the τ lepton, the existing direct limit is too weak to justify the same approximation. Nevertheless it is easy to show that $(s_R^{\nu_\tau})^2$ is bounded by $(s_R^{\nu_\tau})^2 \leq \sum_a (s_R^{\nu_a})^2 = \mathrm{Tr}(E_L^\dagger E_L) \leq \sum_a (s_L^{\nu_a})^2$, and this ensures that it is safe to neglect the corresponding RHC contributions as well.

Using the unitarity relation (12) and the unitarity of K_l, we can introduced common neutrino parameters by writing

$$\begin{aligned} 1 &= [K_l^\dagger (A_L^\dagger A_L + F_L^\dagger F_L) K_l]_{aa} \\ &= (c_L^{\nu_a})^2 + (\lambda_N^a + \lambda_{N^c}^a + \lambda_{\nu^c}^a + \lambda_S^a)(s_L^{\nu_a})^2, \end{aligned} \tag{21}$$

where, e.g., $\lambda_N^a (s_L^{\nu_a})^2 \equiv (K_l^\dagger O_L^\dagger O_L K_l)_{aa}$ describes the amount of mixing with the heavy ordinaries N, and analogous expressions hold for the other λ_n^a parameters that describe the mixing with the exotic. These parameters satisfy $0 \leq \lambda_n^a \leq 1$ and $\sum_n \lambda_n^a = 1$.

4 Simultaneous mixing of gauge bosons and fermions mixing.

The neutral current term of lagrangian for the multiplet Ψ of a given electric charge, for the case when both types of mixing are present, is then

$$-\mathcal{L}^{NC} = \frac{e}{s_W c_W} \sum_{a=L,R} \bar{\Psi}_a^0 \gamma^\mu (D_a, H_a^1, ..., H_a^n)_\mu \Psi_a^0 (Z^0, Z_1^0, ..., Z_n^0)_\mu^T =$$

$$= \frac{e}{s_W c_W} \sum_{a=L,R} \bar{\Psi}_a \gamma^\mu (U_a^\dagger D_a U_a, U_a^\dagger H_a^1 U_a, ..., U_a^\dagger H_a^n U_a)_\mu \Psi_a R (Z, Z_1, ..., Z_n)_\mu^T,$$

where R is the $(n+1) \times (n+1)$ orthogonal matrix that diagonalizes the neutral boson mass matrix; H_a^i are the $(n_a + m_a) \times (n_a + m_a)$ matrices that express the coupling s of the non universal family diagonal (NUFD)

and family changing (FC) gauge bosons to matter. In the simplest case of only one extra neutral gauge boson, the R matrix is

$$R = \begin{pmatrix} \cos\theta & -\sin\theta \\ \sin\theta & \cos\theta \end{pmatrix} \tag{22}$$

and for the lagrangian we have

$$-\mathcal{L}^{NC} = \frac{e}{s_W c_W} \times$$
$$\times \sum_{a=L,R} \bar{\Psi}_a \gamma^\mu U_a^\dagger (D_a \cos\theta + H_a \sin\theta, H_a \cos\theta - D_a \sin\theta) U'_a \Psi_a \begin{pmatrix} Z \\ Z' \end{pmatrix}_\mu .$$

Here $H = \mathrm{diag}(H_0, H_E)$. There are no H_{EO} nor H_{OE} terms in H which would give rise to Z_1^0 mediated transitions between exotic and ordinary fermions as long as the horizontal group commutes with the SM gauge group. The general neutral current lagrangian term in the light sector is

$$-\mathcal{L}^{NC} = \frac{e}{s_W c_W} \sum_{a=L,R} \bar{\Psi}_{la} \gamma^\mu (K_a, K'_a) \Psi_{la} \begin{pmatrix} Z \\ Z' \end{pmatrix}_\mu , \tag{23}$$

where

$$\begin{aligned}
K_L &= \left[\left(F^\dagger F\right)_L (t_{3EL} - t_{3OL}) + t_{3OL} - Q s_W^2\right] \cos\theta + (H_U)_L \sin\theta, \\
K_R &= \left[\left(F^\dagger F\right)_R t_{3ER} - Q s_W^2\right] \cos\theta + (H_U)_R \sin\theta, \\
K'_L &= -\left[\left(F^\dagger F\right)_L (t_{3EL} - t_{3OL}) + t_{3OL} - Q s_W^2\right] \sin\theta + (H_U)_L \cos\theta, \\
K'_R &= -\left[\left(F^\dagger F\right)_R t_{3ER} - Q s_W^2\right] \sin\theta + (H_U)_R \cos\theta.
\end{aligned}$$

It is useful to introduce coupling parameters Λ and Ξ as

$$K_L = (\Lambda_L + t_{3OL} - Q s_W^2) \cos\theta + \Xi_L \sin\theta \tag{24}$$
$$K_R = (\Lambda_R - Q s_W^2) \cos\theta + \Xi_R \sin\theta, \tag{25}$$

where $\Lambda_R = (F^\dagger F)_R\, t_{3ER}$, $\Lambda_L = (F^\dagger F)_L\, (t_{3EL} - t_{3OL})$ and $\Xi_a = (H_U)_a$, $a = L, R$.

Should note that there are two contributions to the FC couplings of the light fermions to the Z, $\sim (F^\dagger F)_a \cos\theta$ and $\sim (H_U)_a \sin\theta$, which may be in principle of the same order. In the limit of no mixing between exotic and ordinary fermions ($F_a \equiv 0$) and no mixing between the Z and Z' ($\theta \equiv 0$)

the SM coupling are recovered. And at last, in the absence of mixing with the exotic fermions the FC couplings of the ordinary fermion (of a given helicity) to the Z may still survive through the term $(H_U)_a \sin\theta$, provided that the family of ordinary fermion of the given helicity transforms nontrivially under horizontal generator H_O.

Since for the light charged fermions, the dimension of Ψ_{lL} and Ψ_{lR} are the same (there is an equal number of left and right handed fermions), we can rewrite the general lagrangian as

$$-\mathcal{L}^{NC} = \frac{e}{2 s_W c_W} \bar{\Psi}_l \gamma^\mu (g_V - g_A \gamma^5, g'_V - g'_A \gamma^5) \Psi_l \begin{pmatrix} Z \\ Z' \end{pmatrix}_\mu , \tag{26}$$

where $g_V = K_L + K_R$ and $g_A = K_L - K_R$.

5 Model independent constraints.

We consider the constraints on mixing parameters from two different processes, a namely, constraints from the lepton family diagonal processes $Z \to l_i \bar{l}_i$ and from lepton family violating processes. For the first ones when both mixing effects are presented the branching ration $B(Z \to l_i \bar{l}_i)$ in the $M_Z \gg m_{l_i}$ approximation, is given as

$$B(Z \to l_i \bar{l}_i) \simeq \frac{1}{\Gamma_{tot}} \frac{G_F M_Z^3}{6\sqrt{2}\pi} \left(\left|g_V^{ii}\right|^2 + \left|g_A^{ii}\right|^2\right) = \tag{27}$$
$$= \frac{1}{\Gamma_{tot}} \frac{G_F M_Z^3}{3\sqrt{2}\pi} \left(|\Lambda_L^{ii} + \Xi_L^{ii}\theta - \frac{1}{2} + s_W^2|^2 + |\Lambda_R^{ii} + \Xi_R^{ii}\theta + s_W^2|^2\right) + \mathcal{O}(\theta^4).$$

The experimental values of the branching ratios are $B_{e\bar{e}} = (3.366 \pm 0.008) \cdot 10^{-2}$, $B_{\mu\bar{\mu}} = (3.367 \pm 0.013) \cdot 10^{-2}$ and $B_{\tau\bar{\tau}} = (3.360 \pm 0.015) \cdot 10^{-2}$. So we have constraints

$$\left|\Lambda_a^{ii} + \Xi_a^{ii}\theta\right| < \text{few} \cdot 10^{-3}. \tag{28}$$

For the branching ration of second types of Z decays we have

$$B(Z \to l_i \bar{l}_j + \bar{l}_i l_j) \simeq 2 \frac{B(Z \to l\bar{l})}{|g_V|^2 + |g_A|^2} (|g_V^{ij}|^2 + |g_A^{ij}|^2) = \tag{29}$$
$$= 4 \frac{B(Z \to l\bar{l})}{|g_V|^2 + |g_A|^2} (|\Lambda_L^{ij} + \Xi_L^{ij}\theta|^2 + |\Lambda_R^{ij} + \Xi_R^{ij}\theta|^2) + \mathcal{O}(\theta^4).$$

¿From ([13]) experimental values are $B_{e\bar{\mu}} < 1.7 \cdot 10^{-6}$, $B_{e\bar{\tau}} < 7.3 \cdot 10^{-6}$ and $B_{\mu\bar{\tau}} < 1.0 \cdot 10^{-5}$. So mixing parameters Λ_a^{ij} are bounded to lie in a circular region centering at $(-\Xi_L^{ij}\theta, -\Xi_R^{ij}\theta)$ and the radius $\sim 10^{-3}$.

6 Conclusions

The lecture is devoted to fermion and gauge boson mixing effects. We see that the new fermions will naturally mix with the known light states and we have outlined a general formalism that allows the study of the simultaneous effects of the new degrees of freedom on electroweak observables. We have shown that flavor–changing neutral interactions could naturally arise in these models, since in general they are not equipped with a GIM mechanism. However, large masses for both the new fermions and the new gauge bosons lead to a natural suppression of the flavor–changing low–energy couplings of the light states, and the FCNC are easily accommodated in these models.

We identified a set of parameters that describe the new physics. The effects of the new gauge boson have been parametrized in terms of a $Z_0 - -Z_1$ mixing angle θ and of its physical mass M_Z'. We have described the fermion mixings in the neutral sector with three parameters $(s_L^\nu)^2$, and we have introduced the additional effective parameters $\Lambda_{0,1}^\nu$ to describe the kind of new states involved in neutrinos mixing. For the charged sector, relying on the very stringent experimental limits on FCNC, we have neglected possible flavor changing couplings of the light fermions. But this restriction is not crucial to derive reliable limits for common fermion and boson mixing parameters Λ_a and Ξ_a.

References

[1] A. De Rujula, S. Glashow, U. Sarid, Nucl. Phys. **B333**, 173 (1990).

[2] E. Nardi, E. Roulet, Phys. Lett. B **245**, 105 (1990).

[3] J. Layssac, F.M. Renard, C. Verzegnassi, Z. Phys. C **53**, 97 (1992).

[4] M.C. Gozalez Garsia, J.W.F. Valle, Phys. Lett. B **259**, 365 (1991).

[5] P. Langacker, M. Luo, Phys. Rev. D **45**, 278 (1992).

[6] F. del Aguila, J.M. Moreno, M. Quiros, Phys. Lett. B **254**, 497 (1991).

[7] P. Langacker, D. London, Phys. Rev. D **38**, 886 (1988).

[8] G. Bhattacharya *et al.*, Phys. Rev. Lett. B **84**, 2870 (1990).

[9] E. Nardi, E. Roulet, D. Tommasini, Nucl. Phys. B **386**, 239 (1992).

[10] E. Nardi, E. Roulet, D. Tommasini, Phys. Rev. D **46**, 3040 (1992).

[11] A.A. Babich, A.A. Pankov, Yad. Fiz. (Sov.J.Nucl.Phys.) **57**, 2061 (1994).

[12] A.A.Babich, A.A. Pankov, N. Paver, Phys. Lett. B **346**, 303 (1995).

[13] Particle Data Group, Eur. Phys. J. C **3**, 1 (1998).

The lowest-order electroweak radiative corrections to the single W-production in hadron-hadron colliders

I.Akushevich[1], A.Ilyichev[1], N.Shumeiko[1], V.Zykunov[2]
[1] NC PHEP, 220040 Minsk, Belarus
[2] GSPU, 246746 Gomel, Belarus; speaker

July 13, 2000

Abstract

The explicit expressions for the lowest-order radiative correction to the single W-production in hadron-hadron collisions are presented with taking consideration the contribution of bremsstrahlung. The calculation is made in the framework of the quark parton model. The infrared divergence is extracted by using the covariant method.

1 Introduction

Precise measurements of the W boson mass - one of the fundamental parameters of the Standard Model (SM) - along with other precision electroweak measurements will lead to more accurate information on the top quark and the Higgs boson masses, that will provide restrictions on the parameters of the supersymmetric extension of the SM. Our current knowledge of the W boson mass ($m_W = 80.43 \pm 0.11$GeV, DØCollaboration [1]) will be significantly improved up to an uncertainty in the range 30-50 MeV at LEP II [2], 20-30 MeV at the Fermilab Tevatron $p\bar{p}$ collider [3] and 15 MeV at the upgrated Tevatron. Besides, the LHC gives opportunity to measure the W boson mass to a precision of better than 15 MeV [4].

To extract the data on m_W with high precision from hadron collider experiments, it is necessary to take into account contribution from electroweak corrections (EWC). The final state photonic corrections were calculated in [5]. More accurate calculation of the lowest-order EWC to the resonant W production at hadronic collisions have been suggested in [6], where both the initial and final state radiation have been included. In this report we present new explicit formulae for EWC to the inclusive single W-production in hadron-hadron collisions. Since in the final state only charged lepton is detected, we suggest to use the covariant Bardin-Shumeiko method [7] for calculation of EWC in that reaction. Indisputable advantage this method is that the final expressions are independent on any poor defined, unphysical parameters (photon 'softness' and so on).

2 Born cross section of process $pp(p\bar{p}) \to l^{\pm}\nu_l$

The process of the single W-boson production is considered in the framework of the quark parton model

$$p + p\ (p + \bar{p}) \to W^{\pm} + X \to l^{\pm} + X. \qquad (1)$$

Notice, that for the partonic process
p_1–4-momenta of the first (anti)quark (flavour i, mass m_1),
p_2–4-momenta of second (anti)quark (i', m_2),
k_1–4-momenta of final charged lepton l^- or l^+ (m),
k_2–4-momenta of (anti)neutrino.

The standard set of Mandelstam invariants is the following:

$$s = (p_1 + p_2)^2,\ t = (p_1 - k_1)^2, u = (k_1 - p_2)^2.$$

The matrix element of the partonic subprocess coincides

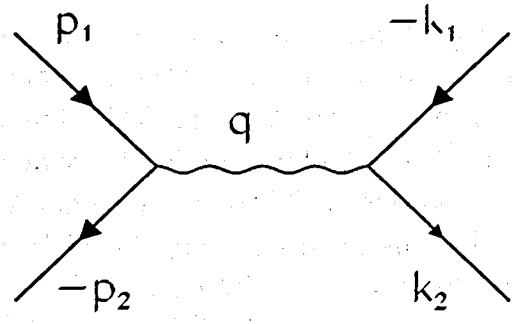

Figure 1: *Feynman graph for the single W-production on partonic level*

with one from [8] (everywhere the W-boson propagator $(s - m_W^2)^2$ replace by $(s - m_W^2)^2 + m_W^2\Gamma_W^2$), and the unpolarized invariant parton-parton cross section has the form

$$d\sigma = \frac{\alpha^2}{4N_c s_w^4 s}\frac{B_{ii'}}{(s-m_W^2)^2}\delta(p_1+p_2-k_1-k_2)\frac{d^3k_1}{k_{10}}\frac{d^3k_2}{2k_{20}},$$

where

$$B_{ii'} = \begin{cases} u^2 - & \text{for } q\bar{q} \to l^-\bar{\nu}_l, \bar{q}q \to l^+\nu_l, \\ t^2 - & \text{for } q\bar{q} \to l^+\nu_l, \bar{q}q \to l^-\bar{\nu}_l. \end{cases}$$

Then we integrate over 4-momenta of an unobservable (anti)neutrino:

$$\int \frac{d^3k_2}{2k_{20}}\delta(p_1+p_2-k_1-k_2) = \delta(s+t+u-m_1^2-m_2^2-m^2),$$

and according to QPM (see for example [9]) substitute $p_{1(2)} \to x_{1(2)}P_{1(2)}$, where $P_{1(2)}$ – 4-momenta of initial hadrons, $x_{1(2)}$ is the fraction of the first(second) hadron's momentum carried by the corresponding struck quark. We shall denote this procedure by a operator "hat". Then we multiply on the parton

densities of the first and second hadrons and integrate over x_1 and x_2.

The integration over x_2 is performed with the help of δ-function taking into consideration that

$$\delta(\hat{s}+\hat{t}+\hat{u}-m_1^2-m_2^2-m^2) \approx \delta(x_1x_2S+x_1T+x_2U) = \frac{1}{x_1S+U}\delta(x_2+\frac{x_1T}{x_1S+U}),$$

and, hence, $x_2 = x_2^0 = -x_1T/(x_1S+U)$. That case corresponds to born kinematics and will denote by the index "0".

S, T, U are Mandelstam variables for $pp(p\bar{p}) \to l\nu_l$:

$$S = 2P_1P_2,\ T = -2P_1k_1,\ U = -2P_2k_1, -\frac{U}{S+T} \le x_1 \le 1.$$

Finally, let us consider the general form of the cross section of the process $pp \to l\nu_l$. In the hadron-hadron collisions the center of the parton-parton masses frame has an undetermined motion along the beam direction. Therefore we use standard in that case variables: the component of the 4-vector of the detected particle transverse to the beam direction $(k_{1\perp})$, and rapidity (y). Integrating over azimuth Φ (it is possible since the initial hadrons are unpolarized) we have phase space $d^3k_1/k_{10} \Rightarrow \pi dy dk_{1\perp}^2$. Hence

$$\frac{d\sigma_{pp\to l\nu_l}}{dydk_{1\perp}^2} = \sum_{i,i'}\int dx_1 f_i(x_1,Q^2)\Sigma_0, \qquad (2)$$

where

$$\Sigma_0 = \Sigma|_{x_2=x_2^0} = \frac{\pi\alpha^2}{4N_c s_w^4 \hat{s}(\hat{s}-m_W^2)^2}\frac{|V_{ii'}|^2\hat{B}_{ii'}f_{i'}(x_2,Q^2)|_{x_2=x_2^0}}{(x_1S+U)} \qquad (3)$$

and the sum is over all types of quarks and antiquarks both of initial hadrons. So, for

$$q\bar{q} \to l^+\nu_l,\ i = u,c,t;\ i' = \bar{d},\bar{s},\bar{b};$$

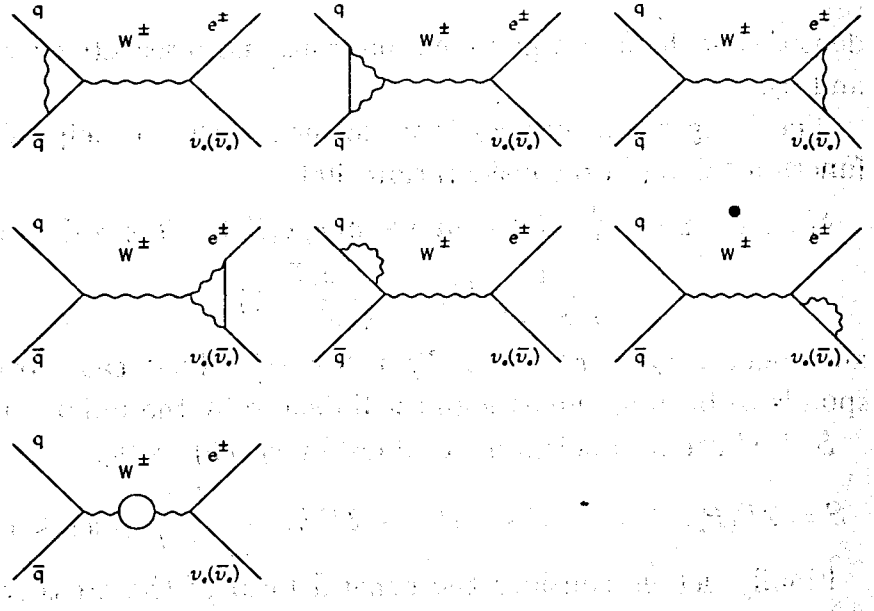

Figure 2: *The full set of Feynman graphs for the contribution of additional virtual particles*

$$\bar{q}q \to l^-\bar{\nu}_l,\ i = \bar{u}, \bar{c}, \bar{t};\ i' = d, s, b;$$
$$q\bar{q} \to l^-\bar{\nu}_l,\ i = d, s, b;\ i' = \bar{u}, \bar{c}, \bar{t};$$
$$\bar{q}q \to l^+\nu_l,\ i = \bar{d}, \bar{s}, \bar{b};\ i' = u, c, t.$$

In the expressions (2), (3) $1/N_c = 1/3$ is the color factor, $V_{ii'}$ is CKM matrix element, $f_i(x_{1(2)}, Q^2)$ are the spin averaged quark densities, Q is a typical momentum transfer in the partonic reaction, so, for the numeric estimations we choose according [6] value $Q^2 = m_W^2$.

3 Contribution of additional virtual particles

The one-loop contribution of additional virtual particles (V-contribution) in the on-mass renormalization scheme and t'Hooft-Feynman gauge is presented. It could be written (for detail see [10],[11])

$$\frac{d\sigma_V}{dydk_{1\perp}^2} = \sum_{i,i'} \int dx_1 f_i(x_1, Q^2)\hat{\delta}_V|_{x_2=x_2^0}\Sigma_0$$

Here the factor δ_V consists of seven terms:

$$\delta_V = \delta_W + \delta_{Vl} + \delta_{Vq} + \delta_{Sl} + \delta_{Sq} + \delta_{\gamma W} + \delta_{ZW}.$$

where

$$\delta_W = 2\Re\frac{\hat{\Sigma}^W(s)}{s - m_W^2}$$

is the W self-energy contribution;

$$\delta_{Vl} = 2\Re\delta F^{We\nu}(s)$$

is leptonic vertex correction;

$$\delta_{Vq} = 2\Re\delta F^{Wud}(s)$$

is quark vertex correction;

$$\delta_{Sl} = \frac{\alpha}{4\pi}Q_l^2\left(\ln\frac{m_Z^2}{m_l^2} - 2\ln\frac{m_l^2}{\lambda^2} + \frac{3}{2}\right)$$

is ν self energy;

$$\delta_{Sq} = -\frac{\alpha}{4\pi}\left[Q_u^2\left(\ln\frac{m_Z^2}{m_u^2} - 2\ln\frac{m_u^2}{\lambda^2}\right) - Q_d^2\left(\ln\frac{m_Z^2}{m_d^2} - 2\ln\frac{m_d^2}{\lambda^2}\right)\right]$$

is u-quark self energy;

$$\delta_{\gamma W} = \frac{2\alpha}{\pi}Q_l c_l(Q_i I_1^{\gamma W}(s,t) + Q_{i'} I_2^{\gamma W}(s,u))$$

is γW box contribution;

$$\delta_{ZW} = \frac{2\alpha}{\pi} c_l[((v_l + a_l)(v_i + a_i) + (v_\nu + a_\nu)(v_{i'} + a_{i'}))I_1^{ZW}(s,t)$$
$$+((v_l + a_l)(v_{i'} + a_{i'}) + (v_\nu + a_\nu)(v_i + a_i))I_2^{ZW}(s,u)]$$

is ZW box contribution.

Here the quantities $I_{1,2}^{\gamma W}$ and $I_{1,2}^{ZW}$ can be found in [11] (see formulae (A.3), (A.4) and (A.6)) IR part of V-contribution can be presented as

$$\delta_V^{IR} = \frac{\alpha}{2\pi} \ln \frac{s}{\lambda^2} (Q_l^2 + Q_i^2 + Q_{i'}^2 - Q_d Q_u \ln \frac{s^2}{m_u^2 m_d^2}$$
$$+Q_l Q_i c_l \ln \frac{t^2}{m_u^2 m_e^2} - Q_l Q_{i'} c_l \ln \frac{u^2}{m_d^2 m_e^2}) \qquad (4)$$

Q_j is the charge of the fermion j expressed in the units of the proton's charge (e.g. $Q_u \equiv Q_{\bar{u}} = +2/3$).

4 Contribution of bremsstrahlung $pp(p\bar{p}) \to l\nu_l\gamma$

Let's present the cross section of bremsstrahlung (R-contribution) according to the covariance method of extraction of the infrared divergence (IRD) [7] in the usual form

$$\frac{d\sigma^R_{pp\to l\nu_l\gamma}}{dy dk_{1\perp}^2} = \frac{d\sigma_R^{IR}}{dy dk_{1\perp}^2} + \frac{d\sigma_R^F}{dy dk_{1\perp}^2}.$$

To get the first part (σ_R^{IR}) we should do operation $k \to 0$ (k is 4-momenta of the real bremsstrahlung photon). So, analogously the form of Born case

$$\frac{d\sigma_R^{IR}}{dy dk_{1\perp}^2} = \sum_{i,i'} \int dx_1 f_i(x_1, Q^2) \hat{\Sigma}_R^{IR},$$

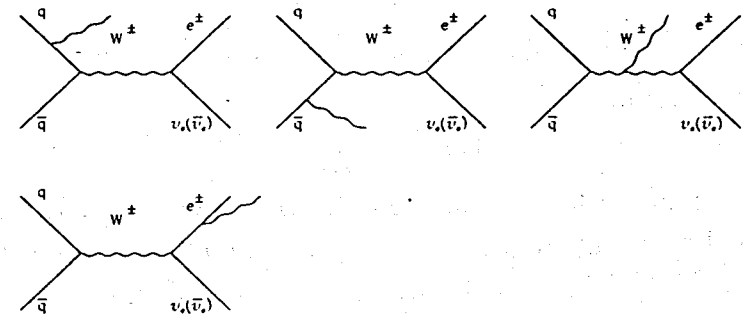

Figure 3: *The full set of Feynman graphs for contribution of the bremsstrahlung*

$$\Sigma_R^{IR} = -\frac{\alpha}{\pi} \int_{v_{min}}^{v_{max}} dv \Sigma I[F^{IR}].$$

Here the substitutions

$$dx_2 = dv/(x_1 S + U)$$

and

$$I[A] = \frac{1}{\pi} \int \frac{d^3k}{k_0} \delta[(p_1 + p_2 - k_1 - k)^2][A].$$

are used.

The quantity F^{IR} is defined as

$$F^{IR} = Q_l^2 \frac{m^2}{z^2} - c_l Q_l Q_i \frac{t}{z z_1} + c_l Q_l Q_{i'} \frac{u}{z u_1} + Q_i^2 \frac{m_1^2}{z_1^2} - Q_i Q_{i'} \frac{s}{z_1 u_1}$$
$$+Q_{i'}^2 \frac{m_2^2}{u_1^2},$$

where

$$c_l = \begin{cases} +1 - & \text{for } q\bar{q} \to l^-\bar{\nu}_l, \bar{q}q \to l^+\nu_l, \\ -1 - & \text{for } q\bar{q} \to l^+\nu_l, \bar{q}q \to l^-\bar{\nu}_l. \end{cases}$$

The kinematic variables read:

$$t_1 = (p_2 - k_2)^2, \; z = 2kk_1,$$
$$z_1 = 2kp_1 = z - t_1 + t,$$

$$u_1 = 2kp_2 = v + t_1 - t,$$
$$v = 2kk_2 = s + u + t - m_1^2 - m_2^2 - m^2,$$

Introducing

$$J(t,v) = v \lim_{\lambda \to 0} I[F^{IR}],$$

where λ is a photon mass as the parameter of IRD, adding and subtracting the terms $-(\alpha/\pi)\Sigma_0 J(t,0)/v$ as well as $-(\alpha/\pi)\Sigma_0 I[F^{IR}]$ we will have three parts of the cross section:

$$\Sigma_R^{IR} = -\frac{\alpha}{\pi}\Sigma_0 J(t,0)\int_{v_{min}}^{v_{max}} \frac{dv}{v} - \frac{\alpha}{\pi}\int_0^{v_{max}} dv(\Sigma - \Sigma_0) I[F^{IR}]$$
$$-\frac{\alpha}{\pi}\Sigma_0 \int_0^{v_{max}} dv\ (I[F^{IR}] - J(t,0)/v).$$

The second and the third addenda are IR-finite. That's why they have the value $v_{min} = 0$, but the first term contains IRD. We will calculate its in the center-of-mass-system of the initial partons [12]. Then $v_{min} = (\vec{k} = 0) = 2\lambda k_{20} = \lambda\sqrt{s_0}$, $v_{max} = (x_{2max} = 1) = x_1(S+T) + U$, and the IRD-part of the cross section has the form

$$-\frac{\alpha}{\pi}\Sigma_0 J(t,0) ln(v_{max}/\lambda\sqrt{s_0}).$$

Summing up IRD-parts V- and R- contribution we get

$$\frac{d\sigma_R^{IR}}{dydk_{1\perp}^2} + \frac{d\sigma_V^{IR}}{dydk_{1\perp}^2} = \sum_{i,i'} \int dx_1 f_i(x_1, Q^2)$$
$$\frac{\alpha}{2\pi}\Sigma_0 J(t,0) ln\frac{\hat{s}_0^2}{v_{max}^2},$$

i.e. the infrared divergence has canceled successfully.

In the process of the integration $I[F^{IR}]$ we were forced to calculate by the next expressions:

$$I[\frac{1}{z^2}] = \frac{1}{m^2 v}, \quad I[\frac{1}{z_1^2}] = \frac{1}{m_1^2 v},$$

$$I[\frac{1}{zz_1}] = -\frac{1}{vt}L_t, \quad I[\frac{1}{zu_1}] = -\frac{1}{vu}L_u,$$
$$I[\frac{1}{z_1 u_1}] = \frac{1}{vs}L_s, \quad I[\frac{1}{u_1^2}] = \frac{1}{m_2^2 v},$$

where

$$L_t = ln\frac{t^2}{m^2 m_1^2}, \quad L_u = ln\frac{u^2}{m^2 m_2^2},$$
$$L_s = ln\frac{s^2}{m_1^2 m_2^2},$$

and $J(t,v)$ has the form

$$J(t,v) = Q_l^2 + c_l Q_l Q_i L_t - c_l Q_l Q_{i'} L_u$$
$$+Q_i^2 - Q_i Q_{i'} L_s + Q_{i'}^2.$$

We turn attention to the fact that if the index "0" is absent, correlation between s, t, u corresponds to the case $v \neq 0$, that is not born kinematics!

After IRD extraction from the cross section of the partonic process remaining part of R-contribution (so called "hard" photon contribution) have the form

$$d\Sigma_R^F = \frac{\alpha^3}{2^6\pi^2 s_w^4}\frac{1}{s}\sum_{j=l,q,w}|R_j|^2 d\Gamma,$$

$$d\Gamma = \frac{1}{4}\frac{d^3k_1}{k_{10}}\frac{d^3k}{k_0}\delta[(p_1 + p_2 - k_1 - k)^2].$$

Here we have integrated over k_2. And then we integrate over whole phase space of the real photon and get following terms in the previous formula

$$\frac{d\Sigma_R^F}{dydk_{1\perp}^2} = \frac{\alpha^3}{8s_w^4 s}|V_{ii'}|^2(Q_l^2\Pi_l^2 V_l + Q_l\Pi_l V_{lq}$$

$$+V_q + Q_l\Pi_l^2 V_{lw} + \Pi_l V_{qw} + \Pi_l^2 V_w).$$

Index of values V corresponds to the particle which radiated photon (l — final lepton, q — initial quarks, w — W-boson). Double index corresponds to the same interference term.

At last, the cross section of inclusive process $pp(p\bar{p}) \to l^{\pm}\nu_l\gamma$ have the form

$$\frac{d\sigma_R^F}{dydk_{1\perp}^2} = \sum_{i,\,i'} \int dx_1 dx_2 f_i(x_1, Q^2) \cdot f_{i'}(x_2, Q^2) \frac{d\hat{\Sigma}_R^F}{dydk_{1\perp}^2}. \tag{5}$$

5 Conclusion

So, in this report the expressions for the lowest-order radiative correction to the single W-production in hadron-hadron collisions are presented. All calculations are made in the framework of the quark parton model. The one-loop contribution of additional virtual particles in the on-mass renormalization scheme and t'Hooft-Feynman gauge is considered. The infrared divergence is extracted from the contribution of bremsstrahlung by using the covariant Bardin-Shumeiko method.

We emphasize that the formulae for lowest order radiative correction have the invariant form, that is allowed one to use them for the numerical estimations in any modern and future inclusive single W-production experiments on the hadron-hadron colliders: Tevatron, and LHC especially.

References

[1] B. Abbott, et.al // Phys.Rev. D58 (1998) 092003 hep-ex/9712029

[2] D.Abbaneo et.al // CERN-PPE/97-154

[3] D.Amidei et al. FERMILAB-Pub-96/082

[4] S.Keller, J.Womersley // Eur.Phys.J. C5 (1998) 249 hep-ph/9711304

[5] F.Berends, R.Kleiss //Z.Phys.C 27, 365 (1985)

[6] U.Baur, S.Keller, D.Wackeroth // Phys.Rev. D59 (1999) 013002 hep-ph/9807417

[7] Bardin D.Yu., Shumeiko N.M. // Nucl.Phys. (1977) V.B127, p.242

[8] D.Wackeroth, W.Hollik // Phys.Rev.D. (1997) V.55, p.6788

[9] Berger, Qiu // Phys.Rev.D. (1989) V.40, N.3

[10] Böhm, Spiesberger //Fortsch.Phys. (1986) V.34 p.687

[11] Böhm, Spiesberger //Nucl.Phys. (1986) V.B304 p.749

[12] Byckling E., Kajantie K "Particle Kinematics", 1973

ON THE REACTION $ep \to ep\gamma$

M.V. Galynsky and M.I. Levchuk *
Institute of Physics, Belarusian Academy of Sciences, Minsk

Abstract

We have studied the reaction $ep \to ep\gamma$ in the kinematics corresponding to electron scattering at small angles and photon scattering at large angles, where proton bremsstrahlung dominates. The analysis is based on the direct evaluation method of the matrix elements in the so-called diagonal spin basis. The results of numerical calculations for electron beam energy $E_e = 200$ MeV in the above kinematics show that the relative contribution of the Bethe-Heitler and interference terms to the reaction cross section is less than 10 %, and the cross section for the reaction $ep \to ep\gamma$ is quite sensitive to the proton polarizability. Owing to the factorization of the squared electric and magnetic form factors of the proton, a compact expression has been obtained for the differential cross section of the Bethe-Heitler emission of a linearly polarized photon by an electron, taking into account the proton recoil and form factors. A covariant expression has been obtained for the lepton tensor in which contributions of states with transverse and longitudinal polarizations of the virtual photon are separated.

1 The reaction $ep \to ep\gamma$ and the proton polarizability

There has recently been much interest in studying Compton scattering on nucleons at low and intermediate energies. The motivation is that the fundamental structure constants of the nucleon, the electric and magnetic polarizabilities, can be determined in this process. The nucleon polarizabilities contain important information about the nucleon structure at large and intermediate distances, in particular, about the radius of the quark core, the meson cloud, and so on. A detailed discussion of these questions can be found in [1, 2]. Knowledge of the amplitudes for Compton scattering on nucleons is also required to interpret the data on photon scattering off nuclei. For example, such studies can answer the question of in what degree the electromagnetic properties of free and bound nucleons differ.

All the experimental results on the proton polarizabilities have been obtained from data on elastic γp scattering below pion photoproduction threshold [3]. However, it has recently been shown that measurements of the proton polarizabilities at the Novosibirsk storage ring with electron beam energy of 200 MeV using an internal jet target appear to be very promising. As proposed in [4], this can be done using the reaction

$$e^-(p_1) + p^+(q_1) \to e^-(p_2) + p^+(q_2) + \gamma(k) \qquad (1)$$

*E-mail: galynski@dragon.bas-net.by, levchuk@dragon.bas-net.by

in the kinematics corresponding to electron scattering at small angles and photon scattering at large angles, i.e. in conditions of small 4-momentum transfer from the initial electron to the final photon and proton. In the lowest order of perturbation theory, the process (1) is described by three graphs shown in Fig.1.

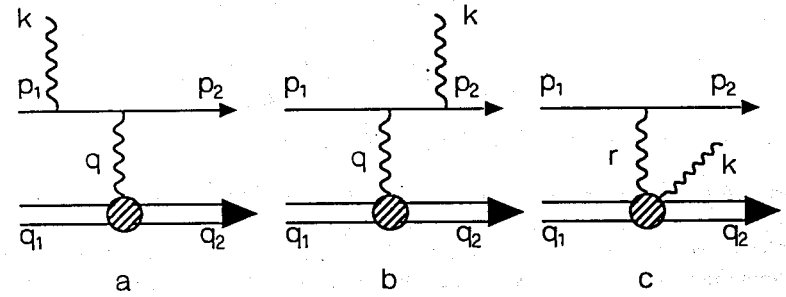

Figure 1: Graphs corresponding to the reaction $ep \to ep\gamma$.

The first two (a) and (b) correspond to electron bremsstrahlung (Bethe-Heitler graphs), and the third (c) corresponds to proton bremsstrahlung (graph with virtual Compton scattering (VCS) on a proton). The kinematics described above was chosen for the following reasons. First, the subprocess of real Compton scattering (RCS) on the proton is realized in it since at small electron scattering angles the virtual photon with 4-momentum $r = p_1 - p_2$ (see Fig.1) becomes almost real. Here the quantity $|r| = \sqrt{-(p_1 - p_2)^2}$ turns out to be small, $|r| \sim m$, where m is the electron mass. Second, for electron scattering at small angles and photon scattering at large angles, the contribution of the graph corresponding to proton bremsstrahlung dominates, being several orders of magnitude larger than the contribution of the Bethe-Heitler graphs to the cross section for the process (1) [5]. This is the main requirement needed to separate the subprocess of Compton scattering on the proton [4] in the reaction $ep \to ep\gamma$.

The estimates in the framework of the method of equivalent photons for a scalar model [4] showed that the reaction (1) offers a good possibility of obtaining high-statistics data on the Compton scattering cross section and the proton polarizability. Measurement of the electric (α_p) and magnetic (β_p) polarizabilities of the proton with higher accuracy than in earlier studies is one of the most important problems to be solved by experiments in the near future [6, 7].

However, to obtain high-statistics data on the cross section for γp scattering and the proton polarizability it is essential to use a theoretical model more accurate than that of [4]. It must include both the spin properties of the particles and parameters characterizing the electromagnetic structure of the hadron. The model can be based on the result of [8], where a general calculation of the reaction $ep \to ep\gamma$ was performed. The cross section was expressed in terms of 12 form factors corresponding to the VCS subprocess on the proton (i.e., the contribution of the graph in Fig.1c) and two form factors corresponding to the Bethe-Heitler graphs.

The differential cross section for the reaction $ep \to ep\gamma$ in the above kinematics was calculated in [9]. It was expressed in terms of the six invariant amplitudes for RCS [1, 10], and also the electric and magnetic form factors of the proton [11].

The matrix element corresponding to the sum of the two Bethe-Heitler graphs (a) and (b) in Fig.1 reads

$$M_1 = \overline{u}(p_2) Q_\epsilon^\mu u(p_1) \cdot \overline{u}(q_2) \Gamma_\mu(q^2) u(q_1) \frac{1}{q^2} , \tag{2}$$

$$Q_\epsilon^\mu = \gamma^\mu \frac{p_1 - k + m}{-2p_1 k} \epsilon + \epsilon \frac{p_2 + k + m}{2p_2 k} \gamma^\mu , \tag{3}$$

$$\Gamma_\mu(q^2) = f_1 \gamma_\mu + \frac{\mu_p}{4M} f_2 (q\gamma_\mu - \gamma_\mu q) , \tag{4}$$

where $u(p_i)$ and $u(q_i)$ are the bispinors of electrons and protons with 4-momenta p_i and q_i, $p_i^2 = m^2$, $q_i^2 = M^2$, $\overline{u}(p_i)\, u(p_i) = 2m$, $\overline{u}(q_i)\, u(q_i) = 2M$, $(i = 1, 2)$, $k = k_\mu \gamma^\mu$, γ^μ are the Dirac matrices, $\gamma^5 = -i\gamma^0\gamma^1\gamma^2\gamma^3$, $\gamma^{5+} = \gamma^5$; μ_p, f_1, and f_2 are respectively the anomalous magnetic moment and the Dirac and Pauli form factors of the proton [11], $q = q_2 - q_1$ is the momentum transfer, ϵ is the polarization 4-vector of a photon with momentum k, $\epsilon k = k^2 = 0$, and M is the proton mass.

In the limit of interest $|r| \sim m$, the matrix element corresponding to the graph of Fig.1c is expressed in terms of the six invariant RCS amplitudes T_i $(i = 1, 2, \ldots, 6)$. It has the form [8]

$$M_2 = \overline{u}(p_2)\gamma^\mu u(p_1) \cdot \overline{u}(q_2) M_{\mu\nu} e^\nu u(q_1) \frac{1}{r^2} , \tag{5}$$

$$M_{\mu\nu} = \frac{C_\mu C_\nu}{C^2} (T_1 + T_2 K) + \frac{D\mu D\nu}{D^2} (T_3 + T_4 K) + \tag{6}$$

$$+ \frac{(C_\mu D_\nu - C_\nu D_\mu)}{D^2} \gamma^5 T_5 + \frac{(C_\mu D_\nu + C_\nu D_\mu)}{D^2} T_6 D . \tag{7}$$

The tensor $M_{\mu\nu}$ is constructed using a set of four mutually orthogonal 4-vectors C, D, B, and K:

$$K = 1/2\ (r + k)\ ,\ Q = 1/2(r - k)\ ,\ R = 1/2(q_1 + q_2)\ ,$$

$$C = R - \frac{(RK)}{K^2} K - \frac{(RB)}{B^2} B\ ,\ B = Q - \frac{(QK)}{K^2} K\ , \tag{8}$$

$$D_\mu = \varepsilon_{\mu\nu\rho\sigma} K^\nu B^\rho C^\sigma\ ,$$

and it satisfies the requirements of parity conservation and gauge invariance:

$$M_{\mu\nu} k^\nu = r^\mu M_{\mu\nu} = 0 . \tag{9}$$

In the unpolarized case it is most efficient to use the standard approach [11] for calculation of the differential cross section of the process (1) together with evaluation of matrix elements in the diagonal spin basis (DSB) [12]-[15]. In the DSB, the spin 4-vectors s_1 and s_2 of particles with 4-momenta p_1 and p_2 $(s_1 p_1 = s_2 p_2 = 0, s_1^2 = s_2^2 = -1)$ belong to the hyperplane formed by the 4-vectors p_1 and p_2:

$$s_1 = -\frac{(v_1 v_2) v_1 - v_2}{\sqrt{(v_1 v_2)^2 - 1}}\ ,\ s_2 = \frac{(v_1 v_2) v_2 - v_1}{\sqrt{(v_1 v_2)^2 - 1}}\ , \tag{10}$$

where $v_1 = p_1/m_1$ and $v_2 = p_2/m_2$. To find the probability for the process (1) it is sufficient to calculate the matrix elements of the electron and proton currents

$$(J_\epsilon^{\pm\delta,\delta})_\mu = \overline{u}^{\pm\delta}(p_2) \gamma_\mu u(p_1)^\delta , \tag{11}$$

$$(J_p^{\pm\delta',\delta'})_\mu = \overline{u}^{\pm\delta'}(q_2) \Gamma_\mu(q^2) u^{\delta'}(q_1) , \tag{12}$$

and also the quantity

$$X_\mu^{\pm\delta',\delta'} = \overline{u}^{\pm\delta'}(q_2) M_{\mu\nu} e^\nu u^{\delta'}(q_1) . \tag{13}$$

The calculations give [12]-[15]:

$$(J_\epsilon^{\delta,\delta})_\mu = 2m(a_0)_\mu\ ,\ (J_\epsilon^{-\delta,\delta})_\mu = -2\delta y_-(a_\delta)_\mu\ ,\ y_- = \sqrt{-p_-^2}/2\ , \tag{14}$$

$$(J_p^{\delta',\delta'})_\mu = 2g_e M(b_0)_\mu\ ,\ (J_p^{-\delta',\delta'})_\mu = -2\delta' y'_- g_m(b_{\delta'})_\mu\ ,\ y'_- = \sqrt{-q_-^2}/2, \tag{15}$$

where

$$a_0 = p_+/\sqrt{p_+^2}\ ,\ a_3 = p_-/\sqrt{-p_-^2}\ ,\ a_2 = [a_0 \cdot a_3]^\times k/\rho\ ,\ a_1 = [a_0 \cdot a_3]^\times a_2\ , \tag{16}$$

$$p_\pm = p_2 \pm p_1\ ,\ a_{\pm\delta} = a_1 \pm i\delta a_2\ ,\ \delta = \pm 1\ ,\ a_2 k = 0\ ,\ a_1^2 = a_2^2 = a_3^2 = -a_0^2 = -1\ . \tag{17}$$

$$b_0 = q_+/\sqrt{q_+^2}\ ,\ b_3 = q_-/\sqrt{-q_-^2}\ ,\ b_2 = [b_0 \cdot b_3]^\times k/\rho'\ ,\ b_1 = [b_0 \cdot b_3]^\times b_2\ , \tag{18}$$

$$q_\pm = q_2 \pm q_1\ ,\ b_{\pm\delta'} = b_1 \pm i\delta' b_2\ ,\ \delta' = \pm 1\ ,\ b_2 k = 0\ ,\ b_1^2 = b_2^2 = b_3^2 = -b_0^2 = -1\ . \tag{19}$$

In Eqs.(16), (18) and below a dot between any two 4-vectors a and b, square parentheses and symbol "$\times$" stands for dyadic product of vectors (but not scalar product) $a \cdot b = (a \cdot b)_{\mu\nu} = (a)_\mu (b)_\nu$, alternating dyadic $[a \cdot b] = a \cdot b - b \cdot a$ and dual operation $[a \cdot b]^\times = ([a \cdot b]^\times)_{\mu\nu} = 1/2 \varepsilon_{\mu\nu\rho\sigma} ([a \cdot b])^{\rho\sigma} = \varepsilon_{\mu\nu\rho\sigma}(a)^\rho (b)^\sigma$, respectively, $\varepsilon_{\mu\nu\rho\sigma}$ is the Levi-Civita symbol $(\varepsilon_{0123} = -1)$; ρ and ρ' are determined from the normalization conditions (17) and (19), finaly, g_e and g_m are just electric and magnetic form factors of the proton (Sachs form factors) [11]:

$$g_e = f_1 + \mu_p \frac{q^2}{4M^2} f_2\ ,\ g_m = f_1 + \mu_p f_2\ . \tag{20}$$

Therefore, in the DSB the matrix elements of the proton current for spin-non-flip and spin-flip transitions are expressed in terms of the electric g_e and magnetic g_m form factor, respectively (see [16]).

Once the matrix elements of the proton current (12) have been determined, the calculation of the contribution of the two Bethe-Heitler graphs reduces to the calculation of VCS on the electron [9, 14, 15]:

$$|M_1^{\pm\delta',\delta'}|^2 = \frac{1}{q^4} |\overline{u}(p_2) \left(J_p^{\pm\delta',\delta'} \frac{p_1 - k + m}{-2p_1 k} \epsilon + \epsilon \frac{p_2 + k + m}{2p_2 k} J_p^{\pm\delta',\delta'} \right) u(p_1)|^2 . \tag{21}$$

Denoting the result of averaging and summing the expression $|M_1^{\pm\delta',\delta'}|^2$ over the polarizations of the initial and final particles by Y_{ee}, one obtains [9, 14, 15]:

$$Y_{ee} = 1/4 \sum_{\delta' e} Tr\{ (p_2 + m)\, \hat{Q}_e^{\pm\delta',\delta'}\, (p_1 + m)\, \hat{\overline{Q}}_e^{\pm\delta',\delta'} \}/q^4 , \qquad (22)$$

where $\hat{Q}_e^{\pm\delta',\delta'} = (Q_e^\mu)\,(J_p^{\pm\delta',\delta'})_\mu$ is the operator in parentheses between the electron bispinors $\overline{u}(p_2)$ and $u(p_1)$ in Eq. (21), and $\hat{\overline{Q}}_e^{\pm\delta',\delta'} = \gamma_0\,(\hat{Q}_e^{\pm\delta',\delta'})^+\gamma_0$. Owing to the factorization of the electric and magnetic form factors g_e and g_m in (15), the Bethe-Heitler term in the cross section for the reaction $ep \to ep\gamma$ Y_{ee} (22) contains only the squares of the Sachs form factors (see [9, 12, 14, 15, 17, 18]).

Similarly, the calculation of the contribution from the graph in Fig.1c reduces to the calculation of quasi-real Compton scattering on the proton. Using the expressions for the electron current (14), one has

$$|\, M_2^{\pm\delta,\delta}\,|^2 = \frac{1}{r^4}\,|\,\overline{u}(q_2)\,\hat{Q}_p^{\pm\delta,\delta}\,u(q_1)\,|^2 , \qquad (23)$$

where $\hat{Q}_p^{\pm\delta,\delta} = (J_e^{\pm\delta,\delta})^\mu\; M_{\mu\nu}\epsilon^\nu$. Denoting the result of averaging and summing Eq. (23) over the polarizations of the initial and final particles by Y_{pp}, we obtain [9]:

$$Y_{pp} = 1/4 \sum_{\delta e} Tr\{ (q_2 + M)\, \hat{Q}_p^{\pm\delta,\delta}\, (q_1 + M)\, \hat{\overline{Q}}_p^{\pm\delta,\delta} \}/r^4 , \qquad (24)$$

where $\hat{\overline{Q}}_p^{\pm\delta,\delta} = \gamma^0\,(\hat{Q}_p^{\pm\delta,\delta})^+\gamma^0$. Finally, to calculate the interference term in the case of unpolarized particles

$$Y_{ep} = 1/4 \sum_{\delta,\delta',\epsilon} 2Re\; M_1\, M_2^* \qquad (25)$$

we shall use the matrix elements of the proton current (15) and also the 4-vectors $X_\mu^{\pm\delta',\delta'}$ (13), which have the form [9]

$$X_\mu^{-\delta',\delta'} = -2\delta' y'_- b_1 k \left(\frac{C_\mu C_\nu}{C^2} T_2 + \frac{D\mu D\nu}{D^2} T_4 + i\delta' y'_+ y'_- \frac{(C_\mu D_\nu + C_\nu D_\mu)}{D^2} T_6 \right) e^\nu ,$$

$$X_\mu^{\delta',\delta'} = 2\left(y'_+ \left(\frac{C_\mu C_\nu}{C^2} \left(T_1 + \frac{\nu_1 M}{1-\tau} T_2 \right) + \frac{D\mu D\nu}{D^2} \left(T_3 + \frac{\nu_1 M}{1-\tau} T_4 \right) \right) + \right. \qquad (26)$$

$$\left. + \delta' y'_- \frac{(C_\mu D_\nu - C_\nu D_\mu)}{D^2}\, T_5 \right) e^\nu ,$$

where $y'_+ = \sqrt{q_+^2}/2 = M\sqrt{1-\tau}$, $\tau = q^2/4M^2$ and $\nu_1 = kq_+/2M^2$. As a result, one has for the matrix element M_2 (5)

$$M_2 = \overline{u}(p_2).X^{\pm\delta',\delta'} u(p_1)/r^2 , \qquad (27)$$

and Eq.(25) reduces to the trace [9]:

$$Y_{ep} = 1/4 \sum_{\delta,\delta',\epsilon} 2R\epsilon\; \{Tr\,((p_2 + m)\hat{Q}_e^{\pm\delta',\delta'}(p_1 + m)\overline{X}^{\pm\delta',\delta'})\}/q^2/r^2 , \qquad (28)$$

where $X^{\pm\delta',\delta'} = \epsilon^\mu\, X_\mu^{\pm\delta',\delta'}$ and $\overline{X}^{\pm\delta',\delta'} = (X_\mu^{\pm\delta',\delta'})^*\gamma^\mu$. The interference term Y_{ep} (28) is a linear combination of the proton electric and magnetic form factors, because the operators $\hat{Q}_e^{\pm\delta',\delta'}$ are expressed linearly in terms of the matrix elements of the proton current: $\hat{Q}_e^{\pm\delta',\delta'} = (Q_\epsilon)^\mu (J_p^{\pm\delta',\delta'})_\mu$, (see Eqs. (3) and (15)). Therefore, the problem of finding the probability for the reaction $ep \to ep\gamma$ in this approach has been reduced to calculations of the traces (22), (24), and (28), which were done making the use of the program REDUCE. For the differential cross section we then obtained [9, 14]:

$$d\sigma = \frac{\alpha^3\,|\,T\,|^2\,\delta^4(p_1 + q_1 - p_2 - q_2 - k)}{2\pi^2\sqrt{(p_1q_1)^2 - m^2M^2}}\; \frac{d^3\vec{p}_2}{2p_{20}}\, \frac{d^3\vec{q}_2}{2q_{20}}\, \frac{d^3\vec{k}}{2\omega} , \qquad (29)$$

$$|\,T\,|^2 = 1/4 \sum_{pol} |\,M_{fi}\,|^2 = Y_{ee} + Y_{ep} + Y_{pp} , \qquad (30)$$

$$Y_{ee} = \frac{8M^2}{q^4}\,(\, g_e^2\, Y_I + \tau\, g_m^2\, Y_{II}\,) , \qquad (31)$$

$$Y_I = -\frac{\lambda_1}{\lambda_2} - \frac{\lambda_2}{\lambda_1} - \frac{m^2q^2}{2}\left(\frac{1}{\lambda_1} - \frac{1}{\lambda_2}\right)^2 - \frac{r^2q^2}{2\lambda_1\lambda_2}$$

$$- \frac{m^2}{2M^2(1-\tau)}\left(\frac{p_1q_+}{\lambda_2} - \frac{p_2q_+}{\lambda_1}\right)^2 - \frac{\tau}{(1-\tau)}\frac{((p_1q_+)^2 + (p_2q_+)^2)}{\lambda_1\lambda_2} , \qquad (32)$$

$$Y_{II} = -\frac{\lambda_1}{\lambda_2} - \frac{\lambda_2}{\lambda_1} - \frac{m^2q^2}{2}\left(\frac{1}{\lambda_1} + \frac{1}{\lambda_2}\right)^2 - \frac{r^2q^2}{2\lambda_1\lambda_2}$$

$$+ \frac{m^2}{2M^2(1-\tau)}\left(\frac{p_1q_+}{\lambda_2} - \frac{p_2q_+}{\lambda_1}\right)^2 + \frac{\tau}{(1-\tau)}\frac{((p_1q_+)^2 + (p_2q_+)^2)}{\lambda_1\lambda_2} \qquad (33)$$

$$- 2\left(\frac{m^2}{\lambda_1} - \frac{m^2}{\lambda_2}\right)^2 + 4\,m^2\left(\frac{1}{\lambda_1} - \frac{1}{\lambda_2}\right) ,$$

$$Y_{ep} = -\frac{32M^3}{r^2q^2(4\nu_4^2 - \nu_2^2)}\left\{ g_e Re\left[y_1\left(T_1 + \frac{\nu_1 M}{1-\tau}T_2\right) + y_2\left(T_3 + \frac{\nu_1 M}{1-\tau}T_4\right)\right]\right.$$

$$\left. + \tau g_m\left[-\frac{\nu_1 M}{1-\tau} Re(y_1T_2 + y_2T_4) + 4M\,Re(z_1T_2 + z_2T_4 + z_3T_6)\right]\right\}, \qquad (34)$$

$$Y_{pp} = -\left\{ (\alpha_1^2\alpha_3 + \nu_3)[(1-\tau)|T_1|^2 + 2\nu_1 M\,Re(T_1T_2^*) + M^2(\nu_1^2 - \nu_2^2)|T_2|^2]\right.$$

$$\left. + (\alpha_2 + \nu_3)[(1-\tau)|T_3|^2 + 2\nu_1 M\,Re(T_3T_4^*) + M^2(\nu_1^2 - \nu_2^2)|T_4|^2] \right. \qquad (35)$$

$$+ \ (\alpha_1^2\alpha_3 + \alpha_2 + 2\nu_3)\tau\left(-\frac{|T_5|^2}{M^4\nu_2^2} + \frac{M^2}{\alpha_3}|T_6|^2\right)\Bigg\}\frac{16M^4}{r^4} \ .$$

For the invariant variables in Eqs. (29) - (35) used in determining the Bethe-Heitler term (Y_{ee}), the interference term (Y_{ep}), and the term corresponding to proton bremsstrahlung (Y_{pp}), we used the notation adopted in [8]:

$$y_1 = 2\alpha_1[\alpha_1\alpha_3(\nu_2\nu_5 - \nu_1\nu_4) + 2\nu_4^2 + \nu_2\nu_3], \ \nu_1 = kq_+/2M^2 \ , \ \nu_2 = -kq_-/2M^2 \ .$$
$$y_2 = 2\alpha_2\ (\nu_2\nu_5 - \nu_1\nu_4) - \alpha_1\nu_2^2, \ \nu_3 = r^2/4M^2, \ \nu_4 = kq_+/4M^2 \ , \ \nu_5 = p_+q_+/4M^2,$$
$$y_3 = -(4\nu_3/\nu_2^2)\ [\alpha_1\alpha_3(\nu_1\nu_2(\nu_2+\nu_3) - 2\nu_4(\nu_1\nu_4 - \nu_2\nu_5)) + \nu_4(4\nu_4^2 - \nu_2^2)] \ .$$
$$\alpha_1 = \nu_5 + \nu_1\nu_4(2\nu_3+\nu_2)/\nu_2^2 \ , \ \alpha_3 = \nu_2^2/(\nu_2^2 + (\nu_2+\nu_3)(\nu_1^2 - \nu_2^2)) \ .$$
$$\alpha_2 = m^2/M^2 - \nu_3 + M^6/D^2[-(\nu_1\nu_4 + \nu_2\nu_5)^2 + 4\nu_3(\nu_4^2 - \nu_1\nu_4\nu_5) - 4\nu_3\nu_4^2(\nu_2+\nu_3)] \ .$$
$$D^2 = M^6\ (\nu_2^2 + (\nu_2+\nu_3)(\nu_1^2 - \nu_2^2)) = M^6\nu_2^2/\alpha_3 \ , \ \lambda_1 = p_1k \ , \ \lambda_2 = p_2k \ ,$$
$$z_1 = \nu_1\nu_4\alpha_1^2\alpha_3 \ , \ z_2 = \nu_2\nu_4\alpha_2 \ , \ z_3 = 1/4\alpha_1\ (2\nu_2(2\alpha_2 + \nu_2 + \nu_3) + 4\nu_4^2 - \nu_2^2) \ .$$

It should be noted that the expression obtained for the differential cross section (29) coincides, within the definition of the initial quantities (the tensor $M_{\mu\nu}$), with the result obtained in [8], if one expresses in the latter the form factors f_1 and f_2 through g_e and g_m. Nevertheless, the Bethe-Heitler term Y_{ee} and the interference term Y_{ep} have a more compact form due to the factorization of the electric and magnetic form factors.

Let us consider contributions of all three graphs to the cross section for the reaction (1) in the selected kinematics when the initial proton is at rest ($q_1 = (M, 0)$), and the electron beam energy is $E_e = 200$ MeV. Performing the required integration over the phase space we obtain [9]:

$$d\sigma = \frac{\alpha^3\omega^2 \mid \vec{q}_2 \mid T \mid^2}{16\pi^2 M \mid \vec{p}_1 \mid (p_2k)}\ dE_{pk}\ d\Omega_{q_2}\ d\Omega_\gamma \ , \qquad (36)$$

where $d\Omega_\gamma$ and $d\Omega_{q_2}$ are the elements of the photon and proton solid angles, and E_{pk} is the kinetic energy of the recoil proton. The differential cross section (36) was calculated numerically in the region $5 \leq E_{pk} \leq 35$ MeVwith the sum and the difference of the electric (α_p) and magnetic (β_p) polarizabilities equal to $\alpha_p + \beta_p = 14$ and $\alpha_p - \beta_p = 10$ (in units of $10^{-4}fm^3$) [1]-[4]. We assume that the reaction kinematics is planar, and that the photon emission and proton scattering angles are $\vartheta_\gamma = 135^0$ and $\vartheta_p = -20.5^0$, respectively (all angles are measured from the direction of the primary electron beam). Calculations show that in the entire range of proton kinetic energy considered, $5 \leq E_{pk} \leq 35$ MeV, for the selected angles $\vartheta_\gamma = 135^0$ and $\vartheta_p = -20.5^0$, the electron scattering angle ϑ_e and the 4-momentum transfer $|r| = \sqrt{-(p_2 - p_1)^2}$ are bounded by the values $|\vartheta_e| \leq 6.4^0$ and $|r| \leq 7.3$ MeV, with the minimum value of $|r|$ corresponding to forward electron scattering [9, 14].

The results of numerical calculations of the cross section (36), $d\sigma/dE_{pk}/d\Omega_{q_2}/d\Omega_\gamma$ in the above kinematics are shown in Fig.2. We see that in the angular range studied the cross section for the reaction $ep \to ep\gamma$ has a sharp peak consisting of two maxima. This peak originates from the factor $1/r^4$ in Eq. (35) for Y_{pp}. The two maxima have a kinematical origin and arise from the interference of two pole graphs corresponding to quasi-real Compton scattering. The cross section (36) has a strong angular dependence,

which, in particular, causes the two maxima to disappear when the proton scattered (or photon emission) angle is changed by only one degree (i.e., for $\vartheta_p = -19.5^0$), so that we have an ordinary peak at $E_{pk} = 25$ MeV.

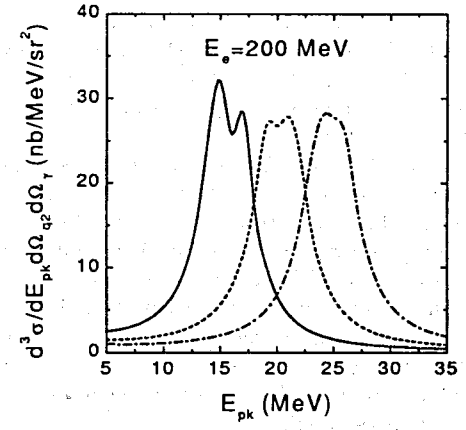

Figure 2: Differential cross section (36) for the reaction (1) in the kinematics where proton bremsstrahlung dominates (see comments in the text). Proton scattering angles are $\vartheta_p = -20.5^0$ (solid line), $\vartheta_p = -20.0^0$ (dashed line), $\vartheta_p = -19.5^0$ (dot-dashed line) and photon emission angle is $\vartheta_\gamma = 135^0$.

The differential cross section (36) shown in Fig.2, is the sum of the Bethe-Heitler (σ_{ee}), the interference (σ_{ep}), and the proton (σ_{pp}) terms (see (30)), where the symbol (σ) denotes the cross section of the form (36) with $\mid T \mid^2$ replaced by Y_{ee}, Y_{ep}, and Y_{pp}, respectively. Numerical calculations show that in the entire range of proton kinetic energy studied, $5 \leq E_{pk} \leq 35$ MeV, the ratios of the Bethe-Heitler term σ_{ee} and the interference term σ_{ep} to the term corresponding to proton emission σ_{pp} are bounded by the values $\sigma_{ee}/\sigma_{pp} < 0.02$ and $|\sigma_{ep}|/\sigma_{pp} < 0.05$. The calculations carried out for another set of angles ($\vartheta_\gamma = 135^0$ and $\vartheta_p = -20^0$) give results which are only slightly different: $\sigma_{ee}/\sigma_{pp} < 0.05$ and $|\sigma_{ep}|/\sigma_{pp} < 0.075$. Since these ratios are much smaller than unity, the main requirement (see [4]) for separation of the background, which is mainly electron bremsstrahlung, is satisfied.

To investigate the sensitivity of the reaction (1) to the proton polarizability we performed numerical calculations of the cross section (36) for the same set of angles ($\vartheta_\gamma = 135^0$ and $\vartheta_p = -20^0$) and fixed sum of the electric and magnetic polarizabilities $\alpha_p + \beta_p = 14$ but different values of the difference: (a) $\alpha_p - \beta_p = 10$ and (b) $\alpha_p - \beta_p = 6$. It turned out that the cross section (36) is about 8% larger for the smaller difference of polarizabilities. Therefore, in this kinematics the cross section for the reaction $ep \to ep\gamma$, is quite sensitive to the proton polarizability [9].

2 Emission of a linearly polarized photon by an electron in the reaction $ep \to ep\gamma$

Let us consider now the emission of a linearly polarized photon by an electron in the reaction $ep \to ep\gamma$, taking into account the proton recoil and form factors. Our study will be limited to the contribution of the two Bethe-Heitler graphs (a) and (b) in Fig.1, which corresponds to the matrix element (2). The contribution of the graph with VCS on a proton can be neglegted when the initial electrons have ultrarelativistic energies, and the photon and final electron are scattered at small forward angles ($\vartheta_\gamma \sim m/E_e$, $\vartheta_e \sim m/E_e$, $m/E_e \ll 1$).

We are interested in these effects for the following reasons. First, even though the Bethe-Heitler process has been intensively studied earlier in the case of the emission of linearly polarized photons [19, 20] and is widely used to obtain them at accelerators [21], up to now the proton recoil and form factors have not been accurately taken into account (in contrast to the unpolarized case). Second, as was shown in [22], the inclusion of these factors in the case of unpolarized photons leads to a strong change of the differential cross section for the Bethe-Heitler process. Since the polarization characteristic of the scattered radiation are expressed in terms of the differential cross section for the emission of an unpolarized photon (see below), it is clear that inclusion of the recoil and form factors is essential.

The covariant expression for the differential cross section for the Bethe-Heitler process (in the Born approximation) taking into account the proton recoil and form factors in the case of emission of a linearly polarized photon has been obtained by us in [23]. It has the form

$$d\sigma_{BH} = \frac{\alpha^3 \mid T_e \mid^2 \delta^4(p_1+q_1-p_2-q_2-k)}{2\pi^2\sqrt{(p_1q_1)^2-m^2M^2}} \frac{d^3\vec{p}_2}{2p_{20}} \frac{d^3\vec{q}_2}{2q_{20}} \frac{d^3\vec{k}}{2\omega} . \tag{37}$$

$$\mid T_e \mid^2 = \frac{4M^2}{q^4} \left(g_e^2 \, Y_I^{\,e} + \tau \, g_m^2 \, Y_{II}^{\,e} \right) , \tag{38}$$

$$Y_I^{\,e} = 2 - \frac{\lambda_1}{\lambda_2} - \frac{\lambda_2}{\lambda_1} - \frac{\tau}{1-\tau} \frac{(kq_+)^2}{\lambda_1\lambda_2} + q^2 \, (ea)^2 + 4 \, (eA)^2 , \tag{39}$$

$$Y_{II}^{\,e} = -2 - \frac{\lambda_1}{\lambda_2} - \frac{\lambda_2}{\lambda_1} + \frac{\tau}{1-\tau} \frac{(kq_+)^2}{\lambda_1\lambda_2} + (q^2+4m^2) \, (ea)^2 - 4 \, (eA)^2 , \tag{40}$$

$$a = \frac{p_1}{\lambda_1} - \frac{p_2}{\lambda_2} , \quad A = b_0 + \frac{(b_0p_2)p_1}{\lambda_1} - \frac{(b_0p_1)p_2}{\lambda_2} . \tag{41}$$

All the quantities entering (37)-(41) are defined in the previous section. Thus, the differential cross section for the Bethe-Heitler process in the case of emission of a linearly polarized photon $d\sigma_{BH}$ (37) is naturally splitted into the sum of two terms containing only the squares of the Sachs form factors and corresponding to the contribution of transitions without ($\sim g_e^2 \, Y_I^{\,e}$) and with ($\sim \tau \, g_m^2 Y_{II}^{\,e}$) proton spin flip.

Let us discuss the properties of the 4-vector a, which is well known from the theory of emission of long-wavelength photons [11], and the 4-vector A. They both satisfy a condition which follows naturally from the requirement of gauge invariance: $a \, k = A \, k = 0$, and, in addition, they are spacelike vectors: $a^2 < 0$ and $A^2 < 0$. This is easily verifed by using the 4-momentum conservation law and the explicit form of a^2 and A^2:

$$a^2 = m^2 \left(\frac{1}{\lambda_1} - \frac{1}{\lambda_2} \right)^2 + \frac{r^2}{\lambda_1\lambda_2} ,$$

$$A^2 = 1 + \frac{m^2}{4M^2(1-\tau)} \left(\frac{q_+p_1}{\lambda_2} - \frac{q_+p_2}{\lambda_1} \right) + \frac{\tau}{1-\tau} \frac{q_+p_1 \cdot q_+p_2}{\lambda_1\lambda_2} .$$

We note that the 4-vector A was first introduced in [23].

Using the electron 4-momenta p_1 and p_2 and the photon 4-momenta k, we construct the 4-vectors of the photon linear polarization $e_\parallel$ and $e_\perp$ ($e_\parallel k = e_\perp k = e_\parallel e_\perp = 0$):

$$e_\parallel = \frac{(p_2k)p_1 - (p_1k)p_2}{\rho'} , \; e_\perp = \frac{[p_1 \cdot p_2]^\times k}{\rho'} ,$$

where ρ' is determined from the normalization conditions: $e_\parallel^2 = e_\perp^2 = -1$. Then the degree of photon linear polarization will be given by the following expressions [23]:

$$P_\gamma = \frac{\mid T_\perp \mid^2 - \mid T_\parallel \mid^2}{\mid T_\perp \mid^2 + \mid T_\parallel \mid^2} = \frac{A_1}{A_2} , \tag{42}$$

where

$$A_1 = \frac{16 \, M^2}{q^4} \left(g_e^2 \, A_{11} + \tau \, g_m^2 \, A_{12} \right) , \tag{43}$$

$$A_2 = \frac{8 \, M^2}{q^4} \left(g_e^2 \, Y_1 + \tau \, g_m^2 \, Y_2 \right) , \tag{44}$$

$$Y_1 = 2 - \frac{\lambda_1}{\lambda_2} - \frac{\lambda_2}{\lambda_1} - \frac{\tau}{1-\tau} \frac{(kq_+)^2}{\lambda_1\lambda_2} - 2 \, \tau M^2 \, a^2 - 2 \, A^2 , \tag{45}$$

$$Y_2 = -2 - \frac{\lambda_1}{\lambda_2} - \frac{\lambda_2}{\lambda_1} + \frac{\tau}{1-\tau} \frac{(kq_+)^2}{\lambda_1\lambda_2} - 2 \, \tau \, M^2 \, a^2 + 2 \, A^2 - 2m^2 \, a^2 . \tag{46}$$

$$A_{11} = A^2 + \tau \, M^2 \, a^2 + 2(e_\perp b_0)^2 ,$$

$$A_{12} = -A^2 + \tau \, M^2 \, a^2 - 2(e_\perp b_0)^2 + m^2 \, a^2 ,$$

$$(e_\perp b_0)^2 = - \frac{4(SD)^2}{M^2(1-\tau)a^2\lambda_1^2\lambda_2^2} ,$$

$$SD = 1/2 \, \epsilon_{\mu\nu\rho\sigma}(p_1)^\mu(p_2)^\nu(q_1)^\rho(q_2)^\sigma ,$$

It is easy to check that A_2 (44) coincides with the expression for Y_{ee} (31) determining the Bethe-Heitler cross section in the case of unpolarized particles: $A_2 = Y_{ee}$, and also that $Y_1 = Y_I$ and $Y_2 = Y_{II}$ (see (32) and (33)).

Therefore, owing to the factorization of the squared form factors g_e and g_m and also the use of the 4-vectors a and A (41), the differential cross section for the Bethe-Heitler process both for linearly polarized photon (38) and unpolarized photon (44), (31), can be written in a rather compact form.

An integration of Eq. (37) over $d^3\vec{q}_2$ and dp_{20} in the rest frame of the initial proton ($q_1 = (M, 0)$) gives the following result:

$$\frac{d\sigma_{BH}}{d\omega\, d\Omega_\gamma\, d\Omega_e} = \frac{\alpha^3\,\omega}{(2\pi)^2}\,\frac{|\vec{p}_2|}{|\vec{p}_1|}\,\frac{|T|^2}{q^4}\,, \tag{47}$$

$$|T|^2 = g_e^2\, Y_I^e + \tau\, g_m^2\, Y_{II}^e\,. \tag{48}$$

Let us consider the limit of the cross section (47) when the proton is a pointlike (structureless) particle with infinite mass, i.e., we assume that $g_e = g_m = 1$ and $q_2 = (M, \vec{q}) \simeq (M, 0)$, where $\vec{q} = \vec{p}_1 - \vec{p}_2 - \vec{k}$ is the momentum transferred to the proton. In this limit ($M \to \infty$), $E_{kp} = \vec{q}^{\,2}/2M \to 0$, $\vec{q}/2M \to 0$, and $b_0 = (1, \vec{q}/2M) \simeq (1, 0)$. We choose the Coulomb gauge for the photon polarization vectors: $e = (0, \vec{e})$ in which one obtains

$$eb_0 = 0,\ ea = \frac{p_1 e}{\lambda_1} - \frac{p_2 e}{\lambda_2},\ eA = p_{20}\,\frac{p_1 e}{\lambda_1} - p_{10}\,\frac{p_2 e}{\lambda_2},\ \tau(q_+k)^2 = \omega^2 q^2\,.$$

Using these expressions we have in the above limit for (48):

$$|T|^2 = 2 - \frac{\lambda_1}{\lambda_2} - \frac{\lambda_2}{\lambda_1} - \frac{\omega^2 q^2}{\lambda_1\lambda_2} + q^2\,(ea)^2 + 4\,(eA)^2\,, \tag{49}$$

or, in expanded form,

$$|T|^2 = 2 - \frac{\lambda_1}{\lambda_2} - \frac{\lambda_2}{\lambda_1} - \frac{\omega^2 q^2}{\lambda_1\lambda_2} + (\,4p_{20}^2 + q^2\,)\left(\frac{p_1 e}{\lambda_1}\right)^2$$

$$+\,(\,4p_{10}^2 + q^2\,)\left(\frac{p_2 e}{\lambda_2}\right)^2 - 2\,(\,4p_{10}p_{20} + q^2\,)\,\frac{p_1 e\cdot p_2 e}{\lambda_1\lambda_2}\,. \tag{50}$$

The expressions (47), (50) for the differential cross section for the Bethe-Heitler process $d\sigma_{BH}/d\omega/d\Omega_\gamma/d\Omega_e$ in the limit where the proton is an infinitely heavy, structureless particle coincide with the result of [19].

3 Virtual-photon polarization in the reaction $ep \to ep\gamma$ ($ep \to eX$)

The reactions $ep \to ep\gamma$ and VCS on the proton have recently become interesting not only at low and intermediate energies [4], but also at high electron energies and 4-momenta transferred to the proton [7], [25]-[28]. The VCS offers greater possibilities for studying hadronic structure than the RCS process, because in it the energy and three-momentum transferred to the target can be varied independently. These attractive properties of VCS have led to the suggestion that it could be used for experimental study of the nucleon structure [25, 26] and have made it necessary to perform a thorough theoretical study of the reaction $ep \to ep\gamma$ (see [7, 27, 28] and references therein). To calculate VCS on the proton, it is necessary to know the hadron ($W_{\mu\nu}$) and lepton ($L_{\mu\nu}$) tensors [7, 29]:

$$L_{\mu\nu} = J_\mu J_\nu^*,\quad J_\mu = \overline{u}(p_2)\gamma_\mu u(p_1)\,, \tag{51}$$

where $u(p_i)$ are electron bispinors, $\overline{u}(p_i)u(p_i) = 2m$, and m is the electron mass ($i = 1, 2$). The interpretation of the results is considerably simplified if the tensor $L_{\mu\nu}$ is expressed in terms of the longitudinal and transverse polarization vectors of the virtual photon. The corresponding expressions can be found in [7] and [29]. However, they have two defects: (1) the electron mass is neglegted, which is of course justified at ultrarelativistic electron energies and large squared 4-momentum of the virtual photon; (2) they have a noncovariant form. A lepton tensor free of these defects was constructed in [24].

Let us consider the question of the polarization state of a virtual photon with 4-momentum $r = p_1 - p_2$ which is exchanged between the electron and proton in the reaction $ep \to epy$ (see Fig.1c). Using the vectors of the orthonormal basis a_A (16) ($A = (0, 1, 2, 3)$):

$$a_0 = p_+/\sqrt{p_+^2}\,,\ a_3 = p_-/\sqrt{-p_-^2}\,,\ a_2 = [a_0\cdot a_3]^\times q_1/\rho\,,\ a_1 = [a_0\cdot a_3]^\times a_2\,, \tag{52}$$

$$p_\pm = p_2 \pm p_1\,,\ a_2 q_1 = 0\,,\ a_1^2 = a_2^2 = a_3^2 = -a_0^2 = -1\,,$$

which satisfies the completeness relation

$$a_0\cdot a_0 - a_1\cdot a_1 - a_2\cdot a_2 - a_3\cdot a_3 = g\,, \tag{53}$$

where $g = (g_{\mu\nu})$ is the metric tensor with signature $g_{\mu\nu} = (+\,---)$, we construct the 4-vectors of the longitudinal (e_3) and transverse (e_1, e_2) polarization of a virtual photon with 4-momentum r [24]:

$$e_1 = \frac{[a_0\cdot a_1]q_1}{\sqrt{(a_3q_1)^2 + q_1^2}}\,,\ e_2 = a_2 = \frac{[a_0\cdot a_3]^\times q_1}{\rho}\,,\ e_3 = \frac{(1 + a_3\cdot a_3)q_1}{\sqrt{(a_3q_1)^2 + q_1^2}}\,, \tag{54}$$

where

$$\rho^2 = (a_1q_1)^2 = \frac{2p_1p_2\cdot p_1q_1\cdot p_2q_1 - M^2((p_1p_2)^2 - m^4) - m^2((p_1q_1)^2 + (p_2q_1)^2)}{(p_1p_2)^2 - m^4}\,.$$

It is easily verifed that the 4-vectors e_i ($i = 1, 2, 3$) are orthogonal to each other ($e_ie_j = 0$, $i \neq j$), and also that $e_ir = e_ia_3 = 0$ and $e_1^2 = e_2^2 = -e_3^2 = -1$. The 4-vectors e_i (54) are not changed when the auxiliary 4-vector q_1 is replaced by $q_1 + p_1 - p_2 = q_2 + k$ (since $p_1 - p_2 = r = -2ya_3$, where $y = \sqrt{-r^2}/2$, and the vectors a_A (52) are orthogonal). For this reason, the virtual-photon polarization vectors e_i (54) in the rest frame of the incident proton or in the c.m. frame of the final proton and photon can be considered as equivalent and their use lead to the same expressions. Below we restrict ourselves to the rest frame of the incident proton, $q_1 = (M, 0, 0, 0)$, where the 4-vectors e_i have the form:

$$e_1 = (0, 1, 0, 0),\ e_2 = (0, 0, 1, 0),\ e_3 = \frac{1}{\sqrt{-r^2}}(|\,\vec{r}\,|, r_0\vec{n}_3)\,, \tag{55}$$

where $\vec{n}_3$ is a unit vector directed along $\vec{r}$ ($\vec{n}_3^{\,2} = 1$), and r_0 is the time component of the 4-vector $r = (r_0, \vec{r})$.

The four mutually orthogonal vectors e_1, e_2, e_3, and a_3 also satisfy the completeness relation:

$$e_3\cdot e_3 - e_1\cdot e_1 - e_2\cdot e_2 - a_3\cdot a_3 = g\,, \tag{56}$$

which allows a_0 and a_1 to be expressed in terms of ϵ_1 and ϵ_3:

$$a_1 = \alpha\epsilon_3 - \beta\epsilon_1 \ , \ a_0 = \beta\epsilon_3 - \alpha\epsilon_1 \ , \ \beta^2 = 1 + \alpha^2 \ , \tag{57}$$

$$\alpha = \epsilon_3 a_1 = a_0\epsilon_1 = \frac{a_1 q_1}{\sqrt{(a_3 q_1)^2 + q_1^2}} \ , \ \beta = \epsilon_1 a_1 = \epsilon_3 a_0 = \frac{a_0 q_1}{\sqrt{(a_3 q_1)^2 + q_1^2}} \ . \tag{58}$$

In the DSB (10) the matrix elements of the electron current have the form of (14). Let us write them in terms of the 4-vectors ϵ_i (54) [24]:

$$(J_\epsilon^{\delta,\delta})_\mu = 2m\,(\beta\epsilon_3 - \alpha\epsilon_1)_\mu \ , \ (J_\epsilon^{-\delta,\delta})_\mu = -2\delta y\,(\alpha\epsilon_3 - \beta\epsilon_1 + i\delta\epsilon_2)_\mu \ . \tag{59}$$

Therefore, for spin-non-flip transitions ($J_\epsilon^{\delta,\delta}$) the virtual-photon polarization vector is a superposition of the longitudinal (βe_3) and transverse linear ($-\alpha e_1$) polarizations, while for spin-flip transitions ($J_\epsilon^{-\delta,\delta}$) it is a superposition of the longitudinal ($\alpha\epsilon_3$) and transverse elliptical [$\epsilon_\delta = (0, \vec{e}_\delta) = -\beta e_1 + i\delta e_2$] polarizations. Here the state of a photon with elliptical polarization vector $\epsilon_\delta = (0, \vec{e}_\delta)$ has degree of linear polarization (equal to the ratio of the difference and sum of the squared semiaxes) [24]:

$$\kappa_\gamma = \frac{\beta^2 - 1}{\beta^2 + 1} = \frac{\alpha^2}{\beta^2 + 1} \ . \tag{60}$$

Inverting this relation, we obtain:

$$\beta^2 = \frac{1 + \kappa_\gamma}{1 - \kappa_\gamma} \ , \ \alpha^2 = \frac{2\kappa_\gamma}{1 - \kappa_\gamma} \ .$$

Now we find the squared moduli of the vectors $\vec{e}_\delta$ and $\vec{a}_\delta$:

$$|\,\vec{e}_\delta\,|^2 = 1 + \beta^2 = \frac{2}{1 - \kappa_\gamma} \ , \ |\,\vec{a}_\delta\,|^2 = (1 + \beta^2)\,(1 + \kappa_L) \ ,$$

$$\kappa_L = \kappa_\gamma \vec{e}_3^{\,2} = \kappa_\gamma \frac{r_0^2}{(-r^2)} \ , \ \vec{e}_3^{\,2} = \frac{r_0^2}{(-r^2)} \ . \tag{61}$$

Let us introduce the normalized vectors $\vec{e}_\delta\,'$ and $\vec{a}_\delta\,'$:

$$\vec{e}_\delta\,' = \frac{\vec{e}_\delta}{\sqrt{1 + \beta^2}} = \sqrt{\frac{1 - \kappa_\gamma}{2}}\,\vec{e}_\delta \ , \ |\vec{e}_\delta\,'|^2 = 1 \ . \tag{62}$$

$$\vec{a}_\delta\,' = \frac{\vec{a}_\delta}{\sqrt{1 + \beta^2}} = \sqrt{\frac{1 - \kappa_\gamma}{2}}\,\vec{a}_\delta \ , \ |\vec{a}_\delta\,'|^2 = 1 + \kappa_\gamma \vec{e}_3^{\,2} = 1 + \kappa_L \ , \tag{63}$$

It is seen that the elliptical-polarization vector $\vec{e}_\delta$ of a virtual photon can be normalized to unity ($|\vec{e}_\delta\,'|^2 = 1$), but the presence of a longitudinal polarization makes this normalization impossible for the total vector $\vec{a}_\delta\,'$ simultaneously. The quantity κ_L (61) corresponding to the inequality $|\vec{a}_\delta\,'|^2 = 1 + \kappa_L \neq 1$ has the meaning of the degree of longitudinal polarization of a virtual photon emitted in a transition with electron spin flip. In the ultrarelativistic limit, when the electron mass can be neglected, the

quantities κ_γ and κ_L can be interpreted as the total degrees of linear and longitudinal polarization of the virtual photon. In this (massless) case we have:

$$(a_3 q_1)^2 + q_1^2 = -M^2\,\frac{\vec{r}^{\,2}}{r^2} \ , \ (a_1 q_1)^2 = M^2\,ctg^2\vartheta/2 \ , \tag{64}$$

$$\kappa_\gamma^{-1} = 1 - 2\,\frac{\vec{r}^{\,2}}{r^2}\,tg^2\vartheta/2 \ , \tag{65}$$

where ϑ is the angle between the vectors $\vec{p}_1$ and $\vec{p}_2$. Equation (65) for κ_γ coincides with the result of [29].

The vector $\vec{a}_\delta\,'$ (63) can also be written as

$$\vec{a}_\delta\,' = \sqrt{\kappa_L}\,\vec{n}_3 - \sqrt{\frac{1 + \kappa_\gamma}{2}}\,\vec{e}_1 + i\delta\sqrt{\frac{1 - \kappa_\gamma}{2}}\,\vec{e}_2 \ ,$$

which makes it easy to construct the polarization density matrix for a virtual photon in the massless limit (both in the polarized case, which for massless particles is helical polarization, and in the unpolarized case; see [29]).

To obtain the complete expression for κ_γ and κ_L arising from the contributions of the matrix elements both without and with spin flip, we construct the lepton tensor averaged over electron spin states. Using the matrix elements (14) this can be easily done [24]:

$$\overline{L}_{\mu\nu} = 4m^2\,(a_0)_\mu (a_0)_\nu + 4y^2\,((a_1)_\mu (a_1)_\nu + (a_2)_\mu (a_2)_\nu) \ . \tag{66}$$

Using the completeness condition (53) and gauge invariance, the tensor $\overline{L}_{\mu\nu}$ can be written as

$$\overline{L}_{\mu\nu} = 4x^2\,(a_0)_\mu (a_0)_\nu - 4y^2\,g_{\mu\nu} \ , \tag{67}$$

where $x^2 = m^2 + y^2$. The tensor $\overline{L}_{\mu\nu}$ (67) is used to reduce the calculation of the contribution of graphs with VCS on a proton to the cross section for the reaction $ep \to ep\gamma$ to calculation of the trace of a product of tensors:

$$Y_{pp} = \overline{L}_{\mu\nu}\,W_{\mu\nu} \ , \ W_{\mu\nu} = V_\mu V_\nu^* \ , \ V_\mu = \overline{u}(q_2)\,M_{\mu\nu}e^\nu\,u(q_1)\,\frac{1}{r^2} \ . \tag{68}$$

Let us express the tensor $\overline{L}_{\mu\nu}$ (66) in the terms of the virtual-photon polarization vectors e_i (54). As a result, it naturally breaks up into the sum of three terms corresponding to the contributions of transverse (L_T) and longitudinal (L_L) states and their interference (L_{LT}) [24]:

$$\overline{L} = 4y^2\,(L_T + L_L + L_{LT}) \ , \tag{69}$$

$$L_T = e_1 \cdot e_1\,(\beta^2 + \alpha^2 m^2/y^2) + e_2 \cdot e_2 \ , \tag{70}$$

$$L_L = e_3 \cdot e_3\,(\alpha^2 + \beta^2 m^2/y^2) \ , \tag{71}$$

$$L_{LT} = -\,(e_1 \cdot e_3 + e_3 \cdot e_1)\,\alpha\beta\,(1 + m^2/y^2) \ . \tag{72}$$

Then the total degree of linear polarization of the virtual photon is given by

$$\kappa_\gamma' = \frac{\beta^2 + \alpha^2 m^2/y^2 - 1}{\beta^2 + \alpha^2 m^2/y^2 + 1} = \frac{\alpha^2}{\beta^2 + 1 - 2m^2/x^2} \ . \tag{73}$$

Since α and β are the same in Eqs. (60) and (73) (see (58)), the inclusion of the electron mass in the ultrarelativistic limit leads only to a slight increase of κ_γ [24]:

$$\kappa'_\gamma \simeq \kappa_\gamma \left(1 + \frac{2m^2}{x^2(1+\beta^2)}\right) . \tag{74}$$

Inverting the relation in (73), we find

$$\beta^2 + \alpha^2 m^2/y^2 = \frac{1+\kappa'_\gamma}{1-\kappa'_\gamma} , \; \alpha^2 + \beta^2 m^2/y^2 = \frac{2\kappa'_\gamma}{1-\kappa'_\gamma} + \frac{m^2}{y^2} . \tag{75}$$

We can separate the completely polarized and unpolarized parts in the transverse tensor: $L_T = e_1 \cdot e_1 \, (\beta^2 + \alpha^2 m^2/y^2 - 1) + e_1 \cdot e_1 + e_2 \cdot e_2 =$
$= \frac{2}{1-\kappa'_\gamma} \, (\kappa'_\gamma \, e_1 \cdot e_1 + (1-\kappa'_\gamma) \, (e_1 \cdot e_1 + e_2 \cdot e_2)/2)$. Therefore, the virtual-photon polarization density matrix ρ_{ij} is obtained from the tensor $\overline{L}_{ij}$ (69) just as in the massless case (see [29]):

$$\rho_{ij} = (1 - \kappa'_\gamma) \, \overline{L}_{ij}/8y^2 . \tag{76}$$

For the degree of longitudinal polarization of the virtual photon we then obtain:

$$\kappa'_L = \frac{r_0^2}{(-r^2)} \kappa'_\gamma \left(1 + \frac{m^2}{y^2} \, \frac{(1-\kappa'_\gamma)}{2\kappa'_\gamma}\right) . \tag{77}$$

The expressions (73) and (77) for κ'_γ and κ'_L with $m = 0$ obviously become κ_γ and κ_L of (60) and (61).

We conclude by noting that the region of applicability of the tensor $\overline{L}_{\mu\nu}$ (69) is not limited to only VCS on the proton. Since in fixed-target experimets the charged-lepton scattering at available energies is mainly determined by virtual photon exchange, the tensor $\overline{L}_{\mu\nu}$ (69) can also be used to study deep-inelastic electron scattering ($e^\pm p \to e^\pm X$), and muon scattering ($\mu^\pm p \to \mu^\pm X$), where inclusion of the mass is more important.

Conclusion

We have studied the reaction $ep \to ep\gamma$ in the kinematics corresponding to electron scattering at small angles and photon scattering at fairly large angles, where proton bremsstrahlung dominates. The results of numerical calculations performed in the rest frame of the initial proton at electron beam energy $E_e = 200$ MeV in the chosen kinematics show that the conditions needed to separate the subprocess $\gamma p \to \gamma p$ from the reaction $ep \to ep\gamma$ are satisfied, because the relative contribution of the Bethe-Heitler and interference terms to the reaction cross section is less than 10 %, and the cross section for the reaction $ep \to ep\gamma$ is quite sensitive to the proton polarizability.

A compact expression was obtained for the differential cross section of the Bethe-Heitler emission of a linearly polarized photon by an electron, taking into account the proton recoil and form factors, owing to the factorization of the squared electric and magnetic form factors of the proton. In the limit where the proton is a pointlike particle of infinite mass, this expression becomes to be the well-known one.

A covariant expression has been obtained for the lepton tensor in which the contribution of states with transverse and longitudinal polarization of the virtual photon is separated. It has been shown that inclusion of the lepton mass tends to increase the degree of linear polarization of the virtual photon.

Acknowledgements

The authors thank to A.I. L'vov for supplying them with a computer code for numerical calculations of the proton RCS amplitudes and for useful discussions. We are also indebted to V.A. Petrun'kin for stimulating discussions of the results.

References

[1] V.A. Petrun'kin, Fiz. Elem. Chast. At. Yadra, **12**, (1981) 692; Sov.J.Part.Nucl. **12**, (1981) 278.

[2] A.I. L'vov and V.A. Petrun'kin, Lecture Notes in Physics, **365**, (1990) 123.

[3] B.E. MacGibbon et al., Phys. Rev. **C52**, (1995) 2097.

[4] A.I. L'vov, V.A. Petrun'kin, S.G. Popov, and B.B. Wojtsekhowski, Preprint No 91-24, Budker-INP (1991); Scanned images of a preprint received at KEK library: 9108320.

[5] P.S. Isaev and I.S. Zlatev, Nucl. Phys. **16**, (1960) 608.

[6] B.B. Wojtsekhovski, A.I. L'vov et al.,"Project: Moscow- Novosibirsk-Gottingen", Preprint Lebedev Physical Institute, Moscow (1992).

[7] P. Kroll, M. Schurmann and P.A.M. Guichon, Nucl. Phys. **A591**, (1995) 606.

[8] R.A. Berg and C.N. Lindner, Nucl. Phys. **26**, (1961) 259.

[9] M.V. Galynsky, Preprint 695, IF AN BSSR, Minsk, (1994) (in Russian).

[10] A.I. L'vov, Yad. Fiz. **34**, (1981) 1075.

[11] V.B. Berestetskii, E.M. Lifshitz, and L.P. Pitaevskii, Quantum Electrodynamics, 2nd ed. (Pergamon Press, Oxford, 1982); Russ: original, Nauka, Moscow, 1989.

[12] S.M. Sikach, Vestsi Akad. Nauk BSSR, Ser. Fiz.-Mat. Nauk, No 2, (1984) 84 (in Russian).

[13] M.V. Galynsky, L.F. Zhirkov, S.M. Sikach, and F.I. Fedorov, Zh.Eksp.Teor.Fiz. **95** (1989) 1921; Sov.Phys.JETP. **68**, (1989) 1111.

[14] M.V. Galynsky and S.M. Sikach, Phys.Part.Nucl.**29** (1998) 469; Fiz.Elem.Chast. Atom.Yadra **29** (1998) 1133; e-print hep-ph/9910284.

[15] M.V. Galynsky and S.M. Sikach, Yad. Fiz. **54**, (1991) 1026.

[16] F. Halsen and A.D. Martin, Quarks and Leptons: an Introductory Course in Modern Particle Physics (Wiley, New York, 1984); Russ: transl., Mir, Moscow, 1987.

[17] A.A. Akhundov, et al., Sov. J. Nucl. Phys **44**, (1986) 988.

[18] A.A. Akhundov, D.Yu. Bardin D.Yu. et al., Z. Phys. **C45**, (1990) 645.

[19] R.L. Gluckstern , M.H. Hull, and G. Breit, Phys. Rev, **90**, (1953) 1026.

[20] H. Olsen and L.C. Maximon, Phys. Rev. **114**, (1959) 887.

[21] J. Asai, H.S. Caplan, and L.C. Maximon, Can. J. Phys. **66**, (1988) 1079.

[22] P.S. Isaev and I.S. Zlatev, Nuovo Cim. **13**, (1959) 1.

[23] M.V. Galynsky, Yad.Fiz.**58**, (1995) 701; Phys. Atom. Nucl. **58**, (1995) 644.

[24] M.V. Galynsky and M.I. Levchuk, Phys.Atom.Nucl. **60**, (1997) 1855; Yad.Fiz. **60**, (1997) 2028.

[25] C. Audit et.al., CEBAF proposal PR 93-050 (1993).

[26] J.F.J. Van den Brand, CEBAF proposal PR 94-011 (1994).

[27] S. Scherer, A.Yu. Korchin, and J.H. Koch, Report MKPH-T-96-4, Mainz (1996).

[28] H.W. Fearing and S. Scherer, Report TRI-PP-96-28, MKPH-T-96-18, Mainz (1996).

[29] A.I. Akhiezer and M.P. Rekalo, Electrodynamics of Hadrons (Naukova Dumka, Kiev, 1977, in Russian).

Exact calculation of the $O(\alpha)$ order QED corrections for the processes $f_1\,\overline{f_1} \to f_2\,\overline{f_2}$ with polarized initial particles

Khotilovich V.G., Shumeiko N.M.

National Scientific and Educational Centre of Particle and High Energy Physics of the Belarusian State University

Abstract

Exact covariant expressions are obtained for the energy spectrum of one of the outgoing fermions, total cross section and polarized asymmetries for the processes $f_1\,\overline{f_1} \to f_2\,\overline{f_2}$ with polarized initial particles in QED to order α^3.

1 Introduction.

The problem of calculation of the radiative corrections (RC) for a process of fermion-antifermion annihilation into another fermion- antifermion

$$f_1 + \overline{f_1} \to f_2 + \overline{f_2} \qquad (1)$$

is one of the best studied both in the Standard Model framework and beyond [1]. Even the calculation of RC in QED for this simple process is a very cumbersome task. But QED-corrections, as background for the effects of more "subtle" physics, are required first of all. So far only one work is known [2] where analytical RC calculation was performed for unpolarized

case without neglecting the particle masses. At present time the perspectives of linear e^+e^-- and $\mu^+\mu^-$-colliders [3, 4] with polarized beams are widely discussed. Therefore we have done here calculation analogous as in [2] but for the case of arbitrary polarized initial particles. In that case we have much more cumbersome expressions and additional difficulties with integration. To overcome these difficulties the tensor integration method have been modified and computer algebra systems were widely used.

2 Method of calculation.

The exact expressions for virtual corrections for the process (1) are well known (e.g. [5]). The infrared divergence is handled with the help of covariant Bardin- Shumeiko method [6]. The main difficulty is fourfold exact analytical integration of the squared matrix element of the bremsstrahlung process

$$f_1(p_1,m,\xi_-)+\overline{f_1}(p_2,m,\xi_+)\to f_2(p_5,M)+\overline{f_2}(p_3,M)+\gamma(p_4,0)\ , \quad (2)$$

where p_i $(i=1..5)$ and m, M are particle momenta and masses, $\xi_\pm$ are polarization vectors of the initial particles.

The main part of the necessary scalar bremsstrahlung integrals was calculated in [7]. To integrate polarization dependent terms we apply the tensor integration method as in [8]. But we have made some modifications in it, making use of basic ideas of the algorithm proposed in [9] for tensor loop intregrals. Using the generalized Kroneker deltas technique allows to fulfill reduction to scalar integrals quickly and in very compact form. If we denote vector and tensor integrals as

$$([p_3^\mu],[p_4^\mu],[p_3^\mu p_3^\nu],[p_4^\mu p_4^\nu],[p_3^\mu p_4^\nu])=\int d\Gamma\ (p_3^\mu,p_4^\mu,p_3^\mu p_3^\nu,p_4^\mu p_4^\nu,p_3^\mu p_4^\nu)\cdot A\ , \quad (3)$$

where $d\Gamma$ is phase space of the reaction (2) and A is some function of integration variables, then we get the results:

$$[p_3^\mu]=[P_3^\mu]\ ,\qquad [p_4^\mu]=[P_4^\mu]\ ,\qquad [p_3^\mu p_3^\nu]=[P_3^\mu P_3^\nu]+\frac{[\Delta_3]}{2\Delta_2^2}\delta^{p_1p_2\mu}_{p_1p_2\alpha}g^{\alpha\nu}\ ,$$
$$[p_4^\mu p_4^\nu]=[P_4^\mu P_4^\nu]+\frac{[\Delta_k]}{2\Delta_2^2}\delta^{p_1p_2\mu}_{p_1p_2\alpha}g^{\alpha\nu}\ ,\ [p_3^\mu p_4^\nu]=[P_3^\mu P_4^\nu]+\frac{[\Delta_{pk}]}{2\Delta_2^2}\delta^{p_1p_2\mu}_{p_1p_2\alpha}g^{\alpha\nu}\ , \quad (4)$$

with

$$P^\mu_{3(4)}=\frac{1}{\Delta_2}(p_1^\mu\delta^{p_1\ p_2}_{p_{3(4)}p_2}+p_2^\mu\delta^{p_1\ p_2}_{p_{3(4)}p_1})\ ,$$

where

$$\Delta_2=\delta^{p_1p_2}_{p_1p_2}\ ,\ \Delta_3=\delta^{p_1p_2p_3}_{p_1p_2p_3}\ ,\ \Delta_k=\delta^{p_1p_2p_4}_{p_1p_2p_4}\ ,\ \Delta_{pk}=\delta^{p_1p_2p_4}_{p_1p_2p_3} \quad (5)$$

are shorthand notations for Gram determinants.

These formula are implemented in REDUCE program, that make all calculations — from squaring matrix element to final results.

3 Results.

After making three analytical integrations we get the fermionic energy spectrum as an intermediate result

$$\begin{aligned}\frac{1}{\sigma_0}\frac{d\sigma}{dx} &= \frac{\alpha}{\pi}\frac{1}{\beta}\Big\{\Big(Q_i^2S_I(x)+Q_f^2S_F(x)(1+2\rho)\Big)\times\\ &\times\left(1+P_L^+P_L^-\frac{1-2\rho}{1+2\rho}+P_{tr}^+P_{tr}^-\cos\Delta\varphi\ \frac{2\rho}{1+2\rho}\right)+\\ &+Q_i^2\left(P_L^+P_L^-\Delta S_L(x)+P_{tr}^+P_{tr}^-\cos\Delta\varphi\ \rho\ \Delta S_{tr}(x)\right)\Big\}\ .\end{aligned}$$

Here

$$\sigma_0 = \frac{4\pi\alpha^2}{3S} Q_i^2 Q_f^2 ,$$

$$\Delta S_L(x) = \frac{1}{\beta^2(1+2\rho)}\Big\{-2x\beta_x\left[1+6\rho+14\rho^2-\rho(1+30\rho-28\rho^2)\frac{L(\beta)}{\beta}\right]+$$
$$+2x^2\beta_x\left[1+9\rho+20\rho^2-\rho(1+42\rho-40\rho^2)\frac{L(\beta)}{\beta}\right]-$$
$$-L(\beta_x)\left[(1+2\rho)(1+2\rho+12\rho\ \rho_f)-2\rho(1+2\rho+4\rho(1-\rho)(1+6\rho_f))\frac{L(\beta)}{\beta}\right]+$$
$$+x(1-x)L(\beta_x)\left[1+2\rho+12\rho^2-24\rho^2(1-\rho)\frac{L(\beta)}{\beta}\right]+$$
$$+L(x,\beta_x)\left[1+6\rho-4\rho^2-4\rho(1+2\rho^2)\frac{L(\beta)}{\beta}\right]\Big\} , \tag{6}$$

$$\Delta S_{tr}(x) = \frac{1}{\beta^2(1+2\rho)}\Big\{x\beta_x\left[8+22\rho-(3+26\rho-44\rho^2)\frac{L(\beta)}{\beta}\right]-$$
$$-2x^2\beta_x\left[11+28\rho-(3+38\rho-56\rho^2)\frac{L(\beta)}{\beta}\right]+$$
$$+L(\beta_x)\left[3(1+2\rho)(1+2\rho_f)-2(1-4\rho+6\rho(1-\rho)(1+2\rho_f))\frac{L(\beta)}{\beta}\right]-$$
$$-x(1-x)L(\beta_x)\left[2+10\rho-(1+10\rho(1-2\rho))\frac{L(\beta)}{\beta}\right]-$$
$$-L(x,\beta_x)\left[4+2\rho-(3-2\rho-4\rho^2)\frac{L(\beta)}{\beta}\right]\Big\} , \tag{7}$$

where $Q_i(Q_f)$ are initial (final) particle charges,

$$S=(p_1+p_2)^2 , \quad x=\frac{p_{30}}{E}\in\left[\frac{M}{E},1\right] , \quad \rho=\frac{m^2}{S} , \quad \rho_f=\frac{M^2}{S} ,$$
$$\beta=\sqrt{1-4\rho} , \quad \beta_x=\sqrt{1-4\rho_f/x^2} , \quad \beta_f=\beta_x|_{x=1}=\sqrt{1-4\rho_f} ,$$
$$L(\beta)=\ln\frac{1+\beta}{1-\beta} , \quad L(x,\beta_x)=\frac{1}{2}\left[L(\beta_x)+\ln\frac{2-x(1-\beta_x)}{2-x(1+\beta_x)}\right] ,$$

E is energy of colliding beems, $P_L^{\pm}$ and $P_{tr}^{\pm}$ are longitudinal and transversal polarizarion degrees of initial particles. Exact expressions for functions $S_I(x)$ and $S_F(x)$ were obtained in [2]. As it is seen from (6) transversal polarization dependent part is proportional to the initial particles masses, and therefore we take it into account only as an example of exact calculation. Polarization structure of the final state radiation is rather simple. It is proportional to unpolarized part. New results are functions $\Delta S_L(x)$ and $\Delta S_{tr}(x)$, that define deviation from this proportionality for the initial state radiation.

Similarly to article [8] we can introduce spin-flip asymmetry

$$A(x,\rho,\rho_f) = \frac{1}{P_L^+P_L^-}\frac{\frac{d\sigma^{\uparrow\uparrow}}{dx}-\frac{d\sigma^{\uparrow\downarrow}}{dx}}{\frac{d\sigma^{\uparrow\uparrow}}{dx}+\frac{d\sigma^{\uparrow\downarrow}}{dx}} = A_0+\frac{Q_i^2\Delta S_L(x)}{Q_i^2S_I(x)+Q_f^2S_F(x)(1+2\rho)} \tag{8}$$

$$\text{where} \quad A_0 = \frac{1-2\rho}{1+2\rho} , \tag{9}$$

which dependence on x is shown in the fig. 1.

Total cross-section of the process $f_1\overline{f_1}\to f_2\overline{f_2}(\gamma)$ with polarized initial particles in the order α^3 is

$$\sigma=\sigma_a+P_L^+P_L^-\sigma_p+P_{tr}^+P_{tr}^-\cos\Delta\varphi\ \sigma_{tr} =$$
$$= \sigma_a^0(1+\delta_a)+P_L^+P_L^-\sigma_p^0(1+\delta_p)+P_{tr}^+P_{tr}^-\cos\Delta\varphi\ \sigma_{tr}^0(1+\delta_{tr}) =$$
$$= (\sigma_a^0+P_L^+P_L^-\sigma_p^0+P_{tr}^+P_{tr}^-\cos\Delta\varphi\ \sigma_{tr}^0)(1+\delta_a)+$$
$$+P_L^+P_L^-\sigma_p^0\Delta\delta_p+P_{tr}^+P_{tr}^-\cos\Delta\varphi\ \sigma_{tr}^0\Delta\delta_{tr} , \tag{10}$$

where

$$\sigma_a^0=\sigma_0\frac{\beta_f}{\beta}(1+2\rho)(1+2\rho_f)$$

is unpolarized born cross-section part, and

$$\sigma_p^0=\sigma_0\frac{\beta_f}{\beta}(1-2\rho)(1+2\rho_f) , \quad \sigma_{tr}^0=\sigma_0\frac{\beta_f}{\beta}\rho(1+2\rho_f)$$

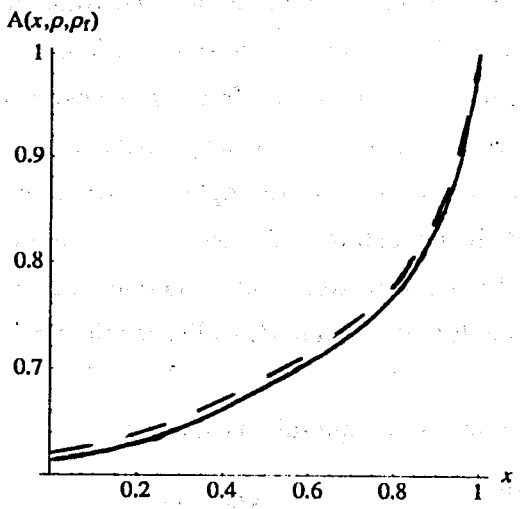

Figure 1: Exact and approximate results for the asymmetry $A(x,\rho,\rho_f)$ for the process $p\bar{p} \to e^+e^-\gamma$ at E=16 GeV.

is longitudinal and transversal polarization dependent born cross- section parts.

Corrections δ_a, δ_p and δ_{tr} equal

$$\delta_a = \delta_I + \delta_F + \delta_{VP}\ , \quad \delta_p = \delta_a + \Delta\delta_p\ , \quad \delta_{tr} = \delta_a + \Delta\delta_{tr}\ , \qquad (11)$$

where

$$\Delta\delta_p = \frac{\alpha}{\pi}Q_i^2\frac{1}{\beta^2(1+\beta^2)}\left\{\frac{3}{2}\frac{L(\beta)}{\beta}\left[\frac{8-8\beta^2+\beta^4-3\beta^6}{3-\beta^2}-2\frac{8-8\beta^2-\beta^4}{3-\beta_f^2}\right]-\right.$$
$$-\frac{2L(\beta_f)}{\beta_f(3-\beta^2)(3-\beta_f^2)}\left[2(9-8\beta^2+3\beta^4)-3\frac{L(\beta)}{\beta}(3+\beta^2)(1-\beta^2)^2\right]-$$
$$\left.-\frac{8}{3(3-\beta^2)}\left[9-2\beta^2-3\beta^4-6\frac{9-5\beta^2}{3-\beta_f^2}\right]\right\}, \qquad (12)$$

$$\Delta\delta_{tr} = \frac{\alpha}{\pi}Q_i^2\frac{1}{\beta^2}\left\{-\frac{L(\beta)}{3\beta}\left[\frac{18+12\beta^2+5\beta^4}{3-\beta^2}-12\frac{3+2\beta^2}{3-\beta_f^2}\right]+\right.$$
$$+\frac{L(\beta_f)}{\beta_f(3-\beta^2)(3-\beta_f^2)}\left[2(9-5\beta^2)-\frac{L(\beta)}{\beta}(9-5\beta^4)\right]+$$

$$\left.+\frac{4}{3(3-\beta^2)}\left[9+\beta^2-6\frac{9-2\beta^2}{3-\beta_f}\right]\right\}. \qquad (13)$$

Correction δ_a (11) corresponds to the unpolarized case. The corrections δ_I (δ_F) were first obtained in [2] and are responsible for initial (final) state corrections. δ_{VP} is the vacuum polarization contribution.

Deviations $\Delta\delta_p$ and $\Delta\delta_{tr}$ from δ_a are the new results. For longitudinal polarization we can again introduce spin-flip asymmetry

$$A(\rho,\rho_f) = \frac{1}{P_L^+P_L^-}\frac{\sigma^{\uparrow\uparrow}-\sigma^{\uparrow\downarrow}}{\sigma^{\uparrow\uparrow}+\sigma^{\uparrow\downarrow}} = \frac{\sigma_p}{\sigma_a} = A_0\frac{1+\delta_p}{1+\delta_a} = A_0(1+\delta_A)\ , \qquad (14)$$

where born asymmetry A_0 and correction δ_A to it are given by

$$A_0 = \frac{\sigma_p^0}{\sigma_a^0}\ , \quad \delta_A = \frac{\Delta\delta_p}{1+\delta_a}\ . \qquad (15)$$

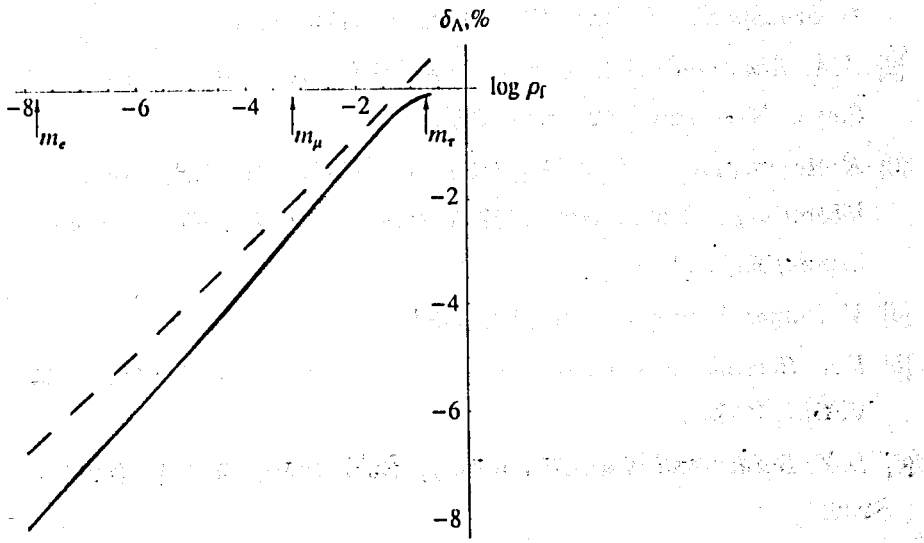

Figure 2: Dependence of the δ_A on the final fermion mass for the process $p\bar{p} \to f\bar{f}(\gamma)$ at E=2 GeV (dashed line - approximate values).

In the fig. 2 the difference between exact and approximate values of δ_A is presented. This difference is noticeable only at close to threshold energies.

4 Conclusion.

We have obtained exact expressions for the fermionic energy spectrum, total cross-section, and corresponding polarization asymmetries for the process $f_1\,\overline{f_1} \to f_2\,\overline{f_2}\,(\gamma)$ with massive fermions to order $O(\alpha^3)$ in QED. Our results generalize the results of [2] in the case of arbitrary polarized initial particles.

References

[1] *D. Bardin et al.* // Nucl. Phys. 1991. V. B351. P. 1. *W. Hollik and C. Schappacher* // Nucl. Phys. 1999. V. B545. P. 98.

[2] *A.A. Akhundov, D.Y. Bardin, O.M. Fedorenko and T. Riemann* // Sov. J. Nucl. Phys. 42, 762 (1985).

[3] *E. Accomando et al. [ECFA/DESY LC Physics Working Group Collaboration]* // Phys. Rept. 1997. V. 299. P. 1. *D.J. Miller* // preprint hep-ex/9901039.

[4] *V. Barger* // preprint hep-ph/9803480.

[5] *F.A. Berends, K.J. Gaemer and R. Gastmans* // Nucl. Phys. 1973. V. B57. P. 381.

[6] *D.Y. Bardin and N.M. Shumeiko* // Nucl. Phys. 1977. V. B127. P. 242.

[7] *A.A. Akhundov, D.Y. Bardin, O.M. Fedorenko and T. Riemann* // JINR communications E2-84-777. Dubna, 1984.

[8] *T.V. Kukhto and N.M. Shumeiko* // Nucl. Phys. 1983. V. B219. P. 412.

[9] *G.J. van Oldenborgh and J.A. Vermaseren* // Z. Phys. 1990. V. C46. P. 425.

Polarization to Probe an Extra Neutral Gauge Boson at e^+e^- Linear Collider

A. A. Pankov [1]

Department of Physics, Technical University, Gomel, Belarus

Abstract

The sensitivity to the Z' couplings of the processes $e^+e^- \to l^+l^-, \bar{b}b$ and $\bar{c}c$ at the linear collider with $\sqrt{s} = 500\,\mathrm{GeV}$ with initial beam polarization, for typical extended model examples are studied. To this aim, the suitable integrated, polarized, observables directly related to the helicity cross sections that carry information on the individual Z' chiral couplings to fermions are used. We discuss the derivation of separate, model-independent limits on the couplings in the case of no observed indirect Z' signal within the expected experimental accuracy. In the hypothesis that such signals were, indeed, observed we assess the expected accuracy on the numerical determination of such couplings and the consequent range of Z' masses where the individual models can be distinguished from each other as the source of the effect.

[1]E-mail: pankov@ggtu.belpak.gomel.by

1 Introduction

Extra neutral gauge bosons are a feature of many models of physics beond the Standard Model (SM). If discovered they would represent irrefutable proof of new physics, most likely that the SM gauge group must be extended [1, 3]. The search for the Z' is included in the physics programme of all the present and future high energy collider facilities. In particular, the strategies for the experimental determination of the Z' couplings to the ordinary SM degrees of freedom, and the relevant discovery limits, have been discussed in the large, and still growing, literature on this subject [1]-[8].

Taking into account the limit $M_{Z'} > 600 - 700\,\mathrm{GeV}$ from 'direct' searches at the Tevatron [9], only 'indirect' (or virtual) manifestations of the Z' can be expected at LEP2 [10] and at the planned e^+e^- linear collider (LC) with CM energy $\sqrt{s} = 500$ GeV [11, 12].

Such effects would be represented by deviations from the calculated SM predictions of the measured observables relevant to the different processes. In this regard, of particular interest for the LC is the annihilation into fermion pairs

$$e^+ + e^- \to \bar{f} + f\,, \tag{1}$$

that gives information on the $Z'ff$ interaction.

In the case of no observed signal within the experimental accuracy, limits on the Z' parameters to a conventionally defined confidence level can be derived, either from a general analysis taking into account the full set of possible Z' couplings to fermions, or in the framework of specific models where characteristic relations among the couplings strongly reduce the number of independent free parameters. Clearly, completely model-independent limits can result only in the optimal situation where the different couplings can be disentangled, by means of suitable observables, and analysed independently so as to avoid potential cancellations. The essential role of the initial electron beam polarization has been repeatedly emphasized in this regard, and the potential of the linear collider along these lines has been extensively reviewed, e.g., in Refs. [7, 8].

The same need of a procedure to disentangle the different Z' couplings arises in the case where deviations from the SM were experimentally observed. Indeed, in this situation, the numerical values of the individual couplings must be extracted from the measured deviations in order to identify the source of these effects and to make tests of the various theoretical

from the mathematical point of view, in the next Section we prefer to use $\sigma_\pm$, that are found more convenient to discuss the expected uncertainties and the corresponding sensitivities to the Z' couplings. Also, it turns out numerically that $z^* = 0.59$ in (10) and (11) maximizes the statistical significance of the results.

The helicity amplitudes $A_{\alpha\beta}$ in Eq. (5) can be written as

$$A_{\alpha\beta} = (Q_e)_\alpha (Q_f)_\beta + g^e_\alpha g^f_\beta \chi_Z + g'^e_\alpha g'^f_\beta \chi_{Z'}, \qquad (13)$$

in the notation where the general neutral-current interaction is written as

$$-L_{NC} = eJ^\mu_\gamma A_\mu + g_Z J^\mu_Z Z_\mu + g^\mu_{Z'} J^\mu_{Z'} Z'_\mu. \qquad (14)$$

Here, $e = \sqrt{4\pi\alpha_{e.m.}}$; $g_Z = e/s_W c_W$ ($s^2_W = 1 - c^2_W \equiv \sin^2\theta_W$) and $g_{Z'}$ are the Z and Z' gauge couplings, respectively. Moreover, in (13), $\chi_i = s/(s - M^2_i + iM_i\Gamma_i)$ are the gauge boson propagators with $i = Z$ and Z', and the g's are the left- and right-handed fermion couplings. The fermion currents that couple to the neutral gauge boson i are expressed as $J^\mu_i = \sum_f \bar\psi_f \gamma^\mu (L^f_i P_L + R^f_i P_R)\psi_f$, with $P_{L,R} = (1 \mp \gamma_5)/2$ the projectors onto the left- and right-handed fermion helicity states. With these definitions, the SM couplings are

$$R^f_\gamma = Q_f; \qquad L^f_\gamma = Q_f; \qquad R^f_Z = -Q_f s^2_W; \qquad L^f_Z = I^f_{3L} - Q_f s^2_W, \qquad (15)$$

where Q_f are fermion electric charges, and the couplings in Eq. (13) are normalized as

$$g^f_L = \frac{g_Z}{e} L^f_Z, \qquad g^f_R = \frac{g_Z}{e} R^f_Z, \qquad g'^f_L = \frac{g_{Z'}}{e} L^f_{Z'}, \qquad g'^f_R = \frac{g_{Z'}}{e} R^f_{Z'}. \qquad (16)$$

In what follows, we will limit ourselves to a few representative models predicting new gauge heavy bosons. Specifically, models inspired by GUT inspired scenarios, superstring-motivated ones, and those with Left-Right symmetric origin [4]. These are the χ model occurring in the breaking $SO(10) \to SU(5) \times U(1)_\chi$, the ψ model originating in $E_6 \to SO(10) \times U(1)_\psi$, and the η model which is encountered in superstring-inspired models in which E_6 breaks directly to a rank-5 group. As an example of Left-Right model, we consider the particular value $\kappa = g_R/g_L = 1$, corresponding to the most commonly considered case of Left-Right Symmetric Model (LR). For all such grand-unified E_6 and Left-Right models the Z' gauge coupling in (14) is $g_{Z'} = g_Z s_W$ [4].

As they are constrained from present low-energy data [2] and from recent data from the Tevatron [9], new vector boson effects at the LC are expected to be quite small and therefore should be disentangled from the radiative corrections to the SM Born predictions for the cross section. To this aim, in our numerical analysis we follow the strategy of Refs. [17]-[18], in particular we use the improved Born approximation accounting for the electroweak one-loop corrections.

3 Model independent Z' search and discovery limits

According to Eqs. (3), (4) and (12), by the measurements of σ_+ and σ_- for the different initial electron beam polarizations one determines the cross sections related to definite helicity amplitudes $A_{\alpha\beta}$. From Eq. (13), one can observe that the Z' manifests itself in these amplitudes by the combination of the product of couplings $g'^e_\alpha g'^f_\beta$ with the propagator $\chi_{Z'}$. In the situation $\sqrt{s} \ll M_{Z'}$ we shall consider here, only the interference of the SM term with the Z' exchange is important and the deviation of each helicity cross section from the SM prediction is given by

$$\Delta\sigma_{\alpha\beta} \equiv \sigma_{\alpha\beta} - \sigma^{SM}_{\alpha\beta} = N_C \sigma_{\rm pt}\, 2\,\mathrm{Re}\left[\left(Q_e Q_f + g^e_\alpha g^f_\beta \chi_Z\right) \cdot \left(g'^e_\alpha g'^f_\beta \chi^*_{Z'}\right)\right]. \qquad (17)$$

As one can see, $\Delta\sigma_{\alpha\beta}$ depend on the same kind of combination of Z' parameters and, correspondingly, each such combination can be considered as a single 'effective' nonstandard parameter. Therefore, in an analysis of experimental data for $\sigma_{\alpha\beta}$ based on a χ^2 procedure, a one-parameter fit is involved and we may hope to get a slightly improved sensitivity to the Z' with respect to other kinds of observables.

As anticipated, in the case of no observed deviation one can evaluate in a model-independent way the sensitivity of process (1) to the Z' parameters, given the expected experimental accuracy on σ_+ and σ_-. It is convenient to introduce the general parameterization of the Z'-exchange interaction used, e.g., in Refs. [8, 13]:

$$G^f_L = L^f_{Z'} \sqrt{\frac{g^2_{Z'}}{4\pi} \frac{M^2_Z}{M^2_{Z'} - s}}, \qquad G^f_R = R^f_{Z'} \sqrt{\frac{g^2_{Z'}}{4\pi} \frac{M^2_Z}{M^2_{Z'} - s}}. \qquad (18)$$

An advantage of introducing the 'effective' left- and right-handed couplings

of Eq. (18) is that the bounds can be represented on a two-dimensional 'scatter plot', with no need to specify particular values of $M_{Z'}$ or s.

Our χ^2 procedure defines a χ^2 function for any observable $\mathcal{O}$:

$$\chi^2 = \left(\frac{\Delta\mathcal{O}}{\delta\mathcal{O}}\right)^2, \tag{19}$$

where $\Delta\mathcal{O} \equiv \mathcal{O}(Z') - \mathcal{O}(SM)$ and $\delta\mathcal{O}$ is the expected uncertainty on the considered observable combining both statistical and systematic uncertainties. The domain allowed to the Z' parameters by the non-observation of the deviations $\Delta\mathcal{O}$ within the accuracy $\delta\mathcal{O}$ will be assessed by imposing $\chi^2 < \chi^2_{\rm crit}$, where the actual value of $\chi^2_{\rm crit}$ specifies the desired 'confidence' level. The numerical analysis has been performed by means of the program ZEFIT, adapted to the present discussion, which has to be used along with ZFITTER [19], with input values $m_{top} = 175$ GeV and $m_H = 300$ GeV.

In the real case, the longitudinal polarization of the beams will not exactly be ± 1 and, consequently, instead of the pure helicity cross section, the experimentally measured $\sigma_\pm$ will determine the linear combinations on the right hand side of Eqs. (3) and (4) with $|P_e|$ (and $|P_{\bar{e}}|$) less than unity. Thus, ultimately, the separation of σ_{RR} from σ_{LL} will be obtained by solving the linear system of two equations corresponding to the data on σ_+ for, e.g., both signs of the electron longitudinal polarization. The same is true for the separation of σ_{RL} and σ_{LR} using the data on σ_-.

In the 'linear' approximation of Eq. (17), and with $M_{Z'} \gg \sqrt{s}$, the constraints from the condition $\chi^2 < \chi^2_{\rm crit}$ can be directly expressed in terms of the effective couplings (18) as:

$$|G^e_\alpha G^f_\beta| < \frac{\alpha_{e.m.}}{2}\sqrt{\chi^2_{crit}}\left(\frac{\delta\sigma^{SM}_{\alpha\beta}}{\sigma^{SM}_{\alpha\beta}}\right)|A^{SM}_{\alpha\beta}|\frac{M_Z^2}{s}. \tag{20}$$

We need to evaluate the expected uncertainties $\delta\sigma_{\alpha\beta}$. To this aim, starting from the discussion of σ_+, we consider the solutions of the system of four equations corresponding to $P_e = \pm P$ and $P_{\bar{e}} = 0$ in Eqs. (3) and (4):

$$\sigma_{\rm LL} = \frac{1+P}{P}\sigma_+(-P) - \frac{1-P}{P}\sigma_+(P), \tag{21}$$

$$\sigma_{\rm RR} = \frac{1+P}{P}\sigma_+(P) - \frac{1-P}{P}\sigma_+(-P), \tag{22}$$

$$\sigma_{\rm LR} = \frac{1+P}{P}\sigma_-(-P) - \frac{1-P}{P}\sigma_-(P), \tag{23}$$

$$\sigma_{\rm RL} = \frac{1+P}{P}\sigma_-(P) - \frac{1-P}{P}\sigma_-(-P). \tag{24}$$

From these relations, adding the uncertainties, e.g. $\delta\sigma_+(\pm P)$ on $\sigma_+(\pm P)$ in quadrature, $\delta\sigma_{RR}$ has the form

$$\delta\sigma_{RR} = \sqrt{\left(\frac{1+P}{P}\right)^2(\delta\sigma_+(P))^2 + \left(\frac{1-P}{P}\right)^2(\delta\sigma_+(-P))^2}, \tag{25}$$

and $\delta\sigma_{LL}$ can be expressed quite similarly. Also, we combine statistical and systematic uncertainties in quadrature. In this case, if $\sigma_+(\pm P)$ are directly measured *via* the difference (10) of the integrated cross sections $\sigma_{1+}(\pm P)$ and $\sigma_{2+}(\pm P)$, one can see that $\delta\sigma^{stat}_+$ has the simple property: $\delta\sigma_+(\pm P)^{stat} = \left(\sigma^{SM}(\pm P)/\epsilon\mathcal{L}_{int}\right)^{1/2}$, where $\mathcal{L}_{int}$ is the time-integrated luminosity, ϵ is the efficiency for detecting the final state under consideration and $\sigma^{SM}(\pm P)$ is the polarized total cross section. For the systematic uncertainty, we use $\delta\sigma_+(\pm P)^{sys} = \delta^{sys}\left(\sigma^2_{1+}(\pm P) + \sigma^2_{2+}(\pm P)\right)^{1/2}$, assuming that $\sigma_{1+}(\pm P)$ and $\sigma_{2+}(\pm P)$ have the same systematic error δ^{sys}. One can easily see that $\delta\sigma_{LL}$ can be obtained by changing $\delta\sigma_+(P) \leftrightarrow \delta\sigma_+(-P)$ in (25) and that the expression for $\delta\sigma_{RL}$ and $\delta\sigma_{LR}$ also follow from this equation by $\delta\sigma_+ \to \delta\sigma_-$.

Numerically, to exploit Eq. (17) with $\delta\sigma_{\alpha\beta}$ expressed as above, we assume the following values for the expected identification efficiencies and systematic uncertainties on the various fermionic final states [20]: $\epsilon = 100\%$ and $\delta^{sys} = 0.5\%$ for leptons; $\epsilon = 60\%$ and $\delta^{sys} = 1\%$ for b quarks; $\epsilon = 35\%$ and $\delta^{sys} = 1.5\%$ for c quarks. Also, $\chi^2_{crit} = 3.84$ as typical for 95% C.L. with a one-parameter fit. We take $\sqrt{s} = 0.5$ TeV and a one-year run with $\mathcal{L}_{int} = 50\, fb^{-1}$. For for polarized beams, we assume 1/2 of the total integrated luminosity quoted above for each value of the electron polarization, $P_e = \pm P$. Concerning polarization, in the numerical analysis presented below we take three different values, P =1, 0.8 and 0.5, in order to test the dependence of the bounds on this variable.

As already noticed, in the general case where process (1) depends on all four independent $Z'ff$ couplings, only the products $G^e_R G^f_R$ and $G^e_L G^f_L$ can be constrained by the σ_+ measurement *via* Eq. (17), while the products $G^e_R G^f_L$ and $G^e_L G^f_R$ can be analogously bounded by σ_-. The exception is lepton pair production ($f = l$) with $(e-l)$ universality of Z' couplings, in which case σ_+ can individually constrain either G^e_L or G^e_R. Also, it is interesting to note that such lepton universality implies $\sigma_{RL} = \sigma_{LR}$ and, accordingly, for $P_{\bar{e}} = 0$ electron polarization drops from Eq. (4) which becomes equivalent to the unpolarized one, with *a priori* no benefit from

Table 1: 95% C.L. model-independent upper limits at LC with $E_{c.m.} = 0.5$ TeV. For polarized beams, we take $\mathcal{L}_{int} = 25\, fb^{-1}$ for each possibility of the electron polarization, $P_e = \pm P$.

couplings		$\lvert G_R^e G_R^f\rvert^{1/2}$ (10^{-3})	$\lvert G_L^e G_L^f\rvert^{1/2}$ (10^{-3})	$\lvert G_R^e G_L^f\rvert^{1/2}$ (10^{-3})	$\lvert G_L^e G_R^f\rvert^{1/2}$ (10^{-3})
observables		σ_{RR}	σ_{LL}	σ_{RL}	σ_{LR}
process	P				
$e^+e^- \to l^+l^-$	1.0	2.1	2.1	3.0	3.2
$e^+e^- \to l^+l^-$	0.8	2.3	2.3	3.3	3.4
$e^+e^- \to l^+l^-$	0.5	2.7	2.7	3.9	4.0
$e^+e^- \to \bar{b}b$	1.0	1.9	2.0	2.5	4.6
$e^+e^- \to \bar{b}b$	0.8	2.2	2.1	2.8	4.8
$e^+e^- \to \bar{b}b$	0.5	3.0	2.3	3.7	5.7
$e^+e^- \to \bar{c}c$	1.0	2.3	2.6	4.1	3.9
$e^+e^- \to \bar{c}c$	0.8	2.5	2.7	4.5	4.1
$e^+e^- \to \bar{c}c$	0.5	3.2	3.0	5.5	4.6

polarization. Nevertheless, the uncertainty in Eq. (25) still depends on the longitudinal polarization P. The 95% C.L. upper bounds on the products of lepton couplings (without assuming lepton universality) are reported in the first three rows of Table 1.

For quark-pair production ($f = c, b$), where in general $\sigma_{RL} \neq \sigma_{LR}$ due to the appearance of different fermion couplings, the analysis takes into account the reconstruction efficiencies and the systematic uncertainties previously introduced, and in Table 1 we report the 95% C.L. upper bounds on the relevant products of couplings.

Also, for illustrative purposes, in Fig. 1 we show the 95% C.L. bounds in the plane (G_R^e, G_R^b), represented by the area limited by the four hyperbolas. The shaded region is obtained by combining these limits with the ones derived from the pure leptonic process with lepton universality. Thus, in general we are not able to constrain the individual couplings to a finite region. On the other hand, there would be the possibility of using Fig. 1 to constrain the quark couplings to the Z' to a finite range in the case where some finite effect were observed in the lepton-pair channel. The situation with the other couplings, and/or the c quark, is similar to the

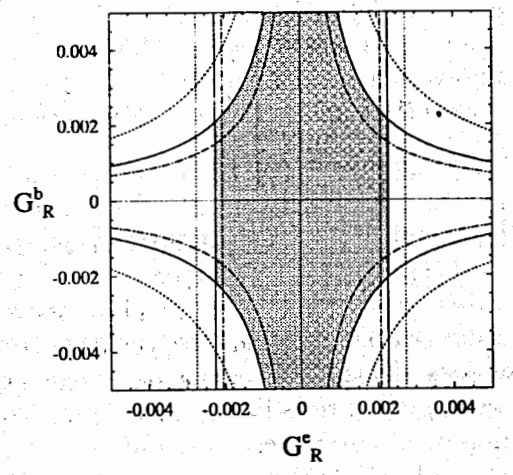

Figure 1: 95% C.L. upper bounds on the model independent Z' couplings in the plane (G_R^e, G_R^b) determined by σ_{RR}. The areas enclosed by vertical straight lines are obtained from the process $e^+e^- \to l^+l^-$, while those enclosed between hyperbolas are from $e^+e^- \to \bar{b}b$ at $\mathcal{L}_{int} = 50$ fb^{-1} and $\sqrt{s} = 500$ GeV. The dot-dash, solid and dotted contours are obtained at $P = 1$, 0.8, 0.5, respectively. The shaded region is derived from the combination of $e^+e^- \to l^+l^-$ and $e^+e^- \to \bar{b}b$ at $P = 0.8$.

one depicted in Fig. 1.

Table 1 shows that the integrated observables σ_+ and σ_- are quite sensitive to the indirect Z' effects, with upper limits on the relevant products $|G_\alpha^e \cdot G_\beta^f|$ ranging from $2.2 \cdot 10^{-3}$ to $4.8 \cdot 10^{-3}$ at the maximal planned value $P = 0.8$ of the electron longitudinal polarization. In most cases, the best sensitivity occurs for the $\bar{b}b$ final state, while the worst one is for $\bar{c}c$. Decreasing the electron polarization from $P = 1$ to $P = 0.5$ results in worsening the sensitivity by as much as 50%, depending on the final fermion channel.

Regarding the role of the assumed uncertainties on the observables under consideration, in the cases of $e^+e^- \to l^+l^-$ and $e^+e^- \to \bar{b}b$ the

expected statistics are such that the uncertainty turns out to be dominated by the statistical one, and the results are almost insensitive to the value of the systematical uncertainty. Conversely, for $e^+e^- \to \bar{c}c$ both statistical and systematic uncertainties are important. Moreover, as Eqs. (3) and (4) show, a further improvement on the sensitivity to the various Z' couplings in Table 1 would obtain if both initial e^- and e^+ longitudinal polarizations were available [12].

4 Resolving power and model identification

If a Z' is indeed discovered, perhaps at a hadron machine, it becomes interesting to measure as accurately as possible its couplings and mass at the LC, and make tests of the various extended gauge models. To assess the accuracy, the same procedure as in the previous section can be applied to the determination of Z' parameters by simply replacing the SM cross sections in Eqs. (19) and (25) by the ones expected for the 'true' values of the parameters (namely, the extended model ones), and evaluating the χ^2 variation around them in terms of the expected uncertainty on the cross section.

4.1 Z' couplings to leptons

We now examine bounds on the Z' couplings for $M_{Z'}$ fixed at some value. Starting from the leptonic process $e^+e^- \to l^+l^-$, let us assume that a Z' signal is detected by means of the observables σ_+ and σ_-. Using Eqs. (22) and (21), the measurement of σ_+ for the two values $P_e = \pm P$ will allow to extract σ_{RR} and σ_{LL} which, in turn, determine independent and separate values for the right- and left-handed Z' couplings $R^e_{Z'}$ and $L^e_{Z'}$ (we assume lepton universality). The χ^2 procedure determines the accuracy, or the 'resolving power' of such determinations given the expected experimental uncertainty (statistical plus systematic).

In Table 2 we give the resolution on the Z' leptonic couplings for the typical model examples introduced in Section 2, with $M_{Z'} = 1$ TeV. In this regard, one should recall that the two-fold ambiguity intrinsic in process (1) does not allow to distinguish the pair of values of $(g'^e_\alpha, g'^f_\beta)$ from the one $(-g'^e_\alpha, -g'^f_\beta)$, see Eq. (17). Thus, the actual sign of the couplings $R^e_{Z'}$ and $L^e_{Z'}$ cannot be determined from the data (in Table 2 we have chosen the signs dictated by the relevant models). In principle, the sign ambiguity of

Table 2: The values of the Z' leptonic and quark chiral couplings for typical models with $M_{Z'} = 1$ TeV and expected 1-σ error bars from combined statistical and systematic uncertainties, as determined at the LC with $E_{c.m.} = 0.5$ TeV and $P = 0.8$.

	χ	ψ	η	LR
$R^e_{Z'}$	$0.204^{+0.042}_{-0.069}$	$-0.264^{+0.052}_{-0.043}$	$-0.333^{+0.038}_{-0.035}$	$-0.438^{+0.029}_{-0.028}$
$L^e_{Z'}$	$0.612^{+0.020}_{-0.020}$	$0.264^{+0.042}_{-0.052}$	$-0.166^{+0.102}_{-0.061}$	$0.326^{+0.036}_{-0.039}$
$R^b_{Z'}$	$-0.612^{+0.110}_{-0.111}$	$-0.264^{+0.111}_{-0.172}$	$0.166^{+0.096}_{-0.075}$	$-0.874^{+0.116}_{-0.138}$
$L^b_{Z'}$	$-0.204^{+0.040}_{-0.042}$	$0.264^{+0.158}_{-0.103}$	$0.333^{+0.230}_{-0.168}$	$-0.110^{+0.080}_{-0.085}$
$R^c_{Z'}$	$0.204^{+0.092}_{-0.090}$	$-0.264^{+0.138}_{-0.207}$	$-0.333^{+0.114}_{-0.145}$	$0.656^{+0.122}_{-0.104}$
$L^c_{Z'}$	$-0.204^{+0.059}_{-0.064}$	$0.264^{+0.222}_{-0.149}$	$0.333^{+0.577}_{-0.326}$	$-0.110^{+0.106}_{-0.134}$

fermionic couplings might be resolved by considering other processes such as, e.g., $e^+e^- \to W^+W^-$.

Another interesting question is the potential of the leptonic process (1) to identify the Z' model underlying the measured signal, through the measurement of the helicity cross sections σ_{RR} and σ_{LL}. Such cross sections only depend on the relevant leptonic chiral coupling and on $M_{Z'}$, so that such resolving power clearly depends on the actual value of the Z' mass. In Figs. 2a and 2b we show this dependence for the E_6 and the LR models of interest here. In these figures, the horizontal lines represent the values of the couplings predicted by the various models, and the lines joining the upper and the lower ends of the vertical bars represent the expected experimental uncertainty at the 95% CL. The intersection of the

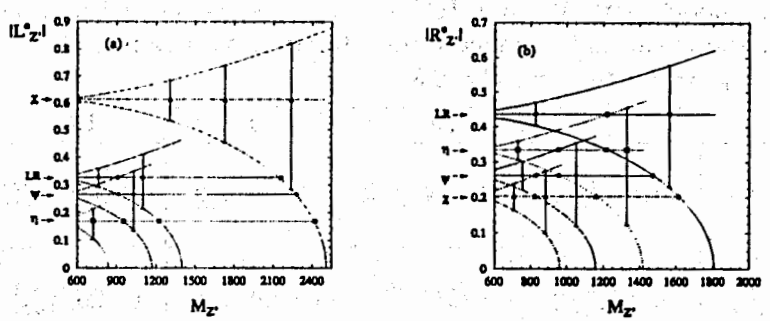

Figure 2: Resolution power at 95% C.L. for the absolute value of the leptonic Z' couplings, $|L^e_{Z'}|$ (a) and $|R^e_{Z'}|$ (b), as a function of $M_{Z'}$, obtained from σ_{LL} and σ_{RR}, respectively, in process $e^+e^- \to l^+l^-$. The error bars combine statistical and systematic uncertainties. Horizontal lines correspond to the values predicted by typical models.

lower such lines with the $M_{Z'}$ axis determines the discovery reach for the corresponding model: larger values of $M_{Z'}$ would determine a Z' signal smaller than the experimental uncertainty and, consequently, statistically invisible. Also, Figs. 2a and 2b show the complementary roles of σ_{LL} and σ_{RR} to set discovery limits: while σ_{LL} is mostly sensitive to the Z'_χ and has the smallest sensitivity to the Z'_η, σ_{RR} provides the best limit for the Z'_{LR} and the worst one for the Z'_χ.

As Figs. 2a and 2b show, the different models can be distinguished by means of $\sigma_\pm$ as long as the uncertainty of the coupling of one model does not overlap with the value predicted by the other model. Thus, the identification power of the leptonic process (1) is determined by the minimum $M_{Z'}$ value at which such 'confusion region' starts. For example, Fig. 2a shows that the χ model cannot be distinguished from the LR, ψ and η models at Z' masses larger than 2165 GeV, 2270 GeV and 2420 GeV, respectively. The identification power for the typical models are indicated in Figs. 2a and 2b by the symbols circle, diamond, square and triangle. The corresponding $M_{Z'}$ values at 95% C.L. for the typical E_6 and LR models are listed in Table 3, where the Z' models listed in first columns should be distinguished from the ones listed in the first row assumed to be the origin

Table 3: Identification power of process $e^+e^- \to \bar{f}f$ at 95% C.L. expressed in terms of $M_{Z'}$ (in GeV) for typical E_6 and LR models at $E_{c.m.} = 0.5$ TeV and $\mathcal{L}_{int} = 25\, fb^{-1}$ for each value of the electron polarization, $P_e = \pm 0.8$.

	σ_{RR}				σ_{LL}			
$e^+e^- \to l^+l^-$	ψ	η	χ	LR	ψ	η	χ	LR
ψ	—	960	830	1470	—	840	2270	920
η	950	—	970	1210	960	—	2420	1220
χ	830	1165	—	1615	1170	840	—	1400
LR	1160	1220	970	—	915	840	2165	—
$e^+e^- \to b\bar{b}$	ψ	η	χ	LR	ψ	η	χ	LR
ψ	—	725	1180	2345	—	710	1120	940
η	700	—	1210	2410	750	—	1250	750
χ	1175	1100	—	2130	1130	1140	—	950
LR	1210	1100	1540	—	940	760	1370	—
$e^+e^- \to c\bar{c}$	ψ	η	χ	LR	ψ	η	χ	LR
ψ	—	865	800	1740	—	620	935	800
η	880	—	880	1580	645	—	1035	665
χ	760	1050	—	1840	935	940	—	810
LR	1050	1280	880	—	780	685	1135	—

of the observed Z' signal. For this reason Table 3 is not symmetric.

Analogous considerations hold also for σ_{LR} and σ_{RL}. These cross sections give qualitatively similar results for the product $L^e_{Z'}R^e_{Z'}$, but with weaker constraints because of smaller sensitivity.

4.2 Z' couplings to quarks

In the case of process (1) with $\bar{q}q$ pair production (with $q = c, b$), the analysis is complicated by the fact that the relevant helicity amplitudes depend on three parameters (g'^e_α, g'^q_β and $M_{Z'}$) instead of two. Nevertheless, there is still some possibility to derive general information on the Z' chiral couplings to quarks. Firstly, by the numerical procedure introduced above one can determine from the measured cross section the products of electrons and final state quark couplings of the Z', from which one derives allowed regions to such couplings in the independent, two-dimensional, planes $(L^e_{Z'}, L^q_{Z'})$ and $(L^e_{Z'}, R^q_{Z'})$. The former regions are determined through σ_{LL},

and the latter ones through σ_{LR}. As an illustrative example, in Fig. 3 we depict the bounds from the process $e^+e^- \to \bar{b}b$ in the $(L^e_{Z'},L^b_{Z'})$ and $(L^e_{Z'},R^b_{Z'})$ planes for the Z' of the χ model, with $M_{Z'} = 1\,\text{TeV}$. Taking into account the above mentioned two-fold ambiguity, the allowed regions are the ones included within the two sets of hyperbolic contours in the upper-left and in the lower-right corners of Fig. 3. Then, to get finite regions for the quark couplings, one must combine the hyperbolic regions so obtained with the determinations of the leptonic Z' couplings from the leptonic process (1), represented by the two vertical strips. The corresponding shaded areas represent the determinations of $L^b_{Z'}$, while the hatched areas are the determinations of $R^b_{Z'}$. Notice that, in general, there is the alternative possibility of deriving constraints on quark couplings also in the case of right-handed electrons, namely, from the determinations of the pairs of couplings $(R^e_{Z'},L^b_{Z'})$ and $(R^e_{Z'},R^b_{Z'})$. However, as observed with regard to the previous analysis of the leptonic process, the sensitivity to the right-handed electron coupling turns out to be smaller than for $L^e_{Z'}$, so that the corresponding constraints are weaker.

The determinations of the Z' couplings with the c and b quarks for the typical E_6 and LR models with $M_{Z'} = 1\,\text{TeV}$, are given in Table 2 where the combined statistical and systematic uncertainties are taken into account. Furthermore, similar to the analysis presented in Section 4.1 and the corresponding Figs. 2a and 2b, we depict in Figs. 4a and 4b the different models identification power as a function of $M_{Z'}$, for the reaction $e^+e^- \to \bar{b}b$ as a representative example. The model identification power of the $\bar{b}b$ and $\bar{c}c$ pair production processes are reported in Table 3.

5 Conclusion

We briefly summarize our findings concerning the Z' discovery limits and the models identification power of process (1) *via* the separate measurement of the helicity cross sections $\sigma_{\alpha\beta}$ at the LC, with $\sqrt{s} = 0.5\,\text{TeV}$ and $\mathcal{L}_{int} = 25\,fb^{-1}$ for each value $P_e = \pm P$ the electron longitudinal polarization. Given the present experimental lower limits on $M_{Z'}$, only indirect effects of the Z' can be studied at the LC. In general, the helicity cross sections allow to extract separate, and model-indpendent, information on the individual 'effective' Z' couplings $(G^e_\alpha \cdot G^f_\beta)$. As depending on the minimal number of free parameters, they may be expected to show some convenience with respect to other observables in an analysis of the experimental data based

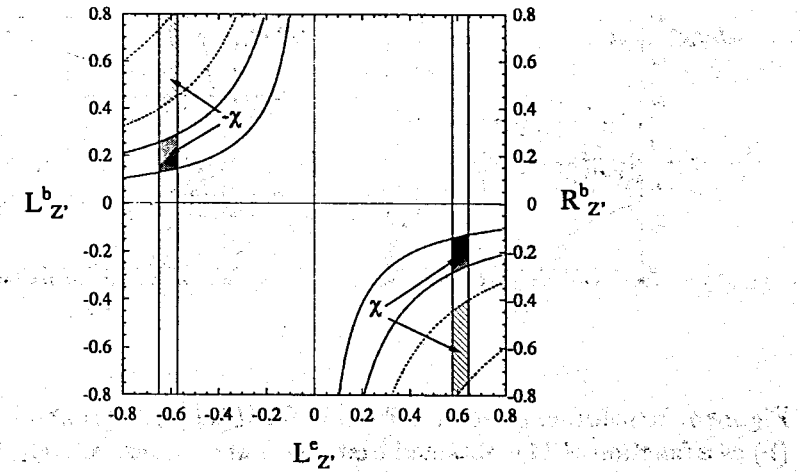

Figure 3: Allowed bounds at 95% C.L. on Z' couplings with $M_{Z'} = 1$ TeV (χ model) in the two-dimension planes $(L^e_{Z'},L^b_{Z'})$ and $(L^e_{Z'},R^b_{Z'})$ obtained from helicity cross sections σ_{LL} (solid lines) and σ_{LR} (dashed lines), respectively. The shaded and hatched regions are derived from the combination of $e^+e^- \to l^+l^-$ and $e^+e^- \to \bar{b}b$ processes. Two allowed regions for each helicity cross section correspond to the two-fold ambiguity discussed in text.

on a χ^2 procedure.

In the case of no observed signal, i.e., no deviation of $\sigma_{\alpha\beta}$ from the SM prediction within the experimental accuracy, one can directly obtain model-independent bounds on the leptonic chiral couplings of the Z' from $e^+e^- \to l^+l^-$ and on the products of couplings $G^e_\alpha \cdot G^q_\beta$ from $e^+e^- \to \bar{q}q$ (with $l = \mu,\tau$ and $q = c,b$). From the numerical point of view, $\sigma_{\alpha\beta}$ are found to just have a complementary role with respect to other observables like σ and A_{FB}.

In the case Z' manifestations are observed as deviations from the SM, with $M_{Z'}$ of the order of 1 TeV, the role of $\sigma_{\alpha\beta}$ is more interesting, specially as regards the problem of identifying the various models as potential

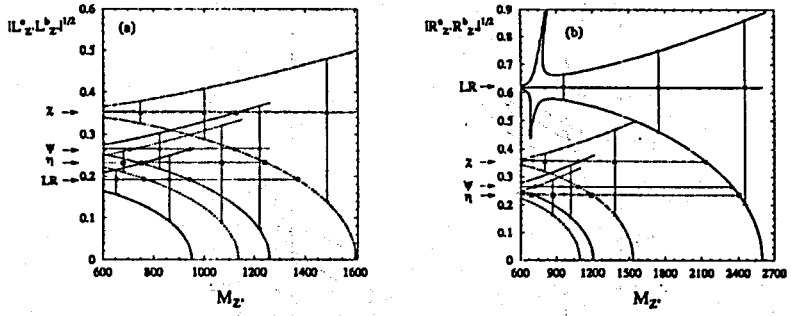

Figure 4: Resolution power at 95% C.L. for $|L^e_{Z'} L^b_{Z'}|^{1/2}$ (a) and $|R^e_{Z'} R^b_{Z'}|^{1/2}$ (b) as a function of $M_{Z'}$ obtained from σ_{LL} and σ_{RR}, respectively, in process $e^+e^- \to \bar{b}b$. The error bars combine statistical and systematic errors. Horizontal lines correspond to the values predicted by typical models.

sources of such non-standard effects. Indeed, in principle, they provide a unique possibility to disentangle and extract numerical values for the chiral couplings of the Z' in a general way (modulo the aforementioned sign ambiguity), avoiding the danger of cancellations, so that Z' model predictions can be tested. Data analyses with other observables may involve combinations of different coupling constants and need some assumption to reduce the number of independent parameters in the χ^2 procedure. In particular, by the analysis combining $\sigma_{\alpha\beta}(l^+l^-)$ and $\sigma_{\alpha\beta}(\bar{q}q)$ one can obtain information of the Z' couplings with quarks without making assumptions on the values of the leptonic couplings. Numerically, as displayed in the previous Sections,for the class of E_6 and Left-Right models considered here the couplings would be determined to about $3-60\%$ for $M_{Z'} = 1$ TeV. Of course, the considerations above hold only in the case where the Z' signal is seen in all observables. Finally, one can notice that for $\sqrt{s} \ll M_{Z'}$ the energy-dependence of the deviations $\Delta\sigma_{\alpha\beta}$ is determined by the SM and that, in particular, the definite sign $\Delta\sigma_{\alpha\alpha}(l^+l^-) < 0$ $(\alpha = L, R)$ is typical of the Z'. This property might be helpful in order to identify the Z' as the source of observed deviations from the SM in process (1).

References

[1] Precision Tests of the Standard Electroweak Model, *Advanced Series on Directions in High Energy Physics*, Vol.14, ed. P. Langacker, 1995, World Scientific.

[2] J. Erler and P. Langacker, Phys. Lett. **B 456** (1999) 68.

[3] G. Altarelli, preprint CERN-TH 97-278 (1997).

[4] For a review see, e.g., L. Hewett and T. G. Rizzo, Phys. Rep. **C183** (1989) 193.

[5] A. A. Pankov and N. Paver, Phys. Rev. D **48** (1993) 63.

[6] F. Del Aguila, M. Cvetic and P. Langacker, Phys. Rev. D **52** (1995) 37.

[7] M. Cvetic and S. Godfrey, Summary of the Working Subgroup on Extra Gauge Boson of the DPF long-range planning study, in *Electro-Weak Symmetry Breaking and Beyond the Standard Model*, eds. T. Barklow, S. Dawson, H. Haber and J. Siegrist (World Scientific, Singapore, 1995).

[8] For an extensive review see, e.g., A. Leike, Phys. Rept. **317** (1999) 143.

[9] J.A. Valls, Representing the CDF and D0 Collaborations, Presented at the *QCD and High Energy Interactions, XXXII Rencontres de Moriond*, Les Arcs, March 22-29, 1997, Fermilab report FERMILAB-Conf-97/135-E.

[10] Z' Physics, in *Physics at LEP2*, eds. G. Altarelli, T. Sjöstrand and F. Zwirner, CERN 96-01, Vol.I, p.577.

[11] Contributions to the Workshops e^+e^- *Linear Colliders: Physics and Detector Studies*, ed. by R. Settles, DESY 97–123E.

[12] E. Accomando *et al.*, Phys. Repts. **299** (1998) 1.

[13] P. Osland and A.A. Pankov, Phys. Lett. **B 403** (1997) 93; **B 406** (1997) 328.

[14] A.A. Babich, A.A. Pankov, and N. Paver, Phys. Lett. B **426** (1998) 375.

[15] A.A. Pankov and N. Paver, Phys. Lett. B **432** (1998) 159.

[16] A.A. Babich, A.A. Pankov, and N. Paver, Phys. Lett. B **452** (1999) 355.

[17] G. Altarelli, R. Casalbuoni, D. Dominici, F. Feruglio and R. Gatto, Nucl. Phys. B **342** (1990) 15.

[18] M. Consoli, W. Hollik and F. Jegerlehner, *in* Z physics at LEP1, ed. G. Altarelli, R. Kleiss and C. Verzegnassi, vol.1, p.7.

[19] S. Riemann, FORTRAN program ZEFIT Version 4.2; D. Bardin et al., preprint CERN-TH. 6443/92, CERN, 1992.

[20] C. Damerall and D. Jackson, in *Proceedings of the 1996 DPF/DPB Summer Study on New Directions for High Energy Physics - Snowmass96*, Snowmass, CO, 25 June - 12 July, 1996.

ON TWO-PHOTON CREATION OF LEPTON PAIRS IN HADRON-HADRON COLLISIONS

N. Shumeiko, A. Soroko, P.Starovoitov
NCPHEP, Belarus

1. Introduction

The modern experiments at hadron colliders (Tevatron, LHC) are of the most interest for studying of the opened HEP questions (such as Higgs boson registration, SUSY particle searches, etc.) Analyzing the observable quantities one can predetermine the validity of the standard theory or, on the other hand, models described so called "new physics" (when find the deviations from the SM predictions). And if these deviations are fixed, we should be sure, that they origin not from the systematics, and are not resulted by the background. In this connection the consideration of double photon leptoproduction in the pp collisions

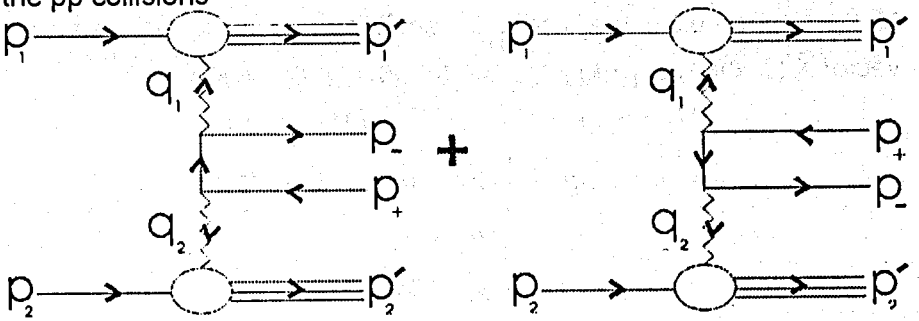

$$p + p \to e^+ e^- + X \quad (1)$$

is actual, since it can be competitive in background with Drell Yan processes. In addition, since at least at ATLAS the luminosity monitoring are planned to be organized through pair production measurements, this is one more motivation for detailed studying of this process.

We have built a programme to calculate exactly (in second order of perturbation theory) three-fold cross section for lepton pair production via two-photon exchange in hadron-hadron collisions when only pair is registered.

2. Kinematics, cross section

The following determinations are used

$$S = p_1 + p_2, J = p_1 - p_2,$$
$$Q = p_+ + p_-, L = p_+ - p_-,$$
$$X = p_1' + p_2'.$$

We use squared pair mass, it's energy and azimuthal angle between pair momenta and collision axis in laboratory system ($\vec{S} = 0$) for description of lepton pair.

$$4m_L^2 \le Q^2 \le (\sqrt{S^2} - (M_1 + M_2 + 2M_\pi))^2,$$
$$\sqrt{S^2 Q^2} \le SQ \le \frac{1}{2}(S^2 + Q^2 - (M_1 + M_2 + 2M_\pi)^2),$$
$$-1 \le \cos\theta_Q \le 1.$$

There are two additional angle variables to desribe leptons

$$0 \le \theta_L \le \pi,$$
$$0 \le \varphi_L \le 2\pi$$

in Q-vector rest frame.

Mass, energy, azimuthal and polar angles of p_2' in the rest frame of vector X ($\vec{S}$ along z-axis) are used for description of jets.

$$(M_2 + M_\pi)^2 \le p_2'^2 \le (\sqrt{X^2} - (M_1 + M_\pi))^2,$$
$$\sqrt{X^2 p_2'^2} \le Xp_2' \le \frac{1}{2}(X^2 + p_2'^2 - (M_1 + M_\pi)^2),$$
$$0 \le \theta_{p_2'} \le \pi,$$
$$0 \le \varphi_{p_2'} \le 2\pi.$$

The formula for three fold cross section is

$$\frac{d^3\sigma}{dQ^2 d(SQ) d\cos\theta_Q} = (2\pi)\left(\frac{\alpha}{4\pi}\right)^4 \frac{M_1 M_2}{\sqrt{-\Delta_2(S,J)X^2 S^2}} *$$
$$* \sqrt{1 - \frac{4m_L^2}{Q^2}} \sqrt{-\Delta_2(Q,S)} *$$
$$* \int dp_2'^2 d(Xp_2') \sqrt{-\Delta_2(X,p_2')} \sin\theta_{p_2'} d\theta_{p_2'} d\varphi_{p_2'} d(-\cos\theta_L) d\varphi_L *$$
$$* \frac{W_{\mu\rho}(q_1,p_1) W_{\nu\sigma}(q_2,p_2)}{(Q_1^2 Q_2^2)^2} L^{\mu\rho\nu\sigma},$$

where $Q_1^2 = -q_1^2, Q_2^2 = -q_2^2$, Δ_2 -Gramm determinant of second order, $W_{\mu\rho}$ -hadron tensor of DIS, $L^{\mu\rho\nu\sigma}$ -lepton tensor.

Integration over L-vector angles is performed analitically in REDUCE environment and the four-dimensional integration over jet variables is fulfiled in FORTRAN code (we use GRV98 structure functions).

3. Numerical analysis

We have calculated the cross section distribution over $\cos\theta_Q$ for electron-positron pair creation in $p\bar{p}$-collisions for Tevatron energy (1.8TeV) for some values of Q^2 and SQ.

The figure shape (as cup with drastic side) demonstrates additional (along with the background measurements) possibilities of studying processes. In contrast to Drell-Yan process which cross section is allocated evenly to the whole kinematical region, the most contribution to the cross section of the process (1) is concentrated near the kinematical boundaries ($\cos\theta_Q = \pm 1$, correspond to the case of forward/backward scattering) and therefore it is suitable to use this process for the purpose of luminosity measurements.

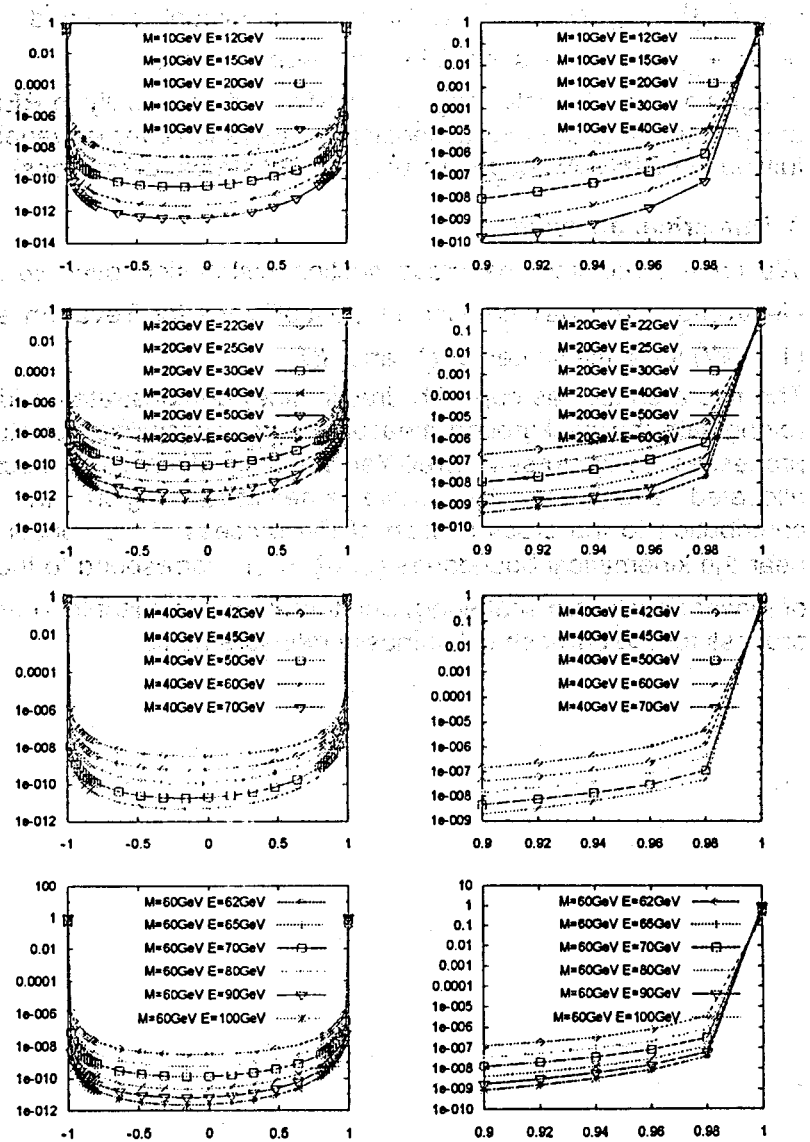

Figure 1. Cross section in mb/GeV^4 ws $\cos\theta_Q$

4. Conclusions

1. We have built a programme to calculate exactly (in second order of perturbation theory) three-fold cross section for lepton pair production via two-photon exchange in hadron-hadron collisions when only pair is registered.
2. Cross section rapidly decreases with increasing of energy and squared mass of lepton pair except the forward/backward region, where it slightly increases.
3. Contribution to the cross section is concentrated near the kinematical boundaries $\cos\theta_Q = \pm 1$ and therefore it is suitable to use this process for the purpose of luminosity measurements. One have to take into account proccess (1), when forward/backward scattering is studied.
4. One need to investigate Z-boson exchange($\gamma - Z, Z - Z$).

5. Reference

1. H. Terazawa: Rev. Mod. Phys **45**, 615 (1973)
2. V. Budnev et al: Phys. Lett. **39B**, 526 (1972)
3. G. Alexander et al: Z. Phys. **34**, 329 (1987)
4. M. Drees et all: hep-ph/9403368
5. T. Gehrmann: DESY-97-014
6. V. Telnov: ATL-PHYS-94-044

Proceedings of International School–Seminar
«Actual Problems of Particle Physics»

Труды международной школы–семинара
«Актуальные проблемы физики частиц»

E1,2-2000-208

Том II

Ответственные за подготовку сборника к печати
П.Старовойтов, С.Шульга

Рукопись сборника поступила 06.09.2000. Подписано в печать 25.09.2000
Формат 60 × 90/16. Офсетная печать. Уч.-изд. листов 14,5
Тираж 170. Заказ 52238

Издательский отдел Объединенного института ядерных исследований
Дубна Московской области